Performance of Continuously Reinforced Concrete Pavements Volume III: Analysis and Evaluation of Field Test Data

PUBLICATION NO. FHWA-RD-94-180

OCTOBER 1998

PB99-128282

U.S. Department of Transportation
Federal Highway Administration

Research and Development
Turner-Fairbank Highway Research Center
6300 Georgetown Pike
McLean, VA 22101-2296

FOREWORD

This report is one volume of a seven-volume set presenting the results of a study to provide the state-of-the-art for the design, construction, maintenance and rehabilitation of Continuously Reinforced Concrete Pavements (CRCP). Through a through literature review of current and past research work in CRCP and extensive field and laboratory testing of 23 in-service CRC pavements, the effectiveness of various design and construction features were assessed; performance of CRCP was evaluated; and procedures for improving CRC pavement technology were recommended. The 23 test pavements were located in six states that participated in this national pooled fund study. In addition the data available for 83 CRCPs included in the General Pavement Study (GPS) number 5 of the Long Term Pavement Performance (LTPP) Program was presented and analyzed. A number of CRCP maintenance and rehabilitation techniques that have been used over the years, including joint and crack sealing, cathodic protection of reinforcing bars, full-depth patching, resurfacing, etc., were also evaluated. This report will be of interest to engineers and researchers concerned with the state-of-the-art design, construction, maintenance and rehabilitation of CRCP including predictive models. The study was made possible with the financial support of Arizona, Arkansas, Connecticut, Delaware, Illinois, Iowa, Louisiana, Oklahoma, Oregon, Pennsylvania, South Dakota, Texas and Wisconsin.

Sufficient copies of this report are being distributed to provide two copies to each FHWA regional office and three copies to each FHWA division office and each state highway agency. Direct distribution is being made to the division offices. Additional copies for the public are available from the National Technical Information Service (NTIS), United States Department of Commerce, 5285 Port Royal Road, Springfield, Virginia 22161.

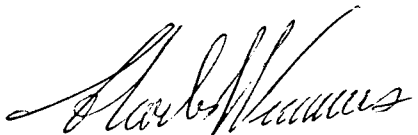

Charles J. Nemmers, P.E.
Director, Office of Engineering
Research and Development

NOTICE

This document is disseminated under the sponsorship of the Department of Transportation in the interest of information exchange. The United States Government assumes no liability for its' contents or use thereof. This report does not constitute a standard, specification or regulation.

The United States Government does not endorse products or manufacturers. Trade and manufacturers' names appear in this report only if they are considered essential to the object of the document.

Technical Report Documentation Page

1. Report No. FHWA-RD-94-180	**2.** PB99-128282	**3. Recipient's Catalog No.**
4. Title and Subtitle PERFORMANCE OF CONTINUOUSLY REINFORCED CONCRETE PAVEMENTS Volume III - Analysis and Evaluation of Field Test Data		**5. Report Date** October 1998 **6. Performing Organization Code**
7. Author(s) Shiraz D. Tayabji, Dan G. Zollinger, Jaganmohan R. Vederey, Jeffrey S. Gagnon		**8. Performing Organization Report No.**
9. Performing Organization Name and Address PCS/Law Engineering A Division of Law Engineering, Inc. 12104 Indian Creek Court, Suite A Beltsville, Maryland 20705		**10. Work Unit No. (TRAIS)** NCP # 3C1A **11. Contract or Grant No.** DTFH61-90-C-00073
12. Sponsoring Agency Name and Address Office of Engineering Research & Development Federal Highway Administration 6300 Georgetown Pike McLean, Virginia 22101		**13. Type of Report and Period Covered** Interim Report Aug 1990 - Dec 1994 **14. Sponsoring Agency Code**

15. Supplementary Notes

Contracting Officer's Technical Representative: Jim Sherwood (current); Roger Larson (previous) (HNR-20)
Subcontractors: Transportation Technologies USA, Inc. (S.D. Tayabji, Principal Investigator)
Texas Transportation Institute (D.G. Zollinger, Co-Principal Investigator)

Special thanks are given to the following highway agencies for their assistance in the conduct of this study: Arizona, Arkansas, Connecticut, Delaware, Illinois, Iowa, Louisiana, Oklahoma, Oregon, Pennsylvania, South Dakota, and Texas.

16. Abstract

This report is one of a series of reports prepared as part of a recent study sponsored by the Federal Highway Administration (FHWA) aimed at updating the state of the art of the design, construction, maintenance, and rehabilitation of CRC pavements. The scope of work of the FHWA study included the following:

1. Conduct of a literature review and prepare an annotated bibliography on CRC pavements and CRC overlays.
2. Conduct of a field investigation and laboratory testing related to 23 existing inservice pavement sections. This was done to evaluate the effect of various design features on CRC pavement performance, to identify any design or construction related problems, and to recommend procedures to improve CRC pavement technology.
3. Evaluation of the effectiveness of various maintenance and rehabilitation strategies for CRC pavements.
4. Preparation of a Summary Report on the current state of the practice for CRC pavements.

Each of the above four items is addressed in a separate report. The following reports have been prepared under this study:

Performance of Continuously Reinforced Concrete Pavements
- Volume I - Summary of Practice and Annotated Bibliography
- Volume II - Field Investigation of CRC Pavements
- Volume III - Analysis and Evaluation of Field Test Data
- Volume IV - Resurfacings for CRC Pavements
- Volume V - Maintenance and Rehabilitation of CRC Pavements
- Volume VI - CRC Pavement Design, Construction, and Performance
- Volume VII - Summary

This report is volume III in the series and presents the results related to the field investigations of selected CRC pavement sections. Also, a summary of data collected to date (1992) for the 83 GPS-5 test sections is presented.

17. Key Words Concrete, concrete pavement, continuously reinforced pavement, nondestructive testing, pavement evaluation, pavement performance, pavement testing, reinforcement.	**18. Distribution Statement** No restrictions. This document is available through: National Technical Information Service, 5285 Port Royal Road, Springfield, VA 22161

19. Security Classification (of this report) Unclassified	**20. Security Classification (of this page)** Unclassified	**21. No. of Pages** 196	**22. Price**

SI* (MODERN METRIC) CONVERSION FACTORS

APPROXIMATE CONVERSIONS TO SI UNITS

Symbol	When You Know	Multiply By	To Find	Symbol
	LENGTH			
in	inches	25.4	millimeters	mm
ft	feet	0.305	meters	m
yd	yards	0.914	meters	m
mi	miles	1.61	kilometers	km
	AREA			
in^2	square inches	645.2	square millimeters	mm^2
ft^2	square feet	0.093	square meters	m^2
yd^2	square yards	0.836	square meters	m^2
ac	acres	0.405	hectares	ha
mi^2	square miles	2.59	square kilometers	km^2
	VOLUME			
fl oz	fluid ounces	29.57	milliliters	mL
gal	gallons	3.785	liters	L
ft^3	cubic feet	0.028	cubic meters	m^3
yd^3	cubic yards	0.765	cubic meters	m^3
NOTE: Volumes greater than 1000 l shall be shown in m^3.				
	MASS			
oz	ounces	28.35	grams	g
lb	pounds	0.454	kilograms	kg
T	short tons (2000 lb)	0.907	megagrams (or "metric ton")	Mg (or "t")
	TEMPERATURE (exact)			
°F	Fahrenheit temperature	5(F-32)/9 or (F-32)/1.8	Celcius temperature	°C
	ILLUMINATION			
fc	foot-candles	10.76	lux	lx
fl	foot-Lamberts	3.426	candela/m^2	cd/m^2
	FORCE and PRESSURE or STRESS			
lbf	poundforce	4.45	newtons	N
lbf/in^2	poundforce per square inch	6.89	kilopascals	kPa

APPROXIMATE CONVERSIONS FROM SI UNITS

Symbol	When You Know	Multiply By	To Find	Symbol
	LENGTH			
mm	millimeters	0.039	inches	in
m	meters	3.28	feet	ft
m	meters	1.09	yards	yd
km	kilometers	0.621	miles	mi
	AREA			
mm^2	square millimeters	0.0016	square inches	in^2
m^2	square meters	10.764	square feet	ft^2
m^2	square meters	1.195	square yards	yd^2
ha	hectares	2.47	acres	ac
km^2	square kilometers	0.386	square miles	mi^2
	VOLUME			
mL	milliliters	0.034	fluid ounces	fl oz
L	liters	0.264	gallons	gal
m^3	cubic meters	35.71	cubic feet	ft^3
m^3	cubic meters	1.307	cubic yards	yd^3
	MASS			
g	grams	0.035	ounces	oz
kg	kilograms	2.202	pounds	lb
Mg (or "t")	megagrams (or "metric ton")	1.103	short tons (2000 lb)	T
	TEMPERATURE (exact)			
°C	Celcius temperature	1.8C + 32	Fahrenheit temperature	°F
	ILLUMINATION			
lx	lux	0.0929	foot-candles	fc
cd/m^2	candela/m^2	0.2919	foot-Lamberts	fl
	FORCE and PRESSURE or STRESS			
N	newtons	0.225	poundforce	lbf
kPa	kilopascals	0.145	poundforce per square inch	lbf/in^2

* SI is the symbol for the International System of Units. Appropriate rounding should be made to comply with Section 4 of ASTM E380.

(Revised September 1993)

ACKNOWLEDGMENTS

The authors wish to sincerely acknowledge the fine support provided by the many State highway agencies during the various phases of the data collection process. Specifically, we would like to thank the many highway agency personnel from Illinois, Iowa, Oklahoma, Oregon, Pennsylvania, and Wisconsin who supplied site specific pavement related data and provided access and traffic control during the testing. Special thanks also go to Oregon DOT for providing more extensive field testing support (FWD testing and coring). The support of the State Technical Advisory Committee and various FHWA staff is gratefully acknowledged.

Finally, the study could not have been possible without the financial support (as part of the pooled-funding) by Arizona, Arkansas, Connecticut, Delaware, Illinois, Iowa, Louisiana, Oklahoma, Oregon, Pennsylvania, South Dakota, and Texas.

TABLE OF CONTENTS

TABLE OF CONTENTS (Continued)

LIST OF FIGURES

LIST OF FIGURES (Continued)

LIST OF FIGURES (Continued)

LIST OF FIGURES (Continued)

LIST OF FIGURES (Continued)

LIST OF TABLES

CHAPTER 1 - INTRODUCTION

General

Continuously reinforced concrete (CRC) pavement is portland cement concrete (PCC) pavement with continuous longitudinal steel reinforcement with no intermediate transverse expansion or contraction joints. The continuous joint-free length of CRC pavements can extend to 305 m (1,000 ft) with breaks provided only at structures. Terminal anchorage is provided at the ends of the CRC pavement to restrain length changes due to temperature variations and drying shrinkage of concrete. The CRC pavements develop a random cracking pattern with cracks generally spaced at about 0.9 to 2.4 m (3 to 8 ft). The cracking pattern is governed by the environment conditions at the time of construction, the amount of steel, and concrete strength. The steel reinforcement restrains the opening of the cracks. Also, the higher the amount of steel reinforcement, the more closely spaced the cracks will be. Most of the cracks form shortly after construction, but additional cracking may develop over the next few years as a result of continued drying shrinkage of concrete, temperature variations, and traffic loading.

Although CRC pavement can be traced back to the late 1930's, the extensive use of CRC pavements began in the early 1960's during the hey-days of the U.S. Interstate System construction program. Currently, there are over 45 060 lane km (28,000 lane mi) of CRC pavements in the U.S. with pavements constructed in at least 35 States. CRC pavements are one of the few pavement types that can truly provide the ideal "zero-maintenance" pavement if they are designed and constructed properly. Many older CRC pavements are considered to have been under-designed leading to premature failures when subjected to ever increasingly heavy truck traffic.

A major concern with CRC pavement is punchout distress. The definition of punchout distress is the area enclosed by two closely spaced (usually less than 0.6 m (2 ft)) transverse cracks, a short longitudinal crack and the edge of the pavement or a longitudinal joint. It also includes "Y" cracks that exhibit spalling, breakup, and faulting. Other distresses associated with punchouts include spalling along transverse cracks and faulting. Other leading causes of CRC pavement failure are wide (and spalled) transverse cracks due to steel rupture and spalling of concrete due to steel corrosion in the presence of heavy deicing salt applications in the northern States. The punchout distress is related to crack spacing, pavement thickness, poor foundation support, and heavy truck loadings. The repair of punchout distress typically consists of full-depth patches. With time, as the number of full-depth patches increase, the pavement may be resurfaced with asphalt concrete or portland cement concrete, or it may be reconstructed.

Over the years, many State agencies have conducted research studies to develop better understanding of the effects of various design and construction features on the performance of CRC pavements. A large number of these studies have focused on pavement thickness, concrete aggregate type, amount of steel reinforcement, and base/subbase type. Studies have

also been conducted to address the benefits of using epoxy-coated reinforcement and the effectiveness of permeable treated base layers under CRC pavements.

This report is one of a series of reports prepared as part of a recent study administered by the Federal Highway Administration (FHWA) aimed at updating the state-of-the-art of the design, construction, maintenance, and rehabilitation of CRC pavements. The study is a national pooled funds study with participation by Arizona, Arkansas, Connecticut, Delaware, Illinois, Iowa, Louisiana, Oklahoma, Oregon, Pennsylvania, South Dakota, and Texas. The scope of work of the FHWA study included the following:

1. Conduct of a literature review and preparation of an annotated bibliography on CRC pavements and CRC overlays.

2. Conduct of a field investigation and laboratory testing related to 23 existing in-service pavement sections. This was done to evaluate the effect of various design features on CRC pavement performance, to identify any design or construction related problems, and to recommend procedures to improve CRC pavement technology.

3. Evaluation of the effectiveness of various maintenance and rehabilitation strategies for CRC pavements.

4. Preparation of a Summary Report on the current state of the practice for CRC pavements.

Each of the above four items is addressed in a separate report. The following reports have been prepared under this study:

Volume I - Summary of Practice and Annotated Bibliography on CRC Pavements

Volume II - Field Investigation of CRC Pavements

Volume III - Analysis and Evaluation of Field Test Data

Volume IV - Maintenance and Rehabilitation of CRC Pavements

Volume V - Resurfacings for CRC Pavements

Volume VI - Synthesis of Recommended Practice

This report is volume III in the series and presents the analysis and evaluation of the field and laboratory test data for the 23 test sections included in the field investigation. Volume II presented the field and laboratory test data and inventory data for each of the 23 test sections. This volume provides a detailed evaluation of the test data, and global analysis of data is presented to identify if behavioral patterns or trends exist for certain pavement design

attributes. Since CRC pavement performance is significantly influenced by crack spacing, the data analysis and evaluation provides a more detailed review of the crack spacing related data. Also, the results of an indepth analysis conducted to compare predicted crack spacing (using available CRCP cracking models) with actual crack spacing are presented. Specifically, the following items were evaluated and are discussed in this report:

1. Overall Trends
    a. Effect of age.
    b. Effect of climatic region.

2. Effect of Design Features
    a. Thickness.
    b. Tied-concrete shoulder.
    c. Permeable base.
    d. Epoxy-coated steel.

3. Predicted Versus Actual Crack Spacings
    a. Crack spacing was predicted using site specific factors (actual or estimated) for each test section and using computer program CRCP-5. The predicted crack spacing was then compared to actual crack spacing.

4. Overall Indicators of Performance
    a. Ride quality.
    b. Pavement stiffness, in terms of radius of relative stiffness, ℓ; modulus of subgrade reaction, k, and slab rigidity, D.

It should be noted that the CRCP behavior and future performance is significantly affected by the temperature and curing conditions at the time of construction. Unfortunately, as is the case with most investigations inservice pavements, the construction time data were generally not available and had to be estimated for the predicted crack spacing study.

This volume also contains a summary of data, available as of August 1993, for the 85 CRC test sections of the GPS-5 experiment of the Long Term Pavement Performance (LTPP) program. A limited analysis of the data is also presented.

Objectives of the Field Investigations

The specific objective of the field investigation was to conduct necessary field investigations and laboratory testing at 20 to 30 existing CRC pavement sections and to evaluate the effect of standard/new design features on CRC pavement performance.

After a detailed evaluation of available project sites in conjunction with participating State highway agencies, 23 project sites were selected as follows:

Illinois	-	5 sites
Iowa	-	3 sites
Oklahoma	-	5 sites
Oregon	-	3 sites
Pennsylvania	-	2 sites
Wisconsin	-	5 sites

At each site, performance of a representative 305-m (1,000-ft) length section was evaluated by performing visual condition surveys, profile measurements, by falling weight deflectometer testing, and by corrosion-related testing. In addition, concrete cores were obtained for strength, stiffness (modulus of elasticity), and coefficient of thermal expansion testing. Samples of base, subbase, and subgrade were also obtained for material characterization. For each project site, available inventory type data related to design, construction, maintenance, performance, and traffic was collected from State agencies.

None of the project sites included rehabilitated pavement sections. Because of the limited budget for field investigations, it was considered that the most benefits would be obtained by focusing on existing original pavement sections.

The work plan for the field investigation consisted of the appropriate data collection for each test section and conduct of the following type of data analysis:

1. *Project Level Evaluation* - Each project would be examined to identify cause-effect relationship. Also, the performance and characteristics of specific groups of projects would be examined and compared.

2. *Crack Spacing Simulations* - Existing crack spacing models would be used to verify the reasonableness of the models in predicting the crack pattern in CRC pavements.

3. *Structural Analysis* - The falling weight deflectometer (FWD) data would be used to characterize the structural capacity of the CRC pavements. Load transfer effectiveness at cracks would be examined.

4. *Distress Modeling* - The validity of the existing CRCP distress models would be examined using project specific data from the CRCP projects.

5. *Corrosion Analysis* - For projects in the northern States, corrosion-related testing would be performed to determine the level of corrosion and to determine the effect of various design, construction, and climatic features on the level of corrosion.

One focus of the data analysis was to try to identify how specific design/construction features affect pavement performance. It should be noted that the study objectives were not to develop distress or performance models with global applicability, as it was realized at the onset

that the limited number of projects considered would not provide the necessary foundation for that. It should also be noted that the primary factors that affect performance of CRC pavements are thickness and crack spacing. Thickness can be controlled as a design factor. However, crack spacing and the consequent crack width cannot be controlled directly, and an ideal workable crack spacing can only be attempted by manipulating various design factors and hoping that placement conditions would be favorable. Although, past experience has indicated that crack spacings in the range of 0.9 to 2.4 m (3 to 8 ft) (and possibly around 1.2 to 1.5 m (4 to 5 ft)) are considered acceptable, we are still not able to achieve the desired spacings with certainty. The actual crack spacings also follow a random pattern whereby on a given length of a CRC pavement, crack spacing may range from 0.6 m (2 ft) or less to over 2.4 m (8 ft) with numerous instances of closely spaced or cluster cracking.

Thus, one of the primary focus in this study was to identify the critical factors that influence crack spacing in CRC pavements. Also, an attempt was made to correlate actual crack spacing to the performance of the pavement in terms of structural capacity, ride, and extent and severity of distress.

The scope of work also included review and analysis of data being collected for the 85 CRC pavement test sections which are being monitored as part of the GPS-5 experiment of the SHRP initiated Long Term Pavement Performance (LTPP) program.

For each project evaluated in the field, all available data related to design, construction, maintenance, rehabilitation, and performance were collected. This was done to complement the information and to extend the study data base. A comprehensive data base was developed to incorporate all CRC projects evaluated as part of the study. A summary of available data and preliminary data analysis results are presented in this volume.

Study Details

This study administered by FHWA is a pooled-funds study with participation by Arizona, Arkansas, Connecticut, Delaware, Illinois, Iowa, Louisiana, Oklahoma, Oregon, Pennsylvania, South Dakota, and Texas. A technical advisory committee (TAC) consisting of selected State agency representatives provided a forum for review of the work plans for the study, specifically for the field investigation portion of the study. The field investigation work plan was presented at a 2-day meeting of the TAC and the plan, as modified based on TAC comments, was implemented. The final field investigation plan, as revised, is included in volume II.

Site Identification and Selection

Based on the literature review and contacts with FHWA and several State highway agencies, a large number of candidate CRCP projects were identified for field testing. Site verification and preliminary technical/background information on the projects were provided by State contacts. Based on a detailed examination of the nominated projects, a total of 23 projects were finally selected for field investigations.

The final list of the test sections selected for field evaluation is given in table 1. As shown in table 1, the selected test sections incorporate a broad range of attributes of interest as follows:

- Design thickness - ranging from 203 to 330 mm (8 to 13 in).
- Epoxy coated reinforcement - 3 sections.
- Permeable base - 2 sections.
- Age - ranging from 0.3 to 22 years.
- Subgrade - both coarse and fine grained soils.
- Base - CTB, LCB, ATB, and granular.
- Steel amount - 0.45 to 0.7 percent.
- Steel placement - tube fed and chairs.
- Shoulder type - 11 AC and 12 PCC.
- Climatic region - wet-freeze (15 sections) and wet-no-freeze (8 sections).

All field testing was performed during the fall of 1991.

Field Data Collection Plan

The field data collection program was aimed at collecting data on the current condition of each 305-m (1,000-ft) long representative test section. The following activities were completed at most of the test sections:

1. Visual condition survey
    - Crack and distress mapping along the 305-m (1,000-ft) section.
    - Joint width measurements.
    - Windshield survey of adjacent 8.05 km (5 mi) of pavement.

2. Nondestructive deflection testing
    - Basin testing (slab interior).
    - Testing at crack locations (mid-slab and edge).

3. Profile testing

4. Corrosion-related testing
    - Corrosion potential measurement.
    - Examination of steel bars (cores).

5. Coring and shallow borings
    - Concrete testing (laboratory testing)
        - Splitting tensile strength.
        - Modulus of elasticity.
        - Coefficient of thermal expansion.
        - Chloride content determination.

Table 1. Final list of test sections.

Test Section ID	Route	Nearest Mile Post	Direction	No. of Lanes	Age as of Fall 1991 Testing, years	SHRP Climatic Region	Terminal Joint Type	Design Thickness, in.	Subgrade Type (AASHTO)	Base Type	Outside Shoulder Type	Long. Steel Amount, %	Steel Placement Method	Epoxy Coated Steel	1,991 2-Way AADT	Design Lane Cumul. ESALs upto 9/91
IL-1	US51	na	SB	4	0.3	wf	wide flange	10	A-7-6	perm. ctb	pcc	0.7	chair	no	na	180,000
IL-2	I72	45	WB	4	15	wf	lug	8	A-6	ctb	ac	0.59	tube	no	7,500	4,800,000
IL-3	US36	st. 5+30	EB	4	20	wf	lug	8	A-7-5	atb	ac	0.6	chair	no	17,700	4,800,000
IL-4	I55	86	EB	6	20	wf	lug	8	A-7-5	atb	ac	0.6	tube	no	17,700	13,700,000
IL-5	US50	na	WB	4	5	wf	wide flange	8	A-7-5	lcb	pcc	0.7	chair	no	na	300,000
IA-1	I29	18	NB	4	20	wf	lug	8	A-2-6	ctb	ac	0.65	tube	no	7,500	3,700,000
IA-2	I80	15	WB	4	22	wf	lug	8	A-6	atb	ac	0.65	tube	no	12,700	8,850,000
IA-3	I380	15	NB	4	15	wf	lug	8	A-6	atb	pcc	0.65	tube	no	27,700	5,300,000
OK-1	I40	231	WB	4	4	wnf	wide flange	9	A-6	atb	pcc	0.5	chair	no	15,000	na
OK-2	US69	na	NB	4	5	wnf	wide flange	9	A-6	atb	pcc	0.5	chair	no	10,000	na
OK-3	I35	148	NB	4	3	wnf	wide flange	10	A-4	atb	pcc	0.5	chair	yes	30,000	na
OK-4	US69	na	SB	4	7	wnf	wide flange	9	A-6	soil-asphalt	pcc	0.5	chair	no	10,000	na
OK-5	I40	299	EB	4	2	wnf	wide flange	10	A-2-6	perm. ctb	pcc	0.61	chair	no	13,000	na
OR-1	I5	184	SN	4	7	wnf	wide flange	13	A-4	granular	ac	0.6	tube	no	29,700	11,300,000
OR-2	I5	184	NB	4	4	wnf	wide flange	10	A-4	ctb	ac	0.6	tube	no	30,300	3,000,000
OR-3	I205	na	SB	4	20	wnf	lug	8	A-6	ctb	ac	0.54	tube	no	59,000	30,000,000
PA-1	I180	23	EB	4	15	wf	wide flange	9	A-2-4	granular	ac	0.45	tube	no	na	na
PA-2	I81	Rt 11	NB	4	22	wf	lug	9	A-2-4	granular	pcc	0.55	chair	no	na	na
WI-1	I43	31	NB	4	18	wf	lug	8	A-2-4	granular	ac	0.65	chair	no	na	na
WI-2	I90	180	EB	4	6	wf	wide flange	10	A-2-4	granular	pcc	0.67	tube	yes	na	na
WI-3	I90/94	136	NB	6	7	wf	lug	10	A-2-7	granular	pcc	0.67	tube	yes	na	na
WI-4	I90/94	111	WB	6	7	wf	na	10	A-2-6	granular	pcc	0.67	tube	no	na	na
WI-5	I90/94	99	EB	4	16	wf	lug	8	A-2-6	granular	ac	0.61	chair	no	na	na
Average					11.3			9.0				0.6				
Std Dev					7.4			1.2				0.1				
Maximum					22.0			13.0				0.7				
Minimum					0.3			8.0				0.5				

(25.4 mm = 1.0 in)

- Material characterization
  - Atterberg limits.
  - Particle size distribution.

6. Reinforcing steel location survey.

7. Photographic and video imaging.

Except for the Oregon testing, all field testing was performed by the contractor staff. In Oregon, the State agency performed deflection testing and the coring and boring operations. No profile testing was done for the Oregon sites. All field testing was accomplished during 1 day of testing with the test crew arriving at the site at dawn and staying at the site until early evening. At a few sites, testing was delayed due to rain. The crew consisted of one project engineer (also operated the profiler), one FWD operator, and two technicians (for coring/ boring and other site activities).

The details of field data collection procedures used are given in appendix A of the volume II report.

Data Compilation

For each test section, the following summary data was developed:

1. Inventory
   - Location and climatic features.
   - Traffic, if available.
   - Structural section.
   - Design/construction, if available.
   - Performance, if available.
   - Maintenance and rehabilitation, if available.

2. Visual Condition Survey
   - Map showing crack spacing within the 305-m (1,000-ft) test section.
   - Crack spacing summaries and statistics.
   - Drainage survey summary.
   - Overall windshield survey summary.
   - Terminal joint survey summary.

3. Deflection Testing
   - Basin deflection data for each of the seven sensors along the 305-m (1,000-ft) length of the test section.
   - Slab temperature profile data.
   - Results of load transfer testing at cracks.

- Average and range of deflections for each sensor for testing conducted at cracks, both at mid-slab and edge locations and for morning and afternoon testing.
- Backcalculated radius of relative stiffness, ℓ, modulus of subgrade reaction, k, and slab rigidity, D, along the length of the test section. Backcalculation was performed using Program ILLI-BACK.[1]

4. Crack Width Measurements
   - Summary of crack width changes between morning and afternoon measurements.
   - Crack widths normalized to -17.8 °C (0 °F) and 4.4 °C (40 °F).

5. Laboratory Testing
   - Concrete test data.
   - Base/subbase/subgrade characterization.
   - Chloride testing.

6. Reinforcement Related Testing
   - Steel location.
   - Steel corrosion evaluation.
     - corrosion potential testing.
     - visual examination of cores over steel bars.

7. Profile Testing
   - International Roughness Index (IRI) data.

Analysis and Evaluation of Data

This section briefly describes the different types of analysis and evaluation that was performed with the field test data. As discussed previously, because the performance of CRC pavements is significantly influenced by crack spacing and the structural integrity of the transverse cracking, the analysis is focused on crack spacing, crack width, and the structural response of the CRC pavement. The structural response of the test sections was characterized by analysis of the falling weight deflectometer test data for testing conducted along the slab interior (basin testing) and at crack locations (at mid-slab and along the lane edge).

Crack Spacing Data Analysis

Crack spacing data was analyzed to determine the total number of cracks within the 305-m (1,000-ft) length of the test section. In addition, average crack spacing and standard deviation of the crack spacing was determined. Also, the average spacing of the closes five cracks was also determined at each crack location. A plot of the average crack spacing of the closest five cracks is useful in identifying incidences and locations of cluster cracking with

average crack spacing of less than 0.6 m (2 ft) and can be easily used when comparing cracking pattern with the overall stiffness characteristics of the pavement.

The crack spacing data were also used to develop crack spacing frequency distribution plots based on the total number of cracks that have spacings equal to or less than the designated spacing and also based on the total length of paving exhibiting crack spacing equal to or less than the designated spacing.

Crack Width Data Analysis

The change in crack width was determined from the crack width measurements made in the morning and the afternoon. In addition, the corresponding change in mid-slab temperature was determined. The two sets of data were used to compute the effective slab length change (over the 30.5-m (100-ft) length of the pavement used for the crack width measurements) in terms of unit length change per unit change in temperature. This value can be used to estimate the "effective coefficient of thermal expansion" for the pavement. Although, at the onset of the testings, it was not clear if reliable crack width data could be measured, the actual crack width data collected did provide values of the "effective coefficient of thermal expansion" that appear to be in the range of expected values compared with actual coefficient of thermal expansion of concretes tested in the laboratory environment.

The crack width data at each section was also used to determine crack widths normalized to 4.4 °C (40 °F) and -17.8 °C (0 °F) to allow comparison of crack widths between sites. The normalization was performed by using the laboratory measured coefficient of thermal expansion and the measured crack widths.

Basin Deflection Testing Data Analysis

Deflection data from the basin testing was used to backcalculate the radius of relative stiffness, ℓ, modulus of subgrade reaction, k, and slab rigidity, D, for the pavement at each test location. ℓ and D are defined as follows:

$$\ell = (Eh^3/12(1 - \mu 2)k)^{0.25} \quad \textbf{(1)}$$

where:

E	=	concrete modulus of elasticity
h	=	slab thickness
μ	=	concrete Poisson's ratio
k	=	modulus of subgrade reaction

and

$$D = Eh^3/12(1 - \mu 2) \quad \textbf{(2)}$$

Program ILLI-BACK was used for this purpose.[1] The backcalculation was performed for all the three load levels used. Backcalculated data indicate that the radius of relative

stiffness values computed for each of the three load levels at each test location were almost identical. Therefore, in subsequent data analysis, only the data for the nominal 40.03 kN (9,000 lb) load were used.

For edge testing, no corrections were made for the boundary conditions (free-edge). Thus, the backcalculated values computed using ILLI-BACK actually represent the "effective" or equivalent radius of relative stiffness, modulus of subgrade reaction, or slab rigidity, as appropriate.

Data Analysis for Deflection Testing at Cracks and Along the Edge

A review of the data obtained from deflection testing at cracks indicated that edge deflections were almost twice as large as mid-slab deflections for both early morning and mid-afternoon testing. However, the backcalculated radius of relative stiffness along the edge was not always "proportionately" less than along the mid-slab. Thus, care must be exercised in interpreting the backcalculated relative stiffness values without considering maximum deflections for edge testing. The radius of relative stiffness values were backcalculated without accounting for the edge boundary condition (free edge or tied shoulder). Thus, these values represent "effective" values and are used primarily to allow comparison of overall pavement stiffness along the edge to the overall pavement stiffness along mid-slab (interior) locations and to identify if tied-shoulder has any effect on the overall pavement stiffness along the edge. Also, as expected, afternoon testing produced lower deflections at both the mid-slab and edge locations. During early morning, the slab edge is curled upwards due to cooler slab surface resulting in a slight loss of support along the free edges. During mid-afternoon, the reverse is true and the slab edge is either in contact with the base/subbase or is close to contact because of the downward curl along the slab edge. However, the range in temperature variations at each site was different depending on cloud cover and rainfall during the days of testing.

The deflection data were also used to backcalculate the modulus of subgrade reaction, k, and slab rigidity, D. As discussed, the radius of relative stiffness values along the edges were not very different from the values for the mid-slab testing even though the maximum deflections along the edges were almost twice as much as at the mid-slab locations. This phenomenon is apparently due to the use of normalized deflection basin areas used for backcalculating the radius of relative stiffness values. However, the backcalculated k and D values along the edge were generally lower than those at the mid-slab locations, clearly indicating the effect of the edge boundary condition. The edge D values generally were between 20 to 60 percent of the mid-slab D values. Thus, the backcalculated D values characterize the slab rigidity along the edge much better than the ℓ values and this approach is strongly recommended for evaluating the deflection based response of CRC pavements.

Comparisons Between Actual and Predicted Crack Spacings

Several computer programs have been developed in the recent years to predict the cracking pattern and the effect of various parameters on the development of the crack spacing. These models include CRCP-5 developed at the University of Texas and the TTICRCP model

developed by the Texas Transportation Institute at Texas A&M University. For this study, CRCP-5 model was used to predict the crack spacing distribution at each of the test sections. The CRCP-5 crack spacing distribution was compared to actual crack spacing distribution which was observed in the field. Variations between the computer simulation results and field observations are noted and discussed in a separate chapter.

Comparisons with Existing Distress/Performance Models

Although CRC pavements have been used widely for over 30 years, there is a noticeable lack of distress and/or performance models for CRC pavements. The American Association of State Highway and Transportation Officials (AASHTO) Guide falls back on the experience with jointed concrete pavements for thickness design of CRC pavements.[2] A limited amount of distress model development work has been done in Texas and Illinois based on state-wide surveys of CRC pavements. Recently, an attempt was made to use the LTPP data from 85 CRC test sections (part of LTPP GPS-5 experiment) to develop distress models. However, because of very little distress in the test sections included in the experiment, a model related to ride quality only was proposed.

As part of this study, some of the viable distress/performance models were used with the test section data to determine the sensitivity and the utility of these models.

Summary

The results of the detailed data analysis are presented in the following chapters. The reader is referred to volume II in this series of reports for more detailed information for each test section. This information includes actual crack mapping for the full 305 m (1,000 ft) long sections and deflections along the length of the test sections.

It should be noted that even though detailed testing at any CRC pavement site may be limited to a 305 m (1,000 ft) length, it is important that a survey of failures (steel ruptures, patches, and punchouts) be conducted over at least 5 to 8 km (3 to 5 mi) length of the project. Also, it is important to note that CRC test sections for monitoring purposes should be at least 305 m (1,000 ft) long to ensure that the test section and the cracking pattern are representative of the project.

CHAPTER 2 - SUMMARY OF TEST DATA

General

As discussed earlier, this volume presents detailed analysis of the field and laboratory test data for each of the 23 CRC pavement test sections included in the field investigation program. One of the major concerns at the beginning of the field study was the availability and reliability of data related to traffic along the test sections. Even though intensive interactions were made with appropriate State highway agencies, traffic data were not made available for many of the test sections - in most cases because the reliable traffic data did not exist or the required traffic data (e.g., ESAL's) were not maintained by the agency. This is not unusual as the same problem has been encountered on many similar pavement data collection programs including the Long Term Pavement Performance (LTPP) program. For the LTPP program, the State agencies have initially provided the best estimates of the ESAL's for the test sections while efforts are underway to perform more indepth traffic data collection using site-specific WIM and AVC equipment. Thus, for this project, traffic effects are indirectly incorporated by considering age (time) effects. However, it should be noted that based on the traffic data that was available, the estimated ESAL's for the test sections ranged from a few hundred thousand ESAL's to over a million ESAL's.

Data Summaries

A summary of the key data elements for each of the 23 test section is presented in table 2. The table includes both raw (as-measured) data and reduced data such as radius of relative stiffness and effective coefficient of thermal expansion (based on joint width change data). As indicated previously, the selected test sections incorporate a broad range of attributes of interest as follows:

- Design thickness - ranging from 203 to 330 mm (8 to 13 in).
- Epoxy coated reinforcement - 3 sections.
- Permeable base - 2 sections.
- Age - ranging from 0.3 to 22 years.
- Subgrade - both coarse and fine grained soils.
- Base - CTB, LCB, ATB, and granular.
- Steel amount - 0.45 to 0.7 percent.
- Steel placement - tube fed and chairs.
- Shoulder type - 11 AC and 12 PCC.
- Climatic region - wet-freeze (15 sections) and wet-no-freeze (8 sections).

Highlights of Data Analysis

Ride Quality and Serviceability

The ride quality of the CRC pavement test sections as denoted by International Roughness Index (IRI) ranged from a low of 837 mm/km (53 in/mi) to a high of 2481 mm/km

(157 in/mi) as shown in table 2. This represents good to very good ride quality considering that the test section ages ranged from 0.3 years to 22 years at the time of testing. Thus, CRCP pavements tend to provide a good riding surface even when a high amount of medium to high severity cracking is present. Figure 1 shows the IRI values plotted as a function of age. Although there is a large amount of scatter in the data points, it appears that there is a slight increase in IRI (rougher ride) with age.

In order to obtain an assessment of the test section performance in terms of the present serviceability index, PSI (as defined by AASHTO), an attempt was made to develop PSI values for each test section using the IRI values. It should be noted that PSI as defined by AASHTO incorporates pavement cracking and patching. It is assumed that the ride quality ((as denoted by IRI) includes the effects of low levels patching and cracking. Thus, for the CRC pavement sections exhibiting little or no distress, the estimation of PSI values from IRI is considered reasonable.

Although not much use has been made in the U.S. of the correlations between PSI and IRI, two procedures have been recently developed as follows:

1. *The World Bank Model* - The following model has been developed based on data from several studies conducted by the World Bank:[1]

$$PSI = 5e^{-(IRI/347)} \quad (3)$$

where PSI ranges from 0 to 5 and IRI is in mm/km (in/mi). The above model was used recently as part of the LTPP data analysis efforts to estimate the PSI values at more than 750 LTPP test sections.

2. *The TRDF Model*[2] - The following model was developed using data obtained from limited testing using LTPP profilometers over a limited number of test sections:

$$PSI = 7.06 - 1.79\log(IRI) \quad (4)$$
$$(r^2 = 0.79)$$

where PSI ranges from 0 to 5 and IRI is in mm/km (in/mi).

The above two models were used to estimate the PSI values as of the testing time. It should be cautioned that the applicability of the models to CRC pavements has not been verified. These models are being utilized only to provide some assessment of performance using an acceptable performance index parameter. The estimated PSI values for each section are summarized in table 3. The PSI values range from 3.2 to 4.2 for the pavements ranging in age from 0.3 to 22 years (using only the ride quality as a measure of PSI). Table 3 also contains PSI (or similar performance indicator converted to 0 to 5 scale) values reported by the State agencies for 1990. As seen, the estimated PSI values compare well with the State reported values.

Table 2. Summary of key data elements.

Test Section ID	Route	Nearest Mile Post	Direction	No. of Lanes	Age as of Fall 1991 Testing, years	Climatic Region	Terminal Joint Type	Design Thickness, in.	Subgrade Type (AASHTO)	Base Type	Outside Shoulder Type	Long. Steel Amount, %	Steel Placement Method	Epoxy Coated Steel	1,991 2-Way AADT	Design Lane Cumul. ESALs upto 9/91
IL-1	US51	na	SB	4	0.3	wet-freeze	wide flange	10	A-7-6	perm. ctb	pcc	0.7	chair	no	na	180,000
IL-2	I72	45	WB	4	15	wet-freeze	lug	8	A-6	ctb	ac	0.59	tube	no	7,500	4,800,000
IL-3	US36	st. 5+30	EB	4	20	wet-freeze	lug	8	A-7-5	atb	ac	0.6	chair	no	17,700	4,800,000
IL-4	I55	86	EB	6	20	wet-freeze	lug	8	A-7-5	atb	ac	0.6	tube	no	17,700	13,700,000
IL-5	US50	na	WB	4	5	wet-freeze	wide flange	8	A-7-5	lcb	pcc	0.7	chair	no	na	300,000
IA-1	I29	18	NB	4	20	wet-freeze	lug	8	A-2-6	ctb	ac	0.65	tube	no	7,500	3,700,000
IA-2	I80	15	WB	4	22	wet-freeze	lug	8	A-6	atb	ac	0.65	tube	no	12,700	8,850,000
IA-3	I380	15	NB	4	15	wet-freeze	lug	8	A-6	atb	pcc	0.65	tube	no	27,700	5,300,000
OK-1	I40	231	WB	4	4	wet-no freeze	wide flange	9	A-6	atb	pcc	0.5	chair	no	15,000	na
OK-2	US69	na	NB	4	5	wet-no freeze	wide flange	9	A-6	atb	pcc	0.5	chair	no	10,000	na
OK-3	I35	148	NB	4	3	wet-no freeze	wide flange	10	A-4	atb	pcc	0.5	chair	yes	30,000	na
OK-4	US69	na	SB	4	7	wet-no freeze	wide flange	9	A-6	soil-asphalt	pcc	0.5	chair	no	10,000	na
OK-5	I40	299	EB	4	2	wet-no freeze	wide flange	10	A-2-6	perm. ctb	pcc	0.61	chair	no	13,000	na
OR-1	I5	184	SN	4	7	wet-no freeze	wide flange	13	A-4	granular	ac	0.6	tube	no	29,700	11,300,000
OR-2	I5	184	NB	4	4	wet-no freeze	wide flange	10	A-4	ctb	ac	0.6	tube	no	30,300	3,000,000
OR-3	I205	na	SB	4	20	wet-no freeze	lug	8	A-6	ctb	ac	0.54	tube	no	59,000	30,000,000
PA-1	I180	seg. 374	EB	4	15	wet-freeze	wide flange	9	A-2-4	granular	ac	0.45	tube	no	na	na
PA-2	I81	seg. 524	NB	4	22	wet-freeze	lug	9	A-2-4	granular	pcc	0.55	chair	no	na	na
WI-1	I43	31	NB	4	18	wet-freeze	lug	8	A-2-4	granular	ac	0.65	chair	no	na	na
WI-2	I90	180	EB	4	6	wet-freeze	wide flange	10	A-2-4	granular	pcc	0.67	tube	yes	na	na
WI-3	I90/94	136	NB	6	7	wet-freeze	lug	10	A-2-7	granular	pcc	0.67	tube	yes	na	na
WI-4	I90/94	111	WB	6	7	wet-freeze	na	10	A-2-6	granular	pcc	0.67	tube	no	na	na
WI-5	I90/94	99	EB	4	16	wet-freeze	lug	8	A-2-6	granular	ac	0.61	chair	no	na	na
Average					11.3			9.0				0.6				
Std Dev					7.4			1.2				0.1				
Maximum					22.0			13.0				0.7				
Minimum					0.3			8.0				0.5				

(25.4 mm = 1 in)

Table 2. Summary of key data elements (continued).

Test Section ID	Average Maximum Deflection (sensor 1) Under 9,000 lb Load, 0.001 in.										% Change in Edge Deflection from Morn. to Afternoon	Edge Deflection as % of Basin Defl. (morning)	Edge Deflection as % of Basin Defl. (afternoon)
	Basin Testing		Morning Mid-Slab Crack Testing		Morning Edge Crack Testing		Afternoon Mid-Slab Crack Testing		Afternoon Edge Crack Testing				
	Average	Std. Dev.	Average	Std. Dev.	Average	Std. Dev.	Average	Std. Dev.	Average	Std. Dev.			
IL-1	2.2	0.4	3.1	0.5	5.2	0.8	2.8	0.3	3.8	0.5	27	236	173
IL-2	4.3	0.7	6.2	1.6	12	3.5	5.4	0.7	10.9	2.4	9	279	253
IL-3	4.9	0.5	5.2	0.2	10	0.9	5	0.1	9.3	0.5	7	204	190
IL-4	3.9	0.2	3.9	0.2	7.9	1.2	3.8	0.1	6.9	1.6	13	203	177
IL-5	4.4	0.7	4.3	0.6	9.3	1.2	4.1	0.4	6.6	0.7	29	211	150
IA-1	4.1	1.2	3.8	1.4	6.9	1.2	4.3	1.3	5.3	0.7	23	168	129
IA-2	5	0.4	5.3	0.5	13.4	1.6	4.7	0.3	9.6	1.2	28	268	192
IA-3	4.2	0.2	4.5	0.1	7.7	0.8	4.5	0.1	9.1	0.5	-18	183	217
OK-1	2.7	0.2	3.1	0.1	5	0.5	3.2	0.2	5.3	0.5	-6	185	196
OK-2	2.7	0.3	3	0.2	4.1	0.9	3	0.2	3.7	0.6	10	152	137
OK-3	2.9	0.3	3.3	0.2	5.2	0.4	3.3	0.2	4.6	0.5	12	179	159
OK-4	3	0.9	5	1	9.3	3.5	3.7	0.5	7.7	2.7	17	310	257
OK-5	3	0.6	4	0.3	5	0.7	3.5	0.2	4.3	0.5	14	167	143
OR-1	2.7	0.3	2.8	0.1	4.1	0.3	na	na	na	na		152	
OR-2	1.9	0.4	2.1	0.3	4.9	0.6	2.1	0.3	3.5	0.2	29	258	184
OR-3	4.7	1.5	4.3	0.6	7.2	1.3	na	na	na	na		153	
PA-1	2.2	0.4	2.3	0.1	4.4	0.7	2.4	0.1	na	na		200	
PA-2	5.3	1.8	4.5	0.9	6.4	0.8	5.5	0.6	5.8	0.9	9	121	109
WI-1	2.8	0.6	3.4	0.9	6.1	1.3	3.2	0.8	4.4	0.9	28	218	157
WI-2	2.8	0.4	2.8	0.3	7	0.9	2.8	0.2	5.4	1	23	250	193
WI-3	2.7	0.3	3.2	0.4	7.4	1.4	3.2	0.4	4.4	0.7	41	274	163
WI-4	3.2	0.4	4.3	0.8	16	4	3.8	0.4	5.1	1	68	500	159
WI-5	5.4	1.1	4.3	0.4	8.5	0.8	5.2	1.3	6.4	0.4	25	157	119
Average	3.5	0.6	3.9	0.5	7.5	1.3	3.8	0.4	6.1	0.9	19.3	218.7	172.9
Std Dev	1.1	0.4	1.0	0.4	3.1	1.0	1.0	0.4	2.2	0.6	17.6	78.6	39.4
Maximum	5.4	1.8	6.2	1.6	16.0	4.0	5.5	1.3	10.9	2.7	68.1	500.0	256.7
Minimum	1.9	0.2	2.1	0.1	4.1	0.3	2.1	0.1	3.5	0.2	-18.2	120.8	109.4

(40.03 kN = 9,000 lb) (0.0254 mm = 1 mil)

Table 2. Summary of key data elements (continued).

Test Section ID	Measured E, million psi	Average Split Ten. Strength, psi	Average Core Thickness, in.	Estimated k, pci	Estimated l, in.	Basin Test l Average, in.	Basin Test l Std. Dev., in.	Morning Mid-slab Crack l Average, in.	Morning Mid-slab Crack l Std. Dev., in.	Morning Edge Crack l Average, in.	Morning Edge Crack l Std. Dev., in.	Afternoon Mid-slab Crack l Average, in.	Afternoon Mid-slab Crack l Std. Dev., in.	Afternoon Edge Crack l Average, in.	Afternoon Edge Crack l Std. Dev., in.
IL-1	5.4	490	10.1	200	39.2	40	9	30	5	27	4	35	5	32	4
IL-2	5.7	578	8.8	200	35.9	37	7	25	3	24	5	28	2	25	5
IL-3	4.9	602	8.3	200	33.1	38	5	35	3	39	3	38	2	39	2
IL-4	4.3	472	9.3	200	34.8	42	3	40	2	41	2	39	2	39	3
IL-5	4.9	483	8.5	200	33.7	38	6	35	4	38	7	36	2	39	4
IA-1	4.4	483	8.2	300	28.8	40	8	40	7	33	4	43	7	33	2
IA-2	4.1	509	8	250	29.1	41	5	36	4	42	2	40	2	40	1
IA-3	5.2	560	8	250	30.9	37	2	35	1	34	1	35	1	35	2
OK-1	5.8	478	9.2	250	35.2	35	4	24	4	25	3	23	4	24	4
OK-2	6.6	573	9.2	250	36.4	40	6	31	3	29	4	31	3	30	4
OK-3	5.2	497	10.3	300	35.6	41	6	37	6	32	5	37	5	35	5
OK-4	6.4	475	9.4	250	36.7	33	8	24	3	26	5	29	3	25	3
OK-5	3.3	482	10.1	250	32.8	34	8	24	1	27	2	26	1	27	2
OR-1	3.6	528	12.4	200	41.4	38	8	33	4	32	2	na	na	na	na
OR-2	4.3	484	10.2	300	33.7	38	8	31	5	30	3	32	6	31	3
OR-3	4.7	448	7.6	200	30.6	35	8	29	3	32	6	na	na	na	na
PA-1	4.2	483	9.2	200	34.4	25	3	20	2	20	2	20	1	na	na
PA-2	4.9	545	9.4	300	32.8	42	12	28	5	23	2	37	10	26	4
WI-1	5.6	663	8.4	300	31.2	26	5	25	2	24	2	24	2	26	3
WI-2	4.5	487	10.2	300	34.1	34	5	33	3	33	8	34	4	30	4
WI-3	3.9	447	10.2	300	32.9	30	4	27	2	30	3	33	4	28	2
WI-4	5.1	633	10.6	300	36.2	38	7	27	3	31	4	35	3	27	4
WI-5	5.3	517	7.9	300	29.4	35	5	28	2	28	2	37	9	30	4
Average	4.9	518.1	9.3	252.2	33.9	36.4	6.2	30.3	3.3	30.4	3.5	33.0	3.7	31.1	3.3
Std Dev	0.8	58.2	1.1	43.9	3.1	4.6	2.3	5.5	1.5	5.8	1.8	6.0	2.5	5.3	1.1
Maximum	6.6	663.0	12.4	300.0	41.4	42.0	12.0	40.0	7.0	42.0	8.0	43.0	10.0	40.0	5.0
Minimum	3.3	447.0	7.6	200.0	28.8	25.0	2.0	20.0	1.0	20.0	1.0	20.0	1.0	24.0	1.0

Notes:

1. l = radius of relative stiffness (RRS)
2. Values of concrete modulus of elasticity and average splitting tensile strength were measured using cores obtained during field testing.

(6.89 kPa = 1 psi) (0.27 MPa/m = 1 pci) (25.4 mm = 1 in.)

Table 2. Summary of key data elements (continued).

Test Section ID	% Change in Mid-Slab Crack l from Morn. to Afternoon	Mid-Slab Crack l as % of Basin l (morning)	Mid-Slab Crack l as % of Basin l (afternoon)	% Change in Edge Crack l from Morn. to Afternoon	Edge Crack l as % of Basin l (morning)	Edge Crack l as % of Basin l (afternoon)	Load Transfer Efficiency at Cracks (Edge), %	Morning Mid-Depth Temp., F	Afternoon Mid-Depth Temp., F	Average Morning Crk Width, .01 mm	Average Afternoon Crk Width, .01 mm	Average Unit Length Change,per F (midslab temp.) (*0.000001)	No. of Cracks Included in Crack Width Study	Measured Coeff. of Thermal Expansion, 0.000001 in./in./F
IL-1	17	75	88	19	68	80	92	44	58	22	16	3.9	28	4.48
IL-2	12	68	76	4	65	68	83	58	73	55	44	6.7	28	4.87
IL-3	9	92	100	0	103	103	94	na	na	48	42	na	25	5.28
IL-4	-3	95	93	-5	98	93	95	64	76	35	27	9.4	43	5.2
IL-5	3	92	95	3	100	103	94	62	75	29	22	6.2	35	4.14
IA-1	8	100	108	0	83	83	93	67	81	46	37	3.2	15	4.29
IA-2	11	88	98	-5	102	98	95	57	73	20	14	2.3	19	4.74
IA-3	0	95	95	3	92	95	93	65	72	47	34	17.7	29	5.22
OK-1	-4	69	66	-4	71	69	88	65	82	63	44	3.7	10	4.94
OK-2	0	78	78	3	73	75	89	42	54	48	38	7.7	28	4.73
OK-3	0	90	90	9	78	85	93	61	78	54	44	3.7	19	3.98
OK-4	21	73	88	-4	79	76	76	40	54	76	70	2.4	17	4.86
OK-5	8	71	76	0	79	79	88	42	47	45	39	5.9	15	7.4
OR-1	na	87	na	na	84	na	93	50	53	31	na	na	21	4.91
OR-2	3	82	84	3	79	82	92	48	53	20	20	na	20	4.83
OR-3	na	83	na	na	91	na	93	49	50	84	na	na	18	4.22
PA-1	0	80	80	na	80	na	86	43	44	155	na	na	19	4.68
PA-2	32	67	88	13	55	62	92	47	58	216	211	3.6	24	4.1
WI-1	-4	96	92	8	92	100	86	55	68	91	69	14.4	26	5.59
WI-2	3	97	100	-9	97	88	92	57	60	58	27	outlier	35	5.67
WI-3	22	90	110	-7	100	93	91	53	64	54	41	11.2	29	5.25
WI-4	30	71	92	-13	82	71	94	50	67	63	45	8.0	23	5.03
WI-5	32	80	106	7	80	86	91	48	64	45	28	9.8	28	4.49
Average	9.5	83.3	90.5	1.3	83.9	84.3				61.1	45.6	7.0	24	4.9
Std Dev	11.8	10.6	11.3	7.7	12.9	12.1				44.4	41.6	4.4	8	0.7
Maximum	32.1	100.0	110.0	18.5	102.6	102.6				216.0	211.0	17.7	43	7.4
Minimum	-4.2	66.7	65.7	-12.9	54.8	61.9				20.0	14.0	2.3	10	4.0

Notes:

1. l = radius of relative stiffness (RRS)
2. Value of concrete coefficient of thermal expansion was measured using a core obtained during field testing.

(0.6°C = 1°F) (25.4 mm = 1 in.) (1.8 mm/mm/°C = 1 in/in/°F)

Table 2. Summary of key data elements (continued).

Test Section ID	Average Depth of Cover Over Steel, in.	Steel Corrossion Level (4 cores)	Average Crack Spacing, feet	Std. Dev. Crack Spacing, feet	Average IRI, in./mile	Terminal Joint Distress Level	No. of Trans. Cracks			Longitud. Cracking Amount, ft & Severity	No. of Patches & Severity	No. of Punchouts & Severity	No. of Miles Visually Surveyed	Total No. of Ptches & Punchouts	Total No. of Ptches & Punchouts per Mile
							Low Severity	Moderate Severity	High Severity						
IL-1	5.1	none	5.1	3.51	93	none	178	0	0	0	0	0	5	0	0.0
IL-2	2.2	1spot	4.22	2.66	127	low	9	221	5	60H	4AC(M),3PCC(L)	0	5	62	12.4
IL-3	3.9	1spt/3sprd	3.58	2.1	152	medium	6	264	5	0	1AC(M),1PCC(L)	0	5	14	2.8
IL-4	3	2spt/2sprd	2.13	1.17	157	medium	9	463	0	0	0	0	5	9	1.8
IL-5	3.2	2spt/2sprd	3.02	2.11	141	none	344	12	0	0	0	0	3	3	1.0
IA-1	4.2	1spt/1sprd	5.89	3.87	72	medium	24	144	0	343L	0	0	5	0	0.0
IA-2	3.1	2spt/2sprd	2.98	2.24	82	medium	35	420	0	4L,49M,14H	1AC(L)	0	5	18	3.6
IA-3	3.2	3spt/1sprd	2.98	1.76	118	none	16	423	0	0	0	0	5	16	3.2
OK-1	3.9	3spt/1sprd	8.44	5.78	53	none	0	124	0	0	0	0	3	1	0.3
OK-2	4.5	1spt	4.57	3.37	na	medium	27	201	1	0	0	0	na	na	na
OK-3	4.8	none	4.75	2.99	74	none	14	210	0	0	0	0	4	0	0.0
OK-4	4.1	4spt	6.36	3.21	na	none	2	130	7	0	0	1L	na	na	na
OK-5	4.6	none	6.13	3.36	50	none	108	48	0	0	0	0	4	2	0.5
OR-1	7.5	none	4.02	2.1	na	low	4	301	0	0	0	0	na	na	na
OR-2	4	none	5.6	3.09	na	low	21	274	0	18L	0	0	na	na	na
OR-3	2.8	none	4.43	2.72	na	low	0	225	0	40M	0	0	na	na	na
PA-1	3.4	2sprd	4.8	2.67	75	low	0	238	84	0	0	0	5	0	0.0
PA-2	2.7	4sprd	4.32	2.47	75	medium	0	256	0	20M	1PCC(L),Map Crk.	3L	5	53	10.6
WI-1	2.8	na	2.88	2.27	112	medium	0	259	0	76L,70M	84AC(L)	0	5	31	6.2
WI-2	4.3	na	2.9	1.42	97	none	30	314	0	0	0	0	5	0	0.0
WI-3	4	na	3.46	1.59	81	low	129	164	0	25L	0	0	5	4	0.8
WI-4	4.8	4sprd	4.58	2.22	126	na	33	192	0	0	1PCC(L)	0	5	7	1.4
WI-5	2.6	4sprd	3.38	1.86	93	medium	14	291	0	416M,249H	11AC(L),13PCC(L)	0	5	107	21.4
Average	3.9		4.4	2.6	98.8										
Std Dev	1.1		1.4	1.0	32.3										
Maximum	7.5		8.4	5.8	157.0										
Minimum	2.2		2.1	1.2	50.0										

Notes:

1. spt = spot corrossion of steel bar
2. sprd = spread corrossion of steel bar
3. Severity levels - L = low; M = moderate; H = high
4. Patching data includes both partial and full depth patching

(25.4 mm = 1 in) (0.305 m = 1 ft) (15.8 mm/km = 1 in/mi) (1.61 km = 1 mi)

Table 3. Estimated PSI values.
(0.305 m = 1 ft) (15.8 mm/km = 1 in/mi)

Test Section ID	Age as of Fall 1991 Testing, years	Average Crack Spacing, feet	Average IRI, in/mi	PSI Using TRDF Equation	PSI Using World Bank Equation	Average Estimated PSI	State Reported 1990 PSI
IL-1	0.3	5.10	93	3.54	3.82	3.68	N/A
IL-2	15	4.22	127	3.29	3.47	3.38	3.60
IL-3	20	3.58	152	3.15	3.23	3.19	N/A
IL-4	20	2.13	157	3.13	3.18	3.15	3.30
IL-5	5	3.02	141	3.21	3.33	3.27	N/A
IA-1	20	5.89	72	3.74	4.06	3.90	3.90
IA-2	22	2.98	82	3.63	3.95	3.79	3.40
IA-3	15	2.98	118	3.35	3.56	3.45	3.30
OK-1	4	8.44	53	3.97	4.29	4.13	N/A
OK-3	3	4.75	74	3.71	4.04	3.88	N/A
OK-5	2	6.13	50	4.02	4.33	4.17	N/A
PA-1	15	4.80	75	3.70	4.03	3.87	N/A
PA-2	22	4.32	75	3.70	4.03	3.87	N/A
WI-1	18	2.88	112	3.39	3.62	3.51	2.50
WI-2	6	2.90	97	3.50	3.78	3.64	4.80
WI-3	7	3.46	81	3.64	3.96	3.80	3.90
WI-4	7	4.58	126	3.30	3.48	3.39	3.40
WI-5	16	3.38	93	3.54	3.82	3.68	4.00
Average	12.1	4.2	98.8	3.5	3.8	3.7	3.6
Std. Dev.	7.6	1.5	32.3	0.3	0.3	0.3	0.6
Maximum	22	8.4	157.0	4.0	4.3	4.2	4.8
Minimum	0.3	2.1	50.0	3.1	3.2	3.2	2.5

The effects of age on the estimated PSI are shown in figure 2. Age does not appear to have a direct relationship to PSI. This is reasonable as these pavements are part of the primary highway system and as such are maintained to ensure an acceptable level of service at "all" times. Similar trends have been observed at other CRC pavement sites. This is one of the reasons that ride quality and PSI (based primarily on ride quality) are not good indicators of CRC pavement performance. Several agencies, therefore, use number of failures (punchouts and patches) as an indicator of CRC pavement performance.

Terminal Joints

The use of lug anchors and wide flange beam terminal joints was equally divided. However, most of the sections using lug anchor joints were older than 15 years (10 sections). Similarly, most of the sections using wide flange beam joints were 7 years old or younger (10 sections). This indicates that the current trend is to use wide flange beams as terminal joints. Wide flange beam joints generally exhibited less distress such as spalling and faulting - primarily because of the young ages.

Deflections Under Load

Average Sensor 1 deflections (maximum deflection under the load plate) ranged from a low of 0.048 mm (1.9 mils) to a high of 0.137 mm (5.4 mils) under the 40.03 kN (9,000 lb) FWD load for the basin (interior) testing. The deflection values are, of course, affected by slab thickness and base/subgrade support. The deflections and the subsequent backcalculated pavement stiffness characteristics therefore represent the conditions at the time of testing only.

The deflections measured at the transverse crack along the mid-slab location were generally comparable to the basin deflections generally measured between crack locations. However, edge deflections measured at transverse crack locations tended to be almost twice as much as the basin (or mid-slab crack location) deflections for the morning testing (upward slab curl along the edges). The edge deflections tended to be less for the afternoon testing but still considerably larger than basin test deflections. The afternoon edge deflections were reduced by about 10 to 30 percent from the morning edge deflections. Figure 3 shows a comparison of edge and mid-slab deflections at crack locations with basin test deflections. The tied-concrete shoulders do not appear to have contributed much to reducing edge deflections.

Also, the change in edge deflection between morning and afternoon testing does not appear to have been affected much by slab support condition - firm support such as LCB, ATB, or CTB versus softer support provided by granular or permeable bases. The edge versus basin deflections are illustrated in table 4 which also contain data on shoulder type and base type.

Loss of Support Analysis

Loss of support analysis was performed using the data from deflection testing along the edge locations. At each test location, FWD loads of 40.03, 53.38, and 71.17 kN (9,000,

Table 4. Edge versus basin deflections.

Test Section ID	Age as of Fall 1991 Testing, years	Subgrade Type (AASHTO)	Long. Steel Amount, %	Maximum Deflection , 0.001 in. Basin Basin Testing Average	Maximum Deflection , 0.001 in. Basin Basin Testing Average	Edge Deflection as % of Basin Defl. (afternoon)	Outside Shoulder Type	Base Type	Average Crack Spacing, feet	No. of Trans. Cracks Mod/High Severity
IL-1	0.3	A-7-6	0.7	2.2	3.8	173	pcc	perm. ctb	5.1	0
IL-2	15	A-6	0.59	4.3	10.9	253	ac	ctb	4.22	231
IL-3	20	A-7-5	0.6	4.9	9.3	190	ac	atb	3.58	274
IL-4	20	A-7-5	0.6	3.9	6.9	177	ac	atb	2.13	463
IL-5	5	A-7-5	0.7	4.4	6.6	150	pcc	lcb	3.02	12
IA-1	20	A-2-6	0.65	4.1	5.3	129	ac	ctb	5.89	144
IA-2	22	A-6	0.65	5	9.6	192	ac	atb	2.98	420
IA-3	15	A-6	0.65	4.2	9.1	217	pcc	atb	2.98	423
OK-1	4	A-6	0.5	2.7	5.3	196	pcc	atb	8.44	124
OK-2	5	A-6	0.5	2.7	3.7	137	pcc	atb	4.57	203
OK-3	3	A-4	0.5	2.9	4.6	159	pcc	atb	4.75	210
OK-4	7	A-6	0.5	3	7.7	257	pcc	soil-asphalt	6.36	144
OK-5	2	A-2-6	0.61	3	4.3	143	pcc	perm. ctb	6.13	48
OR-1	7	A-4	0.6	2.7	na	na	ac	granular	4.02	301
OR-2	4	A-4	0.6	1.9	3.5	184	ac	ctb	5.6	274
OR-3	20	A-6	0.54	4.7	na	na	ac	ctb	4.43	225
PA-1	15	A-2-4	0.45	2.2	na	na	ac	granular	4.8	406
PA-2	22	A-2-4	0.55	5.3	5.8	109	pcc	granular	4.32	256
WI-1	18	A-2-4	0.65	2.8	4.4	157	ac	granular	2.88	259
WI-2	6	A-2-4	0.67	2.8	5.4	193	pcc	granular	2.9	314
WI-3	7	A-2-7	0.67	2.7	4.4	163	pcc	granular	3.46	164
WI-4	7	A-2-6	0.67	3.2	5.1	159	pcc	granular	4.58	192
WI-5	16	A-2-6	0.61	5.4	6.4	119	ac	granular	3.38	291
Average	11.3		0.6	3.5	6.1	172.9			4.4	
Std Dev	7.4		0.1	1.1	2.2	39.4			1.4	
Maximum	22.0		0.7	5.4	10.9	256.7			8.4	
Minimum	0.3		0.5	1.9	3.5	109.4			2.1	

(0.305 m = 1 ft)

12,000, and 15,000 lb) were used. The maximum deflections at each of the 3 load levels were used to extrapolate loss of support conditions along the edge. Figure 4 illustrates the procedure used to estimate the loss of support, which is equal to the "apparent" deflection at zero load. Table 5 presents the loss of support values for each section using the average maximum deflection values for each load level. It is seen that most of the sections do exhibit some loss of support both during the morning and the afternoon testing. The loss of support for the afternoon testing tended to be slightly lower. The data also indicate that for some unexplainable reasons, WI-4 section exhibited very high loss of support during the morning testing which is also reflected in the high deflections measured along the edges during the morning testing.

The net loss of support, the difference in loss of support between early morning and late afternoon testing, provides an indication of the "permanent" loss of support due of moisture warping and base consolidation. Net loss of support in excess of 2 mils (0.002 in) should be considered a cause of concern, with regards to induced concrete flexural stresses under loading and with regards to potential for pumping.

There does not appear to be any significant influence of shoulder type or base type on the magnitudes of the loss of support. However, it should be noted that the data are confounded by actual temperature conditions and pavement thicknesses at each site.

Overall Pavement Stiffness

For concrete pavements, the overall pavement stiffness can be described very effectively using the radius of relative stiffness (RRS), ℓ, value. The ℓ value is an important structural parameter of concrete pavements and has a direct influence on pavement behavior (structural response). The RRS was estimated for each section using the theoretical formula and using the actual slab thickness (average core thickness), laboratory measured modulus of elasticity value, and best estimate of the modulus of subgrade reaction. The RRS values were also backcalculated from the deflection testing using Program ILLI-BACK. These RRS values are presented in table 2. Figure 2 shows a comparison of the estimated RRS and RRS based on the basin (interior) testing. Figure 3 shows a comparison of RRS values from mid-slab and edge testing at transverse crack locations with basin test RRS values. The following is a summary of the comparison of the RRS values:

- For basin testing, the backcalculated RRS values were independent of load levels which ranged from about 40.03 kN (9,000 lb) to about 53.38 kN (16,000 lb). Thus, a single load level of 40.03 kN (9,000 lb) is considered adequate for CRCP basin testing. However, multiple load levels should be used for testing along the pavement edge if loss of support determination is desired.

- RRS values for testing at crack locations were generally lower than those along basin (non-crack) locations.

Table 5. Loss of support along edges.

Test Section ID	Age as of Fall 1991 Testing, years	Subgrade Type (AASHTO)	Base Type	Outside Shoulder Type	Average Core Thickness, in.	Average Crack Spacing, feet	Loss of Support Morning, 0.001 in.	Loss of Support Afternoon, 0.001 in.	Net Loss of Support, 0.001 in.
IL-1	0.3	A-7-6	perm. ctb	pcc	10.1	5.1	0.3	0	0.3
IL-2	15	A-6	ctb	ac	8.8	4.22	1.2	0.3	0.9
IL-3	20	A-7-5	atb	ac	8.3	3.58	0	0	0
IL-4	20	A-7-5	atb	ac	9.3	2.13	0.2	0.1	0.1
IL-5	5	A-7-5	lcb	pcc	8.5	3.02	1.5	0.3	1.2
IA-1	20	A-2-6	ctb	ac	8.2	5.89	1.2	0.6	0.6
IA-2	22	A-6	atb	ac	8	2.98	1.8	0.2	1.6
IA-3	15	A-6	atb	pcc	8	2.98	0	0	0
OK-1	4	A-6	atb	pcc	9.2	8.44	0	0.2	-0.2
OK-2	5	A-6	atb	pcc	9.2	4.57	0	0	0
OK-3	3	A-4	atb	pcc	10.3	4.75	0.5	0.1	0.4
OK-4	7	A-6	soil-asphalt	pcc	9.4	6.36	1.1	0.5	0.6
OK-5	2	A-2-6	perm. ctb	pcc	10.1	6.13	0	0	0
OR-1	7	A-4	granular	ac	12.4	4.02	0.4	na	na
OR-2	4	A-4	ctb	ac	10.2	5.6	0.4	0.2	0.2
OR-3	20	A-6	ctb	ac	7.6	4.43	1	na	na
PA-1	15	A-2-4	granular	ac	9.2	4.8	0.2	na	na
PA-2	22	A-2-4	granular	pcc	9.4	4.32	0.1	0	0.1
WI-1	18	A-2-4	granular	ac	8.4	2.88	0.6	0.4	0.2
WI-2	6	A-2-4	granular	pcc	10.2	2.9	2.1	0.6	1.5
WI-3	7	A-2-7	granular	pcc	10.2	3.46	1.4	0	1.4
WI-4	7	A-2-6	granular	pcc	10.6	4.58	7.2	0.2	7
WI-5	16	A-2-6	granular	ac	7.9	3.38	0.7	0.4	0.3
Average	11.3				9.3	4.4	1.0	0.2	0.8
Std Dev	7.4				1.1	1.4	1.5	0.2	1.6
Maximum	22.0				12.4	8.4	7.2	0.6	7.0
Minimum	0.3				7.6	2.1	0.0	0.0	-0.2

Notes:

1. Negative loss of support values were considered to be zero.
2. Loss of support values determined from average of maximum deflections at each of 3 load levels.

(25.4 mm = 1 in.) (0.305 m = 1 ft) (0.0254 mm = 1 mil)

- The estimated RRS values compared well with the basin RRS values. However, the estimated RRS values are somewhat dependent upon the modulus of subgrade reaction values used.

- There was some increase in RRS values for mid-slab crack location from morning to afternoon testing. However, there was very little increase in the edge crack location RRS values from morning to afternoon testing even though actual deflection values were lower.

- The crack location RRS values for edge testing were only slightly lower than for the mid-slab testing. However, this decrease was not at all "proportional" to the difference in magnitudes of deflections at the mid-slab and edge locations. It should be noted that the RRS values computed for the edge testing are "effective" or equivalent values as no allowance was made in the backcalculation analysis for edge boundary conditions. It appears that the normalized deflection basin areas for edge testing are similar to the normalized deflection basin areas for the mid-slab testing, thus compensating for the high deflection values measured for edge testing. The backcalculated RRS values are determined using the normalized deflection basins.

- The use of concrete shoulder appears to have mixed effect on the backcalculated RRS values. The IL-5, IA-3, and WI-3 sections exhibited edge crack test RRS values almost equal to the basin test RRS. However, all five Oklahoma test sections, IL-1, and WI-4 exhibited much lower RRS values for the edge crack testing compared to the basin testing RRS values. Thus, it appears that concrete shoulders may not be very effective in all cases for structural strengthening of the mainline CRC pavements. The use of concrete shoulder may still be strongly desired for other reasons such as maintenance-free shoulder, effective joint sealing, etc.

  It appears that the most effective way to strengthen the mainline CRC pavement along the edge is to use widened lanes which eliminate much of the free-edge loading conditions. The widened lanes may be used more effectively with tied-concrete shoulders.

The deflection test data were further analyzed to backcalculate the modulus of subgrade reaction, k, and the slab rigidity, D. The relationship between RRS, k, and D is as follows:

$$RRS = (D/k)^{0.25} \quad (5)$$

and

$$D = (Eh^3/12(1 - \mu^2)) \quad (6)$$

where: E = concrete modulus of elasticity

h	=	slab thickness
μ	=	concrete Poisson's ratio

While the RRS term describes the overall stiffness of the total pavement system, the D term describes the rigidity of the concrete slab only. As discussed above, the RRS values along the slab edge were very similar to the values at the mid-slab locations. The explanation for this behavior is as follows:

Given: $RRS(edge) = (D_{edge}/k_{edge})^{0.25}$

Assume: $k_{edge} = 0.5\ k_{interior}$ (slab curling effects)

$D_{edge} = 0.5\ D_{interior}$ (slab edge boundary condition)

Then:
$$RRS(edge) = (0.5\ D_{interior}/0.5\ k_{interior})^{0.25}$$
$$= (D_{interior}/k_{interior})^{0.25}$$
$$= RRS_{interior}$$

Thus, RRS is not a good descriptor for evaluating the slab integrity along the edge.

The modulus of subgrade reaction (backcalculated using Program ILLI-SLAB) and D values are given in table 2. The following is a summary of the average values for the various parameters for all 23 test sections.

	Average Values		
	ℓ, mm (in)	k, MPa/m (pci)	D, kN-m (million lb-in^3)
Basin Testing	914 (36)	81 (300)	546,000 (480)
Mid-Slab Crack Testing			
Morning Testing	762 (30)	103 (380)	341,000 (300)
Afternoon Testing	838 (33)	92 (340)	391,000 (344)
Edge Crack Testing			
Morning Testing	762 (30)	54 (200)	171,000 (150)
Afternoon Testing	787 (31)	62 (230)	216,000 (190)

Thus, it is seen that the effective k values along the edges are about 60 to 70 percent of the values for the mid-slab locations and that the D values along the edge are about 30 to 60 percent of the values for the mid-slab locations. The basin testing (uncracked locations) resulted in the highest D values. These trends in k and D values are what one would expect and appear to be more descriptive of the actual physical condition (edge) of the pavement system. It is also likely that the backcalculated D value would be much lower at those edge locations that exhibit the beginning of a punchout or exhibit wide cracks. Thus, it is recommended that the D and k values be used in interpreting the results of edge testing, in addition to the use of RRS.

A review of the D values indicate that the tied-concrete shoulder did not contribute to the rigidity of the mainline slab as the ratios of edge D to the mid-slab D values are very similar for sections with tied-concrete shoulder and sections without tied-concrete shoulder.

Crack Spacing Analysis

The average crack spacings for each site are shown in figure 7. During the study, it was realized that a good method for characterizing the cracking pattern for CRC pavements did not exist. In the past use has been made of the cumulative frequency distributions for representing the total number of cracks that have spacings equal to or less than the designated crack spacing. This is certainly a good method providing a clear visual description of the cracking pattern. The cumulative frequency plots for each of the test sections are given in figure 8. These plots are arranged by States. These plots can be used to identify the number of cracks (by percent) that are greater than or less than the designated crack spacing. A summary of the cumulative frequency plot data is presented later in this section.

The cumulative frequency plots of the type presented in figure 8 do not, however, represent the true picture of the cracking pattern as the focus of these plots is the number of cracks. A more representative characterization is the cumulative frequency based on the length of paving exhibiting a designated crack spacing. Thus, as an example, if 40 percent of the cracks (by number) have crack spacing equal to or less than 0.9 m (3 ft), the length of paving exhibiting crack spacing equal to or less than 0.9 m (3 ft) may be only 20 percent or less. Similarly, if 10 percent of the cracks (by number) have crack spacing greater than 3.0 m (10 ft), the length of paving exhibiting crack spacing greater than 3.0 m (10 ft) may exceed 20 percent. It is the length of paving that exhibits a certain cracking pattern that is equally important (if not more important) than the number of cracks that exhibit a certain cracking pattern. The cumulative frequency plots based on length of paving are given in figure 9.

Table 6 shows a comparison of the crack spacing characterization using the frequency distributions based on the number of cracks and the length of paving involved. The length of paving definition appears to be more descriptive. For cluster cracking, it indicates the potential for cluster cracking related problems based on the amount (by length) of cracking that is less than 0.9 m (3 ft). It also clearly indicates the length of paving that incorporates undesirable longer crack spacing, in excess of 3.0 m (10 ft). A concern with longer spaced cracks is the development of crack spalls, steel rupture, and punchout at companion closely spaced cracks. These problem items are also better characterized by the number of crack locations where these problems may develop in the future. Thus, for problem cluster cracking, the involved length of paving is more significant than the number of cracks. For longer spaced cracks, it is the number of cracks that is more significant than the involved length of paving.

From table 6, the following can be ascertained:

1. IL-1 has a large number of cracks having spacings in excess of 3.0 m (10 ft). However, this section was only a few months old and had not yet gone through a winter cycle.

Table 6. Crack spacing distributions.

Test Section ID	Route	Age as of Fall 1991 Testing, years	Base Type	Outside Shoulder Type	Long. Steel Amount, %	Basin Test I Average in.	Total No. of Cracks (1,000 ft)	% of Cracks = or < 3 ft Spacing (by no.)	% Length with Cracks = or < 3 ft Spacing	% of Cracks > 6 ft Spacing (by no.)	% Length with Cracks > 6 ft Spacing	% of Cracks > 10 ft Spacing (by no.)	% Length with Cracks > 10 ft Spacing	No. of Patches & Severity	No. of Punchouts & Severity
IL-1	US51	0.3	perm. ctb	pcc	0.7	40	195	37	16	33	60	9	25	0	0
IL-2	I72	15	ctb	ac	0.59	37	237	45	22	23	43	3	7	4AC(M),3PCC(L)	0
IL-3	US36	20	atb	ac	0.6	38	279	51	30	10	21	1	1	1AC(M),1PCC(L)	0
IL-4	I55	20	atb	ac	0.6	42	470	86	79	1	2	0	0	0	0
IL-5	US50	5	lcb	pcc	0.7	38	329	67	44	10	25	0	0	0	0
IA-1	I29	20	ctb	ac	0.65	40	169	33	10	49	73	15	27	0	0
IA-2	I80	22	atb	ac	0.65	41	336	65	40	8	23	2	8	1AC(L)	0
IA-3	I380	15	atb	pcc	0.65	37	334	61	41	6	10	0	0	0	0
OK-1	I40	4	atb	pcc	0.5	35	118	28	5	58	88	43	73	0	0
OK-2	US69	5	atb	pcc	0.5	40	217	40	18	25	50	8	21	0	0
OK-3	I35	3	atb	pcc	0.5	41	210	36	16	29	52	7	17	0	0
OK-4	US69	7	soil-asphalt	pcc	0.5	33	156	15	5	51	72	13	25	0	1L
OK-5	I40	2	perm. ctb	pcc	0.61	34	164	24	9	45	67	13	26	0	0
OR-1	I5	7	granular	ac	0.6	38	248	36	18	12	23	1	1	0	0
OR-2	I5	4	ctb	ac	0.6	38	179	25	10	34	53	8	20	0	0
OR-3	I205	20	ctb	ac	0.54	35	227	41	21	23	43	3	9	0	0
PA-1	I180	15	granular	ac	0.45	25	208	33	15	28	47	3	7	0	0
PA-2	I81	22	granular	pcc	0.55	42	231	39	20	20	38	2	6	1PCC(L),Map Crack.	3L
WI-1	I43	18	granular	ac	0.65	26	347	69	38	9	25	1	2	84AC(L)	0
WI-2	I90	6	granular	pcc	0.67	34	345	68	52	2	6	0	0	0	0
WI-3	I90/94	7	granular	pcc	0.67	30	288	48	32	5	10	0	0	0	0
WI-4	I90/94	7	granular	pcc	0.67	38	218	34	17	25	41	0	0	1PCC(L)	0
WI-5	I90/94	16	granular	ac	0.61	35	295	54	34	7	14	0	0	11AC(L),13PCC(L)	0
Average		11.3			0.6	36.4	252	45	26	22	39	6	12		
Std Dev		7.4			0.1	4.6	82	18	18	17	24	9	17		
Maximum		22.0			0.7	42.0	470	86	79	58	88	43	73		
Minimum		0.3			0.5	25.0	118	15	5	1	2	0	0		

Notes:

1. spt = spot corrossion of steel bar
2. sprd = spread corrossion of steel bar
3. Severity levels - L = low; M = moderate; H = high
4. Patching data includes both partial and full depth patching

(25.4 mm = 1 in) (0.305 m = 1 ft)

2. IL-4, IL-5, IA-2, IA-3, and WI-2 have more than 40 percent length exhibiting crack spacing equal to or less than 0.9 m (3 ft).

3. IA-1, IL-1, all Oklahoma sections, and OR-2 have more than 50 percent length exhibiting crack spacing in excess of 1.8 m (6 ft).

4. IA-1, IL-1, all Oklahoma sections, and OR-2 also have more than 15 percent length exhibiting crack spacing in excess of 3.0 m (10 ft). OK-1 has 73 percent length exhibiting crack spacing in excess of 3.0 m (10 ft). The large incidence of larger crack spacings can only be considered as potential problem areas (except for IL-1 as it can be expected to develop a more normal crack spacing pattern with time).

5. It is not clear why IA-1 (20 years age), OK-1 (4 years age), and OR-2 (4 years age) have comparatively different cracking patterns (compared to other in-state test sections). It appears that construction time concrete placement conditions may have influenced the cracking pattern, for lack of any other identifiable cause. However, the placement conditions generally affect only the early crack spacing pattern as the crack spacing tends to stabilize after several cold season (winter) periods. IA-1 and OK-1 did have CTB layers.

6. The larger crack spacings for OK-1, OK-2, OK-3, and OK-4 are due to the use of lower steel amount (0.5 percent).

7. The two sections with permeable bases (IL-1 and OK-5) did have higher amounts of cracks with longer spacings. It is not clear if this is a real trend as the data are confounded by age (newer pavements).

8. The use of epoxy-coated reinforcing bars did not appear to have any effect on the overall cracking pattern.

9. The older pavements (over 15 years old) generally had very few or no cracks with spacings in excess of 3.0 m (10 ft).

10. The Illinois and Wisconsin sections had very few or no cracks with spacings in excess of 3.0 m (10 ft), irrespective of age, thickness, and other design features.

In order to relate the crack spacing to the structural response of the pavements, the concept of the average of several closest crack spacings was developed. The crack spacing pattern for IA-1 is shown in figure 10, based on individual crack spacing. This type of pattern is very difficult to relate to structural response that is provided by the effective length (or area) of the CRC pavement. The effective length is generally considered to be about 1.5 to 2.0 times the RRS value on each side of the applied load - about 1.2 to 1.8 m (4 to 6 ft) on each side of the load. Thus, it was necessary to develop a different way to represent the crack

spacing pattern that would incorporate better the effective length of the pavement. The concept that was developed was to use the average spacing of a certain number of closest cracks.

Figure 11 shows a comparison of the average crack spacings based on 3 and 5 closest cracks. The cracking patterns are very similar and more importantly do not exhibit the random pattern shown in figure 11. Because a large number of projects exhibit very small crack spacings (< 0.6 m (2 ft)), it was decided to use the average spacing of the closest five cracks (ASCFC) to characterize the cracking pattern for evaluation of structural response due to loading.

The plot of the ASCFC with distance is also useful in identifying locations of cluster cracking (groups of cracks with average spacing of less than about 0.6 m (2 ft)). Similarly, cracking patterns with large crack spacings can also be easily identified (e.g., at OK-1 where ASCFC exceeded 3.0 m (10 ft) at several locations). The ASCFC trends provide a more visual definition of crack spacing pattern than use of the standard deviation or the coefficient of variation parameters. The ASCFC plot (with distance) can also be used to identify the extent of a pavement section that exhibits "acceptable" cracking pattern. For example, if acceptable values of ASCFC are assumed to be between 0.9 and 1.8 m (3 and 6 ft), then as shown in figure 12, the length of the pavement section outside the acceptable limits can be easily identified. It is possible that this length can be used as a performance indicator and compared with the extent of other manifested distresses such as punchout/patching, ride quality, etc.

The RRS values were compared with crack spacing for each test section. The plot of basin test RRS values along side the average spacing of five closest cracks indicate that pavement stiffness is not very dependent on crack spacing as long as there is high load transfer efficiency at the transverse cracks. The load transfer effectiveness was generally greater than 90 percent for most of the test sections. However, there appears to be some interaction between cluster cracking (average crack spacing of less than 0.6 m (2 ft)) and RRS. The RRS in many instances were lower for lower average crack spacing especially for the older test sections.

Overall, the variability in the RRS values along the test section appears to be more influenced by the "apparent" variability in the support condition. The extent of variability does not appear to be influenced by the base type (stabilized versus granular) nor by the subgrade type (fine-grained versus coarse-grained).

The effect of the following design features on crack spacing development was evaluated:

- Thickness.
- Tied-concrete shoulder.
- Permeable base.
- Epoxy coated bars.

Thickness Effects

Figure 13 shows the average crack spacing categorized by concrete thickness - less than 254 mm (10 in) and equal to or greater than 254 mm (10 in). No clear trends are apparent. The data are also confounded by age, percent steel, and climatic region.

Tied-Concrete Shoulder Effects

Figure 13 shows the average crack spacing categorized by outside shoulder type - AC or PCC shoulder. No definitive trends are apparent. The data are also confounded by age, percent steel, and climatic region.

Permeable Base Effects

Figure 13 shows the average crack spacing categorized by base layer - permeable cement treated base or non-permeable base. The two sections with permeable base did exhibit slightly higher average crack spacings. However, both of these sections were young - IL-1 was only a few months old and OK-5 was only 2 years old. Therefore, it is likely that within the next few years, these two sections would exhibit cracking patterns similar to the sections with the non-permeable CTB. One of the concerns with the use of the permeable CTB is that it may contribute to the thickness of the concrete slab through bonding which would then require use of a slightly higher steel percentage to ensure acceptable cracking pattern.

In order to further study the effect of permeable CTB, data from an additional CRC section constructed on a permeable CTB were obtained. This section was located along I-295 in Virginia (just south of Exit 9B sign, near Milepost 8). The section details are as follows:

Date Constructed: Summer/Fall 1991

Pavement Details:

- Slab thickness = 229 mm (9 in).
- Permeable CTB thickness = 102 mm (4 in).
- CTB thickness = 152 mm (6 in).
- Percent steel = 0.65 percent.
- No tubes or chairs used - concrete placed in two lifts with the steel placed at surface of bottom lift.
- Permeable CTB cement content = 131 kg/m^3 (220 lb/yd^3).
- Permeable CTB aggregate = ASTM No. 57.
- Shoulder type = jointed plain concrete.

A 305-m (1,000-ft) length of the section was surveyed on May 17, 1994. The section exhibited the following cracking pattern:

Crack Spacing, m (ft)	Percent of Cracks
0-0.3 (0-1)	9.6
0.3-0.6 (1-2)	20.8
0.6-0.9 (2-3)	29.5
0.9-1.2 (3-4)	12.8
1.2-1.5 (4-5)	10.2
1.5-1.8 (5-6)	9.7
1.8-2.1 (6-7)	4.9
2.1-2.4 (7-8)	1.6
2.4-2.7 (8-9)	0.6
2.7-3.0 (9-10)	0.3

Total number of cracks/305 m (1,000 ft) = 322
Average crack spacing = 0.95 m (3.11 ft)
Standard deviation of crack spacing = 0.54 m (1.78 ft)

The above data indicate that 3 years after construction, the crack spacing along the permeable base section exhibits acceptable cracking pattern. Most of the cracks either exhibited no distress or were of low severity. Thus, the concern that CRC pavements constructed over permeable CTB may not exhibit acceptable cracking pattern (because of "interlocking/bonding" with the permeable base) may not be justifiable. However, it should be stressed that adequate percent steel ($\geq$ 0.65 percent) should be used to minimize any potential problems related to use of the permeable CTB.

Epoxy Coated Bar Effects

Figure 13 shows the average crack spacing categorized by bar coating - epoxy coated or not epoxy coated. The three sections with epoxy-coated bars did exhibit lower average crack spacing. Although the sample size is small, it appears that the use of epoxy coated reinforcement may not result in undesirable cracking pattern. The current FHWA Technical Advisory T 5080.14, dated June 5, 1990, recommends that the bond area should be increased 15 percent to increase the bond strength between the concrete and reinforcement of epoxy-coated steel reinforcement is used. This implies that 15 percent more steel should be used if epoxy-coated bars are used. The sections with epoxy-coated bars had the following steel amounts:

OK-3 = 0.5 percent steel
WI-2 and WI-3 = 0.67 percent steel

Thus, it appears that use of 15 percent more steel bars (or increase in steel content by about 0.1 percent for the same size of steel bars) may not be warranted provided the steel content is properly estimated.

Effect of Age on Crack Spacing

The effect of age on crack spacing development is shown in figure 14. There appears to be a trend toward a decrease in crack spacing with age with crack spacing stabilizing after about 8 to 10 years. The effect of crack spacing on ride quality and estimated PSI are shown in figure 15. Crack spacing appears to have an effect on ride quality and estimated PSI. Shorter crack spacing result in higher IRI (and lower PSI) values indicating that cluster cracking does result in poorer riding surface.

Load Transfer Efficiencies at Cracks and Crack Width Analysis

Load transfer efficiencies were determined using the data from the morning and afternoon testing at crack locations. All sections, except the Oklahoma sections and WI-1 exhibited high load transfer efficiencies (> 90 percent) at crack locations. The Oklahoma sections have the widest crack spacings due to lower steel amount. This may be contributing to the development of the poor load transfer at crack locations.

Crack widths at the test section ranged from 0.20 mm to about 0.84 mm (ignoring the apparent high values noted at the two Pennsylvania sites) during the mornings. The morning slab mid-depth temperatures during crack width measurements ranged from 4.4 °C (40 °F) to about 18.3 °C (65 °F). The cracks did close a little bit during the afternoon when mid-slab temperatures increased from about -15.0 to -9.4 °C (5 to 15 °F). For each section the crack widths were normalized to mid-depth slab temperatures of 4.4 °C (40 °F) and -17.8 °C (0 °F) to allow comparisons between sites. The normalization was performed by using the laboratory measured coefficient of thermal expansion. The normalized crack width data are shown in table 7 and figure 16. These data are for the 30.5 m (100 ft) subsection used for crack width measurements and not for the full 305 m (1,000 ft) section.

As shown in table 7, the normalized crack width (at 4.4 °C (40 °F)) range from 0.24 mm at IL-1 to 1.01 mm at OK-1 and WI-1. The average normalized crack width at 4.4 °C (40 °F) is 0.59 mm. The small crack width at IL-1 is explainable in that IL-1 section was only a few months old. The large normalized crack width at OK-1 is the result of the large average crack spacing. Table 7 also indicates that IA-1 with the larger crack spacing exhibits larger normalized crack widths.

Criteria for limiting crack width for CRC pavements are presented in the AASHTO Guide based on studies performed in Texas. The maximum crack width to avoid spalling is recommended to be 1.07 mm. For the wet-freeze region test sections, using the crack width data normalized to -17.8 °C (0 °F), it is seen that IA-1, WI-1, and WI-4 are marginal with respect to the AASHTO crack width criteria. It should be noted that WI-1 also had somewhat lower load transfer efficiency at the crack locations.

Figure 17 shows the relationship between normalized crack widths and average crack spacing. No clear trend is evident as the data is confounded by concrete material type, age, and percent steel.

Table 7. Crack widths

Test Section ID	Morning Mid-Depth Temp., F	Afternoon Mid-Depth Temp., F	Average Morning Crk Width, .01 mm	Average Afternoon Crk Width, .01 mm	Average Unit Length Change,per F (midslab temp.) (*0.000001)	No. of Cracks Included in Crack Width Study	Measured Coeff. of Thermal Expansion, 0.000001 in./in./F	Normalized Crack Width at 40 F Temp at Mid-Depth 0.01 mm	Normalized Crack Width at 0 F Temp at Mid-Depth 0.01 mm
								Normalized @ 40 F	Normalized @ 0 F
IL-1	44	58	22	16	3.9	28	4.48	24	43
IL-2	58	73	55	44	6.7	28	4.87	65	86
IL-3	na	na	48	42	na	25	5.28	na	na
IL-4	64	76	35	27	9.4	43	5.2	44	59
IL-5	62	75	29	22	6.2	35	4.14	37	51
IA-1	67	81	46	37	3.2	15	4.29	70	104
IA-2	57	73	20	14	2.3	19	4.74	33	63
IA-3	65	72	47	34	17.7	29	5.22	61	83
OK-1	65	82	63	44	3.7	10	4.94	101	161
OK-2	42	54	48	38	7.7	28	4.73	49	70
OK-3	61	78	54	44	3.7	19	3.98	67	93
OK-4	40	54	76	70	2.4	17	4.86	76	111
OK-5	42	47	45	39	5.9	15	7.4	48	108
OR-1	50	53	31	na	na	21	4.91	38	67
OR-2	48	53	20	20	na	20	4.83	26	55
OR-3	49	50	84	na	na	18	4.22	90	119
PA-1	43	44	outlier	outlier	na	19	4.68	na	na
PA-2	47	58	outlier	outlier	na	24	4.1	na	na
WI-1	55	68	91	69	14.4	26	5.59	101	127
WI-2	57	60	58	27	outlier	35	5.67	66	86
WI-3	53	64	54	41	11.2	29	5.25	61	83
WI-4	50	67	63	45	8.0	23	5.03	70	96
WI-5	48	64	45	28	9.8	28	4.49	49	68
Average			49.2	36.9	7.3	24	4.9	59	87
Std Dev			19.6	15.2	4.4	8	0.7	23	29
Maximum			91.0	70.0	17.7	43	7.4	101	161
Minimum			20.0	14.0	2.3	10	4.0	24	43

(0.6 °C = 1 °F) (25.4 mm = 1 in) (1.8 mm/mm/ °C = 1 in/in/ °F)

Effect of Steel Amount

The longitudinal reinforcement has a significant influence on performance of CRC pavements. Higher amounts of reinforcement result in smaller crack spacing for a given set of conditions (concrete quality, climatic conditions). Figure 18 shows the effect of steel amount on crack spacing. Considering that the data points incorporate a broad range of pavement age, concrete quality, and climatic conditions, there is a strong overriding linkage between percent steel and crack spacing. At a steel percentage of about 0.8 percent, average crack spacing may approach about 0.6 m (2 ft) which borders on undesirable crack spacing in the presence of poor support conditions - results in a very high incidence of cluster cracking and a high potential for future punchouts when the support condition is marginal. A percent steel in the range of 0.6 to 0.7 percent appears to provide average long-term crack spacing in the range of 0.9 to 1.5 m (3 to 5 ft).

The effect of steel amount on ride quality is shown in figure 19. Again, there is a some linkage between percent steel and ride quality (IRI) considering a wide range of support (base/subgrade) conditions. This is, however, not surprising as figure 19 represents a composite of figures 15 and 18. Figure 15 showed that a smaller crack spacing provided a comparatively rougher ride. Thus, it can be concluded that a higher steel amount (percent) may lead to closer crack spacing, which would lead to comparatively poorer ride. It should be noted that the poor ride is a function of the condition of the transverse cracking and patching/punchouts. Thus, it appears that pavement distresses can be expected to be higher for sections with closely spaced transverse cracks or, as a corollary, for sections incorporating higher amounts of steel percentage for the currently used range of concrete strengths. It is possible that a different conclusion would be reached if concrete strengths used were much higher than conventionally used concrete strengths having average splitting tensile strengths in the range of 3.10 to 4.48 MPa (450 to 650 lbf/in^2) (all ages). Also, it must be pointed out that some of the European experiences indicate that close crack spacing (average crack spacing of about 0.6 m (2 ft)) due to use of steel amount of 0.85 percent can still provide excellent performance under heavy truck traffic, provided that a good support condition is constructed.

The above discussion should not be interpreted as indicating higher steel amounts are not preferable. There appears to be an optimum range of steel amount - about 0.6 to about 0.7 percent for conventionally specified concrete strengths. Smaller amounts of steel would result in larger transverse crack spacing with attendant problems of steel ruptures and more frequent punchout incidences. Similarly, larger amounts of steel would result in closely spaced transverse cracking (cluster cracking), which creates a potential for punchouts on poor base/subbase/subgrade.

During the design process, the amount of steel determined to obtain acceptable crack spacing/crack width/steel stresses is based on the assumption that the design concrete strength will be obtained. However, for a given (design) steel content, if a higher concrete strength is actually obtained, that crack spacings may be larger than anticipated. Similarly, if lower concrete strength is actually obtained during construction, then a much closer crack spacing may result. This is very important to establish especially when using marginal amount of steel

- less than 0.6 percent. The larger crack spacing may result in higher steel stress and wider cracks resulting in premature failures. Therefore, if the possibility exists that higher than specified concrete strengths may be obtained on any given project, then the prudent course would be to specify a slightly higher steel content to accommodate the expected higher concrete strength.

Based on the data obtained as part of this study, use of steel in the amount less than 0.60 percent is not recommended as the cracking pattern that develops is very marginal (as exhibited by the Oklahoma test sections). The larger crack spacings that develop as a result of low steel amount create potential locations for steel ruptures and punchouts at closely spaced cracking adjacent to widely spaced (> 3.7 m (12 ft)) cracks.

Summary of Distresses

A summary of data related to various distress items and potential associated causative factors are listed in table 8. Pavements 15 years old and older generally exhibit moderate severity of spalling at transverse cracks. The older pavements also exhibit various amounts of patching. Sections WI-1 and WI-5 exhibited the most number of patches (partial and full-depth) within the 305-m (1,000-ft) sections tested. Only two sections (OK-4 and PA-2) exhibited punchouts that had not been patched. There does not appear to be any correlation between patching amount and ride quality indicating that the patches if constructed properly are not detrimental to ride quality. The Oklahoma sections (ranging in age from 2 to 7 years) exhibited very little distress other than low to moderate severity of transverse cracking. These sections also had the lowest percent of longitudinal steel reinforcement and above average crack spacing.

Steel corrosion based on core examination was found to be present at most of the sections in the wet-freeze regions with the exception of sections where epoxy-coated reinforcement was used. Also, there appeared to be a strong correlation between observed corrosion, based on core examinations, and the corrosion potential measured in the field using the copper-copper sulphate half-cell potentiometer. Corrosion potential measurements lower than about -0.30 volts indicated that potential for corrosion did exist at the site as verified by core examination.

Analysis of Data Using Distress Performance Models

As indicated previously, there are very few distress/performance models that exist for CRC pavements. The models that have been based on past studies include the following:

1. SHRP LTPP Ride Quality Model for CRC pavements.

2. AASHTO Design Guide (prediction of cumulative equivalent single axle loads (CESAL's), estimation of slab thickness and reinforcement design).

3. Illinois and Texas distress models based on number of failures.

Table 8. Various distress items.

Test Section ID	Route	Age as of Fall 1991 Testing, years	Climatic Region	Subgrade Type (AASHTO)	Base Type	Outside Shoulder Type	Long. Steel Amount, %	Average Core Thickness, in.	Steel Steel Corrossion Level (4 cores)	Average Crack Spacing, feet	Average IRI, in./mile	Terminal Joint Distress Level	No. of Trans. Cracks			Longitud. Cracking Amount, ft & Severity	No. of Patches & Severity	No. of Punchouts & Severity	Total No. of Ptches & Punchouts per Mile
													Low Severity	Moderate Severity	High Severity				
IL-1	US51	0.3	wet-freeze	A-7-6	perm. ctb	pcc	0.7	10.1	none	5.1	93	none	178	0	0	0	0	0	0.0
IL-2	I72	15	wet-freeze	A-6	ctb	ac	0.59	8.8	1spot	4.22	127	low	9	221	5	60H	4AC(M),3PCC(L)	0	12.4
IL-3	US36	20	wet-freeze	A-7-5	atb	ac	0.6	8.3	1spt/3sprd	3.58	152	medium	6	264	5	0	1AC(M),1PCC(L)	0	2.8
IL-4	I55	20	wet-freeze	A-7-5	atb	ac	0.6	9.3	2spt/2sprd	2.13	157	medium	9	463	0	0	0	0	1.8
IL-5	US50	5	wet-freeze	A-7-5	lcb	pcc	0.7	8.5	2spt/2sprd	3.02	141	none	344	12	0	0	0	0	1.0
IA-1	I29	20	wet-freeze	A-2-6	ctb	ac	0.65	8.2	1spt/1sprd	5.89	72	medium	24	144	0	343L	0	0	0.0
IA-2	I80	22	wet-freeze	A-6	atb	ac	0.65	8	2spt/2sprd	2.98	82	medium	35	420	0	4L,49M,14H	1AC(L)	0	3.6
IA-3	I380	15	wet-freeze	A-6	atb	pcc	0.65	8	3spt/1sprd	2.98	118	none	16	423	0	0	0	0	3.2
OK-1	I40	4	wet-no freeze	A-6	atb	pcc	0.5	9.2	3spt/1sprd	8.44	53	none	0	124	0	0	0	0	0.3
OK-2	US69	5	wet-no freeze	A-6	atb	pcc	0.5	9.2	1spt	4.57	na	medium	27	201	1	0	0	0	na
OK-3	I35	3	wet-no freeze	A-4	atb	pcc	0.5	10.3	none	4.75	74	none	14	210	0	0	0	0	0.0
OK-4	US69	7	wet-no freeze	A-6	soil-asphalt	pcc	0.5	9.4	4spt	6.36	na	none	2	130	7	0	0	1L	na
OK-5	I40	2	wet-no freeze	A-2-6	perm. ctb	pcc	0.61	10.1	none	6.13	50	none	108	48	0	0	0	0	0.5
OR-1	I5	7	wet-no freeze	A-4	granular	ac	0.6	12.4	none	4.02	na	low	4	301	0	0	0	0	na
OR-2	I5	4	wet-no freeze	A-4	ctb	ac	0.6	10.2	none	5.6	na	low	21	274	0	18L	0	0	na
OR-3	I205	20	wet-no freeze	A-6	ctb	ac	0.54	7.6	none	4.43	na	low	0	225	0	40M	0	0	na
PA-1	I180	15	wet-freeze	A-2-4	granular	ac	0.45	9.2	2sprd	4.8	75	low	0	238	84	0	0	0	0.0
PA-2	I81	22	wet-freeze	A-2-4	granular	pcc	0.55	9.4	4sprd	4.32	75	medium	0	256	0	20M	1PCC(L),Map Crack.	3L	10.6
WI-1	I43	18	wet-freeze	A-2-4	granular	ac	0.65	8.4	na	2.88	112	medium	0	259	0	76L,70M	84AC(L)	0	6.2
WI-2	I90	6	wet-freeze	A-2-4	granular	pcc	0.67	10.2	na	2.9	97	none	30	314	0	0	0	0	0.0
WI-3	I90/94	7	wet-freeze	A-2-7	granular	pcc	0.67	10.2	na	3.46	81	low	129	164	0	25L	0	0	0.8
WI-4	I90/94	7	wet-freeze	A-2-6	granular	pcc	0.67	10.6	4sprd	4.58	126	na	33	192	0	0	1PCC(L)	0	1.4
WI-5	I90/94	16	wet-freeze	A-2-6	granular	ac	0.61	7.9	4sprd	3.38	93	medium	14	291	0	416M,249H	11AC(L),13PCC(L)	0	21.4
Average		11.3					0.6	9.3		4.4	98.8								
Std Dev		7.4					0.1	1.1		1.4	32.3								
Maximum		22.0					0.7	12.4		8.4	157.0								
Minimum		0.3					0.5	7.6		2.1	50.0								

Notes:

1. spt = spot corrossion of steel bar
2. sprd = spread corrossion of steel bar
3. Severity levels - L = low; M = moderate; H = high
4. Patching data includes both partial and full depth patching

(25.4 mm = 1 in) (0.305 m = 1 ft)
(15.8 mm/km = 1 in/mi) (1.61 km = 1 mi)

4. Highway Performance Monitoring System (HPMS) model.

SHRP LTPP Ride Quality Model[3]

A model was recently developed using data collected as part of the LTPP GPS-5 experiment involving performance evaluation of in-place CRC pavements. The model has the following form:

$$IRI = 262.05 + 1.47 * CESAL - 2.94 * THICK - 232.3 * PSTEEL - WIDENED - 16.8 * SUBGRADE \quad (7)$$

where:

IRI	=	International Roughness Index, mm/km (in/mi)
CESAL	=	Cumulative 80.07 kN (18,000 lb) ESAL in traffic lane, millions
THICK	=	Concrete slab thickness, mm (in)
PSTEEL	=	Percent steel (longitudinal reinforcement)
WIDENED	=	1 for widened lane, 0 for 3.7-m (12-ft) wide lane
SUBGRADE	=	1 for coarse-grained soils, 0 for fine-grained soils

The model was based on data from 42 152-m (500-ft) long test sections and has a R^2 of 0.55.

For fine-grained soils, slab thickness of 254 mm (10 in), and standard lane width of 3.7 m (12 ft), the model reduces to the following:

$$IRI = 232.65 + 1.47 * CESAL - 232.2 * PSTEEL \quad (8)$$

For a CESAL of 10,000,000, the IRI value expected is given by:

$$\begin{aligned} IRI &= 247.35 - 232.2 * PSTEEL \quad (9) \\ &= 131 \text{ for } PSTEEL = 0.5 \text{ percent} \\ &= 108 \text{ for } PSTEEL = 0.6 \text{ percent} \\ &= 85 \text{ for } PSTEEL = 0.7 \text{ percent} \\ &= 62 \text{ for } PSTEEL = 0.8 \text{ percent} \end{aligned}$$

Similar results are obtained for coarse grained subgrades. The model indicates that a smoother ride can be obtained with higher steel amounts. This is somewhat contradictory to the trend noticed with data from the current study. Data obtained from the reported study indicate that higher steel amounts may cause a rougher ride because of closely spaced cracks in presence of weak or variable subgrade support.

AASHTO Design Guide Models

The AASHTO Guide incorporates CRC pavement thickness design procedure within the procedures for jointed concrete pavements. As such no realistic predictions can be made

using the AASHTO Design Guide equation relating CESAL's to various pavement parameters for CRC pavements.

Given the following conditions:

Modulus of subgrade reaction	=	81.4 MPa/m (300 pci)
Concrete modulus of rupture	=	4.48 MPa (650 lbf/in^2)
Concrete modulus of elasticity	=	31 030 MPa (4,500,000 lbf/in^2)
Terminal PSI	=	3.0
Design reliability	=	90 percent

The following levels of CESAL's can be expected to be carried by the pavement:

- 38.4 million CESAL's for thickness of 305 mm (12 in)
- 12.2 million CESAL's for thickness of 254 mm (10 in)
- 3.3 million CESAL's for thickness of 203 mm (8 in)

Unfortunately, reliable estimates for CESAL's at many sites were not available. Where the estimates were available, it became quickly apparent that the actual CESAL's (estimates provided by state agencies) are generally much higher than those predicted by the AASHTO Guide. The AASHTO Guide tends to be very conservative with predicting allowable/acceptable cumulative ESAL's for concrete pavements.

The AASHTO Guide also includes models to allow computation of the appropriate amount of steel to be used for CRC pavements. These models can be used indirectly to estimate the crack spacing, crack width, and the longitudinal steel stress.

These models have, however, been supplanted in reliability by the recent improvements in the CRCP mechanistic models developed at the University of Texas. Therefore, no further evaluation is presented here with the AASHTO design models. The following chapter presents a more comprehensive evaluation of the field data in relation to predicted crack spacing and crack width using one of the mechanistic models.

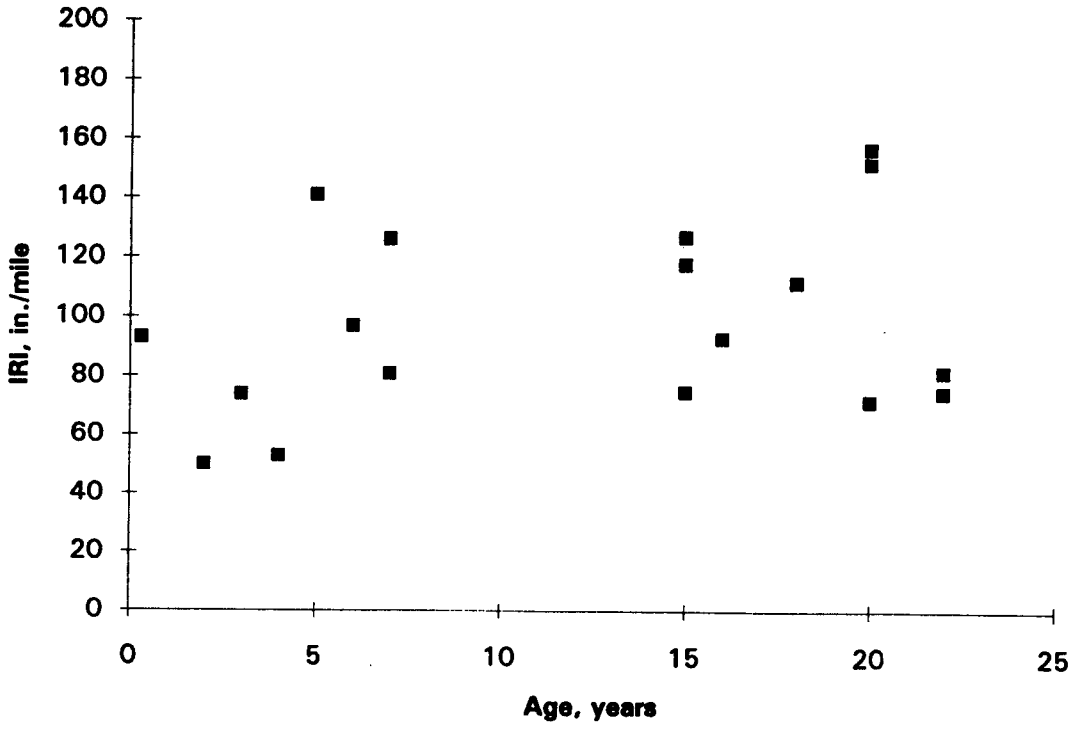

(15.8 mm/km = 1 in/mi)

Figure 1. Ride quality as a function of age.

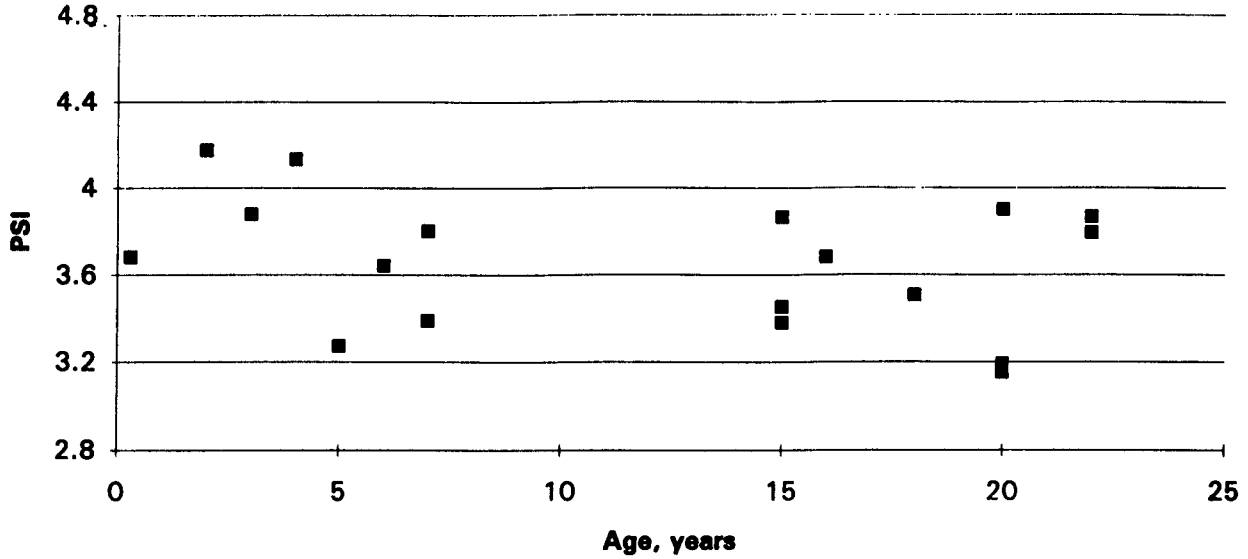

Figure 2. Estimated PSI as a function of age.

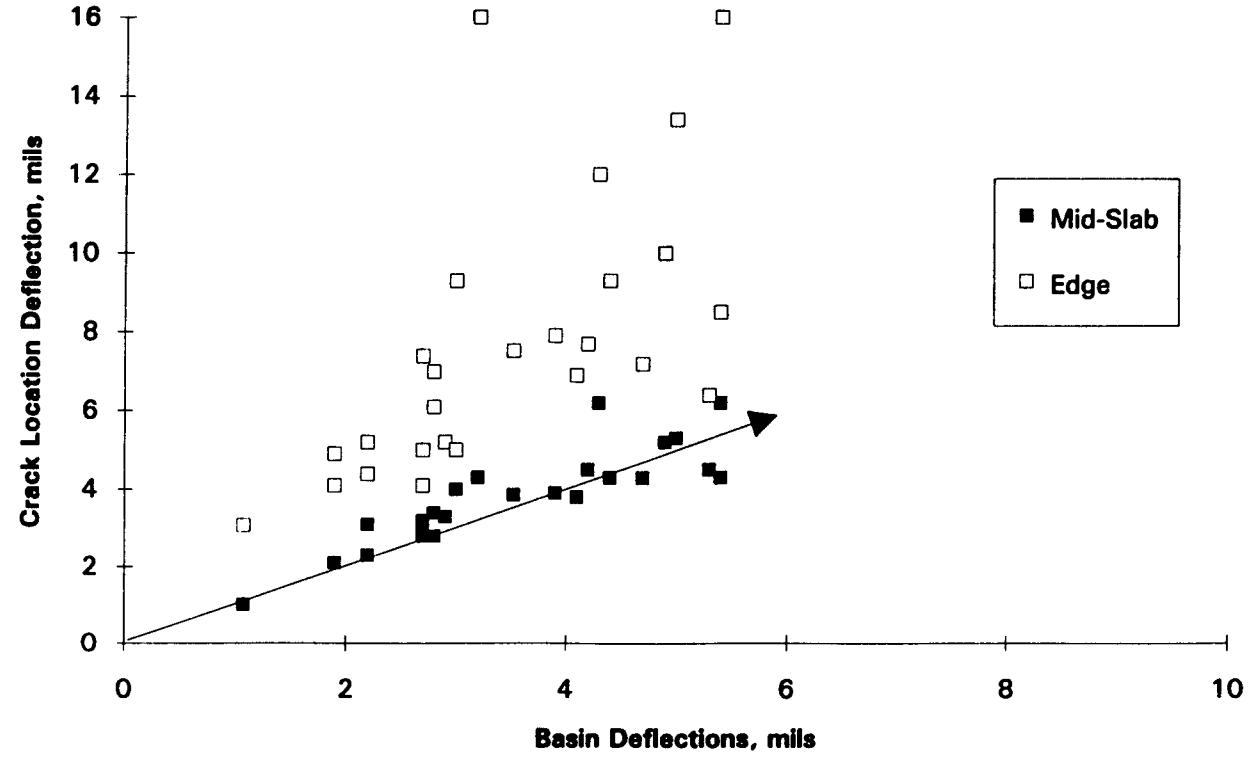

(0.0254 mm = 1 mil)

Figure 3. Comparison of basin and crack location deflections.

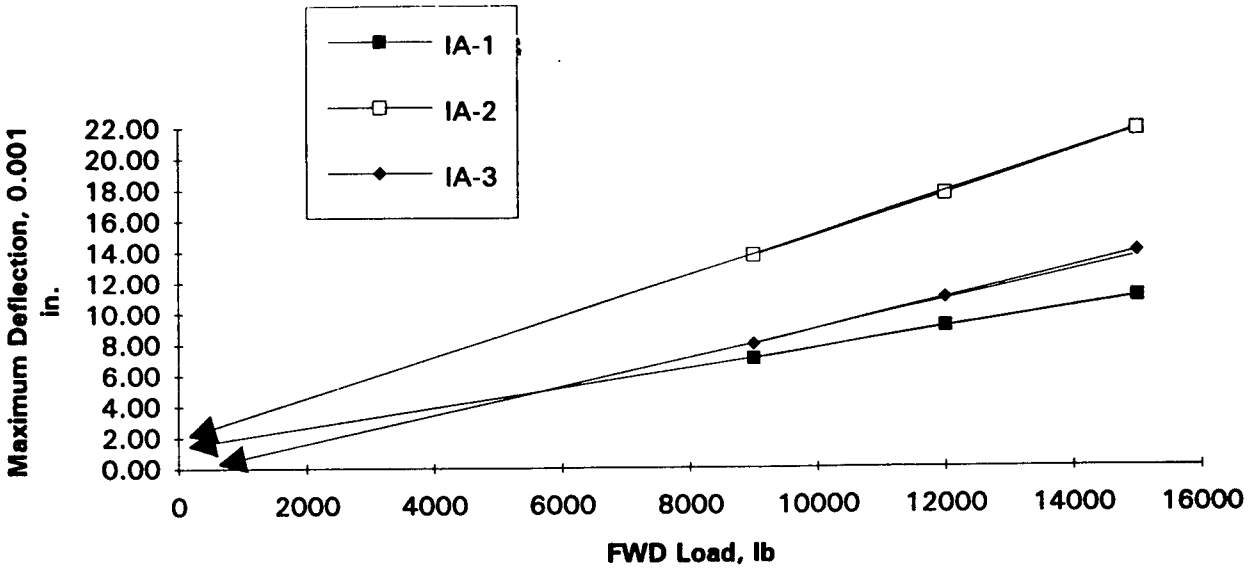

(0.0254 mm = 1 mil) (4.45 kN = 1,000 lb)

Figure 4. Determination of loss of support along edges.

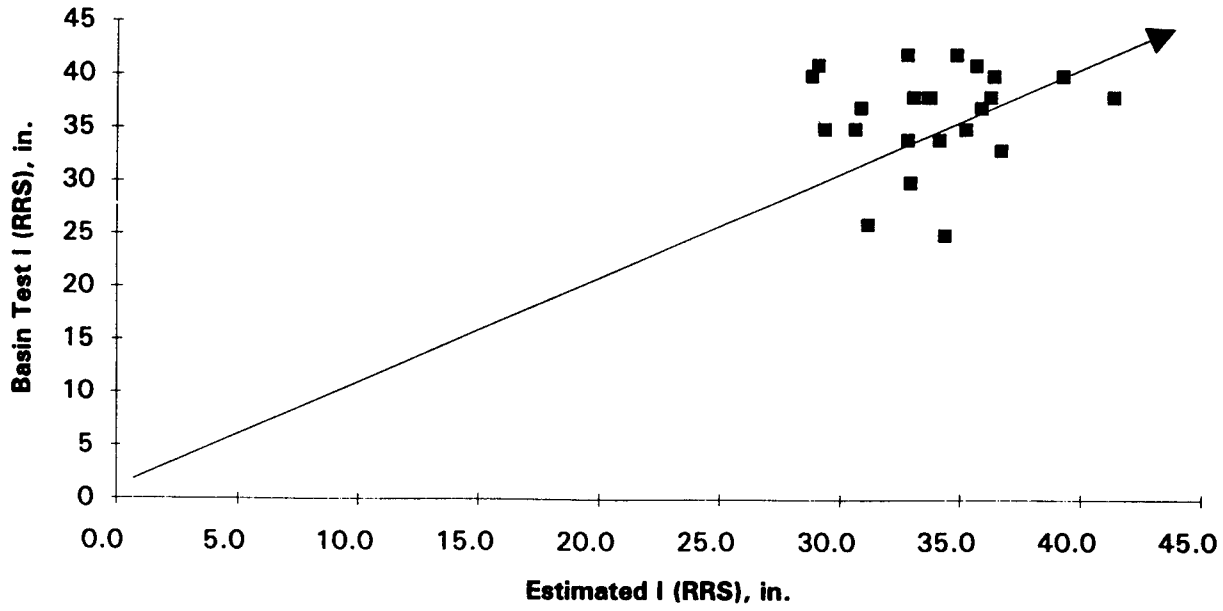

(25.4 mm = 1 in)

Figure 5. Comparison of basin and estimated radius of relative stiffness (RRS) values.

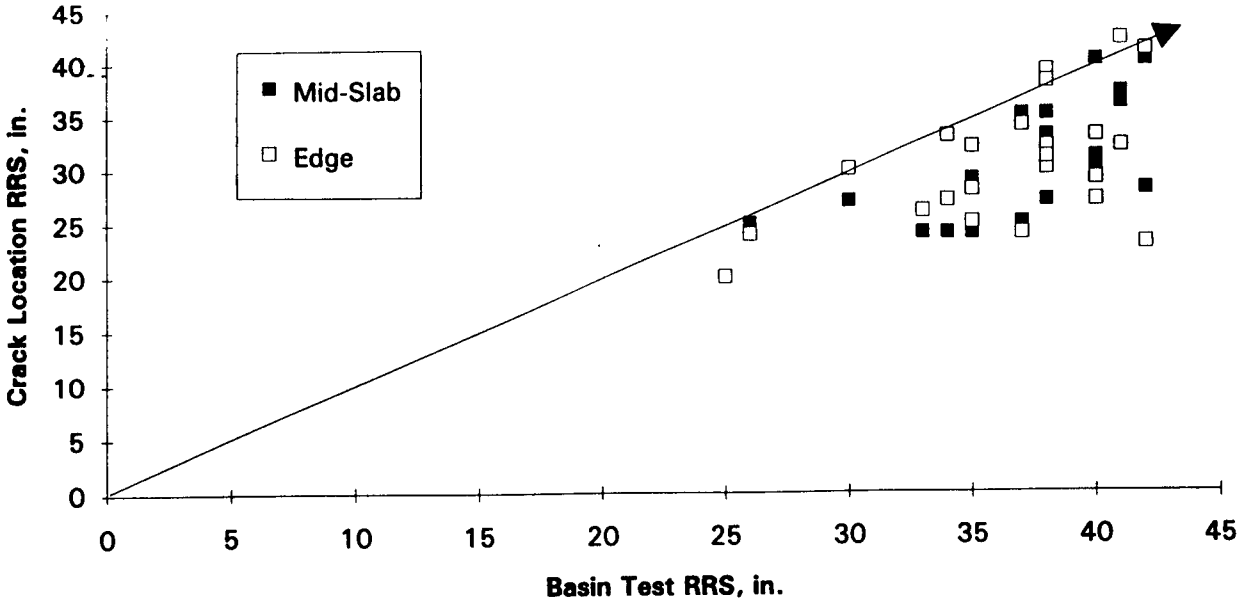

(25.4 mm = 1 in)

Figure 6. Comparison of basin and crack location test RRS values.

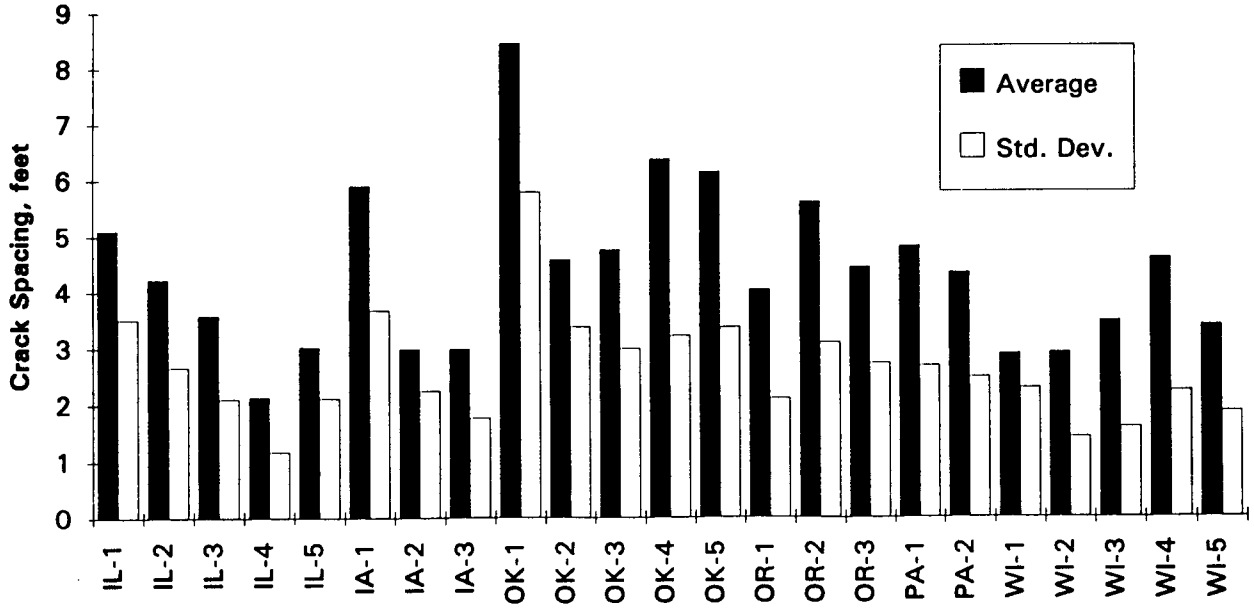

(0.305 m = 1 ft)

Figure 7. Crack spacing summary.

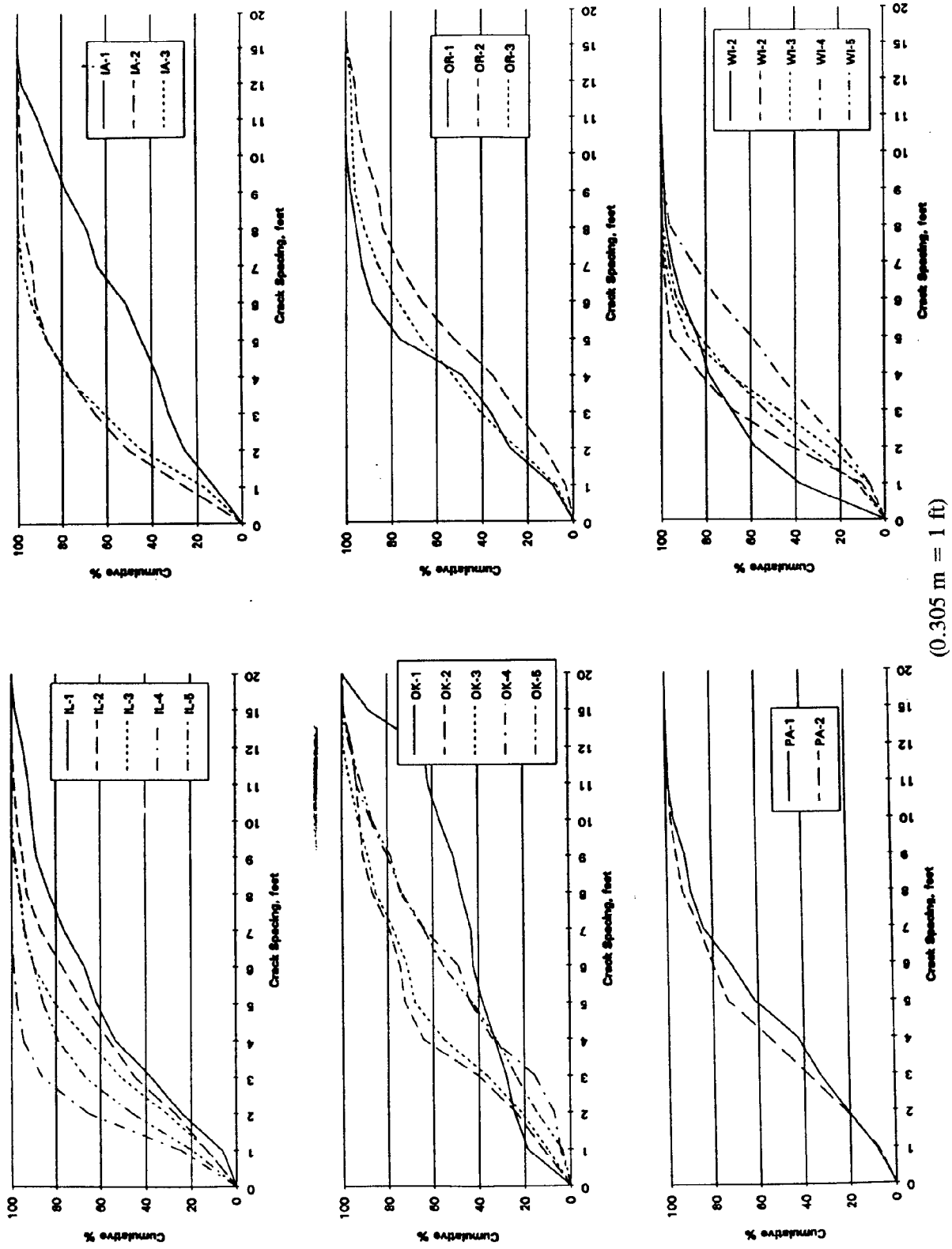

(0.305 m = 1 ft)

Figure 8. Crack spacing distribution (by number of cracks).

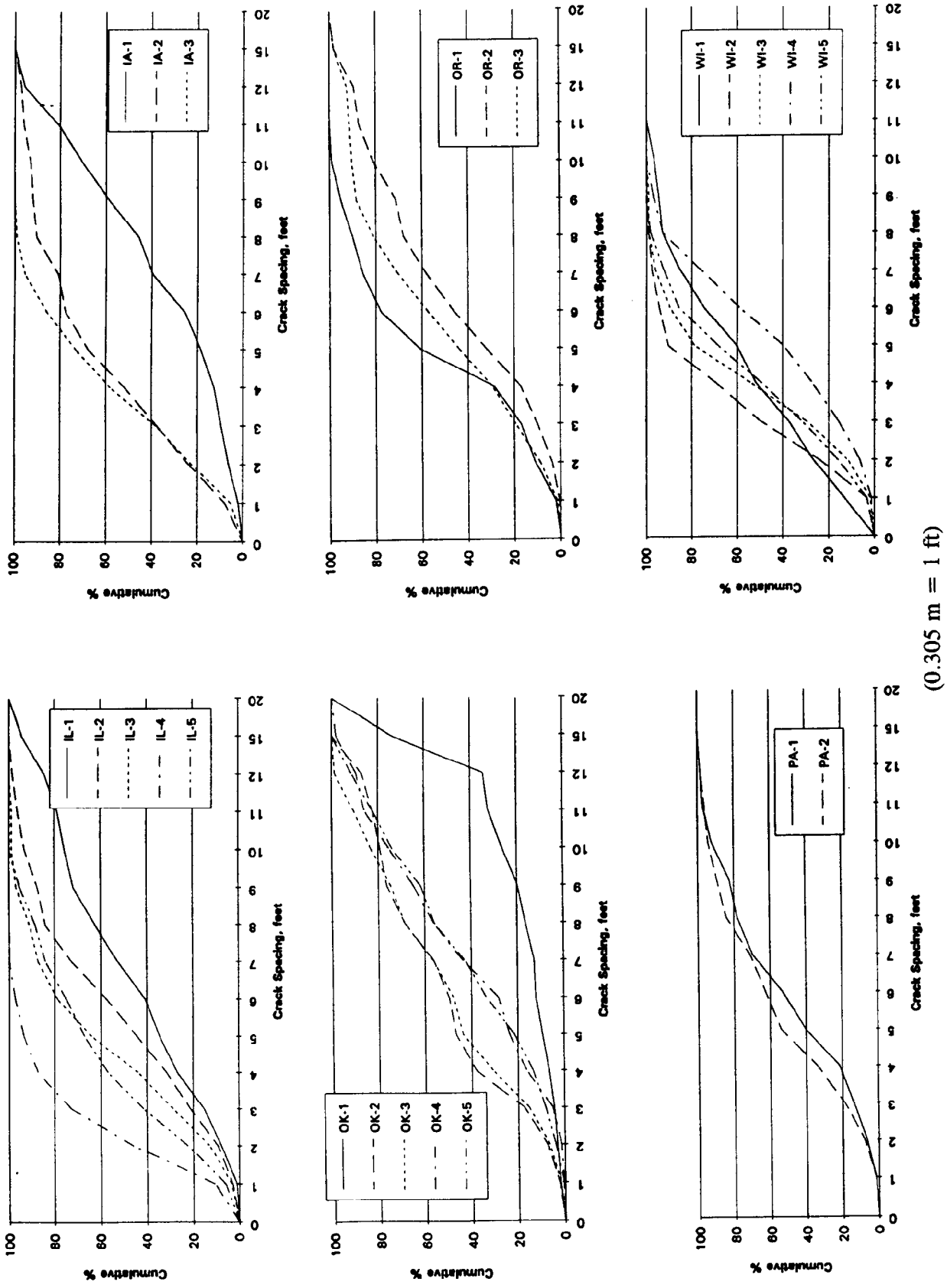

(0.305 m = 1 ft)

Figure 9. Crack spacing distribution (by length of paving)

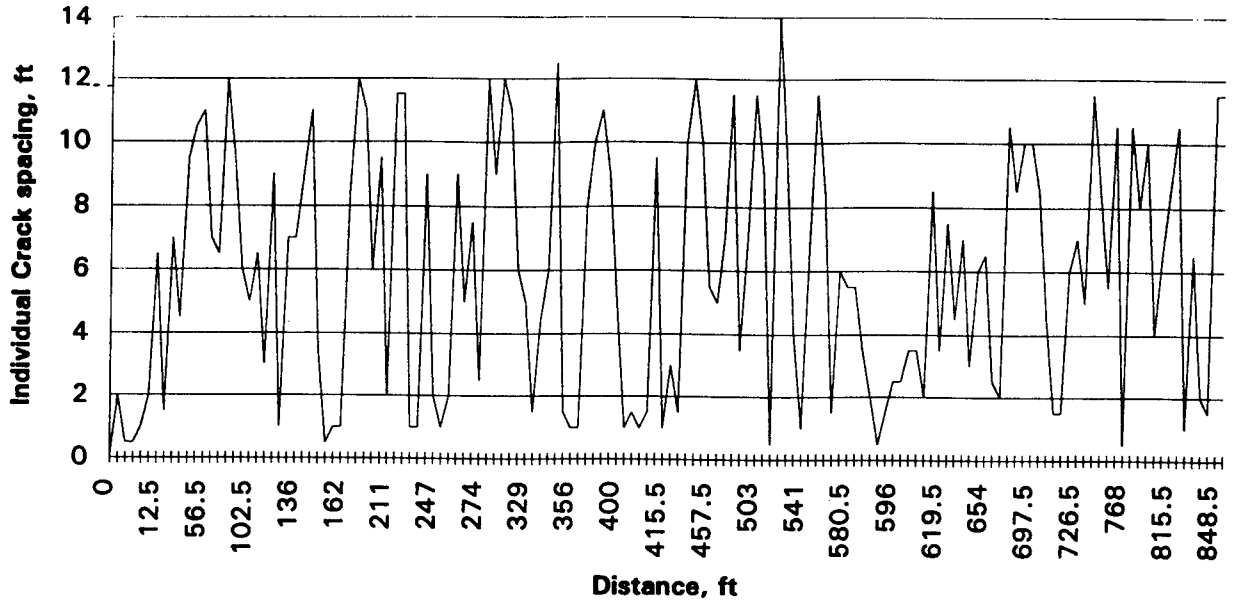

(0.305 m = 1 ft)

Figure 10. Crack spacing pattern for IA-1 - individual crack spacings.

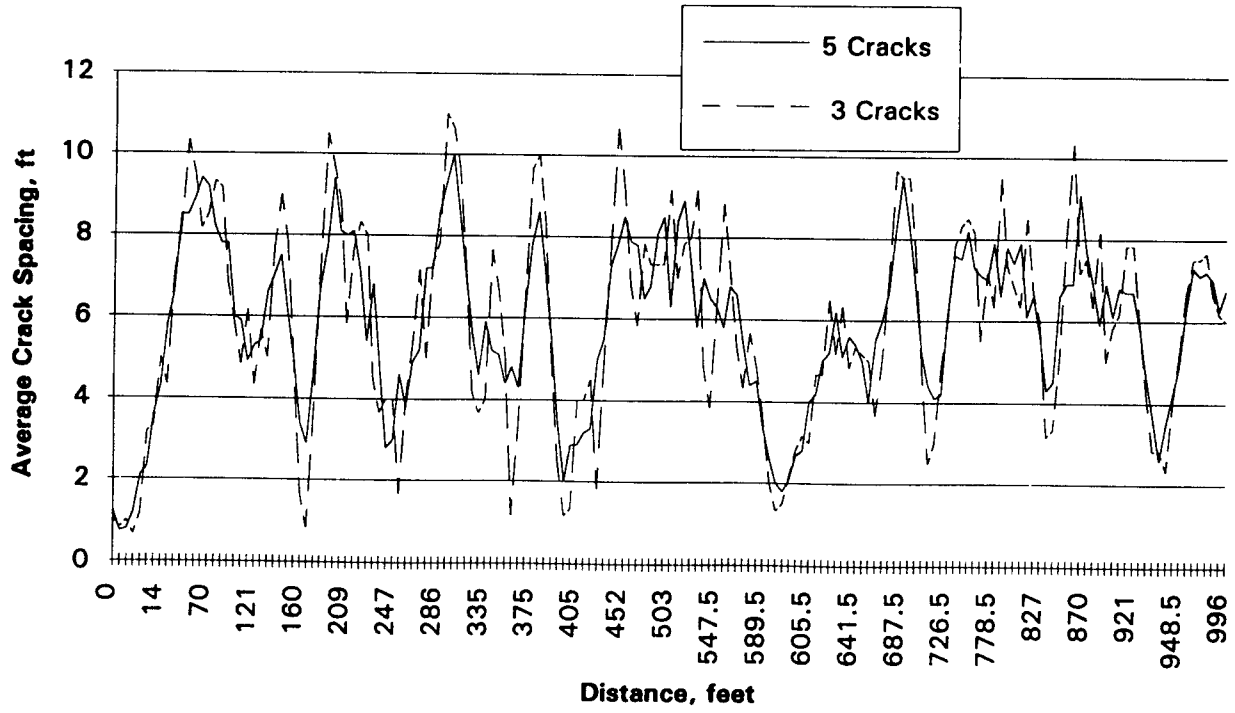

(0.305 m = 1 ft)

Figure 11. Crack spacing pattern for IA-1 based on closest 3 or 5 cracks.

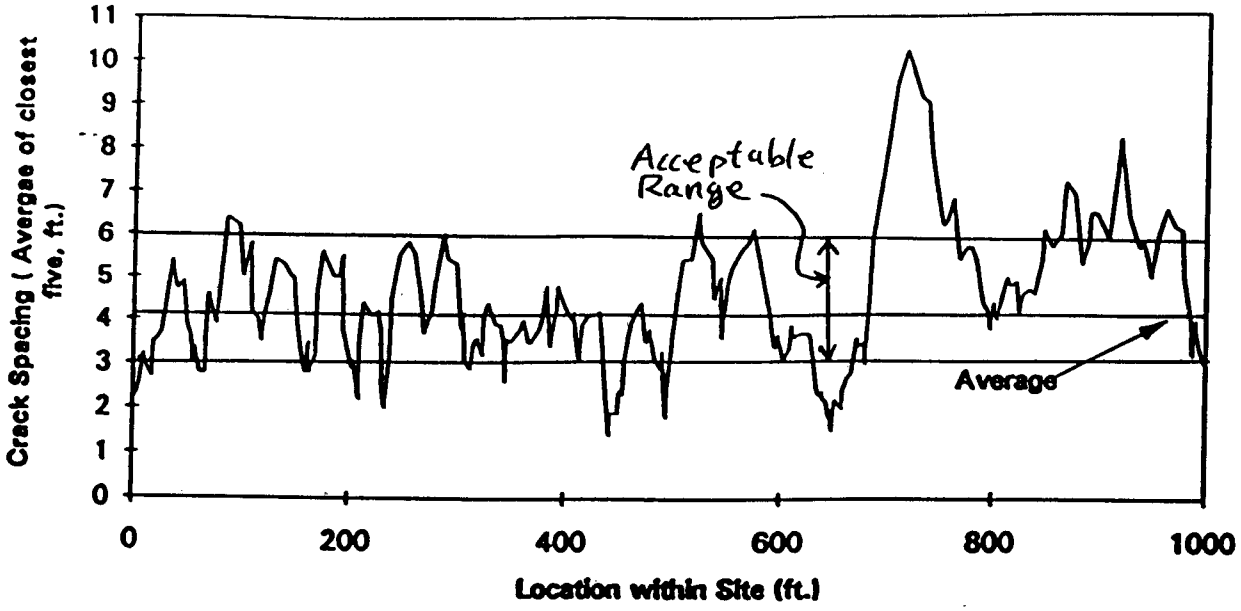

Crack Spacing Pattern at IL-2

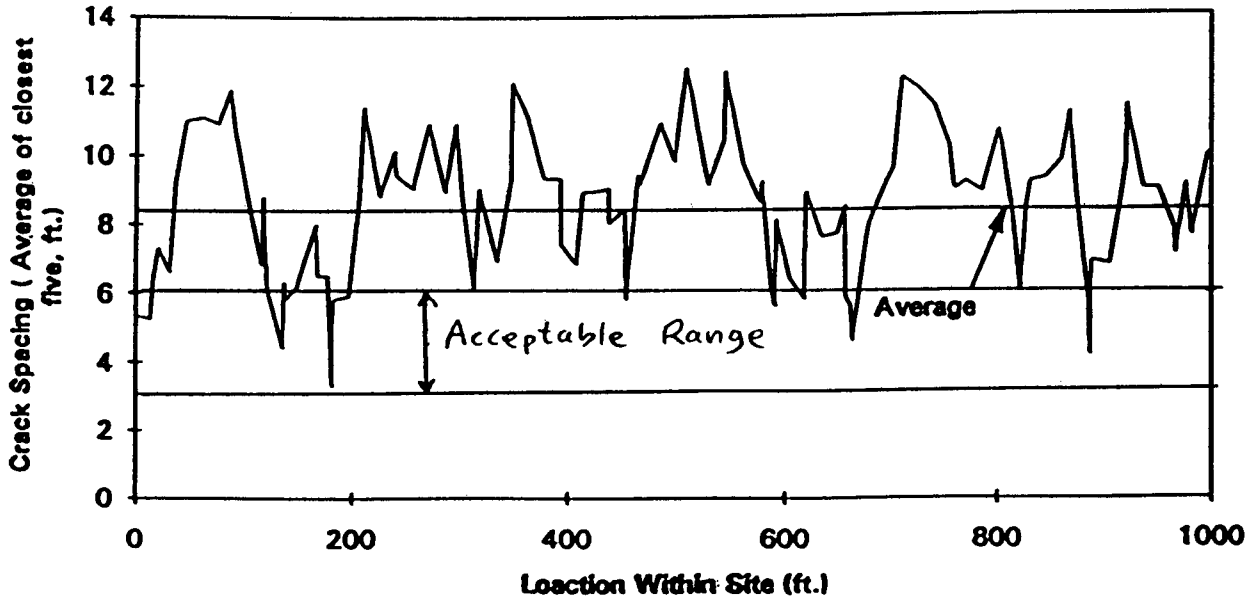

Crack Spacing Pattern at OK-1

(0.305 m = 1 ft)

Figure 12. Illustration of procedure to identify extent of marginal cracking pattern.

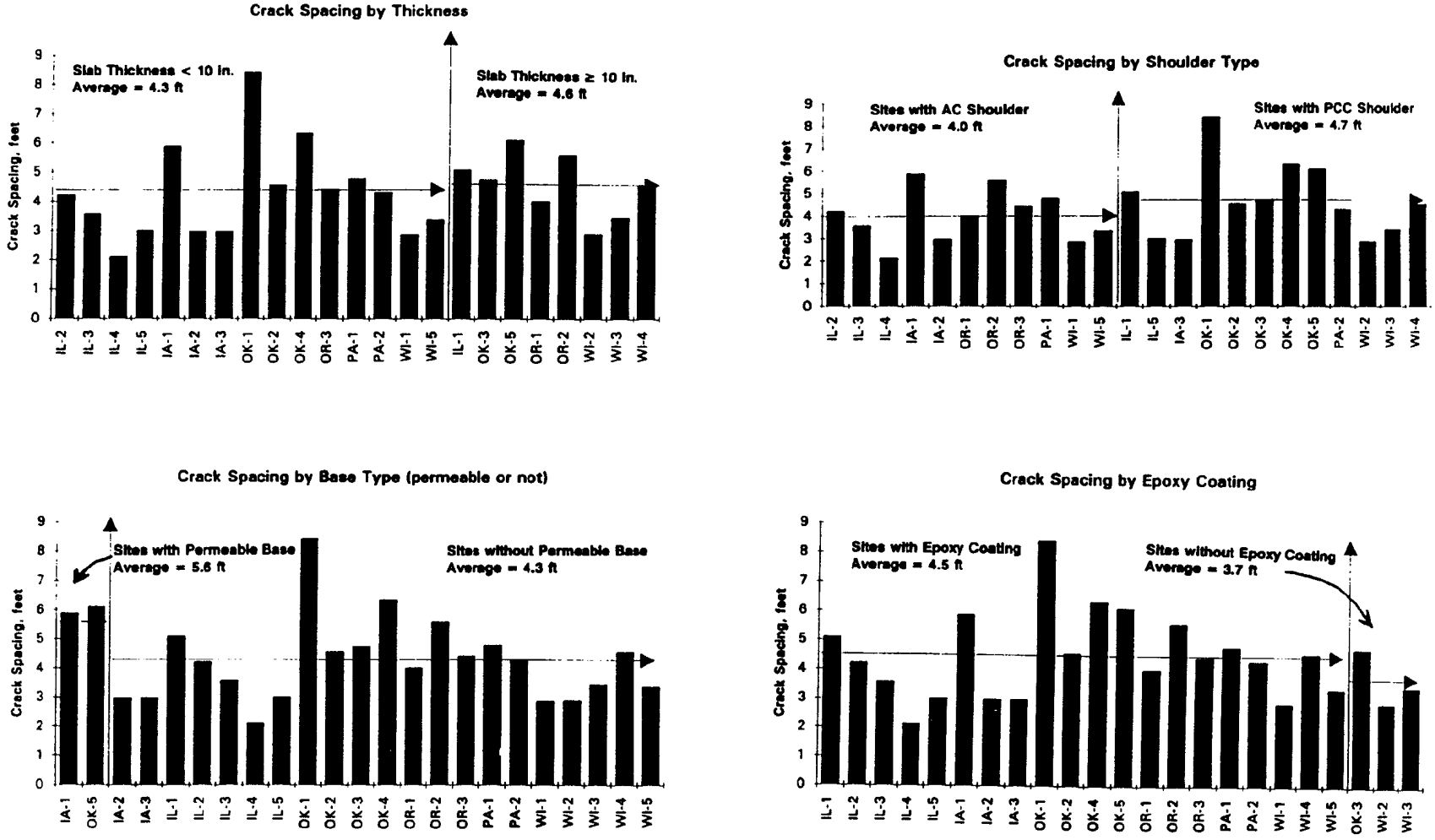

(0.305 m = 1 ft)

Figure 13. Crack spacings as affected by various design related attributes.

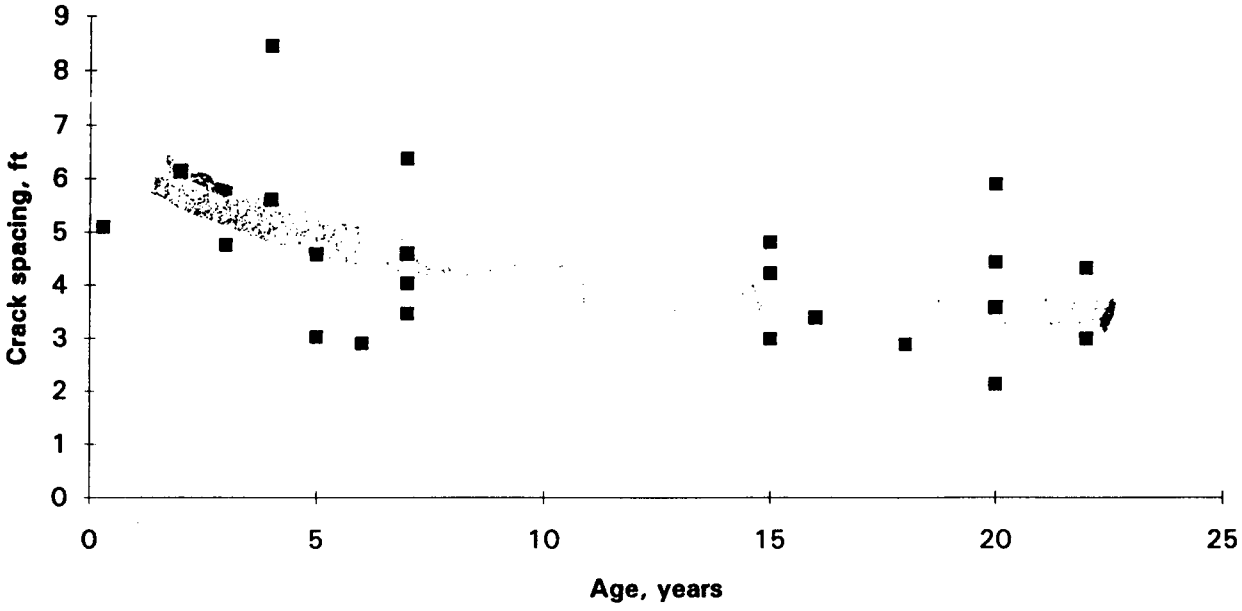

(0.305 m = 1 ft)

Figure 14. Average crack spacing as a function of age.

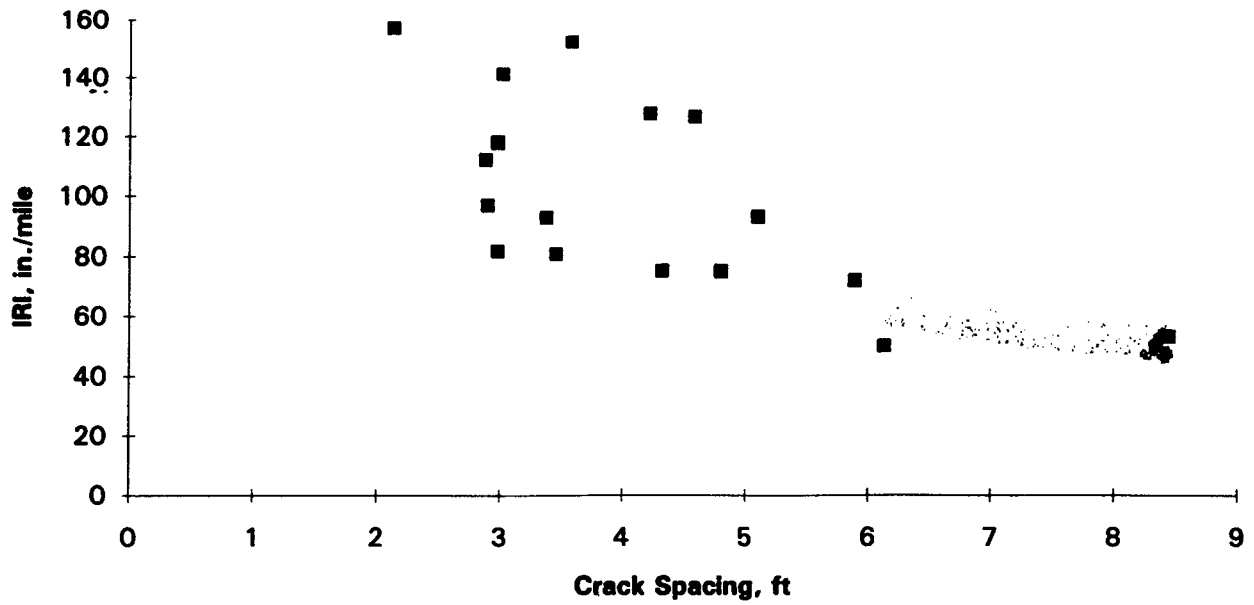

(15.8 mm/km = 1 in/mi) (0.305 m = 1 ft)

Ride quality (IRI) as a function of average crack spacing.

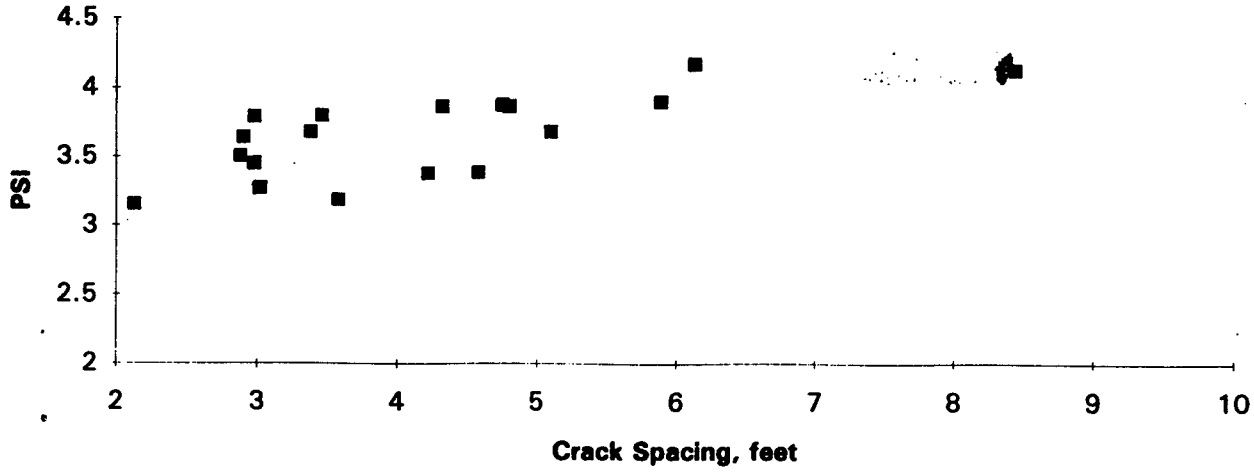

(0.305 m = 1 ft)

Estimated PSI as a function of average crack spacing.

Figure 15. Ride quality and PSI as a function of average crack spacing.

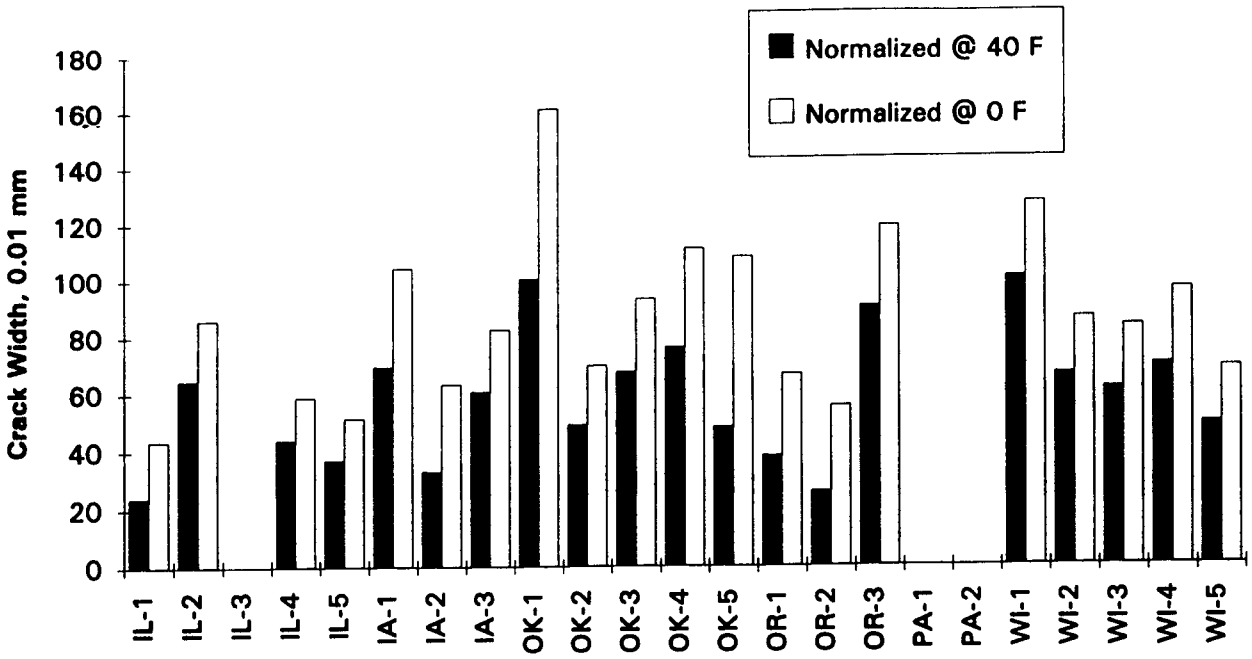

(0.6 °C = 1 °F) (25.4 mm = 1 in)

Figure 16. Normalized crack widths.

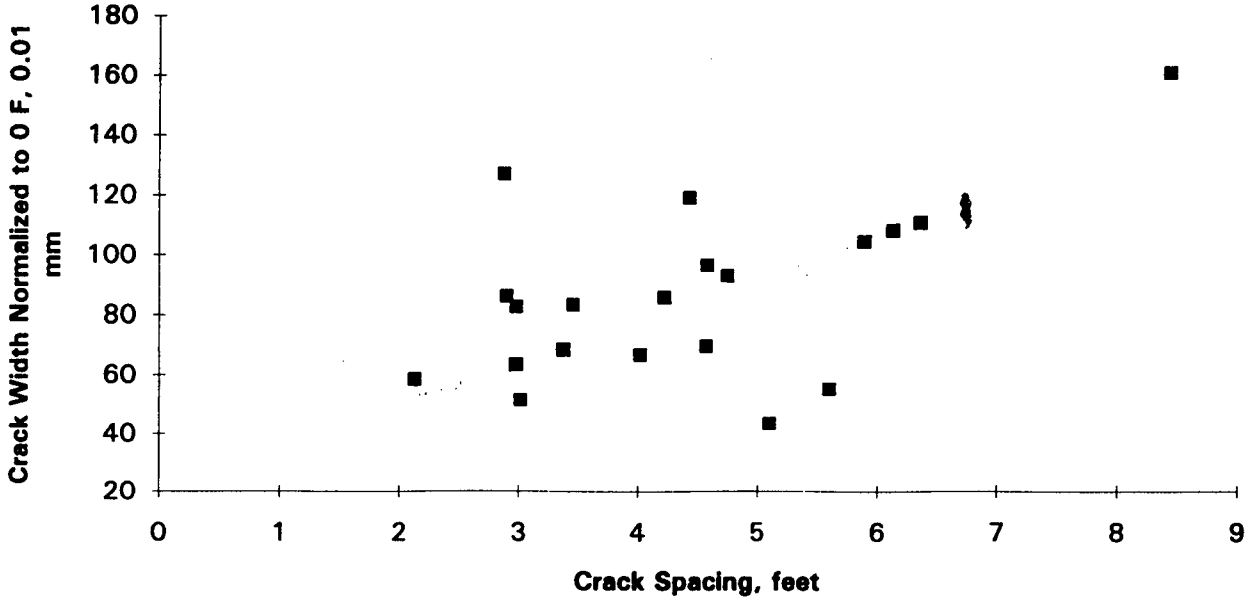

(0.6 °C = 1 °F) (25.4 mm = 1 in) (0.305 m = 1 ft)

Figure 17. Normalized crack width as a function of crack spacing.

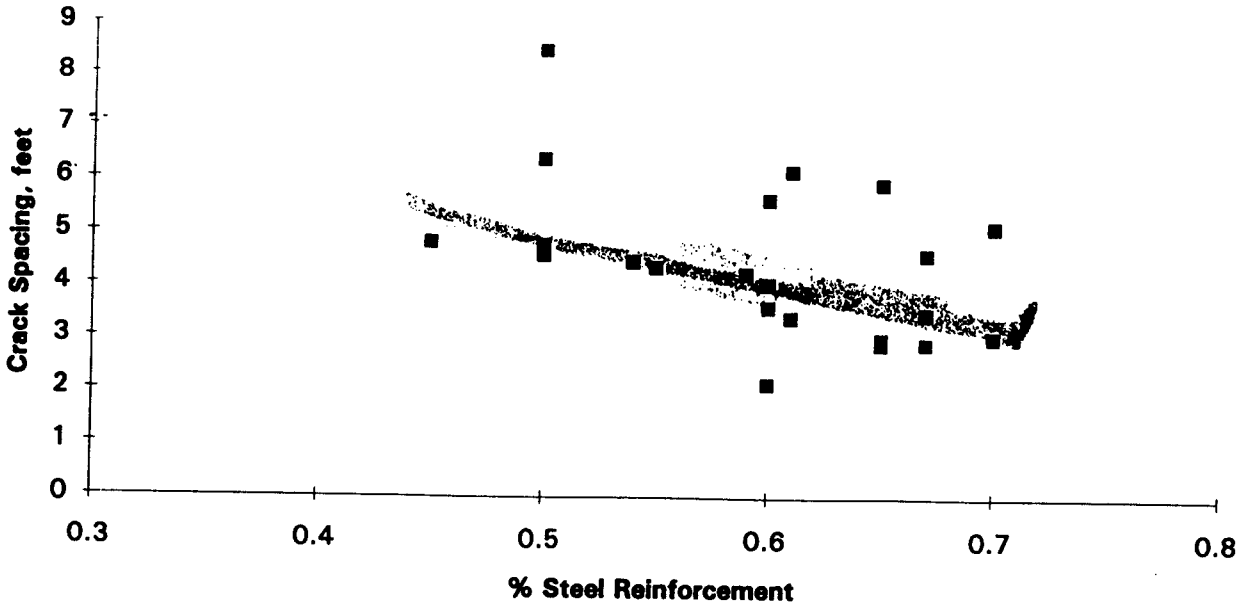

(0.305 m = 1 ft)

Figure 18. Average crack spacing as a function of percent steel reinforcement.

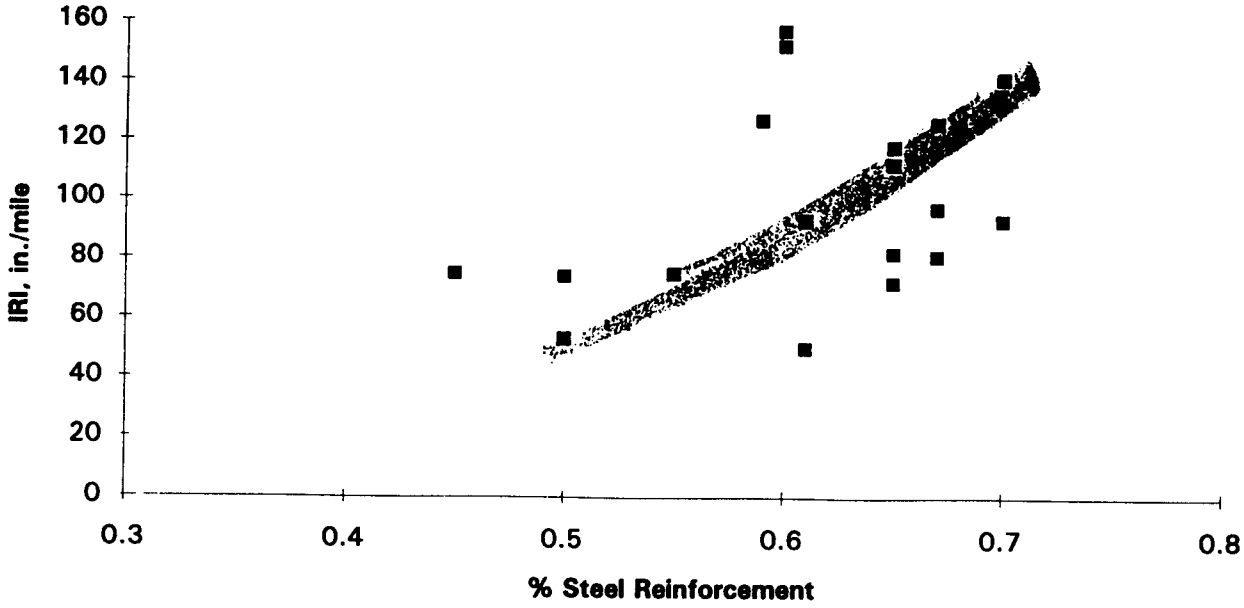

(15.8 mm/km = 1 in/mi)

Figure 19. Ride quality as a function of percent steel reinforcement.

CHAPTER 3 - PREDICTIONS OF CRC PAVEMENT CRACKING

General

Analysis to predict crack spacing were conducted for a total of twenty 305-m (1,000-ft) sections from Iowa, Illinois, Pennsylvania, Oklahoma, and Wisconsin. The Oregon sections were not analyzed. This chapter provides a background on the various crack spacing models and presents the results of crack spacing analysis performed using the CRCP-5 program.

Crack Spacing Computer Models

Since the transverse cracking process in CRC pavement involves an on going sequence of change in concrete strength and environmental conditions, it is advantageous to computerize certain stress and strain distributions, as shown in figure 20, in the form of algorithms to model the pavement crack spacing. To simplify the analysis, certain assumptions are made with regard to material properties and environmental conditions. The computer models are useful for the purpose of predicting crack spacing, crack width, and the stresses in concrete and steel for a given set of environmental and material conditions. In this study CRCP-5, developed at the Center for Transportation Research at the University of Texas at Austin, and TTICRCP, developed at the Texas Transportation Institute, were reviewed. However, only the CRCP-5 model was used in this study since it was the most currently available at the time of this study in this series of CRC pavement design/analysis tools.

CRCP-5 Model[5]

CRCP-5 was developed for the prediction of cracking in CRC pavements due to in-plane stresses caused by drying shrinkage and temperature drop. Included in the model is equilibrium analysis of stress in the concrete, steel reinforcement, and resistance due to friction at the base/subbase interface. The friction on the base/subbase is considered as a function of the pavement displacement which depends upon temperature and material properties. The model also accounts for the age/tensile strength relationship of the concrete which allows for analysis of crack formation with time as the internal tensile stress exceeds the tensile strength of the concrete. Basically, CRCP-5 consists of two parts. One part is to analyze the structural response of the pavement system and predicts transverse crack spacing distributions. The other part estimates pavement life in terms of distress manifestations. In the first part, the Monte Carlo Method is applied to include material variabilities in the mechanistic analysis. A calibrated fatigue relationship directly representing the behavior of concrete and the relationship between wheel load stress (and indirectly those stresses resulting from curling and warping effects) and crack spacings are utilized in the second part to provide a predictive model of pavement performance.

The CRCP-5 model incorporates equations developed for force equilibrium of bond, steel, and subbase friction in the pavement system for the prediction of structural responses due to contraction restraint in CRC pavement. The model assumes a crack forms when the concrete stress calculated from the equilibrium equations is greater than the concrete strength

at that location. The model assumes the stress in the concrete at a crack is zero. The stresses due to volummetric changes are also assumed to be uniformly distributed throughout the slab thickness. Since the model contains an algorithm for the change in concrete strength with time, the criteria for cracking can be adjusted with time. The following assumptions are made in the CRCP-5 model:

1. A crack occurs when the concrete stress exceeds the concrete strength; after cracking, the concrete stress at the location of the crack is zero.

2. Concrete and steel properties are linearly elastic.

3. In the fully bonded sections of the concrete slab, there is no relative movement between the steel and the concrete; stresses are assumed to be uniformly distributed with depth in the slab.

4. The force-displacement curve which characterizes the frictional resistance between the concrete slab and the underlying base is elastic.

5. Material properties are independent of space.

6. Effects of concrete creep and slab warping are neglected.

7. Temperature variations and shrinkage due to drying are uniformly distributed throughout the slab; hence, a one dimensional axial structural model is adopted for the analysis of the problem.

The model also assumes fixed end conditions at the mid-slab location and for the reinforcement at the crack centerline. No condition for variable depth of cover is included. Fully restrained conditions are used as a basis for the development of the equations since the total length of steel bars is assumed to be constant. The model limits variable frictional resistance between the concrete slab and the underlying base between existing cracks.

The basic equations for the CRCP-5 model are derived by considering a full length of CRC pavement in which a free body diagram is developed in (figure 20). By considering overall equilibrium:

$$F_{sx} + F_{cx} = F_{sc} + {}_{x}^{l}F_i dx \qquad \textbf{(10)}$$

where

F_{sc} = force in the steel at the crack
F_i = friction force per unit length along the slab length
F_{sx} = force in the steel at location, x and
F_{cx} = force in the concrete at the location x.

Compatibility equations are included in the model for volummetric changes in the concrete pavement under environmental effects in which:

$$\sigma_{cx} = \frac{\sigma_{sx}}{n} + E_c\left[(\alpha_c - \alpha_s)\Delta T + \epsilon_{sh}\right] \quad (11)$$

where

σ_{cx}	=	stress in the concrete at location x
σ_{sx}	=	stress in the steel at location at x
α_c	=	thermal coefficient of expansion of the concrete
α_s	=	thermal coefficient of expansion of the steel
ΔT	=	temperature change, positive if temperature decreases
ϵ_{sh}	=	drying shrinkage of the concrete
E_s	=	elastic modulus of the steel
E_c	=	elastic modulus of the concrete
n	=	E_s/E_c (modular ratio)

The material characteristics indicated above can be found from standard test procedures, references, or design relationships. The above generalized compatibility equation applies to the region in which the steel and concrete are fully bonded. The effect of subbase friction (F_i) was also included in equations expressing the change in steel and concrete stress with length:

$$\frac{d\sigma_{sx}}{dx} = \frac{-F_i}{\left(A_c(\frac{1}{n} + p)\right)} + \frac{4u}{d_b} \quad (12)$$

$$\frac{d\sigma_{cx}}{dx} = -\frac{F_i}{A_c} - \frac{4up}{d_b} \quad (13)$$

where

A_c	=	cross-sectional area of concrete
p	=	ratio of cross-sectional area of steel to concrete
u	=	uniformly distributed bond stress
d	=	rebar diameter

These expressions are important since they describe how the stresses in the reinforcing steel and the concrete vary from the crack face (where the concrete stress (σ_c) is assumed to be zero) to the fully bonded region of the slab segment. However, these expressions have application to the fully bonded region but the change in either the concrete or the steel stress in the fully bonded region is assumed to be small since the change in bond stress and friction effects is small in that region.

The CRCP-5 program also contains a model for prediction of punchout development based on fatigue damage accumulation due to wheel load stresses developing at potential longitudinal crack locations. Longitudinal cracking is significant in the development of punchout distress. The damage accumulation determined by this model, shown below, incorporates the crack spacing distribution obtained from the program results to generate a relative estimate of the punchout performance in terms of:

$$N = A \left\{ \frac{f}{\sigma} \right\}^{B} \qquad \textbf{(14)}$$

where

A,B	=	Regression coefficients to be determined
σ	=	Flexural stress
f	=	Flexural strength

The above expression is useful in determining relative comparisons of pavement life between different designs of CRC pavements, for a given combination of crack spacing distributions, support conditions, and climatic conditions.

TTICRCP Model[6]

The model developed at the TTI designated TTICRCP takes a different approach to cracking in the CRC pavement by characterizing the bond stress distribution between the steel and the concrete which is not based on an assumption of uniform bond distribution. No direct relationship is assumed between the bond stress and the crack width.

The basic assumptions of the TTICRCP model are similar to those used in CRCP-5 and are as follows:

1. The concrete and the reinforcing steel are linearly elastic.
2. The base material underneath the slab is rigid, and will not deflect under loading by the horizontal friction force.
3. All materials are homogeneous.
4. All temperature and shrinkage induced strains are uniformly distributed throughout the depth and the width of the CRCP slab.
5. The effect of warping, curling, and creep are neglected.

6. All behavior in the slab is symmetrical about the midpoint of the slab.

Cumulative Distributions

Analysis of data collected from the field test sections is discussed in the following sections on a State by State basis. The pavement sections consist of 305-m (1,000-ft) sections located in Iowa, Illinois, Pennsylvania, Oklahoma, and Wisconsin selected for this study. The Oregon sections are not included in this analysis. The characterization of the data is generally described with respect to cumulative crack distributions and cluster cracking. Data on several Texas sections are provided in this study with respect to cluster cracking.

In order to obtain a representative cracking sample of the pavement from each 305-m (1,000-ft) section, two 30.5-m (100-ft) sections from each of the previously described 305-m (1,000-ft) sections were selected at random for detailed data analysis. The recorded crack spacing in each 30.5-m (100-ft) section was placed in an ascending order. The cumulative probability for each crack spacing was calculated in terms of the cumulative distribution of the crack spacing for a given sample. The cumulative probability for a particular crack spacing was found by dividing the number of cracks less than a given crack spacing by the total number of cracks included in the sample.

Given the cumulative probability, each of the crack patterns derived from each 30.5-m (100-ft) section were tested for both normal and lognormal distribution. This test was made by determining the fit between the calculated cumulative probability and the associated crack spacing. For this purpose, two graphs were plotted with cumulative probability on x-axis and crack spacing on y-axis. One graph with a linear scale on y-axis and other with a log scale on y-axis. The regression was done for both the graphs. Both linear and log distributions of the crack spacing were considered in the regression analysis. The coefficient of correlation (r^2) value was calculated for both curves where the linear distribution was assumed to be normally distributed and the log distribution was assumed to be lognormally distributed. The regression having maximum coefficient of correlation was chosen as the distribution of that 305-m (1,000-ft) section. Table 9 lists the type of distributions for all the twenty sections referred to in appendix H and illustrated in appendices A through E with graphs for each test section.

In order to obtain a more representative distribution for each 305-m (1,000-ft) section, a pooled variance and pooled mean were calculated from the individual variances and means of two 30.5-m (100-ft) sample sections. The pooled variance was used to calculate the pooled standard deviation. The following formulas were used to calculate the pooled variance and pooled mean.

$$S_p^2 = \frac{(n_1 - 1)S_1^2 + (n_2 - 1)S_2^2}{(n_1 - 1) + (n_2 - 1)} \quad \textbf{(15)}$$

Table 9. Distribution table for the test sections.
(0.305 m = 1 ft)

Test Section (305 m (1,000 ft))	Type of Distribution
PENNSYLVANIA-1	Normal
PENNSYLVANIA-2	Normal
ILLINOIS-1	Normal
ILLINOIS-2	Normal
ILLINOIS-3	Lognormal
ILLINOIS-4	Lognormal
ILLINOIS-5	Lognormal
OKLAHOMA-1	Normal
OKLAHOMA-2	Normal
OKLAHOMA-3	Lognormal
OKLAHOMA-4	Lognormal
OKLAHOMA-5	Normal
WISCONSIN-1	Lognormal
WISCONSIN-2	Lognormal
WISCONSIN-3	Normal
WISCONSIN-4	Normal
WISCONSIN-5	Normal
IOWA-1	Normal
IOWA-2	Lognormal
IOWA-3	Normal

$$\mu = \frac{(n_1\mu_1 + n_2\ \mu_2)}{n_1 + n_2} \quad (16)$$

where

S_p^2 = pooled variance
n_1 = number of cracks in sample 1
n_2 = number of cracks in sample 2
S_1^2 = variance of sample 1
S_1^2 = variance of sample 2
μ_p = pooled average crack spacing, m (ft)
μ_1 = average crack spacing, m (ft) of sample 1
μ_2 = average crack spacing, m (ft) of sample 2

To determine the probability that any measured crack spacing will fall in the interval from μ_p to some Y crack spacing, the number of standard deviations that Y lies away from the mean is calculated using the formula (for normal distribution):

$$Z = \frac{Y - \mu_p}{\sigma_p} \quad (17)$$

where

Z = standard normal deviate
Y = crack spacing
σ_p = pooled standard deviation

The value of Z computed using this formula is sometimes referred to as the Z score associated with the Y value. Using the computed value of Z, the appropriate probability is determined from the probability tables listed for a normal distribution. Similar approach is taken for a lognormal distribution except:

y = ln y,
μ = ln μ_p, and
σ = σ [ln y]

The previously described cumulative field distribution curves illustrate the level of probability associated with a specified cracking interval. These trends, shown in appendixes A through E, indicate the range of crack spacing and the likelihood of cracking intervals outside the desired range of 0.9 and 2.4 m (3 and 8 ft). Also, these curves are compared against cracking distribution developed for the same sites from computer results (using CRCP-5) for all the sections.

As pointed out before, the CRCP-5 program gives the cumulative probability for a particular combination of materials, design, and climatic conditions. The CRCP-5 plots were

superimposed on actual crack spacing distributions from the inservice CRC pavements from Iowa, Illinois, Pennsylvania, Oklahoma, and Wisconsin. Efforts were made to simulate the actual field data curves using the CRCP-5 program, but for all of the sections either the tensile strength of the concrete or coefficient of variation of concrete or both the parameters were modified in order to match the field data. However, past modeling efforts using CRCP-5 have predicted crack spacing distribution that are more closely spread than that indicated by the field data. The adjusted and unadjusted CRCP-5 analysis plots were superimposed on the pooled data curves. The reasons for any noted variation are provided in the later part of this chapter on site by site basis.

Detailed results of the crack spacing analysis are presented in appendixes as follows:

Appendix A - Illinois Sections
Appendix B - Iowa Sections
Appendix C - Oklahoma Sections
Appendix D - Pennsylvania Sections
Appendix E - Wisconsin

The following data are presented in the appendixes for each test section:

1. Field crack spacing distribution data for two 30.5-m (100-ft) subsections and pooled data.
2. Crack spacing distribution predicted by CRCP-5 for two assumed curing temperatures.
3. Crack spacing frequency.
4. Probability of cluster cracking (2, 3, and 4 consecutive cracks).

The following appendixes are also included:

Appendix F - Development of CRCP-5 Input Data (steel, concrete, and other material and climatic data)
Appendix G - Correlations of Cluster Ratios (results of correlations of cluster ratios with different attributes)
Appendix H - Correlations of Y Cracking (results of correlations of Y cracking with different attributes)

The average crack spacing and the cluster ratios determined for each test section are given in table 10. The lower the value of the cluster ratio (which is discussed later), the lower the incidence of cluster cracking.

Cluster Cracking

It is generally recommended in design that the crack spacing for CRC pavement should be selected such that the crack width is small enough to minimize the entrance of water and to provide the necessary load transfer through aggregate interlock. Consequently, cracking

Table 10. Field mean crack spacing values.
(0.305 m = 1 ft)

Section	Mean Crack Spacing, m (ft)	Standard Deviation of Crack Spacing, m (ft)	Cluster Ratio
IA-1	1.80 (5.89)	1.18 (3.87)	.55
IA-2	0.91 (2.98)	0.68 (2.24)	.42
IA-3	0.91 (2.98)	1.54 (1.76)	.23
PA-1	1.46 (4.80)	0.81 (2.67)	.17
PA-2	1.32 (4.32)	0.75 (2.47)	.22
OK-1	2.57 (8.44)	1.76 (5.78)	.85
OK-2	1.39 (4.57)	1.02 (3.37)	.32
OK-3	1.45 (4.75) Epoxy	0.91 (2.99)	.27
OK-4	1.94 (6.36)	0.98 (3.21)	.20
OK-5	1.87 (6.13)	1.02 (3.36)	.40
IL-1	1.55 (5.10)	1.07 (3.51)	.36
IL-2	1.29 (4.22)	0.81 (2.66)	.21
IL-3	1.09 (3.58)	0.64 (2.10)	.25
IL-4	0.65 (2.13)	0.36 (1.17)	.21
IL-5	0.92 (3.02)	0.64 (2.11)	.28
WI-1	0.88 (2.88)	0.69 (2.27)	.31
WI-2	0.88 (2.90) Epoxy	0.43 (1.42)	.24
WI-3	1.05 (3.46) Epoxy	0.48 (1.59)	.09
WI-4	1.40 (4.58)	0.68 (2.22)	.27
WI-5	1.03 (3.38)	0.57 (1.86)	.10

design criteria have evolved over time to include shorter cracking intervals. Early recommendations suggested design crack spacing should be between 1.5 and 2.4 m (5 and 8 ft) based on deflection test results and steel corrosion studies. Most recently the minimum crack spacing recommendation has changed to as low as 0.9 m (3 ft) based on load transfer and pavement stiffness requirements (9). The maximum crack spacing recommended to minimize spalling at the transverse cracks is a range between 1.8 to 2.4 m (6 to 8 ft). As pointed out previously, punchout distress may occur at a greater frequency in pavement sections with crack spacing of 0.3 to 0.6 m (1 to 2 ft). In spite of noted reinforcing steel effects in design, a certain percentage of crack spacing usually falls below the specified minimum crack interval. Consequently, a very short cracking interval as occurs in cluster cracking, has been recognized as an undesirable feature, especially for poor support conditions.

The percentage frequency of cracks occurring in clusters were calculated for all CRC pavement sample sections. The crack spacing frequency distribution was determined and given in appendixes A through E and grouped in crack spacing ranges of 0.6 to 0.9 m (2 to 3 ft), 0.9 to 1.2 m (3 to 4 ft), 1.2 to 1.5 m (4 to 5 ft), and 1.5 to 1.8 m (5 to 6 ft). This type of information provides an indication of the level of cluster cracking within each 305-m (1,000-ft) section. The crack spacing data were also plotted against the probability of two, three, or four consecutive cracks occurring within a certain distance.

Cluster cracking is a type of "distress" in CRC pavements. Consequently, cluster cracks typically will act as a locus for punchout development under repeated application of traffic loads particularly in area of poor subbase support. Stress in the reinforcement and the pavement may be higher in these groups of cracks possibly leading to wide crack widths and contributing to punchout distresses at these locations. Generally speaking, cluster cracks occur within a distance of 0.3, 0.6, or 0.9 m (1, 2, or 3 ft) intervals. The probability of two, three or four consecutive cracks were chosen for analysis of occurring within a range of distances to evaluate the evidence of cluster cracking manifest within a particular pavement segment. The probability was calculated for two consecutive cracks occurring within less than a 0.3-m (1-ft) distance, a 0.6-m (2-ft) distance and so on. Similarly, probabilities were calculated for other previously described combinations. A simple algorithm was developed to calculate the probability of cluster cracking. The crack spacing data from the different State survey data bases were used as a input to calculate the number of combinations that a certain number of consecutive cracks lie in less than 0.3-, 0.6-, 0.9-, and 1.2-m (1-, 2-, 3-, and 4-ft) distances. This algorithm also calculates the total number of combinations of possible consecutive crack combinations in a given population of cracks. The number of combinations is calculated by deducting (r - 1) from the total number of cracks where `r' is the number of consecutive cracks under consideration.

The probability of cluster cracking is the total number of combinations that a certain group of consecutive cracks lie within a certain distance divided by the total number of combinations. A graph is provided for each section illustrating the trend in the cumulative probability as it varies with the number of consecutive cracks in appendixes A through E. Prior to further discussion of the field results the following observations are made. It should be noted that cluster cracking for ideal CRC pavement cracking distributions (where the

pavement cracking is uniformly distributed) would appear for 2 consecutive cracks (at 0.6-m (2-ft) intervals) and 3 consecutive cracks as shown in figure 21. A characteristic of an ideal crack spacing distribution would be reflected in how well the curve for 2 consecutive cracks reflects the curve for 3 consecutive cracks (at the same intervals) if it were superimposed upon the curve for 3 consecutive cracks by doubling the crack distance interval at any probability. In other words, the curve for 2 consecutive cracks can, so to speak, be converted into a curve for 3 consecutive cracks by shifting the curve to the right the interval distance associated with the interval between two consecutive cracks.

Elaborating on this line of reasoning, the information provided in figure 21 for each sample section can be used to determine a "cluster ratio" to serve as a measure of cluster cracking manifest by a particular crack pattern. The cluster ratio can be found from dividing the crack distance interval for 3 consecutive cracks based upon doubling the crack interval distance associated with any probability along the curve for 2 consecutive cracks by the crack location (at the same probability) corresponding to the curve associated with 3 consecutive cracks and subtracting this quantity from one as shown below:

$$Cluster \quad Ratio = 1 - \frac{2 * X_1}{X_2} \tag{18}$$

where X_1 and X_2 are the crack distant intervals for 2 and 3 consecutive cracks, respectively. Cluster cracking is discussed later in the state by state analysis. The lower the cluster ratio the lower the evidence of cluster cracking in the crack pattern. Cluster ratios for various test sections are listed in table 10. As discussed later, it is recommended that cluster ratios be limited to less than 20 percent.

State by State Cracking Distributions

Illinois Sample Sections (Appendix A)

Five 305-m (1,000-ft) CRC pavement sections were selected in the State of Illinois as part of the detailed data collection. These sections are located in a wet freeze region. The IL-1 section was constructed in June 1990 with a permeable concrete base and is on US-51 South Bound. The IL-2 section was constructed in the year 1971 with a cement treated base and is located on I-72 West Bound. The IL-3 section was constructed in May 1976 with an asphalt treated base and is located on US-36 East Bound. The IL-4 section was constructed in year 1971 with an asphalt treated base and is located I-55 on East Bound. The IL-5 section was constructed in June 1986 with a lean concrete base and is situated on US-50 on West Bound.

The mean crack spacing for the IL-1 section is higher than the other Illinois sections. A permeable stabilized concrete subbase was used for IL-1 section and that this section was only a few months old. However, little guidance on the selection of frictional resistance for permeable stabilized subbases was available in the literature. Therefore, the value of frictional resistance listed in table 21 in appendix F corresponds to the crack spacing distribution that fit

the field distribution reasonably well. It is interesting to note that a relatively low frictional resistance resulted from this analysis which tends to indicate that a certain amount of "displacement" may occur prior to "interlocking" developing at the subbase interface. This hypothesis tended to be supported from the resulting higher mean crack spacing for the IL-1 section and from the possibility that the "interlock" effect may be manifest in the relatively higher cluster ratio for the IL-1 section. On this basis, a lower subbase frictional resistance was assigned to the IL-1 section in the analysis than other Illinois sections because of the type of subbase. Although some effect due to the asphalt treated subbase is noted, the primary factors for the low mean crack spacing for the IL-4 section may be due to the high curing temperature and low tensile strength of the concrete.

Crack distribution plots (figures 45, 46, 49, 50, 53, 54, 57, 58, 61, and 62) of the CRCP-5 analysis for Illinois sections tend to be on the high side of the field crack distribution curves. This trend for the sections with an asphalt treated subbase may indicate that the listed friction resistance is too low for these sections. Also, all the sections may have been subjected to curling conditions at a greater temperature than that listed for these projects.

Figures 48, 52, 56, 60, and 64 show the crack spacing frequency and probability of cluster cracking curves for the Illinois sections. It appears from the above figures that only one or two of the Illinois sections indicate strong cluster cracking. The higher curing temperature, noted in appendix F, may have caused a lower average crack spacings in IL-4 and IL-5 sections. No strong trends appears between the crack spacing frequency distributions and the cluster cracking characteristics of the Illinois sample sections. The remaining figures in appendix A for measured crack widths will be discussed in chapter 4.

Iowa Test Sections (Appendix B)

Three 305-m (1,000-ft) sections were selected from different CRC pavements in the State of Iowa. The section IA-1 was constructed in the year 1971 on a cement treated subbase and is located on I-29 North Bound, the section IA-2 was constructed in the year 1969 on an asphalt treated subbase and is located on I-80 West Bound, and the Section IA-3 was constructed in the year 1976 on an asphalt treated subbase and is located on I-380 North Bound.

The percent of longitudinal steel was same for all the sections. The field mean crack spacings for these sections were listed in table 10. The mean crack spacing is same for IA-2 and IA-3 sections which are lower than the mean crack spacing of IA-1 section. In light of the subbase types and the curing conditions listed for these sections, the crack pattern trends are not easily explained. However, even though a lower tensile strength is associated with the IA-2 and IA-3 sections (as noted in appendix F) but it is difficult to attribute the entire magnitude of the differences in the field and predicted cracking trends to this alone.

Upon comparison of the CRCP-5 results (figures 71, 75, and 79) for all the Iowa sections, the prediction curves are on the high side of the field curves. Ideally the field and prediction curves should overlap each other. The IA-1 simulated results (figure 71) do not as

match well with the field results as the match indicated with other two Iowa test sections (figures 75 and 79). The field data provided for each section were used to the extent possible. Since the was some uncertainty in the curing temperature, a range of temperatures were analyzed to bracket the possible analytical results. None of the Iowa sample sections fell within these limits. It is not entirely clear why the fit is not better than illustrated.

The concrete elastic modulus, compressive strength, and flexural strength of the concrete were assumed to be related to the tensile strength of the concrete. Graphs illustrating the crack spacing frequency and probability of cluster cracking are shown for these sections. The crack spacing frequency data indicate the number of cracks that occur within certain crack spacing ranges. The cluster cracking data indicates the probability of a certain number of cracking occurring within a given interval. The comparison of the crack spacing frequency distribution and probability of cluster cracking (figures 73 and 77) shows that the IA-1 and the IA-2 sections display the greatest amount of cluster cracking. The cluster ratio is tabulated (as is the mean crack spacing and the standard deviation of cracking) for each section shown in table 10.

A significant amount cluster cracking was determined for the IA-1 and IA-2 sections. The curing temperature and the cracking standard deviation apparently may be related to the potential of cluster cracking. The IA-1 section had a higher curing temperature and a crack spacing standard deviation than the other two Iowa pavement sections. However, temperature at curing seems to show only a moderate correlation to cluster cracking. Pavements that typically are cured at higher temperatures have a shorter average crack spacing than those cured at lower curing temperatures. Figure 72 for IA-1 section reveals that nearly 8 percent of the cracks are in the 0.6- to 0.9-m (2- to 3-ft) range. Figure 73 (cluster cracking) shows that the change in the probability of two consecutive cracks occurring within the range of crack locations is not evenly distributed as it is in section IA-2 or IA-3 (particularly for two and three consecutive cracks) both of which contained asphalt treated bases. What also worth noting is the character of the frequency distribution of the crack spacing shown in figure 73 and 77 with high cluster ratios to figure 81 manifesting a lower cluster ratio. Even though ambient temperature condition at the time of construction has some affect on cluster cracking, some interaction is also apparent due to subbase type (where granular bases tend to be the least contributory).

Oklahoma Sample Sections (Appendix C)

Analysis was done for five 305-m (1,000-ft) sections in Oklahoma. The OK-1 section was constructed in October 1987 and it was opened to traffic in March 1989. This section is located on I-40 West Bound. OK-2 section was constructed in August 1986 and is located on US-69 North Bound. This section was opened to traffic in September 1988. OK-3 is located on I-35 North Bound and it was constructed in August 1988. The traffic was permitted in May 1989 on this Interstate. OK-4 section was constructed in May 1984 and was opened to traffic in August 1985. This section is located on US-69. The OK-5 section is located on I-40 East Bound and was constructed in May 1989. This pavement was opened to traffic in November 1990.

The field mean crack spacing is very high for OK-1 section. The field mean crack spacings are also comparatively high for OK-2 and OK-3 sections. Sites OK-1 through OK-3 consisted of a asphalt treated subbase. Permeable concrete was used as the subbase material for OK-5 section. The OK-1 section was constructed at a time when the temperatures were very low and this may have contributed to the large average crack spacing observed in this pavement section.

Figures 84, 88, 92, 96, and 100 show the crack distribution plots for Oklahoma sections. The plots show that the numerical results for sample section OK-4 and OK-5 nearly matched the field data. But the curves for other sections were not close to the field data.

Figures 85, 86, 89, 90, 93, 94, 97, 98, 101, and 102 gives the percentage frequency and cluster cracking probability plots for Oklahoma sections. Cluster cracking is evident in the OK-1 and the OK-2 sample sections. The crack spacing distribution displayed in these two sample sections are similar to the one shown in the IA-1 sample section and appears to be undesirable cracking distribution.

Pennsylvania Sample Sections (Appendix D)

Two 305-m (1,000-ft) sections were selected from two CRC pavements in the State of Pennsylvania. These sections are located in wet and freeze zones. The PA-1 section was constructed in the year 1976 and is located on I-180 East Bound. The PA-2 section is located on I-81 North Bound. A granular material was used as a subbase for both the sections.

Comparison of CRCP-5 results and field data (figures 109 and 113) shows that the numerical results for the PA-1 test section nearly matched the field data. The PA-2 CRCP-5 curve is not as close to the field curve when compared to PA-1. Again it is not clear why in one case the fit is adequate whereas in the other the comparison is not satisfactory. Even though sections PA-1 and PA-2 had 0.45 and 0.55 percent steel, respectively, no potential problems related to performance were noted in the data collected from these sites.

Comparison of probability of cluster cracking (as indicated by the cluster ratio) and cracking spacing frequency results (figures 110, 111, 114, and 115) of the Pennsylvania sections shows that the PA-1 section has a lower level of cluster cracking than the crack pattern in section PA-2. However, based on the characteristics of figure 110 (a gap in crack intervals occurring between 0.9 and 1.2 m (3 and 4 ft)), one may expect a high cluster ratio to result.

Wisconsin Sample Sections (Appendix E)

Five 305-m (1,000-ft) sections were selected for analysis from different CRC pavements in Wisconsin. WI-1 section was constructed in year 1973 and is located on I-43 North Bound. WI-2 section was constructed in the year 1985 and is located on I-90 East Bound. WI-3 and WI-4 sections were selected from I-90/94 West Bound and was constructed in the year 1984. WI-5 section was constructed in the year 1975 and is located on I-90/94 East Bound. Figures 118, 122, 126, 130, and 134 shows the plots of CRCP-5 analysis. It appears

a good fit resulted between the predicted and field crack distribution except for the sample section WI-4.

It is appears from the percentage frequency and cluster probability plots (figures 119, 120, 123, 124, 127, 128, 131, 132, 135, and 136) that the WI-2 and 4 show the greatest amount of cluster cracking. Little can be stated as to how the frequency distribution corresponds to the tendency of cluster cracking within a given crack pattern for a CRC pavement. However, based on this data by itself, it is difficult to indicate if epoxy-coated rebar causes any detrimental effects on cluster cracking or the development of poor crack pattern characteristics.

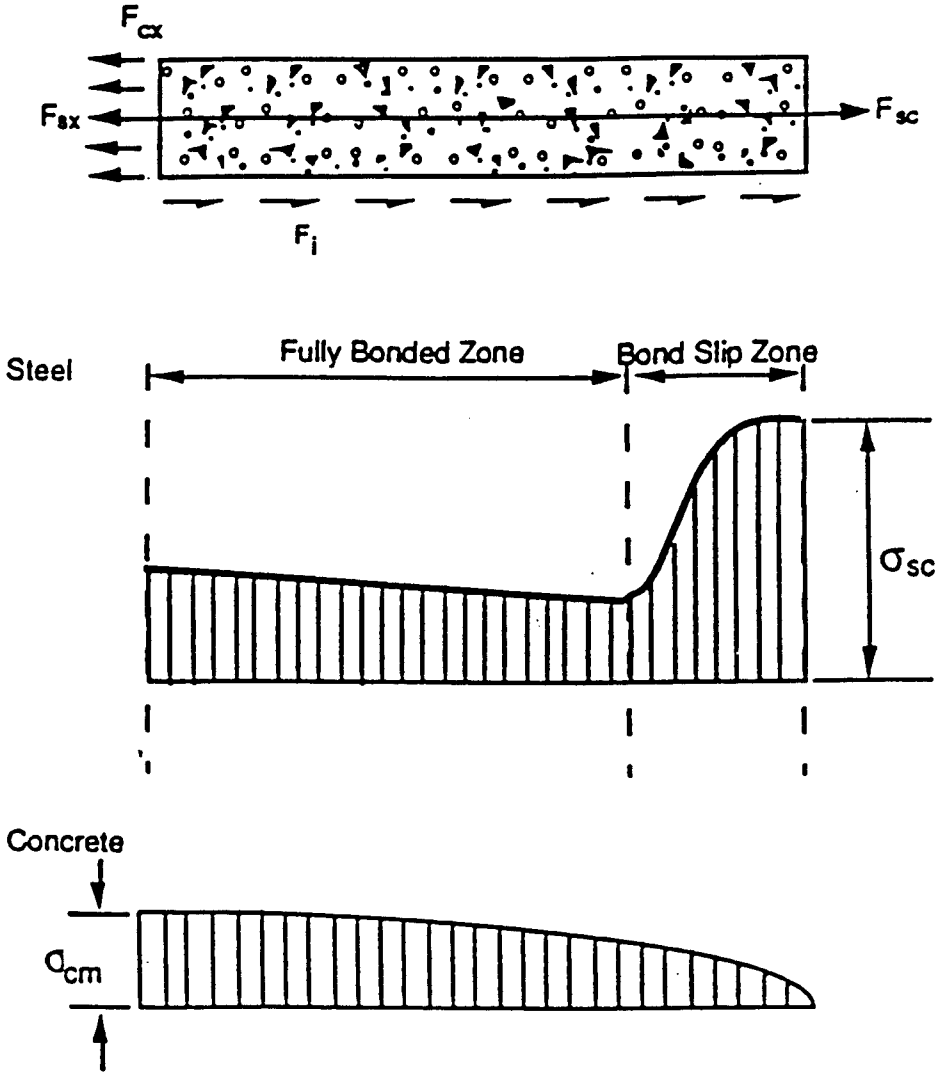

Figure 20. Freebody of CRCP segment and stress distribution in the concrete and steel.

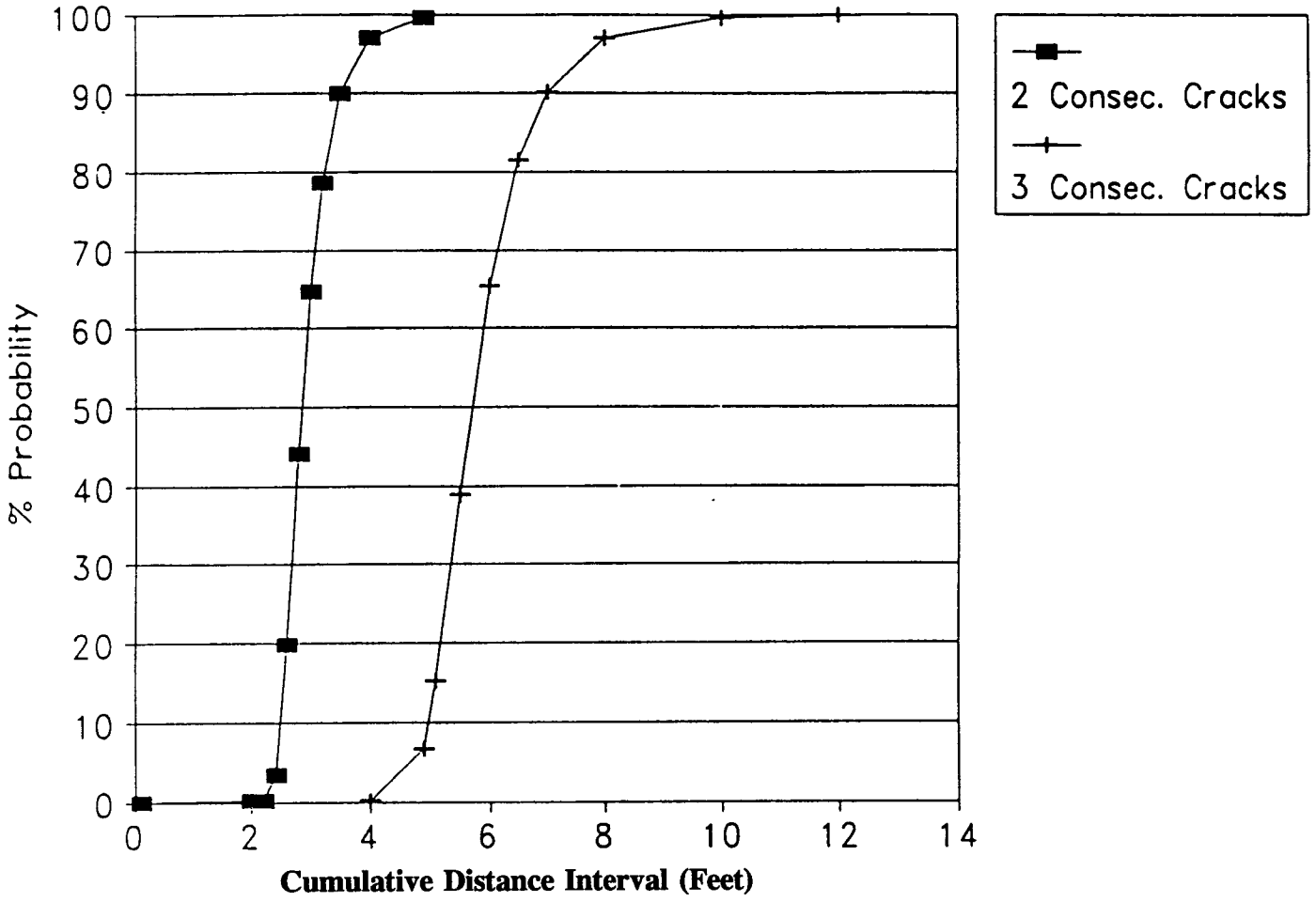

(0.305 m = 1 ft)

Figure 21. Ideal CRC pavement cluster cracking probability.

CHAPTER 4 - ADDITIONAL EVALUATION OF CRACK SPACING DATA

General

In this chapter further analysis of the collected field data is accomplished in terms of the variation of crack width and variations in parameters associated with the crack spacing characteristics (i.e., Y cracking, cluster ratio, etc.). This variation is examined with respect to pavement thickness, tied-concrete shoulders, permeable subbases, epoxy-coated reinforcement, amount of steel reinforcement, and other design parameters. The characterization of the data, as presented in chapter 3, with the respect to cumulative crack distributions and cluster cracking will be useful in this regard.

Crack Width and Crack Spacing

Crack width and crack spacing are characteristically thought of as indicators of pavement performance. Although Zuk developed a theoretical relationship between these two parameters as a function of steel percentage, concrete shrinkage, and temperature coefficients, other parameters such as pavement age and depth of steel cover may also be important.[7] Each of these factors is examined in light of the data that were collected at each sample site; some of which are included in the Zuk expression for crack width:

$$cw = L*(z + \alpha_c t_t) - \frac{\sigma_f}{E_c} * L - \frac{d_b \sigma_f}{4up} \quad (19)$$

where L = Crack spacings
z = Drying shrinkage
α_c = Concrete coefficient of thermal expansion
t_t = Temperature drop at level of steel curing temperature - pavement temperature at time of measurement
d_b = Steel reinforcement diameter
p = Percent reinforcement
u = Bond strength of concrete
σ_f = Concrete tensile strength
Ec = Concrete modulus of elasticity

Crack width measurements from the Illinois, Oklahoma, and Wisconsin test sections were considered for detail analysis. The crack width measurements were taken at the sections in the morning and in the afternoon. The crack widths measurements taken in the morning hours were typically greater than the crack width measurements taken in the afternoon.

Table 11 shows the average crack widths for several measurements taken in both the morning and afternoon time periods. It can be observed from table 11 that the WI-1 section has the higher average crack width. The average crack spacing for WI-1 section is 0.88 m

(2.88 ft). Because of the lower average crack spacings for WI-1 section, the lower average crack width would be expected for this section. The size of the longitudinal bar used for this section was #4. This may have caused cracks to become wider. The IL-1 section has the lower crack width. The IL-1 section has the largest percent of longitudinal steel when compared to all the other sections when the crack widths were measured. IL-1 was also only a few months old when tested.

The variation of crack width with crack spacing and variation of average crack width/crack spacing ratio with percent reinforcement, pavement age, and depth of cover is shown in figures 65 to 68, figures 103 to 106, and figures 137 to 140 for Illinois, Oklahoma, and Wisconsin test sections, respectively. A small difference is noted in between the theoretical crack width found from Zuk's expression for crack width (w) and the measured crack widths. It is interesting to note how well the theoretical expression predicts the trend in crack widths as a function of steel percentage and steel spacing. The area of steel reinforcement is also important but only affects the crack width indirectly in how in affects the actual crack spacing.

The crack width trend is as expected with respect to steel percentage as shown in figure 67 and is similar to crack width and crack spacing shown in figure 65. Figure 67 shows an increase in crack width with pavement age. The trends with respect to traffic (accumulated ESAL noted in parenthesis) seem to show a similar trend, however some anomalies are associated with both of these trends. The trends shown in figure 68seem to be generally unexpected which suggest indirectly that the depth of cover does not affect crack width. The trends in measured crack width data for Oklahoma and Wisconsin (figures 103 to 106 and 137 to 140) show similar characteristics as the crack width curves for the Illinois sections and tend to be well represented by Zuk's crack width model. Crack width versus pavement age appeared to show a strong effect. WI-2, WI-3, and OK-3 contained epoxy-coated rebar but the crack width trends with the design parameters noted above that were observed in these sections did not appear to be significantly different from the trends observed in the sections containing conventional reinforcement.

From observation of the field data illustrated in figure 22, the tensile strength of the concrete appears to have some effect on the cumulative crack spacing distribution. Although a considerable amount of scatter exists in this figure, theoretical models suggest that the trend in data of this nature must indicate an increase in mean crack spacing as the concrete strength increases. Therefore, as the tensile strength of the concrete increases, the average crack spacing tends to increase according to the illustrated data. Figure 23 indicates the curing temperature has little effect on the average crack spacing within the ranges included in this study. One would expect that the lower the curing temperature, the greater the average crack spacings. However, it appears that even though curing temperatures may affect the early age crack spacing pattern, the long-term crack pattern does not appear to be affected by the curing temperature. The cement treated base designation in these figures includes both CTB and lean concrete bases.

Table 11. Average crack width data for Illinois, Oklahoma, and Wisconsin sections.
(0.305 m = 1 ft) (25.4 mm = 1 in)

Test Section (30.5 m (100 ft))	Average Crack Width (0.01 mm)	
	Morning	Afternoon
IL-1	22	16
IL-2	57	44
IL-3	48	42
IL-4	35	27
IL-5	29	22
OK-1	63	44
OK-2	48	38
OK-3	54	44
OK-4	76	70
OK-5	45	39
WI-1	91	69
WI-2	58	27
WI-3	54	41
WI-4	63	45
WI-5	46	28

Cluster Ratio and Y Cracking

The definition of the cluster ratio was provided in chapter 3 and is based upon the characteristics of the crack pattern being distinct from the distress of Y cracking. The cluster ratio is tabulated (as is the mean crack spacing and the standard deviation of cracking) in table 10 for a majority of the test sections included in the study. The utility of the cluster ratio will be presented later in this section. However, it is also worthwhile to point out that the percent of Y cracking (number of cracks associated with a Y crack divided by those which are not in a given crack pattern multiplied by 100) may also be useful in CRC pavement evaluation analysis. Discussion is provided below to assess the correlation of these parameters to depth of steel cover, curing conditions, as other design characteristics in terms of subbase type.

Appendix G was prepared to provide a summary of possible correlations taken from the collected data base of cluster ratio to the above mentioned characteristics. Cluster ratios are plotted for different subbase types included in the pavement samples versus curing temperature, standard deviation of crack spacing, mean and standard deviation of depth of steel cover, percent of reinforcement, and total shrinkage strain in the figures illustrated in appendix G. It is interesting to note that the trend in the cluster ratio versus curing temperature is not particularly strong but is with respect to deviation of crack spacing. This appears to be characteristic of the trend line indicating the variation in mean crack spacing with curing temperature noted previously in figure 23. Other illustrated comparisons show varying correlation strengths. Correlation of cluster ratio to depth of cover indicated some correlation while correlations between cluster ratio and standard deviation of steel cover and percent of reinforcement was very low.

It is not surprising that a reasonably strong correlation is evident between the cluster ratio and the standard deviation of crack spacing. The illustrated trend suggests that as the deviation in crack spacing increases so does the cluster ratio. The other strong trend is indicated with total shrinkage strain as determined from the sample crack width measurements. As the total strain (i.e., drying shrinkage) increases, reduction in cluster ratio results (as the crack density increases). Assuming that a minimum tolerable cluster ratio can be established based upon certain performance criteria (i.e., ride quality, punchouts described in failures per mile (FPM)), it may be possible to suggest that a given level of drying shrinkage should be "allowed" to occur in order to maximize performance of the pavement. This concept tends to suggest a need to "manage" concrete pavement curing (i.e., time of curing placement, type, etc.) to achieve predetermined desired results that ultimately affect the long term performance of the pavement.

Similar comparisons as those made with cluster ratio were also illustrated in appendix H with respect to Y cracking again in terms of different subbase types. Of these comparisons, none of them were particularly strong, however two of them are noteworthy. Y cracking decreases as the depth of steel cover increases. It is also interesting to note that the trend in cluster ratio with this parameter indicated a distinctive opposite effect. A similar circumstance exists with the comparison of Y cracking to total shrinkage strain. Although, only a moderate correlation exists, the trend in Y cracking is again opposite that of cluster ratio. The percent

of Y cracking is listed for each sample section in table 12. No strong correlations appeared with respect to subbase type to percent Y cracking.

It is also important to note the correlation of the standard deviation of steel cover with the depth of steel cover illustrated in figure 24. As has been noted in previous studies, as the depth of steel cover increases so does the variability in depth of cover. In fact, there appears to be little difference in whether the method of placement was by either the use of chairs or by tube feeding procedures. Although, it is not illustrated, there was some correlation between pavement thickness and the deviation in steel cover. As the thickness increased, the deviation in steel cover increased. However, it should be noted that little correlation existed between the pavement thickness and the cluster ratio.

In light of these observations and those indicated in the above figures and in appendices G and H, it does not appear that any one type of subbase included in this study stands out in causing more cracking related distress or a form of potential distress than any of the other subbase types. The evaluation of permeable subbase pavements indicate that they have no more potential for cluster cracking (table 10) than other subbase types.

As shown in figure 25, which illustrates cluster ratios for the SH-6 CRC pavement study sites located in Houston, Texas, the cluster ratio is also sensitive to aggregate type. These sections, which contained both winter and summer placements, consisted of 279 mm (11 in) CRC pavement placed on a 152 mm (6 in) CTB with an AC bond breaker using a single mat of deformed reinforcing steel. Although several items of interest are shown in this figure, one conclusion, based on this data, appears to suggest that the river gravel tend to produce lower amounts of cluster cracking if placed under winter conditions. Steel percentage may have some effect on controlling the amount of cluster cracking that a pavement may experience but the trends indicated in appendix G did not appear to be strong. Aggregate type for the test sections is shown in table 12.

Punchout Related Performance

Pavement performance predictions varied widely across all sections. They are summarized in figure 26 in terms of the number of failures per mile (FPM). The average crack spacing can be an important factor in the overall performance of a CRC pavement system. It appears from the trend indicated in figure 26 that the mean cracking interval should be at least 1.2 to 1.5 m (4 to 5 ft) to minimize the incidence of punchout distress. Other factors are also involved in the development of this type of distress. However, it is evident that characteristics of the crack pattern such as mean crack spacing, standard deviation in crack spacing, and pattern uniformity should not be overlooked in the construction of quality CRC concrete pavements.

Information illustrated in the performance figures referred to above was compared to the calculated cluster ratios and noted Y cracking in figure 27. Although the scatter in the plotted data is quite wide, there is some indication that both the cluster ratio and the percent Y cracking should be kept below a limit of 20 percent to enhance the level of performance of the

Table 12. Percent Y cracks data.
(0.305-m = 1 ft)

Test Section (30.5-m (100-ft))	Percent Cracks	Base Type	Aggregate Type
IL-1	4	Permanent CTB	Crushed Stone
IL-2	18	CTB	Crushed Stone
IL-3	17	ATB	Crushed Stone
IL-4	15	ATB	Crushed Stone
IL-5	18	LCB	Crushed Stone
OK-1	19	ATB	Crushed Stone
OK-2	7	ATB	Crushed Stone
OK-3	12	ATB	Crushed Stone
OK-4	3	Soil-Asphalt	Crushed Stone
OK-5	2	Permanent CTB	Crushed Stone
WI-1	23	Granular	Stone (Quartz)
WI-2	10	Granular	
WI-3	7	Granular	
WI-4	10	Granular	
WI-5	13	Granular	
PA-1		Granular	Crushed Gravel
PA-2		Granular	Crushed Gravel

pavement system. Environmental conditions are indirectly inferred as significant factors from the correlations illustrated in appendixes G and H. Management of the pavement curing process during construction is one measure which can be taken to minimize both the cluster ratio and the percent Y cracking.

Summary of Observations

It appears that the crack space distribution can be predicted to some extent. However, a certain amount of variation occurs which is not entirely explainable on the basis of information obtainable for this study. None of the design features of interest (i.e., thickness, tied-concrete shoulders, permeable subbases, epoxy-coated rebars, and the percent of steel reinforcement) indicated a particularly strong influence in any of the correlations considered in this analysis probably because of the small number of sections included in this study. However, the most useful approach in determining the influence of any of these design features may be through examination of the effect each may have on the resultant crack pattern (except for tied shoulders).

Pavement Thickness

The effect of pavement thickness appeared to be well represented in the Zuk equation for crack prediction. Thicker CRC pavement tends to manifest greater degrees of steel cover variability which leads to greater cluster ratios and crack space deviations. Any gains obtained from thicker pavement sections performance-wise may be offset by lower quality crack patterns if steel placement is not adequately controlled. Pavement thickness requirements are determined based on design considerations which are thoroughly discussed in reference 9. However, it is well to point out that load transfer capacity of a CRC pavement system is a function of the thickness design and the resulting widths of the transverse cracks. Normal variability in crack width (coefficient variation of 10 to 15 percent) can be offset by increasing the thickness of CRC pavement on the average by one inch.

Permeable Bases

The effect of subbase type was examined in several ways in this study. In most comparisons, the permeable bases tended to have higher cluster ratios than the other sections. However, so did the other factors the cluster ratios were correlated with. Even in those comparisons where climatic related factors were involved, pavements constructed with permeable bases fell within the data trends. Therefore, it is suspected that the effect of permeable bases on development of poor crack patterns is less significant that of climatic conditions. The potential negative impact on the cracking pattern from the use of permeable subbases was not evident in the data base collected from the sample sites. However, based on experience in Texas, the restraint causes by high friction interfaces at the boundary between a main slab and a stabilized base has significantly affected the resulting crack pattern. For this reason, the standard of using an asphalt bond breaker was adopted in Texas to alleviate this negative effect.

Epoxy-Coated Reinforcement

The effect of epoxy-coated reinforcement appeared to be minimal on the various crack pattern characteristics identified in this study. No distinguishing features regarding the trends examined in the plotted data with respect to epoxy-coated rebars could be identified.

Percent Steel Reinforcement

In the analysis of the characteristics of the various crack patterns, no identifiable trends were noted. This would suggest that in terms of methods to control or improve the crack pattern, technology focusing on the variation of steel percentage may not be as sensitive as methods which focus on improved quality construction and variability. However, this conclusion is qualified for the range of conventional concrete strengths and the range of steel amounts considered in this study. The use of higher concrete strength in conjunction with higher steel amounts needs to be investigated. Such a design may greatly alleviate crack spalling and minimize punchout related distresses.

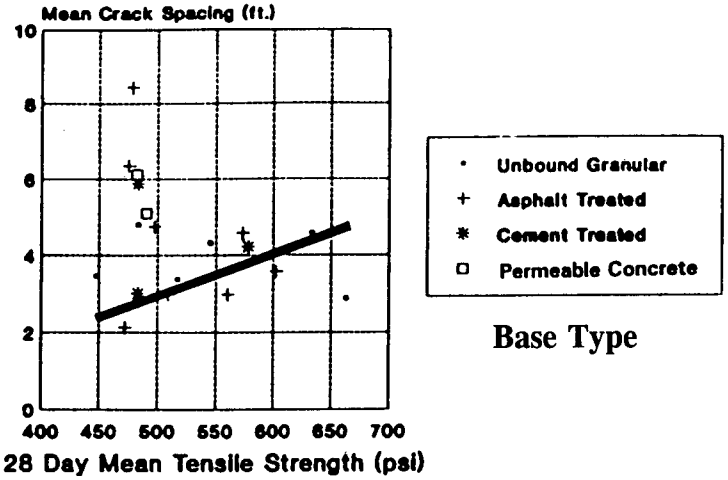

(0.305-m = 1 ft) (6.89 kPa = 1 lbf/in^2)

Figure 22. Correlation of concrete strengths and mean crack spacing.

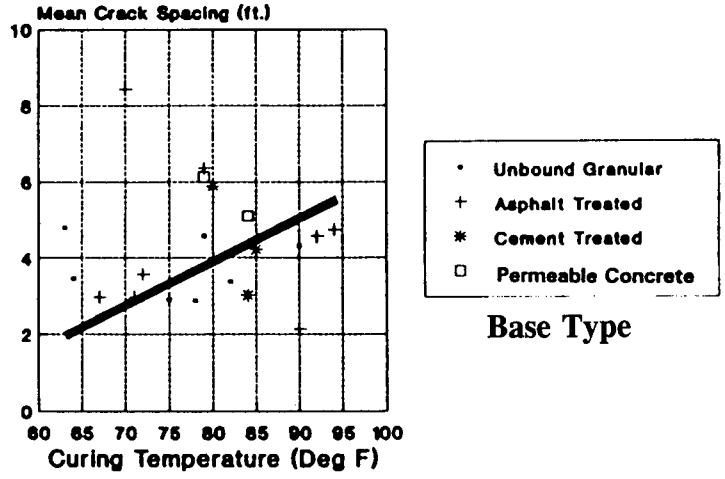

(0.305-m = 1 ft) (0.6 °C = 1 °F)

Figure 23. Correlation of mean crack spacing to curing temperature.

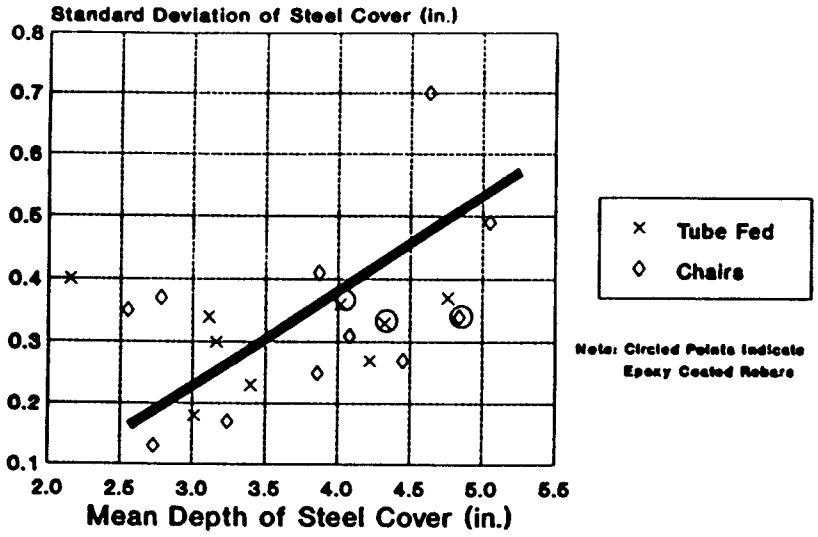

Figure 24. Variation in standard deviation of steel cover with mean depth cover. (25.4 mm = 1 in)

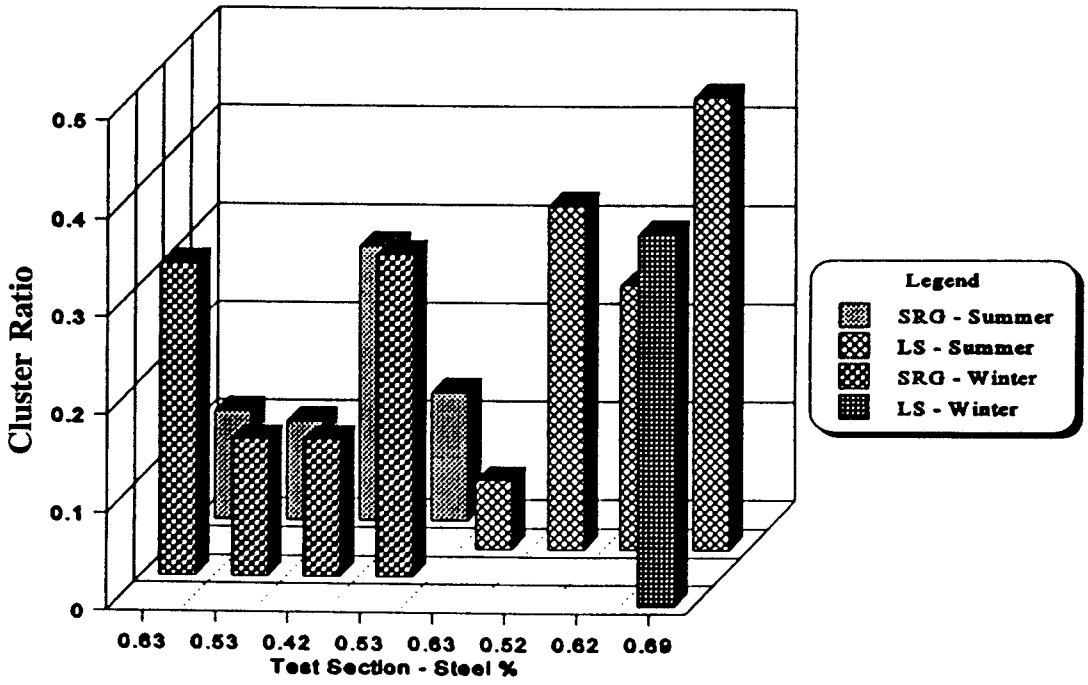

Figure 25. Texas sample sections: Cluster ratio versus aggregate type.

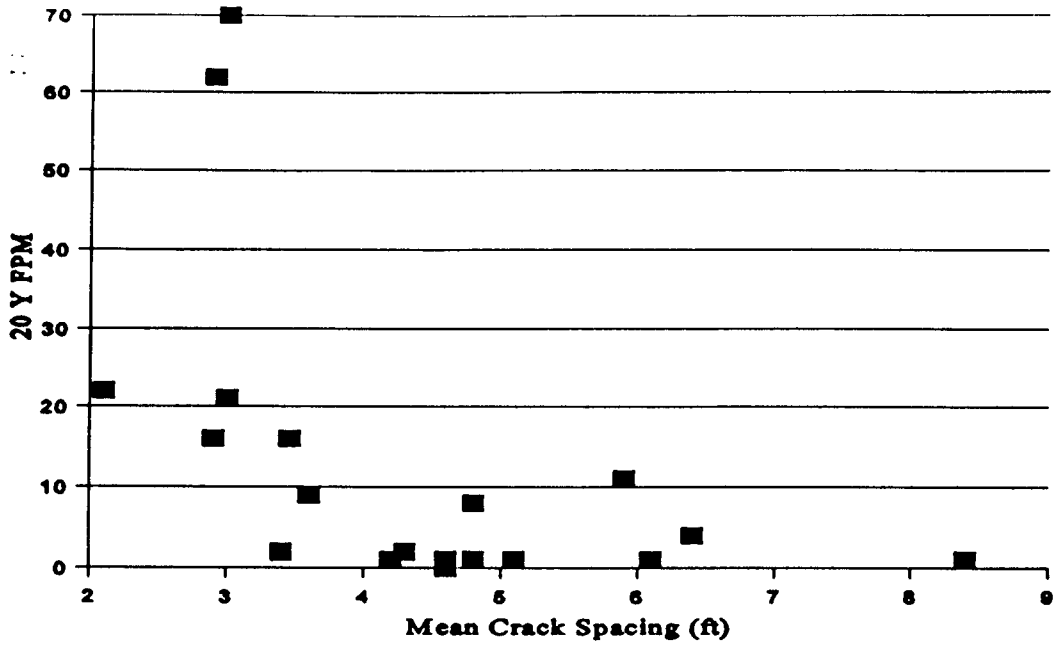

Figure 26. 20 year FPM as a function of mean crack spacing. (0.305 m = 1 ft)

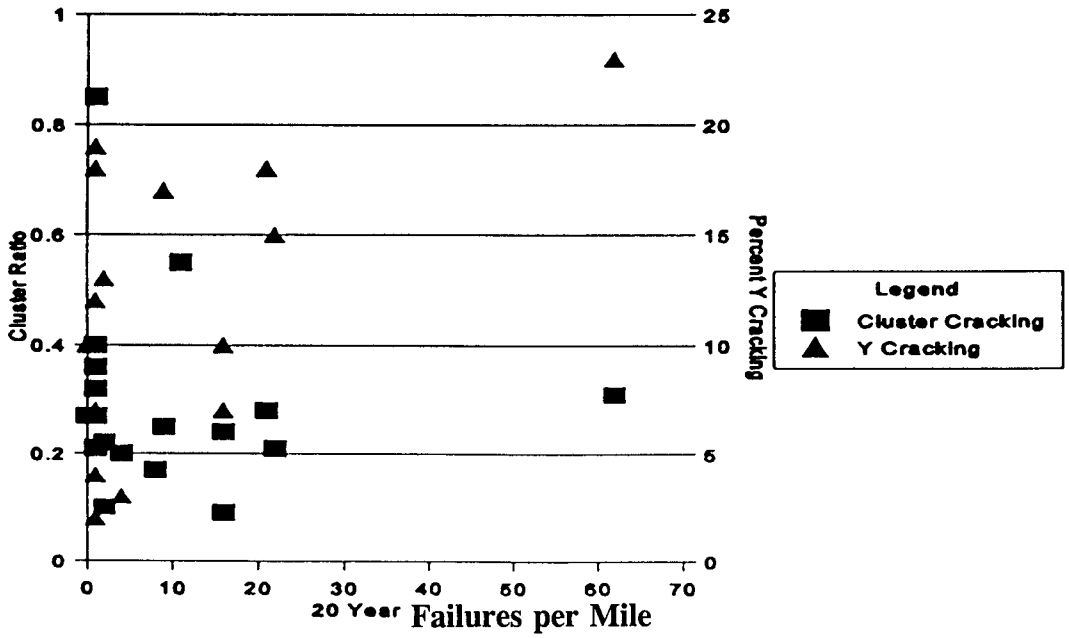

Figure 27. Correlation of cluster ratio and Y cracking to CRC pavement performance.

CHAPTER 5 - ANALYSIS OF GPS-5 DATA

Introduction

During the early 1980's, the Transportation Research Board (TRB) of the National Research Council, under the sponsorship of the Federal Highway Administration (FHWA) and with the cooperation of the American Association of State Highway and Transportation Officials (AASHTO) undertook a thorough study of the deterioration of the nation's highway and bridge infrastructure system. The study recommended that a Strategic Highway Research Program (SHRP) be initiated to focus research and development activities that would make major contributions to improving highway transportation. The study report published as TRB Special Report 202 during 1984, emphasized six research areas, with the Long Term Pavement Performance (LTPP) program as one of the key research areas. During 1985 and 1986, the detailed research programs were developed for SHRP by independent contractors. The detailed programs were published in May 1986 as a TRB Report entitled, "Strategic Highway Research Program - Research Plans."

The Long Term Pavement Performance was envisioned as a comprehensive program to satisfy "the total range of pavement information needs." It draws on "technical knowledge of pavements presently available and seeks to develop models that will better explain how pavements perform. It also seeks to gain knowledge of the specific effects on pavement performance of various design features, traffic and environment, use of various materials, construction quality, and maintenance practices." As sufficient data becomes available with time, analysis will be conducted by various agencies to provide better performance prediction models for use in design and pavement management, to provide much better understanding of the effects of many variables on pavement performance, and to provide new techniques for pavement design and construction.

The LTPP Program incorporates two primary types of studies. The General Pavement Studies (GPS) involve 800 in-service pavement test sections throughout the U.S. and Canada. The Specific Pavement Studies (SPS) are intensive studies of few specific variables involving new construction, maintenance treatments, or rehabilitation activities.

The General Pavement Studies include the following experiments:

GPS-1 - Asphalt Concrete (AC) on Granular Base
GPS-2 - AC on Bound Base
GPS-3 - Jointed Plain Concrete
GPS-4 - Jointed Reinforced Concrete
GPS-5 - Continuously Reinforced Concrete
GPS-6A - Existing AC Overlay on AC Pavements
GPS-6B - New AC Overlay on AC Pavements
GPS-7A - Existing AC Overlay on Portland Cement Concrete (PCC)
GPS-7B - New AC Overlay on PCC Pavements
GPS-9 - Unbounded PCC Overlays on PCC Pavements

This report presents a summary of the data collected to date for the GPS-5 experiment related to CRC pavements. A preliminary analysis of the data is also presented to identify key factors that affect the behavior and performance of CRC pavements.

The GPS-5 Experiment

Pavements in the GPS-5 experiment include continuously reinforced portland cement concrete pavements placed directly on a base layer or upon unstabilized coarse grained subgrade. One or more subbase layers can exist but were not required. A seal coat (prime coat) is also permissible just above a granular base layer.

Sampling template factors and levels for GPS-5 are summarized below:

Moisture:	Wet (Refer to figure 1) Dry (Refer to figure 1)
Temperature:	F - Freeze (Refer to figure 1) NF - Non-Freeze (Refer to figure 1)
Subgrade Type:	F - Fine C - Coarse
Traffic Rate:	L - Less than 300 KESAL/Year H - Greater than or equal to 300 KESAL/Year
Percent Reinforcing:	L - Less than or equal to 0.61 percent G - Greater than 0.61 percent
PCC Thickness:	L - Less than 216 mm (8.5 inches) H - Greater than or equal to 216 mm (8.5 inches)

The sampling template for GPS-5 is shown as table 13.

Experimental Design Philosophy

The development of the experimental design of each specific experiment of the GPS and the SPS was based on identifying factors considered to have significant influence on pavement performance. Three factors were selected as a basis of the sampling factorials and were defined as qualitative (distinct levels) or quantitative (continuous numerical levels). The qualitative factors used in most of the GPS and SPS experiments include the following:

1. Moisture conditions - wet or dry
2. Temperature conditions - freeze or non-freeze
3. Subgrade type - fine or coarse

The generalized moisture and temperature zones defined for the LTPP program are shown in figure 28. A wet zone is one having annual precipitation greater than 508 mm

Table 13. Sampling template for GPS-5.

MOISTURE		WET								DRY							
TEMPERATURE		FREEZE				NO FREEZE				FREEZE				NO FREEZE			
SUBGRADE TYPE		F		C		F		C		F		C		F		C	
TRAFFIC RATE		L	H	L	H	L	H	L	H	L	H	L	H	L	H	L	H
PCC THICKNESS	% REINFORCEMENT																
L	L	1	5	9	13	17	21	25	29	33	37	41	45	49	53	57	61
	H	2	6	10	14	18	22	26	30	34	38	42	46	50	54	58	62
H	L	3	7	11	15	19	23	27	31	35	39	43	47	51	55	59	63
	H	4	8	12	16	20	24	28	32	36	40	44	48	52	56	60	64

Factor Midpoints:

Traffic Rate	300 KESAL/Year
% Reinforcement	0.61%
PCC Thickness	216 mm (8.5 inches)

(20 in.). A freeze zone is one having annual air freezing index greater than 83 °C-Days (150 °F-Days). A subgrade is defined as being fine if it has more than 50 percent material passing the #200 sieve.

For the quantitative factors for GPS, mid-points were established for these factors based on expected numerical ranges, so that all values below the mid-point were considered low and all values above the mid-point were considered high. The qualitative factors vary for each GPS experiment and in general include factors such as layer thicknesses and traffic levels. Two distinct levels were defined for all GPS quantitative factors with the exception of three levels (low, medium, and high) for asphalt concrete thickness in GPS-1.

Test Section Layout

Each test section in the GPS-5 experiment consists of a 152 m (500 ft) monitoring length and a 15.2 m (50 ft) section at each end of the monitoring length used for material sampling. The overriding philosophy of the LTPP program is not to permit any destruction sampling within the 152 m (500 ft) monitoring length of the section. The monitoring lengths are used for collecting the specific monitoring data (FWD, profilometer, surface distress, skid (friction), and transverse profile) at each site.

LTPP Data Collection and Storage

The LTPP program involves extensive data collection. The following data are collected for each test section.

1. Inventory
2. Materials Testing
3. Climatic
4. Maintenance
5. Rehabilitation
6. Traffic
7. Monitoring (Falling Weight Deflectometer (FWD), profilometer, surface distress, friction, and transverse profile)

Data are collected for each test section by Regional Contractors (funded initially by SHRP and since 1992, by FHWA). The Regional Contractors also perform deflection and profile testing and conduct manual pavement distress surveys. Photographic distress surveys are performed by another Contractor.

To ensure uniform and consistent data collection and construction, detailed guidelines have been prepared and implemented. These guidelines incorporate collection of inventory data, traffic data, monitoring data, materials testing data, and maintenance and rehabilitation data. Details of various data collection requirements are given in References 9, 10, 11, and 12.

Each of the seven LTPP data modules is composed of numerous tables, with each table representing a collection of related information. The tables contain individual records that store information for a specific pavement test section, layer, etc. LTPP data are stored in the National Information Management System (NIMS) located at TRB in Washington, DC. The data base is expected to evolve during the course of the LTPP program to accommodate the data collected and the needs of researchers as they are identified. LTPP data are available to the public only from the NIMS. Before any data are released to the public, a series of quality assurance checks are performed to ensure the integrity of the data.

New and updated data from the LTPP IMS are released once a year. The 5th public release of the LTPP IMS data took place during August 1993.

Summary of GPS-5 Data

At the time of the 5th public release of LTPP IMS data (August 1993), the status of GPS-5 was as follows:

	No. of Sections
Wet-Freeze Region	35
Wet-No Freeze Region	36
Dry-Freeze Region	7
Dry-No Freeze Region	7
Total	85

Four sections have been released, were overlaid and are now being monitored as part of GPS-7B - New AC Overlay on PCC Pavements. The test sections range in age from 1.7 to 28.5 years (as of January 1992) and can be found in 29 States. Texas has the largest number of test sections - 19. A summary of the GPS-5 data is given in table 14.

Inventory/Climatic Data Summary

The following data is summarized in a graphical form:

Figure 29 - Age Summary
Figure 30 - Percent Longitudinal Steel Summary
Figure 31 - Annual Freezing Index Summary
Figure 32 - Annual Precipitation Summary
Figure 33 - Average Design and Core Thickness Summary
Figure 34 - Traffic Data Summary

Table 14. GPS-5 data summary.

(0.305 m = 1 ft) (25.4 mm = 1 in)

Section No.	Section ID	State	LTPP Region	Age yrs as 1-Jan-92	Current Status	Av IRI 1991/92	Manual Av. Crack Spac,ft	PADIAS Av. Crack Spac,ft	Tran Bar Diam., in.	Tran Bar Spac,in.	Long Bar Diam., in.	Long % Steel	1989 2-way AADT	1989 ESAL	elev	MR Age days
1	13998	AL	3	19.43		42	ns	10.00	0.50	30	0.63	0.59	AADT	ESAL	130	7
2	15008	AL	3	15.59		58	ns	4.39	0.50	38	0.75	0.68	19330	623000	1023	7
3	47079	AZ	4	2.84		66	ns	6.58	0.63	34	0.63	1.16			1151	
4	55803	AR	3	18.52			3.23	3.31					76050	98000	383	
5	55805	AR	3	16.18			2.31	4.07	0.50	30	0.63	0.61	36810	203000	305	
6	67455	CA	4	20.68		78	2.26		0.50	60	0.63	0.56	13500	864000	52	14
7	95001	CT	1	10.51		117	ns	5.56	0.63	34	0.63	0.60	64400	990000	534	14
8	105004	DE	1	14.59		79	ns	6.49			0.63	0.60	21968	698000	14	
9	105005	DE	1	20.60		70	ns	5.05			0.63	0.60	11446	94000	25	
10	135023	GA	3	17.80		90	6.25				0.63	0.60			25	14
11	165025	ID	4	19.35		140	ns	4.13			0.75	0.60			4979	14
12	175020	IL	2	5.67		77	5.26	35.71	0.50	48	0.75	0.73			459	
13	175151	IL	2	26.02	78		3.91		0.25	48	0.63	0.69			665	
14	175843	IL	2	10.01		78	6.58	7.69	0.50	48	0.75	0.71			780	14
15	175849	IL	2	21.01		97	2.33	2.16			0.70				765	
16	175854	IL	2	11.34		132	4.00	3.94							693	14
17	175869	IL	2	12.43		108	4.67	5.21							669	
18	185022	IN	2	20.01		136	6.49	6.67			0.60				836	7
19	185043	IN	2	23.01		135	3.82	4.27	0.38		0.63	0.60			446	8
20	185518	IN	2	21.27	78	84	3.03		0.38		0.75	0.61			543	11
21	195042	IA	2	16.35			3.57				0.75	0.65	6251	333000	1183	7
22	195046	IA	2	16.35			8.33	55.56			0.75	0.65	6251	333000	1142	7
23	199116	IA	2	19.60	78		2.38				0.75	0.65			1268	14
24	245807	MD	1	3.33		170	ns	38.46	0.50	54	0.75	0.55			107	
25	265363	MI	2	16.01		110	3.38				0.75	0.70			840	
26	275076	MN	2	21.27		48	ns	2.20							985	
27	283099	MS	3	21.10	78		2.10		0.50	42	0.63	0.61			468	7
28	285006	MS	3	12.51			2.91	3.76	0.50	36	0.63	0.59			329	28
29	285025	MS	3	13.51			3.91	4.17	0.50	36	0.62	0.59			420	28
30	285803	MS	3	12.09			4.63	6.25	0.50	36	0.63	0.59			530	28
31	285805	MS	3	16.35	78		3.25	3.52	0.50	30	0.63	0.59			30	28
32	295047	MO	2	20.27		101	5.05	5.26	0.50	48	0.62	0.60			461	
33	315052	NE	2	23.01		68	4.90	3.94	0.68	36	0.68	0.75			1188	
34	375037	NC	1	19.26		75	ns	5.26	1.00	12	0.50	0.60	28500	620000	2110	14
35	375826	NC	1	14.59		84	ns	5.15	1.00	30	0.50	0.65	21100	947000	1140	
36	375827	NC	1	18.85		61	ns	8.06	1.00	30	0.50	0.60	7126	142000	630	
37	385002	ND	2	18.26		82	ns		0.63	48	0.63	0.60	5200	139000	916	
38	395003	OH	2	3.59		69	ns	ns	0.50	30	0.88	0.96			753	5
39	395010	OH	2	17.01	78	116	3.55								1160	
40	404158	OK	3	2.59			5.56		0.63	44	0.75	0.61			731	
41	404166	OK	3	1.67			5.15		0.63	44	0.79	0.72			621	
42	405021	OK	3	4.25			3.94	5.15							634	
43	415005	OR	4	6.25		85	ns	15.15	0.50	60	0.75	0.51			240	28
44	415006	OR	4	18.60		87	ns	4.46	0.50	60	0.63	0.51			2713	
45	415008	OR	4	19.60		58	ns	2.81	0.50	60	0.63	0.51			2729	28
46	415021	OR	4	5.51		73	ns	3.38	0.50	60	0.75	0.51			559	28
47	415022	OR	4	7.25		64	ns	5.38	0.50	60	0.75	0.51			521	7
48	417081	OR	4	3.33		48	ns	166.67	0.50	36	0.75	0.70			585	
49	421598	PA	1	17.01		107	ns	6.67	0.50	34	0.63	0.65			460	
50	421617	PA	1	19.60	78	143	ns		0.50	34	0.63	0.64			340	28
51	425020	PA	1	13.85		120	ns	4.59	0.50	34	0.75	0.65			130	
52	455017	SC	3	12.92		130	5.38	5.62	0.50	30	0.63	0.57			396	14
53	455034	SC	3	16.68		90	4.95		0.50	30	0.63	0.64	13500	457000	178	14
54	455035	SC	3	16.26		80	2.98		0.50	30	0.63	0.64	14938	506000	140	14
55	465020	SD	2	19.43		117	2.50	2.44	0.63	48	0.63	0.59			3932	
56	465025	SD	2	17.18		78	2.03	2.16	0.63	48	0.63	0.59			2588	
57	465040	SD	2	28.52		135	ns		0.63	44	0.63	0.65			1513	
58	483719	TX	3	27.35		152	4.03	5.10	0.50	24	0.63	0.51	29000	344000	21	
59	483779	TX	3	13.59		136	ns		0.50	36	0.63	0.51			3778	7
60	485024	TX	3	10.51		163	4.03		0.50	36	0.75	0.60	3100	103000	210	7
61	485026	TX	3	6.17		107	3.57	5.68	0.75	24	0.75	0.56			18	
62	485035	TX	3	12.34		118	3.70	ns	0.50	36	0.63	0.61			559	7
63	485154	TX	3	20.52		97	4.76	5.15	0.50	36	0.63	0.52			355	7
64	485274	TX	3	18.85		109	6.85	7.58	0.50	36	0.63	0.51	309000	77000	641	7
65	485278	TX	3	16.60		105	2.91	3.52	0.50	36	0.63	0.61			2868	
66	485283	TX	3	4.17		75	5.62	15.63	0.50	24	0.75	0.52			560	7
67	485284	TX	3	4.25		139	6.76	21.74	0.50	24	0.75	0.50	55000	218000	562	7
68	485287	TX	3	18.43		125	3.82	4.39	0.50	36	0.63	0.51			679	7
69	485301	TX	3	9.92		109	4.72	5.68	0.50	36	0.75	0.60	29000	175000	704	7
70	485310	TX	3	4.51		133	6.17	7.04	0.50	24	0.75	0.50			911	7
71	485317	TX	3	9.76		144	7.14	8.62	0.50	36	0.63	0.51			650	7
72	485323	TX	3	12.68		116	2.13	2.63	0.50	36	0.75	0.61			3290	7
73	485328	TX	3	16.35		104	3.79	3.91	0.50	36	0.63	0.61			1033	7
74	485334	TX	3	21.77		73	2.40	2.33	0.50	30	0.63	0.51			2302	7
75	485335	TX	3	12.68		133	2.34	2.72	0.50	36	0.75	0.61			3265	7
76	485336	TX	3	8.42		91	3.13	5.75	0.50	36	0.75	0.61	5800	207000	3551	
77	512564	VA	1	22.93		61	ns	2.29			0.63	0.60			22	
78	515008	VA	1	14.43		140	ns	2.62			0.63	0.60			13	
79	515009	VA	1	12.43		143	ns	4.63			0.63	0.60			133	
80	515010	VA	1	3.67		99	ns	ns			0.75	0.60			155	
81	545007	WV	1	14.59		145	ns	2.91				0.65			1225	
82	555037	WI	2	18.35		77	5.88	4.27			0.75	0.61			1064	
83	556040	WI	2	11.17		150	4.31	5.56			0.75	0.60			690	
Aver.				14.54		101.84	4.20	9.86	0.54	38.14	0.68	0.61	37,013	398,619	942	
St. Dev.				6.39		31.26	1.52	22.16	0.13	10.62	0.07	0.10	65,474	306,363	1,030	
Max.				28.52		170.00	8.33	166.67	1.00	60.00	0.88	1.16	309,000	990,000	4,979	
Min.				1.67		42.00	.03	2.16	0.25	12.00	0.50	0.50	3,100	77,000	13	

Table 14. GPS-5 data summary (continued).

(0.305 m = 1 ft) (25.4 mm = 1 in)

Section No.	Section ID	State	LTPP Region	Age yrs as 1 Jan 92	Current Status	Av IRI 1991/92	Manual Av. Crack Spac.ft	PADIAS Av. Crack Spac.ft	Tran Bar Diam., in	Tran Bar Spac.in	Long Bar Diam., in	Long. % Steel	1989 2-way AADT	1989 ESAL	elev	MR Age days
1	13998	AL	3	19.43		42	ns	10.00	0.50	30	0.63	0.59	AADT	ESAL	130	7
2	15008	AL	3	15.59		58	ns	4.39	0.50	36	0.75	0.66	19330	823000	1023	7
3	47079	AZ	4	2.84		66	ns	6.58	0.63	34	0.63	1.16			1151	
4	55803	AR	3	18.52			3.23	3.31					76050	98000	383	
5	55806	AR	3	16.18			2.31	4.07	0.50	30	0.63	0.61	36810	203000	305	
6	67456	CA	4	20.68		78	2.26		0.50	60	0.63	0.56	13500	864000	52	14
7	95001	CT	1	10.51		117	ns	5.56	0.63	34	0.63	0.60	64400	990000	534	14
8	105004	DE	1	14.59		79	ns	6.49			0.63	0.60	21968	698000	14	
9	105006	DE	1	20.60		70	ns	5.05			0.63	0.60	11446	94000	25	
10	135023	GA	3	17.60		80	6.25				0.63	0.60			25	14
11	165025	ID	4	19.35		140	ns	4.13			0.75	0.80			4979	14
12	175020	IL	2	5.67		77	5.26	35.71	0.50	48	0.75	0.73			459	
13	175161	IL	2	26.02	78		3.91		0.25	48	0.63	0.69			665	
14	175843	IL	2	10.01		78	6.58	7.69	0.50	48	0.75	0.71			780	14
15	175849	IL	2	21.01		97	2.33	2.16			0.70				765	
16	175854	IL	2	11.34		132	4.00	3.94							693	14
17	175869	IL	2	12.43		108	4.67	5.21							669	
18	185022	IN	2	20.01		136	6.49	6.67			0.60				836	7
19	185043	IN	2	23.01		135	3.82	4.27	0.38		0.63	0.60			446	8
20	185518	IN	2	21.27	78	84	3.03		0.38		0.75	0.61			643	11
21	195042	IA	2	16.35			3.57				0.75	0.65	6251	333000	1183	7
22	195046	IA	2	16.35			8.33	55.56			0.75	0.65	6251	333000	1142	7
23	199116	IA	2	19.60	78		2.38				0.75	0.65			1268	14
24	245807	MD	1	3.33		170	ns	38.46	0.50	64	0.75	0.66			107	
25	265363	MI	2	16.01		110	3.38				0.75	0.70			640	
26	275076	MN	2	21.27		48	ns	2.20							985	
27	283089	MS	3	21.10	78		2.10		0.50	42	0.63	0.61			468	7
28	285008	MS	3	12.51			2.91	3.76	0.50	36	0.63	0.59			329	28
29	285026	MS	3	13.51			3.91	4.17	0.50	36	0.62	0.59			420	28
30	285803	MS	3	12.08			4.63	6.25	0.50	36	0.63	0.59			530	28
31	285806	MS	3	16.35	78		3.25	3.62	0.50	30	0.63	0.59			30	28
32	295047	MO	2	20.27		101	6.05	5.26	0.50	48	0.62	0.60			461	
33	315062	NE	2	23.01		66	4.90	3.94	0.68	36	0.68	0.78			1188	
34	375037	NC	1	19.26		75	ns	5.26	1.00	12	0.50	0.60	28500	620000	2110	14
35	375826	NC	1	14.59		84	ns	5.16	1.00	30	0.50	0.65	21100	947000	1140	
36	375827	NC	1	18.85		61	ns	8.06	1.00	30	0.50	0.60	7126	142000	630	
37	385002	ND	2	16.26		82	ns		0.63	48	0.63	0.60	5200	139000	916	
38	395003	OH	2	3.59		69	ns	ns	0.50	30	0.88	0.98			763	5
39	395010	OH	2	17.01	78	116	3.55								1160	
40	404158	OK	3	2.59			5.56		0.63	44	0.75	0.61			731	
41	434108	OK	3	1.67			5.16		0.63	44	0.79	0.72			821	
42	406021	OK	3	4.26			3.94	5.16							634	
43	415006	OR	4	6.25		85	ns	15.15	0.50	60	0.75	0.61			240	28
44	415008	OR	4	18.60		87	ns	4.48	0.50	60	0.63	0.61			2713	
45	415008	OR	4	19.60		58	ns	2.81	0.50	60	0.63	0.61			2729	28
46	415021	OR	4	5.51		73	ns	3.38	0.50	60	0.75	0.61			559	28
47	415022	OR	4	7.25		64	ns	5.38	0.50	60	0.75	0.61			521	7
48	417081	OR	4	3.33		48	ns	166.67	0.50	36	0.75	0.70			585	
49	421598	PA	1	17.01		107	ns	6.67	0.50	34	0.63	0.65			460	
50	421617	PA	1	19.60	78	143	ns		0.50	34	0.63	0.64			340	28
51	425020	PA	1	13.85		120	ns	4.59	0.50	34	0.75	0.65			130	
52	455017	SC	3	12.92		130	5.38	5.62	0.50	30	0.63	0.67			396	14
53	455034	SC	3	16.68		90	4.95		0.50	30	0.63	0.64	13500	457000	178	14
54	455036	SC	3	16.26		80	2.98		0.50	30	0.63	0.64	14938	508000	140	14
55	465020	SD	2	19.43		117	2.80	2.44	0.63	48	0.63	0.59			3932	
56	465026	SD	2	17.18		78	2.03	2.16	0.63	48	0.63	0.59			2588	
57	465040	SD	2	28.82		136	ns		0.63	44	0.63	0.66			1513	
58	483719	TX	3	27.35		152	4.03	5.10	0.50	24	0.63	0.51	29000	344000	21	
59	483779	TX	3	13.59		136	ns		0.50	36	0.63	0.51			3778	7
60	485024	TX	3	10.51		163	4.03		0.50	36	0.75	0.60	3100	103000	210	7
61	485026	TX	3	6.17		107	3.57	5.66	0.75	24	0.75	0.64			18	
62	485036	TX	3	12.34		116	3.70	ns	0.50	36	0.63	0.61			559	7
63	485164	TX	3	20.62		97	4.76	5.16	0.50	36	0.63	0.62			356	7
64	485274	TX	3	18.85		109	6.85	7.58	0.50	36	0.63	0.61	309000	77000	641	7
65	485278	TX	3	16.60		105	2.91	3.62	0.50	36	0.63	0.61			2868	
66	485283	TX	3	4.17		75	5.62	15.63	0.50	24	0.75	0.62			560	7
67	485284	TX	3	4.25		139	6.76	21.74	0.50	24	0.75	0.60	55000	218000	562	7
68	485287	TX	3	18.43		125	3.82	4.39	0.50	36	0.63	0.61			679	7
69	485301	TX	3	9.92		109	4.72	5.68	0.50	36	0.75	0.60	29000	175000	704	7
70	485310	TX	3	4.61		133	6.17	7.04	0.50	24	0.75	0.60			911	7
71	485317	TX	3	9.76		144	7.14	8.62	0.50	36	0.63	0.61			650	7
72	485323	TX	3	12.68		116	2.13	2.63	0.50	36	0.75	0.61			3290	7
73	485328	TX	3	16.35		104	3.79	3.91	0.50	36	0.63	0.61			1033	7
74	485334	TX	3	21.77		73	2.40	2.33	0.50	30	0.63	0.51			2302	7
75	485336	TX	3	12.68		133	2.34	2.72	0.50	36	0.75	0.61			3266	7
76	485338	TX	3	8.42		91	3.13	5.75	0.50	36	0.75	0.61	5800	207000	3551	
77	512864	VA	1	22.93		81	ns	2.29			0.63	0.60			22	
78	515008	VA	1	14.43		140	ns	2.62			0.63	0.60			13	
79	515009	VA	1	12.43		143	ns	4.63			0.63	0.60			133	
80	515010	VA	1	3.67		99	ns	ns			0.75	0.60			165	
81	545007	WV	1	14.59		145	ns	2.91				0.65			1226	
82	555037	WI	2	18.35		77	5.68	4.27			0.75	0.61			1064	
83	555040	WI	2	11.17		150	4.31	5.56			0.75	0.60			690	
Aver				14.54		101.84	4.20	9.86	0.54	38.14	0.68	0.61	37,013	398,619	942	
St. Dev.				6.39		31.26	1.62	22.16	0.13	10.62	0.07	0.10	66,474	306,383	1,030	
Max.				28.82		170.00	8.33	166.67	1.00	60.00	0.88	1.16	309,000	990,000	4,979	
Min.				1.67		42.00	2.03	2.16	0.25	12.00	0.50	0.60	3,100	77,000	13	

Table 14. GPS-5 data summary (continued).

Section No.	Section ID	State	Aver. Annual KESAL	ESAL Record Years	Latest Annual KESAL	Latest KESAL Year
			*1000		*1000	
1	13998	AL	966	15	673	88
2	15008	AL	650	13	823	89
3	47079	AZ	.	.	.	.
4	55803	AR	66	18	98	89
5	55806	AR	106	16	203	89
6	67455	CA	776	21	864	90
7	95001	CT	829	11	990	90
8	105004	DE	735	13	687	88
9	105006	DE	74	19	94	89
10	135023	GA	855	17	1095	89
11	165025	ID	752	19	1921	89
12	175020	IL	54	7	68	91
13	175151	IL	630	25	1107	89
14	175843	IL	698	11	1030	91
15	175849	IL	556	21	766	91
16	175854	IL	92	11	140	91
17	175869	IL	127	13	199	91
18	185022	IN	3597	20	5224	90
19	185043	IN	14	23	18	90
20	185518	IN	3239	22	4635	90
21	195042	IA	409	17	623	91
22	195046	IA	409	17	623	91
23	199116	IA	896	17	649	88
24	245807	MD	5826	3	5826	89
25	265363	MI	225	16	306	91
26	275076	MN	282	23	481	91
27	283099	MS	100	21	234	89
28	285006	MS	692	10	176	89
29	285025	MS	95	13	129	89
30	285803	MS	306	11	508	89
31	285806	MS	632	16	1063	89
32	295047	MO	300	19	426	89
33	315052	NE	254	23	317	90
34	375037	NC	359	17	620	89
35	375826	NC	872	15	801	91
36	375827	NC	432	19	175	91
37	385002	ND	277	19	153	91
38	395003	OH	2581	3	158	90
39	395010	OH	162	15	319	89
40	404158	OK	566	3	566	92
41	404166	OK	1931	3	1931	91
42	405021	OK	743	3	765	91
43	415005	OR	1936	6	2273	89
44	415006	OR	566	17	890	89
45	415008	OR	566	18	1269	89
46	415021	OR	1480	17	1874	89
47	415022	OR	1813	7	2131	89
48	417081	OR	440	3	454	89
49	421598	PA	984	17	1130	89
50	421617	PA	.	.	.	.
51	425020	PA	502	12	622	89
52	455017	SC	354	12	836	89
53	455034	SC	232	16	457	89
54	455035	SC	254	16	506	89
55	465020	SD	306	20	75	91
56	465025	SD	38	19	65	91
57	465040	SD	50	28	88	91
58	483719	TX	320	26	344	89
59	483779	TX	678	13	735	89
60	485024	TX	139	9	103	89
61	485026	TX	111	2	111	89
62	485035	TX	763	12	561	89
63	485154	TX	428	20	363	89
64	485274	TX	270	16	293	89
65	485278	TX	390	17	59	89
66	485283	TX	357	3	354	89
67	485284	TX	220	3	218	89
68	485287	TX	200	16	187	89
69	485301	TX	174	9	175	89
70	485310	TX	1679	6	387	89
71	485317	TX	382	8	352	89
72	485323	TX	547	11	519	89
73	485328	TX	443	16	462	89
74	485334	TX	399	21	536	89
75	485335	TX	556	11	519	89
76	485336	TX	241	4	207	89
77	512564	VA	479	21	589	89
78	515008	VA	779	14	246	89
79	515009	VA	164	11	93	89
80	515010	VA	31	3	29	89
81	545007	WV	116	6	141	89
82	555037	WI	118	18	257	89
83	555020	WI	493	11	419	89
Aver.			656		721	
St. Dev.			878		1,019	
Max			5,826		5,826	
Min			14		18	

Monitoring Data Summary

The monitoring data available for GPS-5 consists of crack spacing, deflection, profile, and visual condition survey data.

Crack Spacing

Two types of condition surveys may be performed at each GPS-5 site. The survey procedure of choice for the LTPP program is based on 35mm photographic surveys using the PADIAS system. The PADIAS procedure is intended to identify the extent and severity of most surface distresses. The second procedure is the manual (walking) condition survey in which the type extent, and severity of distresses are noted and mapped. A review of the results of the two types of surveys indicate that the PADIAS system cannot reliability identify low and no severity cracking in CRC pavements and as such the total number of cracks per section cannot be obtained using the PADIAS system. Therefore, the average cracking spacing data was developed using the results of the manual surveys. Figure 35 provides a summary of average crack spacing at each GPS-5 section for which manual survey data were available. Average crack spacing ranges from 0.62 to 2.54 m (2.03 to 8.33 ft).

Profile Data

For the LTPP program, the profile of a pavement section is characterized by the International Roughness Index (IRI). A summary of the IRI data is given in figure 36. The IRI values determined from measurements made in 1992 and 1993 range from 664 to 2686 mm/km (42 to 170 in/mi).

Distress Data

Although many test sections in the GPS-5 experiments are over 15 years of age and 14 sections are over 20 years of age, the test sections do not exhibit noticeable amounts of patching and punchout distress. Also, most sections had very little medium to high severity cracking reported. However, at the same time 4 sections have been overlaid, probably as a result of the need for overlaying adjacent length of the CRC pavement. Only one of the overlaid sections exhibited patches within the monitoring length.

It thus appears that the distress data as being collected under the LTPP program is either not being recorded/interpreted correctly or the test section data collected in the present form is not representative of the appropriate pavement project. Based on the results of the current FHWA sponsored study on CRC pavement performance, it is clear that performance evaluation of CRC pavements must incorporate longer lengths of pavement to ensure that failure conditions in the pavement are reliably obtained. Thus, the visual condition survey must include a survey of 4.83 to 8.05 km (3 to 5 mi) length of the CRC project in addition to a detailed survey of the 152 m (500 ft) monitoring length of the test section. The visual condition survey should record the number and severity of patches and punchouts.

CRC pavement behavior is characterized by crack spacing (average crack spacing and cumulative frequency type statistics for crack spacing) and CRC pavement performance is characterized by number of failures (patches and punchouts), ride quality, and structural capacity (deflection testing). For the GPS-5 experiment, it appears that cracking related data must be obtained by manual surveys and actual crack mapping must be done to allow appropriate crack spacing statistics to be determined. Also, the GPS-5 monitoring plan must include visual survey of 4.83 to 8.05 km (3 to 5 mi) length of the project to allow reliable determination of number of failures (punchout/patches) per kilometer (mi). Crack width data is also important and should be collected over a representative subsection of the monitoring length.

As a result of the above discussed lack of appropriate data, no additional discussion is presented on distress related data.

Deflection Data

Deflection testing at the GPS-5 sites has been conducted over different seasons and varying ambient and in-situ conditions. As such, the deflection data is confounded by many factors. As a result no discussion of the deflection data is presented. Currently, a seasonal monitoring program is in progress at almost 60 test sections. It is expected that the results of this program may allow normalization of the deflection test data so that deflection responses at different sections can be compared more reliably. A limited analysis of the deflection data indicates that deflections along the pavement (lane) edge ranged from almost 100 percent to 200 percent of the deflections along the mid-lane locations.

Data Analysis

The effects of age on average crack spacing are shown in figures 37 and 38 for no-freeze and freeze areas, respectively. No clear trends are apparent. Figures 39 and 40 show the effect on average crack spacing for percent steel less than 0.62 percent and equal to or more than 0.62 percent. Once again, no clear trends are noticeable.

The effect of percent steel on crack spacing is shown in figure 41. However, because of wide variation in the data, no clear trends are evident.

The effect of age, percent steel, and crack spacing on IRI (profile index) are shown in figures 42, 43, and 44, respectively. Once again, no clear over-riding trends are evident.

Recently, as part of the analysis of LTPP data, attempts were made to develop distress prediction models.[3] However, because of very little distress existing within the 152 m (500 ft) monitoring lengths of the GPS-5 test sections, no distress prediction models could be developed. A performance model was developed using ride quality as the performance indicator. This model has the following form:

$$IRI = 262.05 + 1.47 * CESAL - 2.94 * THICK - 232.3 * PSTEEL - WIDENED - 16.8 * SUBGRADE \quad (20)$$

where:

IRI	=	International Roughness Index, mm/km (in/mi)
CESAL	=	Cumulative 80.07 kN (18,000 lb) ESAL in traffic lane, millions
THICK	=	Concrete slab thickness, millimeters (in)
PSTEEL	=	Percent steel (longitudinal reinforcement)
WIDENED	=	1 for widened lane, 0 for 3.66 m (12 ft) wide lane
SUBGRADE	=	1 for coarse-grained soils, 0 for fine-grained soils

The model was based on data from 42 sections and has a R^2 of 0.55. For slab thicknesses ranging from 203 to 305 mm (8 to 12 in), standard lane width of 3.7 m (12 ft), and traffic ranging from 10 to 20 million ESAL's, the model can be approximated as follows:

$$IRI = 246.30 - 232.2 * PSTEEL \quad (21)$$

The above "reduced" model indicates that use of higher steel percentage should improve the ride quality.

As for the effect of traffic on IRI, no analysis was conducted because of the very limited amount of reliable traffic data available.

Summary

This supplemental report presents a summary of key data related to the GPS-5 experiment. Only a limited data analysis was possible at this time. This limited evaluation of data has pointed out several limitations in the data collection procedures for the GPS-5 experiment. These limitations are summarized below:

1. Reliable crack spacing data must be collected to allow average crack spacing and other crack spacing related statistics (including individual crack spacing) to be developed. Crack spacing is a very important (if not the most important) characteristic of CRC pavements.

2. The PADIAS system should not be relied on for crack spacing data. Manual condition surveys should be mandatory for the GPS-5 experiment.

3. Crack width data (and slab temperature data) should be collected for a representative subsection of each section. Currently, a limited amount of crack width data is collected in conjunction with FWD testing at crack locations.

4. Visual condition surveys should be extended to 4.83 to 8.05 km (3 to 5 mi) of the project at each test section to obtain data on number of failures (patches and punchouts) per kilometer (mi). The 152 m (500 ft) monitoring lengths are too

short to develop such information. The number of failures per kilometer (mi) is a key performance indicator for CRC pavements.

The limited analysis presented was conducted to identify if there were strong influences of certain parameters on crack spacing, ride quality, and failures. No such specific trends stand out because crack spacing is affected by many factors including the ambient conditions during the construction of the pavement (concrete placement).

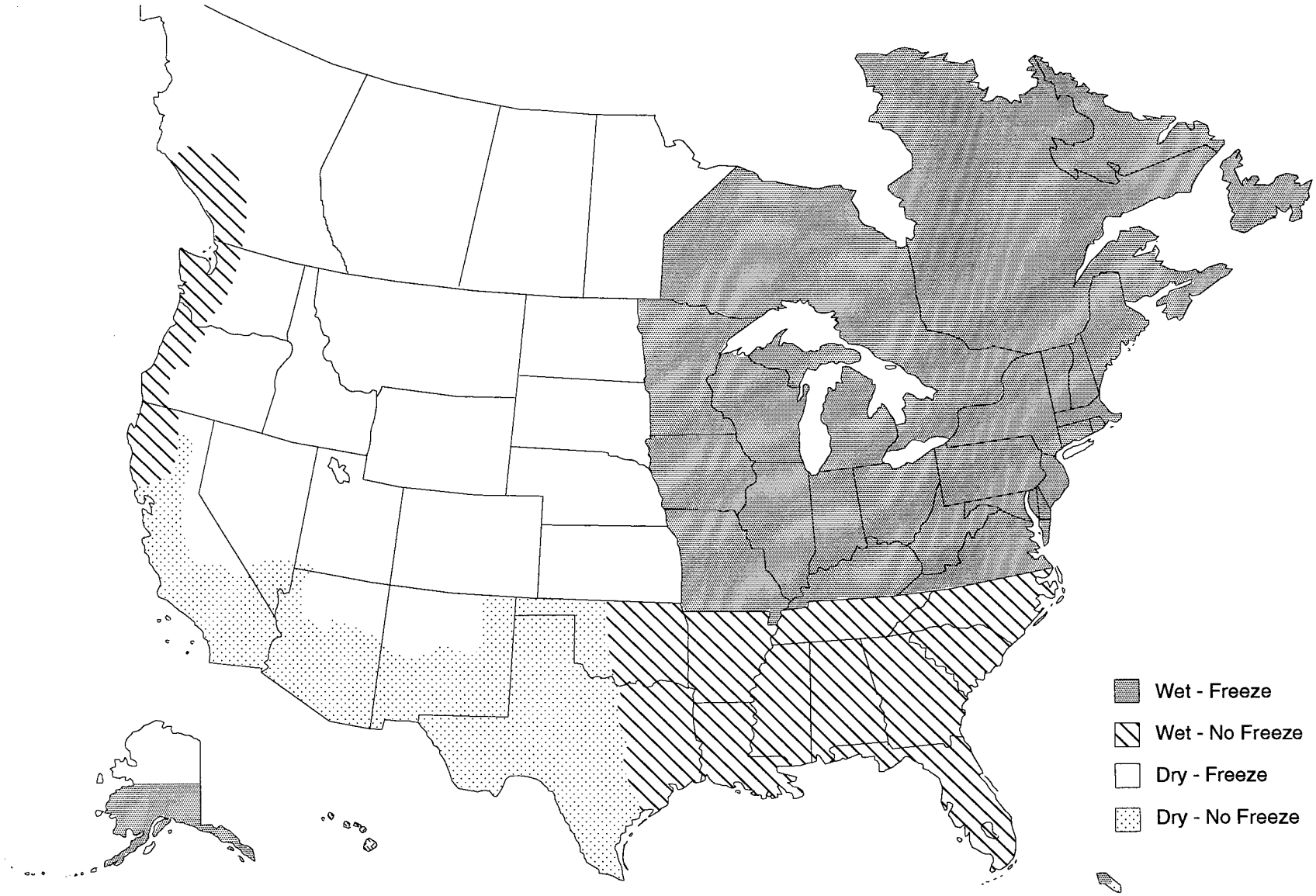

Figure 28. SHRP-LTPP environmental zones.

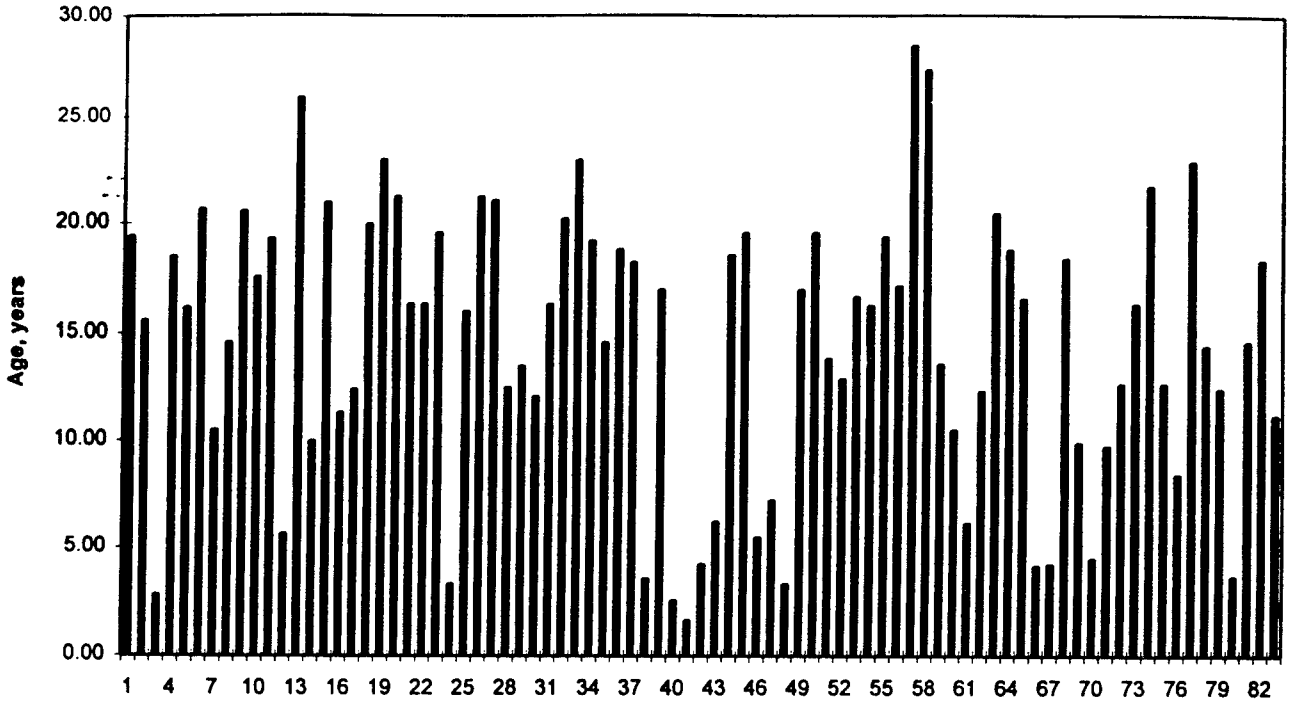

Figure 29. Age summary.

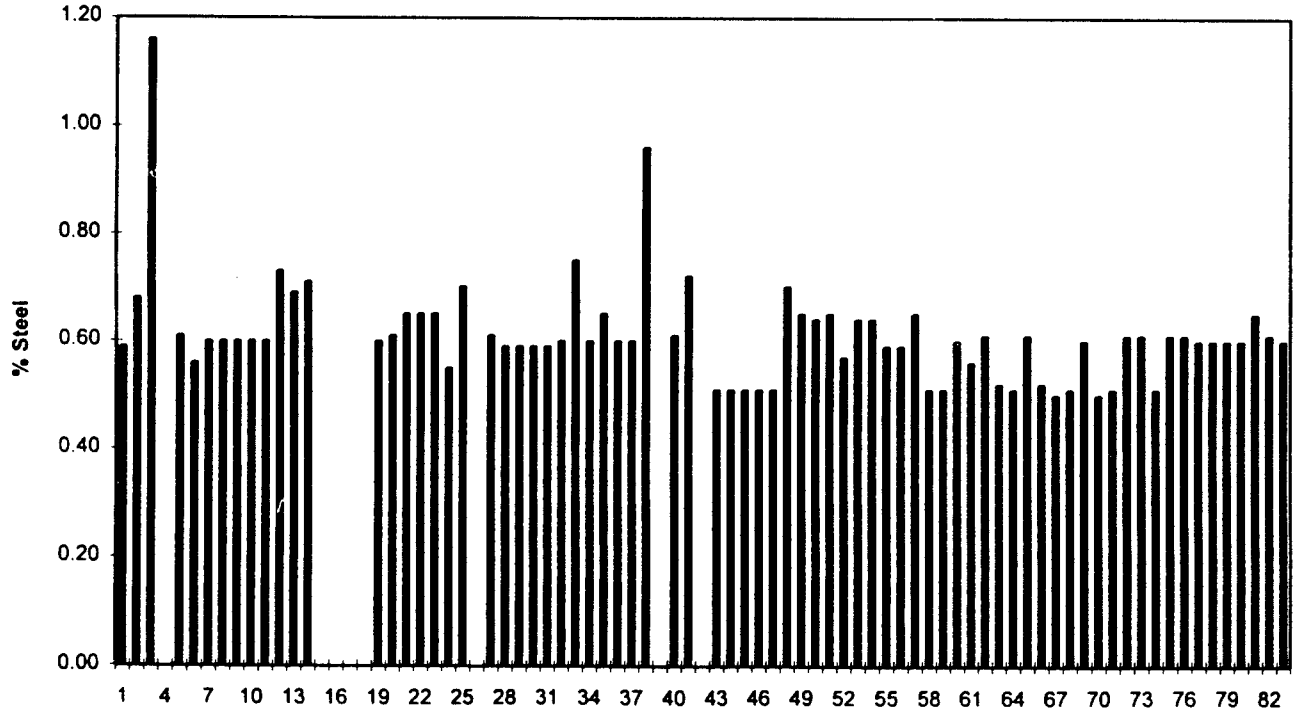

Figure 30. Percent longitudinal steel summary.

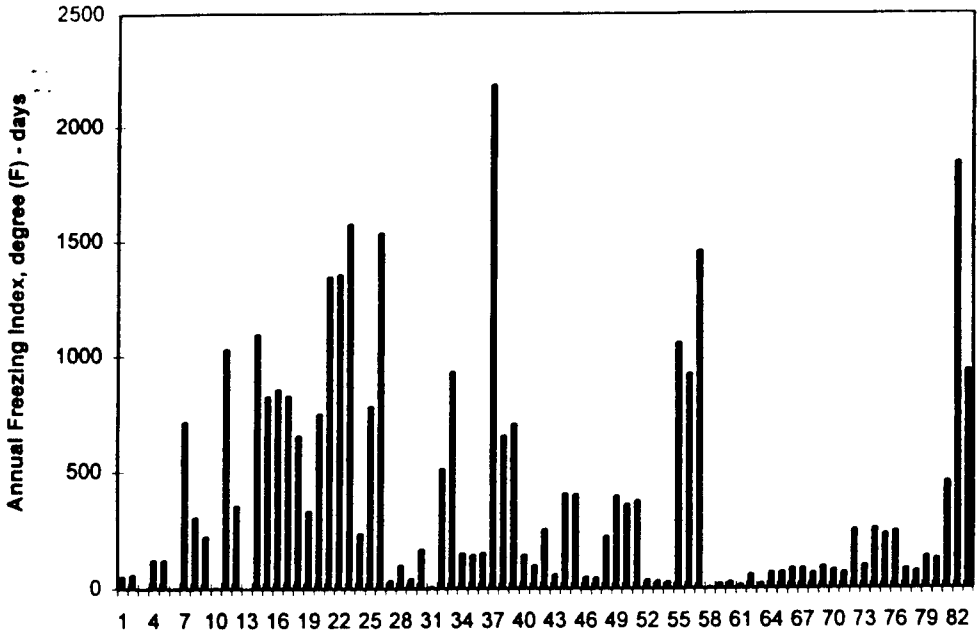

(0.6 °C = 1 °F)

Figure 31. Annual freezing index.

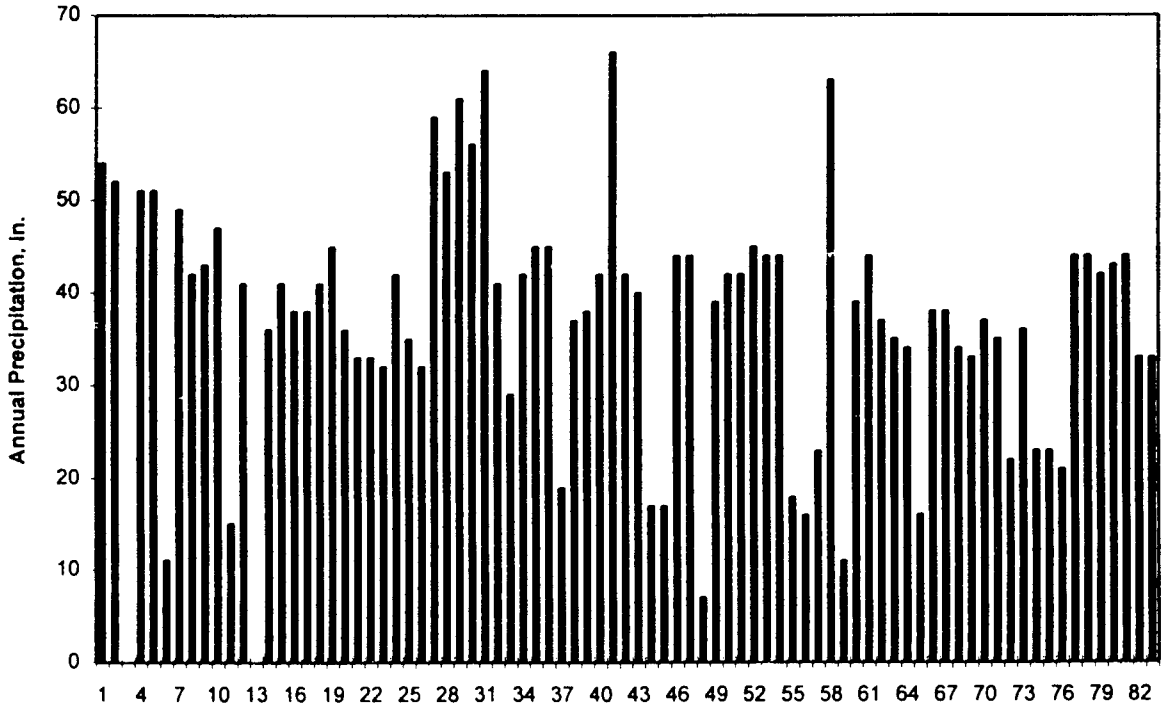

(25.4 mm = 1 in)

Figure 32. Annual precipitation summary.

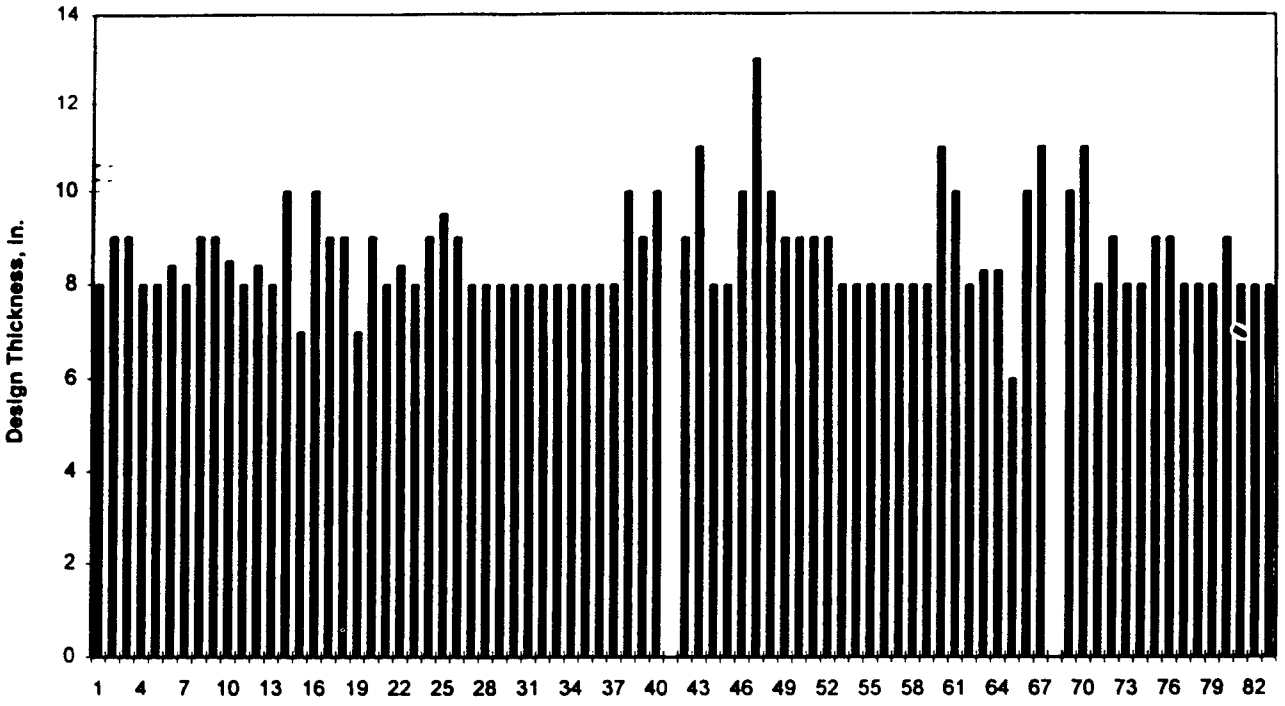

(25.4 mm = 1 in)

Figure 33. Design thickness summary.

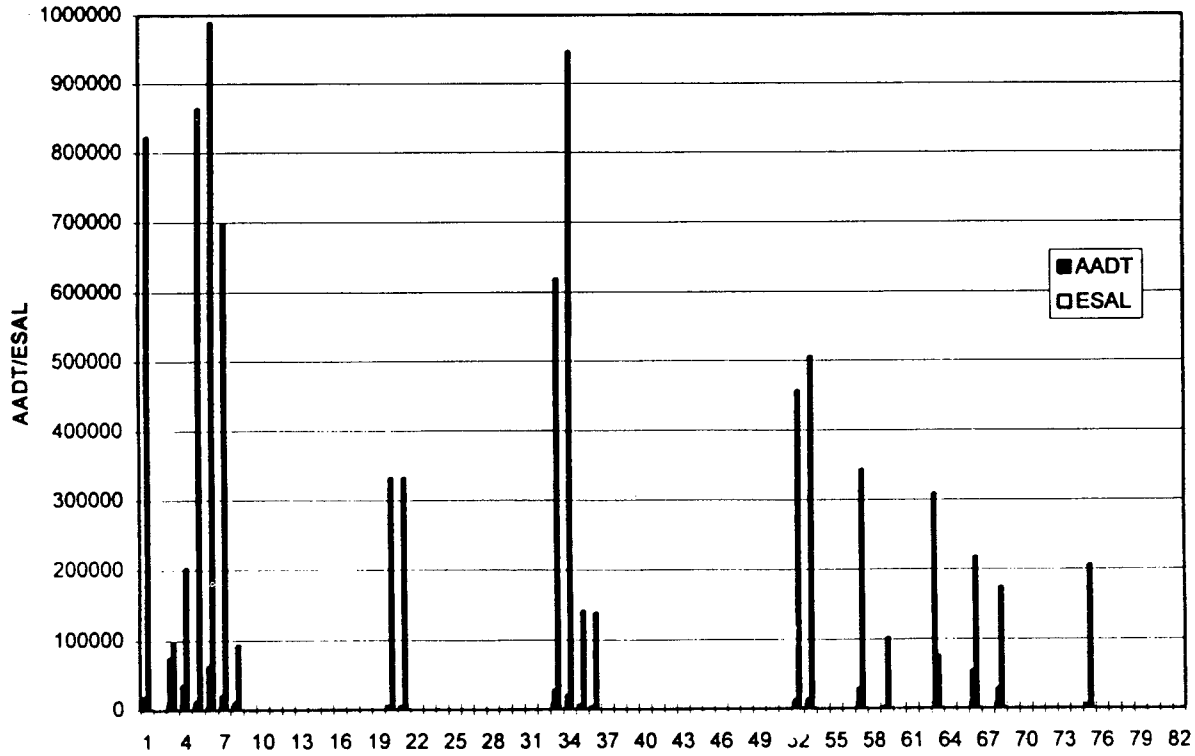

Figure 34. 1989 AADT (2-way) and ESAL.

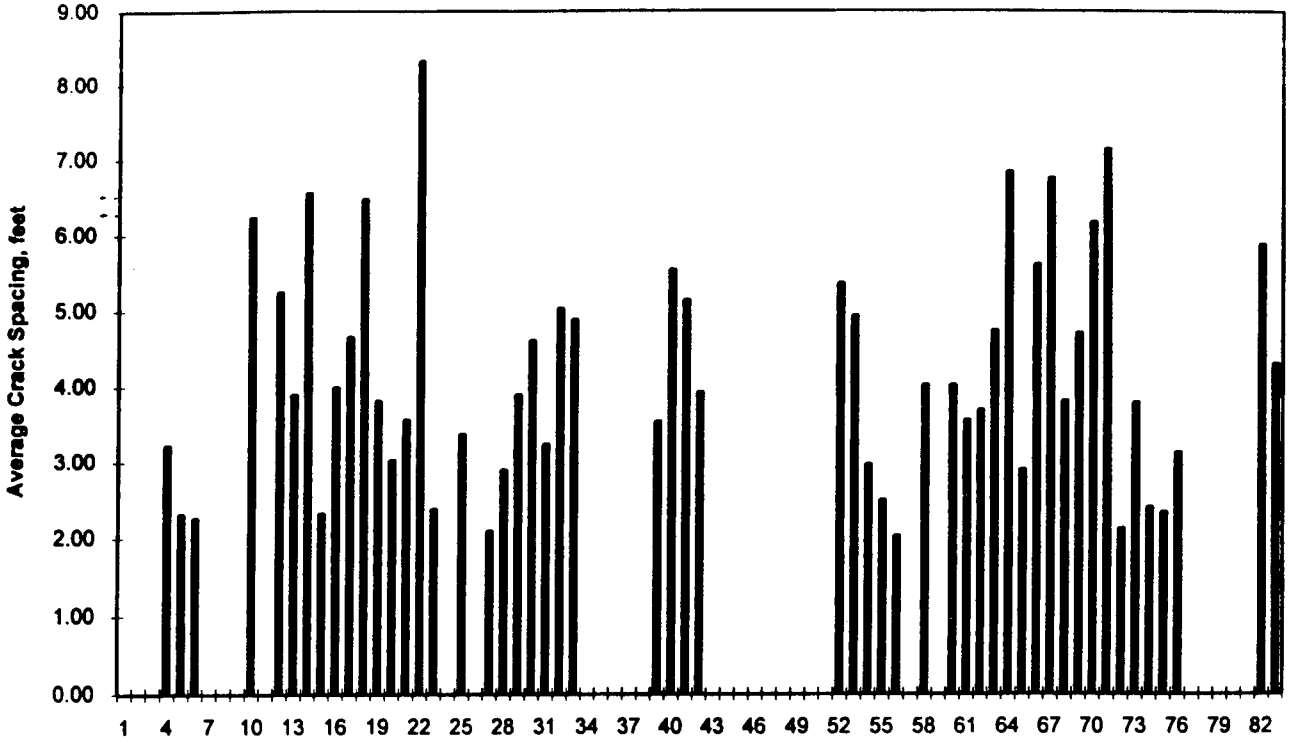

(0.305 m = 1 ft)

Figure 35. Average crack spacing summary (manual).

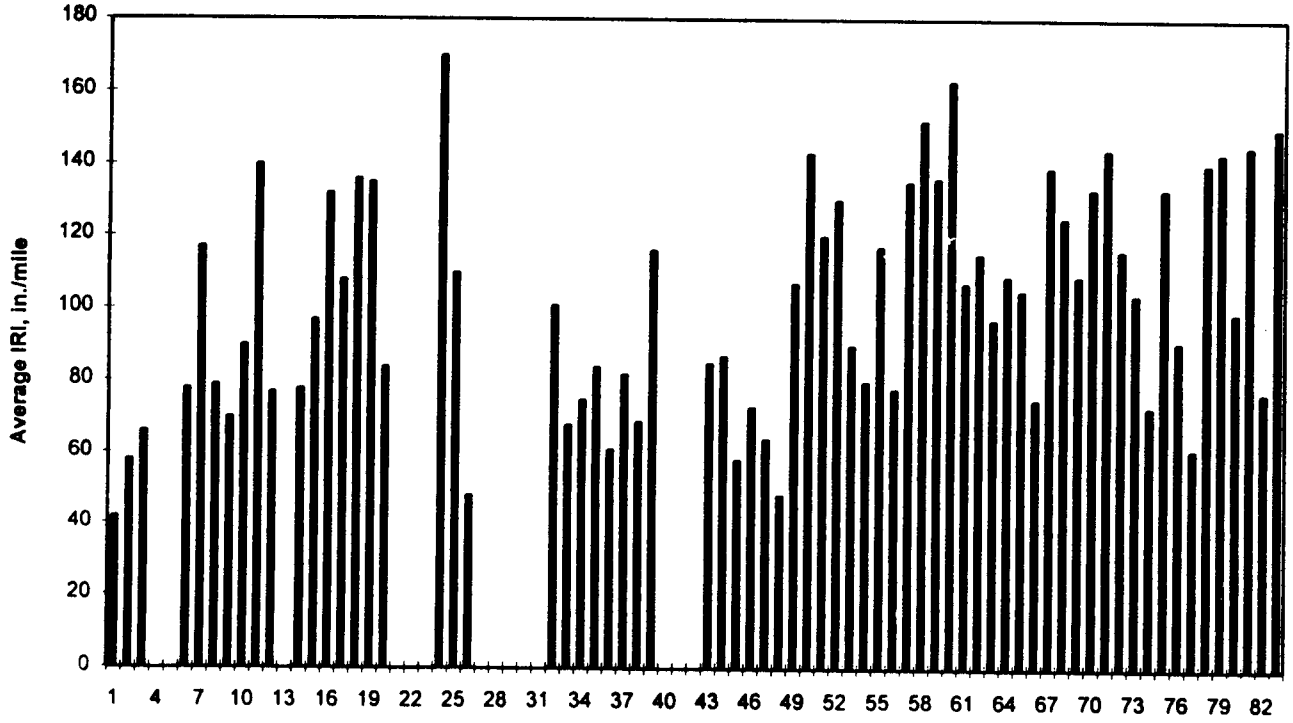

(15.8 mm/km = 1 in/mi)

Figure 36. Average IRI summary.

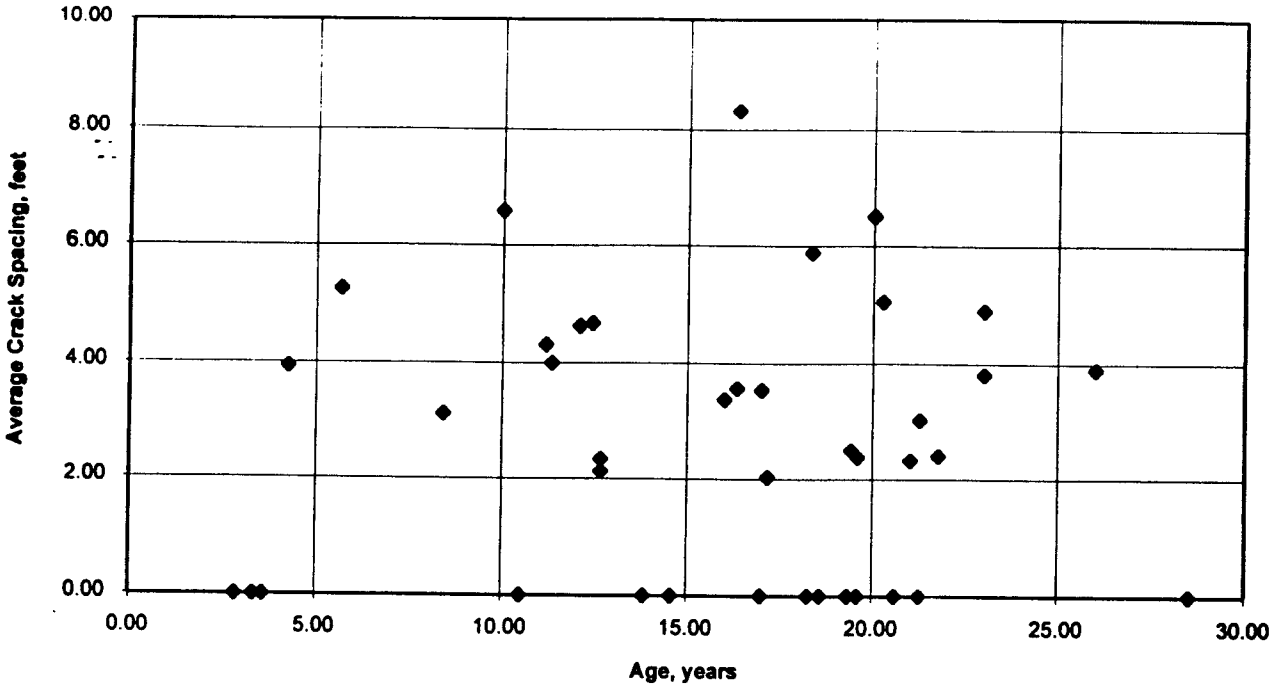

(0.305 m = 1 ft)

Figure 37. Crack spacing versus age - freeze sections.

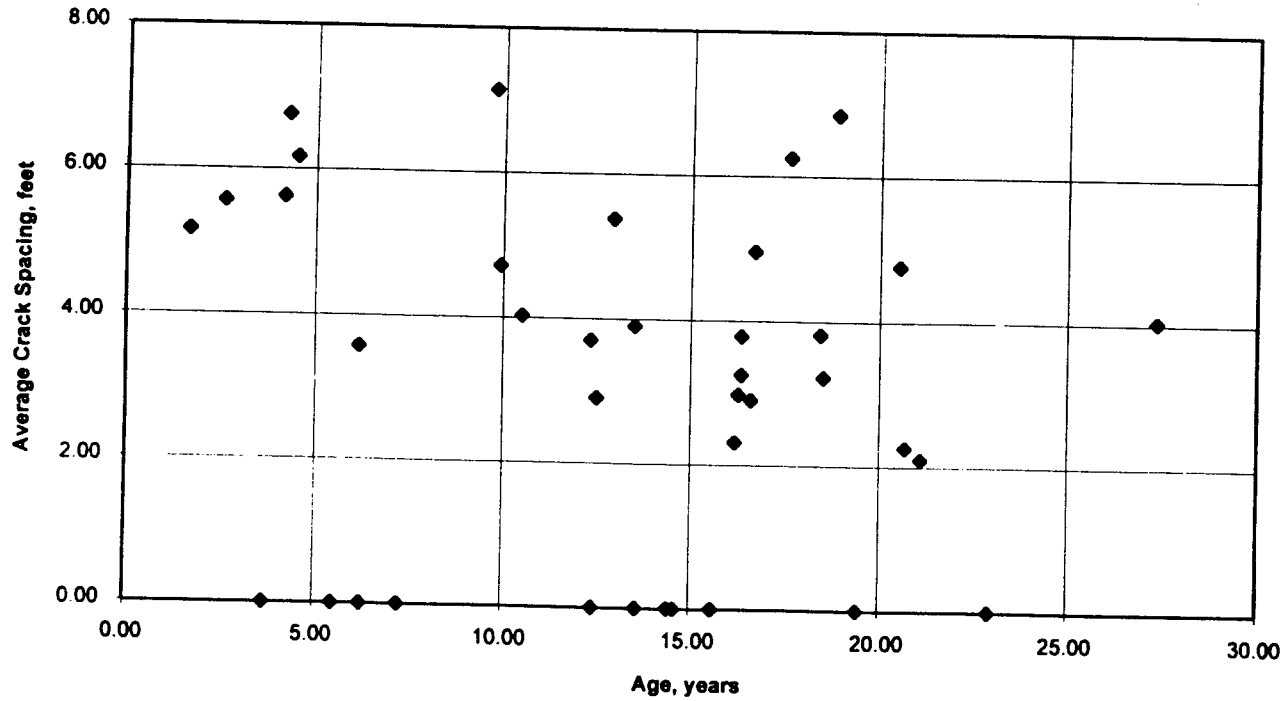

(0.305 m = 1 ft)

Figure 38. Crack spacing versus age - no-freeze sections.

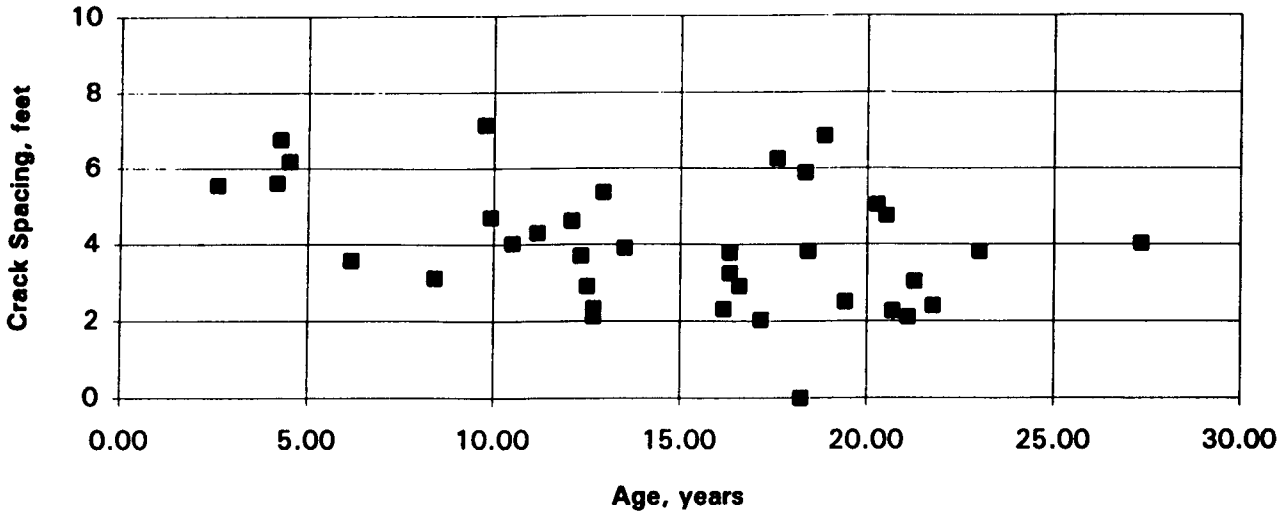

(0.305 m = 1 ft)

Figure 39. Crack spacing versus age (% steel < 0.62%).

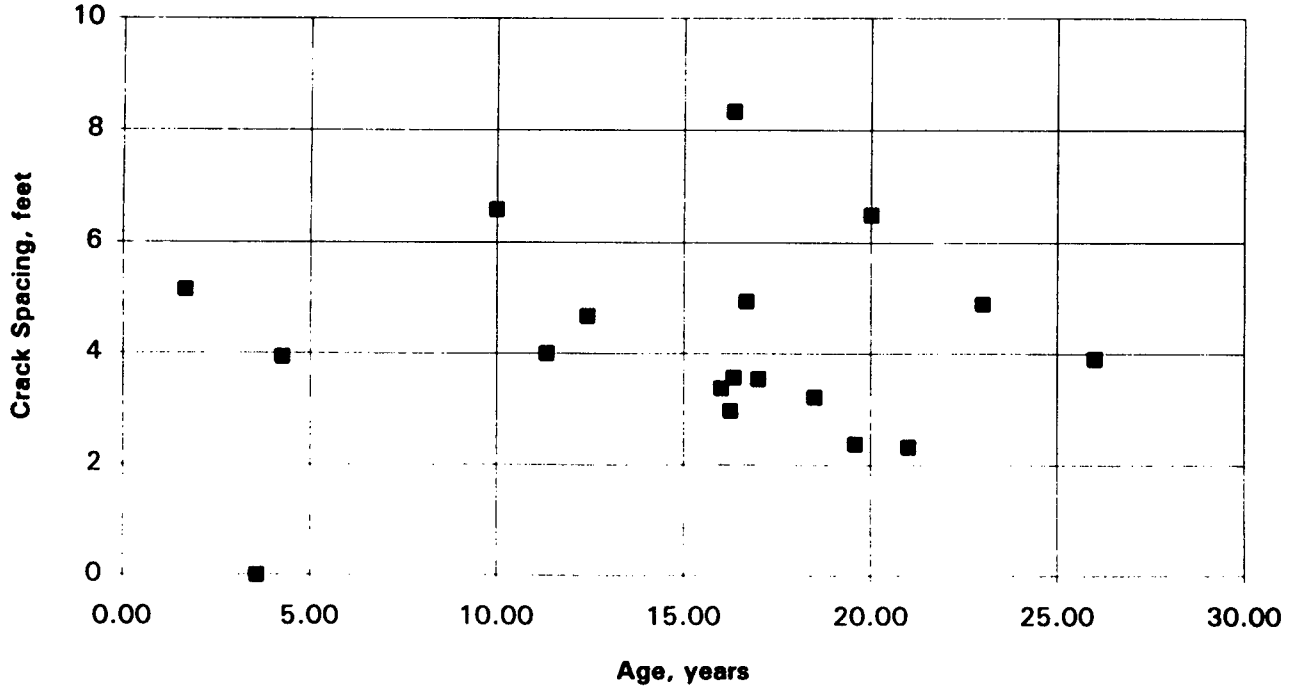

(0.305 m = 1 ft)

Figure 40. Crack spacing versus age (% steel > 0.62%).

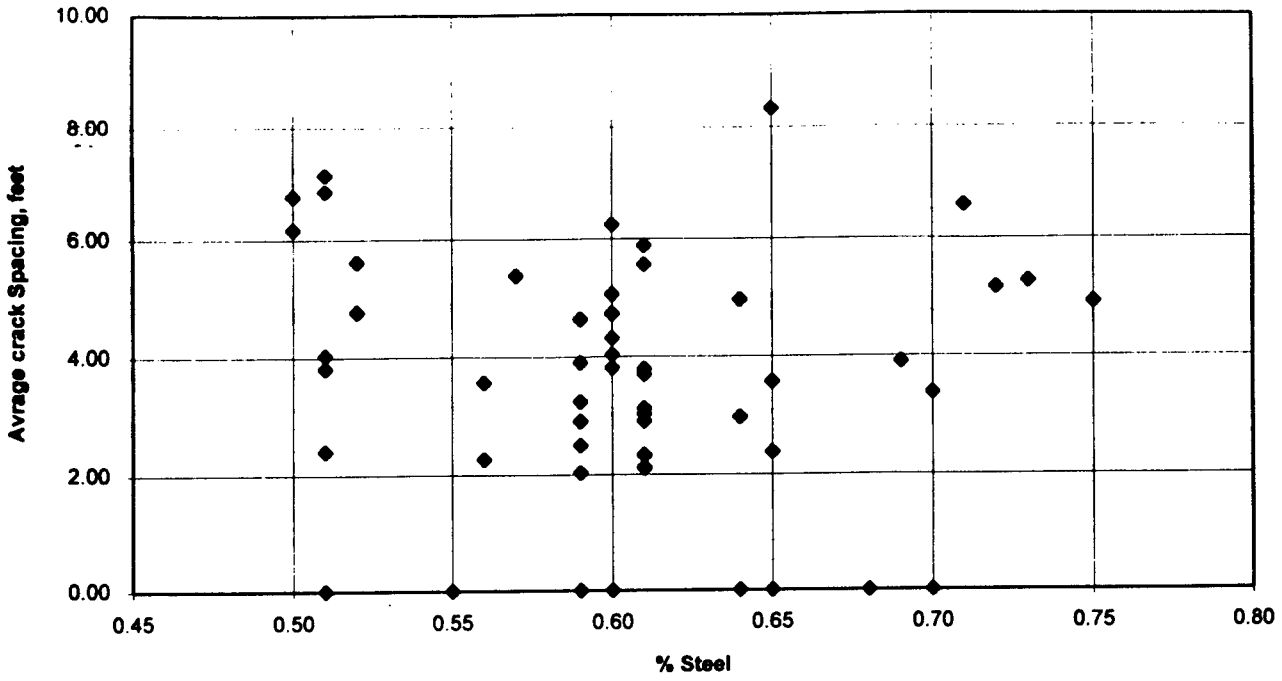

(0.305 m = 1 ft)

Figure 41. Crack spacing versus percent steel.

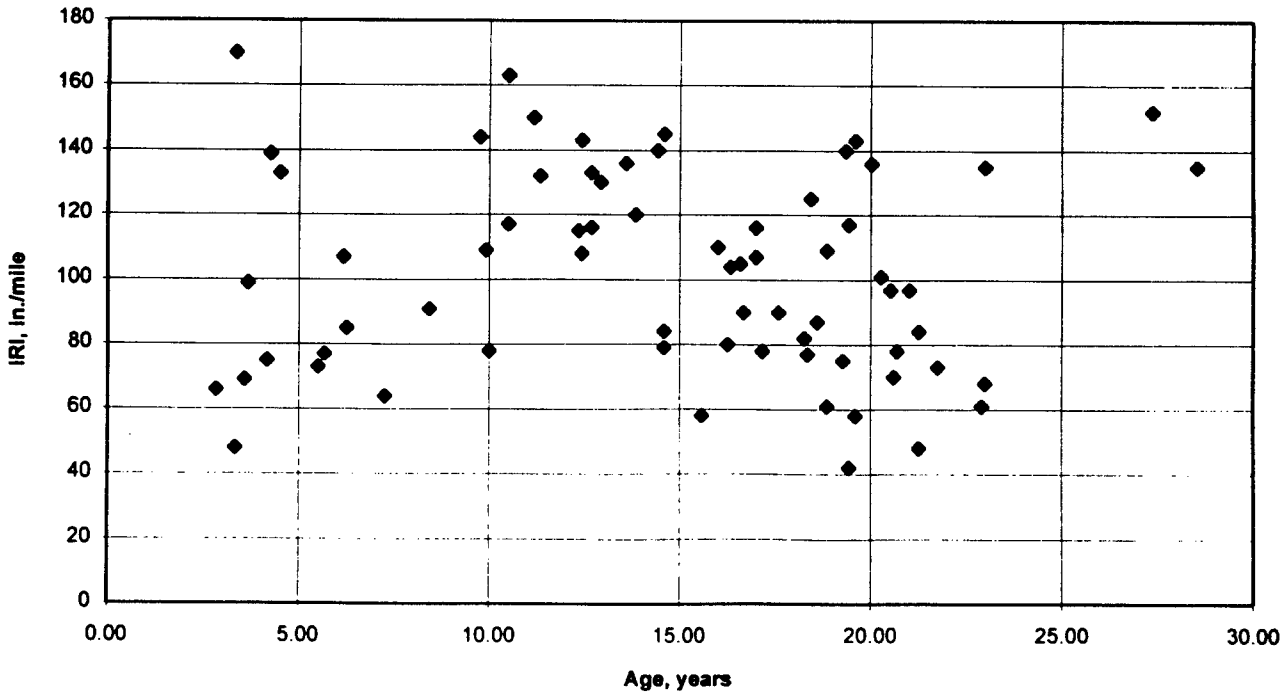

(15.8 mm/km = 1 in/mi)

Figure 42. IRI versus age.

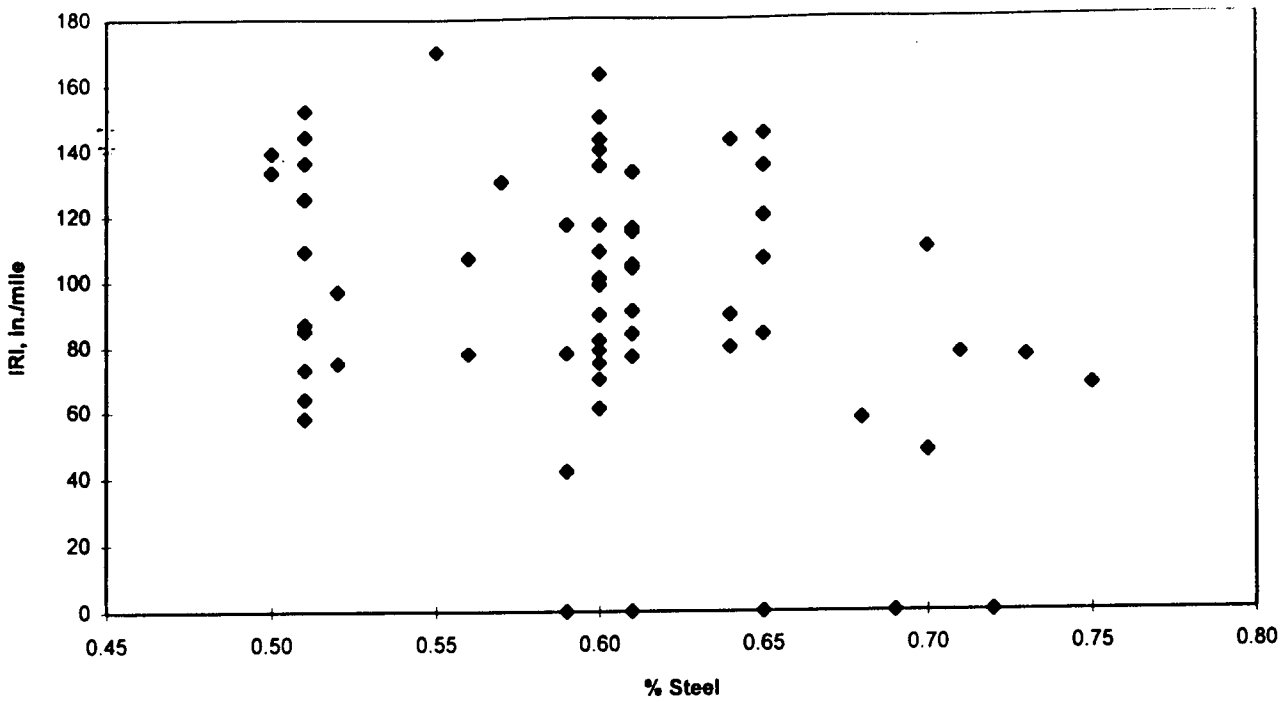

(15.8 mm/km = 1 in/mi)

Figure 43. IRI versus percent steel.

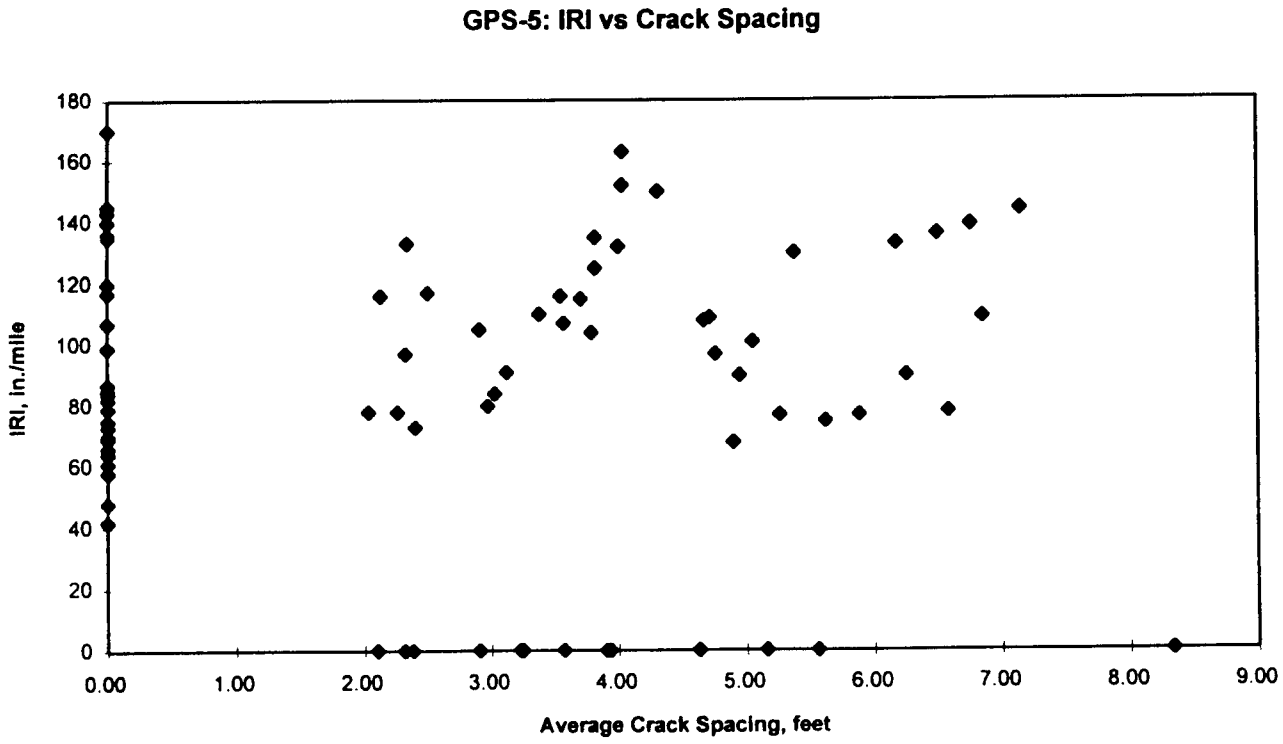

(15.8 mm/km = 1 in/mi) (0.305 m = 1 ft)

Figure 44. IRI versus crack spacing.

CHAPTER 6 - SUMMARY AND RECOMMENDATIONS

Summary

The analysis of the field data from a select number of CRC pavement test sections was presented in the previous chapters. Because of funding constraints, only a small number of sections were investigated. However, this was not a major disadvantage as the major focus of the study was to evaluate the performance of each section in detail and determine cause and effect relationships between various pavement characteristics and performance (functional and structural). No global regression analysis based relationships are presented here because of the small sample size and because of the interactions of many confounding factors.

This study has highlighted some new concepts and approaches of evaluating different aspects of CRC pavement performance incorporating the results of distress surveys (cracking pattern), crack width measurements, deflection testing along the edge and crack locations, and ride quality evaluation. An attempt was made to determine why certain CRC pavement sections behaved (in terms of cracking pattern) significantly differently than other sections with many factors being similar for these sections. The different cracking patterns at IA-1, OK-1, and OR-2 (compared to other in-state sections) could not be explained directly. It is quite possible that the ambient temperature conditions and curing conditions at these sections may have contributed to the development of the cracking pattern.

It should be noted that no attempt was made in this study to conduct an indepth analysis of specific "known" problem factors such as D-cracking, alkali-silica reactivity (ASR), and local aggregate effects. These known issues were unfortunately not accounted for in earlier concrete pavement construction, but are taken into account in new construction now.

Based on the results of the study, it appears that there may be a threshold value for percent steel for the currently used range of concrete strengths (splitting tensile strength in the range of 3.10 to 4.48 MPa (450 to 650 lbf/in^2)). Use of higher steel amount with conventional concrete strengths may result in more closely spaced cracking. While closely spaced cracking is not in itself a problem, it can lead to excessive punchout related problems in presence of poor support conditions.

There is a strong interaction between percent steel, concrete strength, and crack spacing. For conventionally used concrete strengths (splitting tensile strength at 28 days of about 2.76 to 3.45 MPa (400 to 500 lbf/in^2)), steel in the amount of 0.6 to 0.7 percent appears to provide desirable long-term average crack spacing in the range of 0.9 to 1.5 m (3 to 5 ft). The use of steel content less than 0.6 percent is cautioned as it is clear from the Oklahoma test sections and a recent Maryland project along U.S. 50 (not reported here) that use of 0.5 percent steel will result in longer crack spacings and possible premature development of punchouts at closely spaced cracks adjacent to longer spaced cracks. The use of 0.65 percent as the minimum steel content is strongly recommended with the conventional concrete strengths typically used in the U.S. If higher steel content is to be used, then appropriately

higher strength concrete should be specified to maintain desirable average crack spacing in the range of 0.9 to 1.5 m (3 to 5 ft) or a stabilized base must be specified.

The measured crack widths normalized to -17.8 °C (0 °F) generally appear to be within the recommended limit of about 1 mm. However, some sections were marginal with respect to desired crack width. Recent studies[9] have indicated the cracks less than 1 mm in width may be required for heavily trafficked CRC pavements under 330 mm (13 in) in thickness to ensure adequate performance.

The effect of tied concrete shoulder could not be classified as very positive with respect to improving the structural response of the CRC pavements (as indicated by deflection testing along the edges). Use of tied-concrete shoulders may have other advantages and as such may be used in conjunction with CRC pavements. The use of widened lane for CRC pavement appears to be promising and should be seriously considered as a design option. Based on the good performance of the three Oregon sections (each incorporating a 4.0 m (13 ft) wide outside lane), the use of widened lane should not be a cause for concern because of the longer aspect ratio for each cracked portion of the pavement.

The effect of base type on CRC performance was not very pronounced. The effect of the use of a "hard" support (e.g., LCB) could not be clearly addressed. However, the two sample sections (IL-1, OK-5) containing permeable bases did exhibit greater cluster ratios and average crack spacing. Both of these sections were relatively new and the section in Oklahoma was constructed with a lower amount of steel. Also, a separate evaluation of a 3-year old Virginia CRC pavement constructed with a permeable CTB indicated that adequate crack spacing can develop in CRC pavements incorporating permeable CTB.

The use of epoxy-coated reinforcement did not result in undesirable cracking pattern. The FHWA Technical Advisory T5080.14, dated June 5, 1990, recommends that the bond area should be increased 15 percent to increase the bond strength between the concrete and reinforcement if epoxy-coated steel reinforcement is used. This implies that 15 percent more steel should be used if epoxy-coated bars are used. Based on the limited field data, it appears that the use of 15 percent more steel may not be warranted provided the steel content is properly estimated. However, additional data need to be compiled to verify this observation.

Based on the deflection testing, the following summary is presented:

1. Load transfer efficiencies at transverse cracks of CRC pavements, even after many years of service, remain high - generally greater than 90 percent, provided adequate steel amount is used. The Oklahoma sections with 0.5 percent steel exhibited lower load transfer efficiencies.

2. Edge deflections measured at transverse crack locations tended to be twice as high as the base or midslab crack location deflections.

3. Edge deflections measured at transverse crack locations were higher during early morning than during afternoon testing.

4. The radius of relative stiffness, ℓ, did not characterize well the effective pavement stiffness along the edge. The better parameter to describe the edge "structural stiffness" is the slab rigidity, D. The D values were found to be considerably lower along the edge that at the interior. The backcalculated D value may be a better indicator of potential punchout locations.

5. Deflection data did not correlate well with the cracking pattern indicating that the pavement stiffness is not very dependent on crack spacing as long as there is high load transfer efficiency at the transverse cracks. Overall, the variability in the deflections and the backcalculated pavement stiffness values appears to be more influenced by the apparent variability in the support condition.

The profile data indicate that CRC pavements generally provide good ride even after many years of service. Although ride quality may decrease with age, age (and cumulative traffic) by itself was not a major contributor to decrease in ride quality. As the data indicated, many CRC pavement continue to provide a good ride (IRI between 72 and 157) even after 15 years of service. This was confirmed by the profile testing data from the GPS-5 test sections.

Other specific findings based also on the theoretical analysis of crack spacing development are summarized below.

1. Based on the results discussed in chapters 3 and 4, development of early cracking patterns is most significantly affected by climatic conditions at the time of construction. In other words, design variables such as the percent of reinforcement, concrete strength, type of rebar coating, subbase type appeared to be secondary in nature. The long term cracking appears to be affected by amount of steel, age, and concrete strength. The cracking development appears to slow down (stabilize) after about 3 to 4 years.

2. Construction related variability (i.e. depth of steel cover and concrete strength) and degree or quality of curing appears to be most significant in affecting cluster cracking in the crack pattern.

3. The crack spacing distribution predicted by CRCP-5 program showed variable results when compared to the measured field values. In order to simulate the field values, a range in possible curing temperatures were considered based on climatological data for a given state or area. It was assumed in the study that the compressive strength of the concrete, elastic modulus, and flexural strength of the concrete were dependent on the tensile strength of the concrete as was the drying shrinkage in the concrete. Thus, CRCP-5 program was not always able to simulate field cracking pattern.

4. As pointed out above, curing temperature has an effect on the crack spacing distribution. The higher the curing temperature and the lower the minimum temperature condition following construction, the shorter the crack spacing interval. The lower the curing temperature, the larger the average crack spacings.

5. The crack width depends on many of the design parameters previously recognized that influence its prediction. However, other parameters such as the depth of cover and the age of the pavement are also important. As expected, older pavements tend to have wider crack widths than the new pavements.

6. Although analysis programs suggest that the average crack spacing are greater for pavements placed on bases/subbases with lower frictional resistance values, the field results did not substantiate this fact. It appears that in actual practice, once initial cracking develops, the effect of base/subbase friction is not as significant for the shorter lengths of pavement between cracks.

7. There is some evidence to suggest that cluster cracking potential increases if the pavements are cured at higher temperatures. Some interaction may exist with the curing temperature and the degree of drying shrinkage. Cluster cracking decreases as shrinkage increases or apparently as the degree of cracking increases.

8. Theoretically predicted crack widths decreased with an increase in percent of longitudinal steel. Some evidence was apparent in the field data to support this observation.

The performance of CRC pavement systems are affected by many factors related to material, design, climatic, and support parameters. The first three factors affect CRC pavement performance primarily through their effect on the development of the crack pattern and subsequently the resulting crack widths. Extensive discussion has been previously presented in volume I describing the role these factors play in crack development. Some of the important material properties are the strength and the thermal coefficient of expansion of the concrete. Elastic modulus is not as important because of the offsetting affects it has on crack spacing and crack width. Typically, however, as the thermal coefficient of expansion increases the crack pattern will become more dense and as the concrete strength increases the less dense the crack pattern becomes. Closely spaced crack patterns have traditionally become locations of punchout development typically if these locations are incidental with poor subgrade/subbase support conditions. For this reason it is recommended that close crack patterns be avoided. The use of high strength concrete may be appropriate for some coarse aggregate types, particularly those which have a tendency to develop close cracking intervals - otherwise the development of high strength may result in widely spaced crack patterns. The effect of high strength concrete can be offset in this regard by using greater percentages of reinforcing steel but this may result in an expensive costruction alternative. Ultimately, the design engineer must employs the right combination of steel reinforcement, coarse aggregate, Portland cement

content, and curing methodology to achieve a crack pattern that manifests tight crack widths and high load transfer qualities.

Recommendations

Further research and development for CRC pavement should focus on improving the cracking pattern of the pavement through improved construction and design technology and the use of positive crack control techniques. An over abundance of evidence manifest in this and past studies have pointed to the importance of the crack pattern as key to successful pavement performance. For many years the design of CRC pavement has focused on the percent of steel reinforcement and the expected drop in pavement temperature over the course of a year. However, it is apparent the crack pattern of CRC pavement cannot be controlled by the steel design alone and that other considerations deserving of further research should be included in the design process such as the type of aggregate, method of curing, and shrinkage potential, depth of steel cover, rate of strength gain in the first three days after construction, among others. Recent research efforts in Texas have indicated that positive crack control methods employed during the construction process show a high potential of providing improved crack patterns with less viability than those which occur on a random basis. The use of techniques such as this will forgo the need for high percents of steel reinforcements since the design engineer will have greater control over the resulting crack pattern. Since the use of high strength concrete will have a tendency to result in large average crack spacings, positive crack control techniques should offset this effect and allow for the use of such materials in CRC pavement systems.

Future research should consider investigating the concept of dynamic design of CRC pavements. With this concept, the amount of steel and concrete strength would be adjusted at the time of construction based on anticipated ambient temperature conditions or temperature restrictions may need to be imposed for paving.

CRC pavement has probably the greatest potential of all concrete pavement types of providing zero-maintenance service. This potential can be realized through the use of available technology to achieve longer service life and greater pavement performance at a lower cost to the tax payer. However, this can only be achieved if the design and construction features of CRC pavements are managed well on an active basis. The design process for a CRC pavement should continue through the construction and not end as soon as the plans and specifications are prepared. A more active interaction between the design process and actual ambient conditions during construction needs to be developed to achieve CRC pavements that will have acceptable cracking pattern. This may require imposing of guidelines on acceptable ambient conditions for placement of CRC pavements and overlays.

APPENDIX A - ILLINOIS TEST SECTIONS DATA ANALYSIS

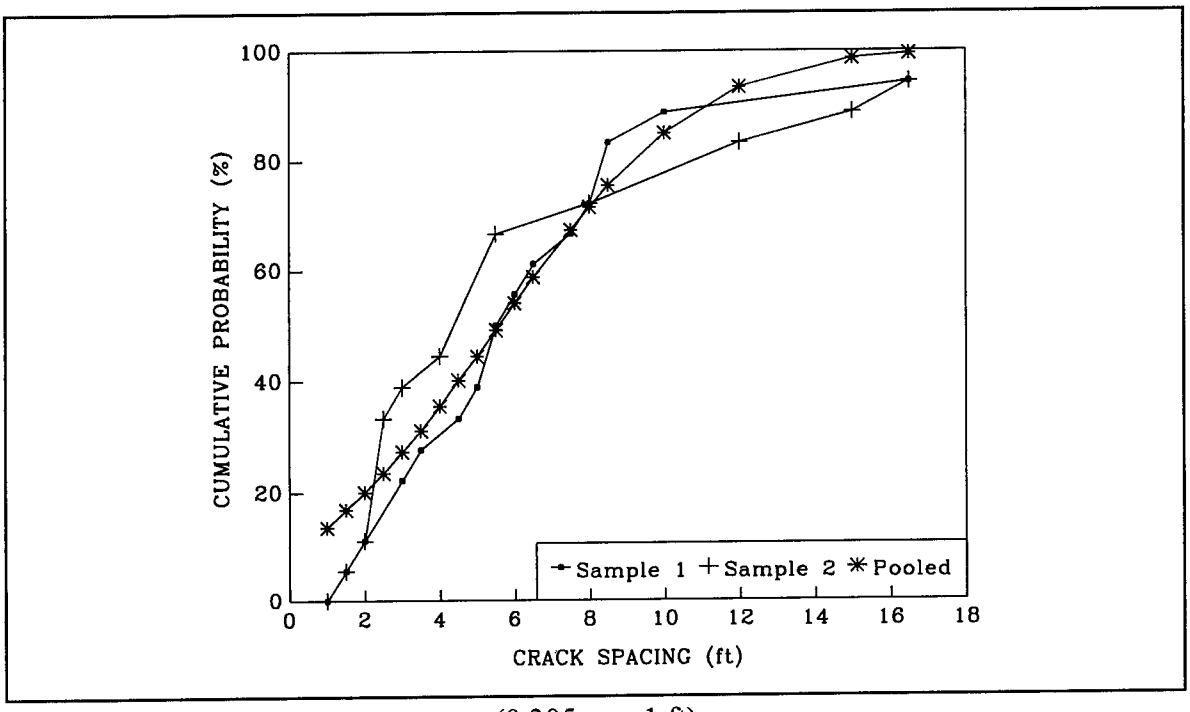

(0.305 m = 1 ft)

Figure 45. Field crack spacing distribution data: sample section Illinois-1.

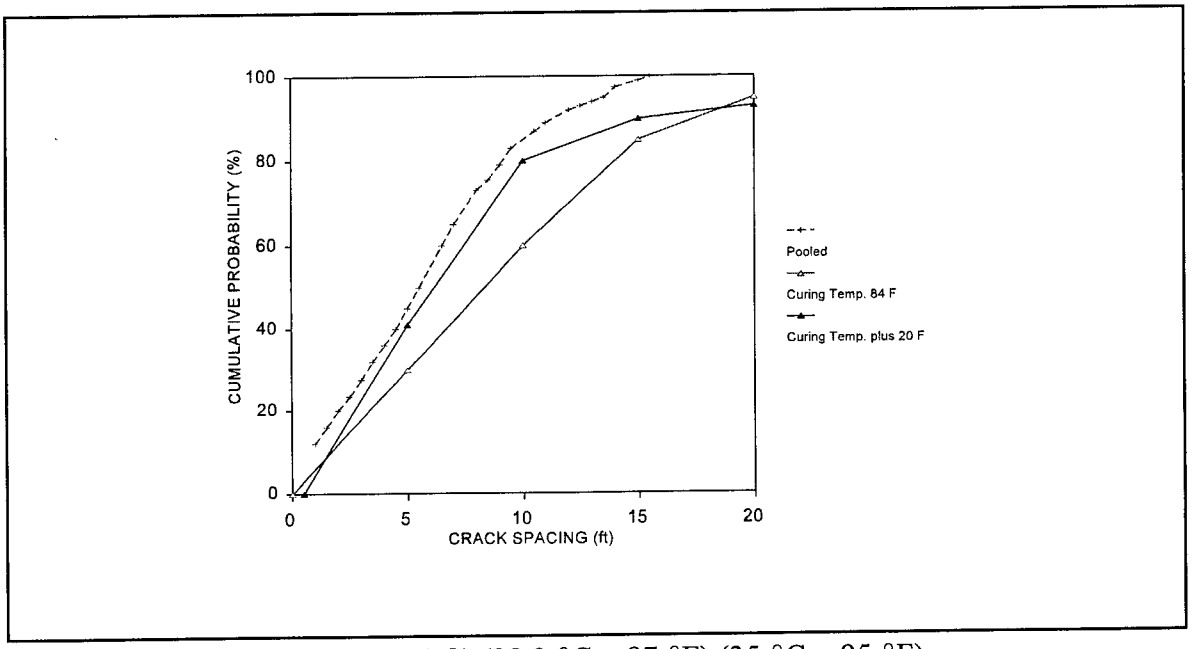

(0.305 m = 1 ft) (28.9 °C = 87 °F) (35 °C = 95 °F)

Figure 46. CRCP-5 crack distribution analysis for two curing temperatures from section Illinois-1.

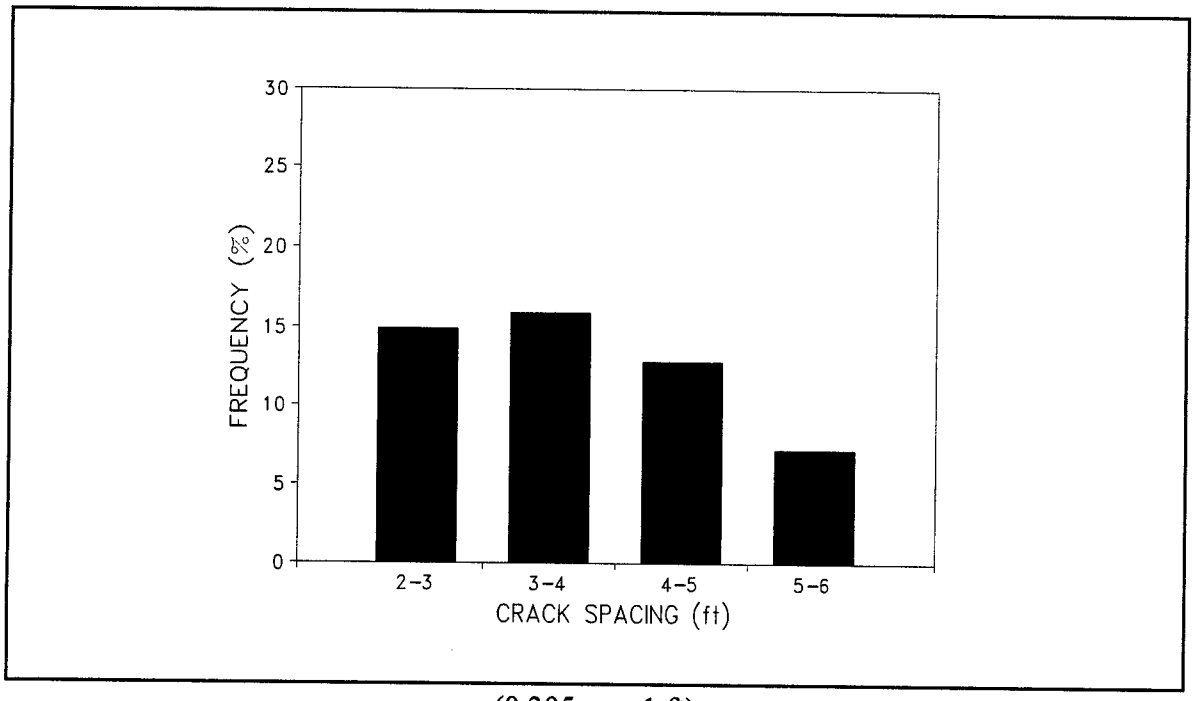

(0.305 m = 1 ft)

Figure 47. Crack spacing frequency: sample section Illinois-1.

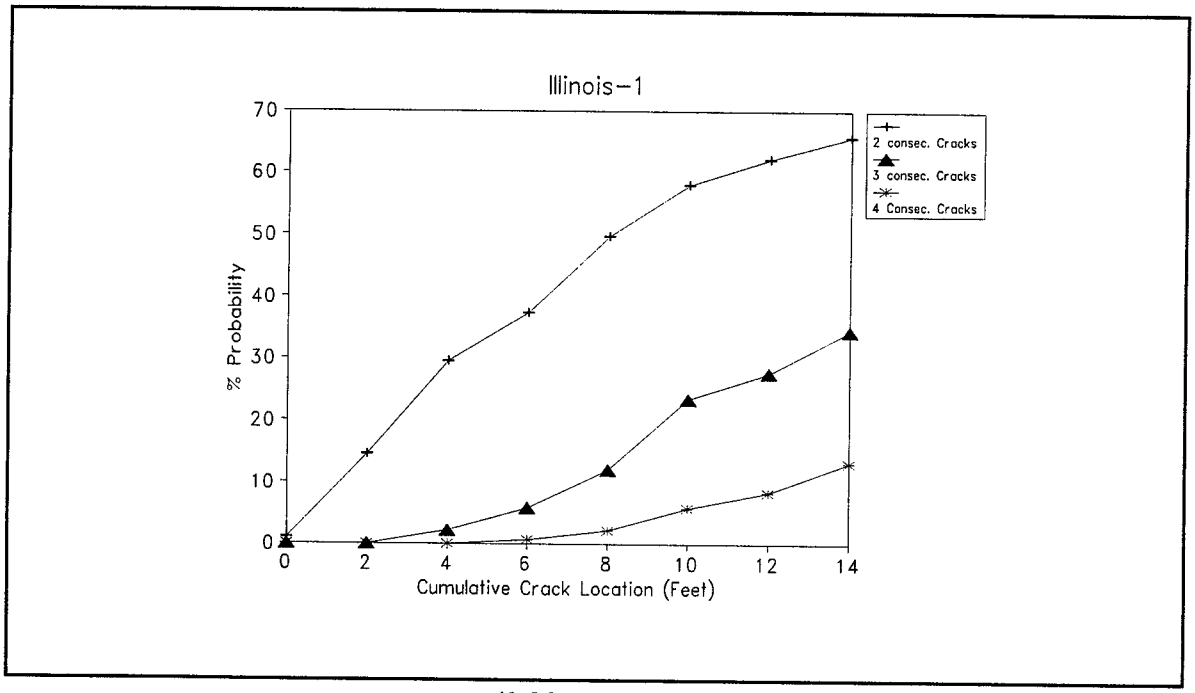

(0.305 m = 1 ft)

Figure 48. Probability of cluster cracking from sample section Illinois-1.

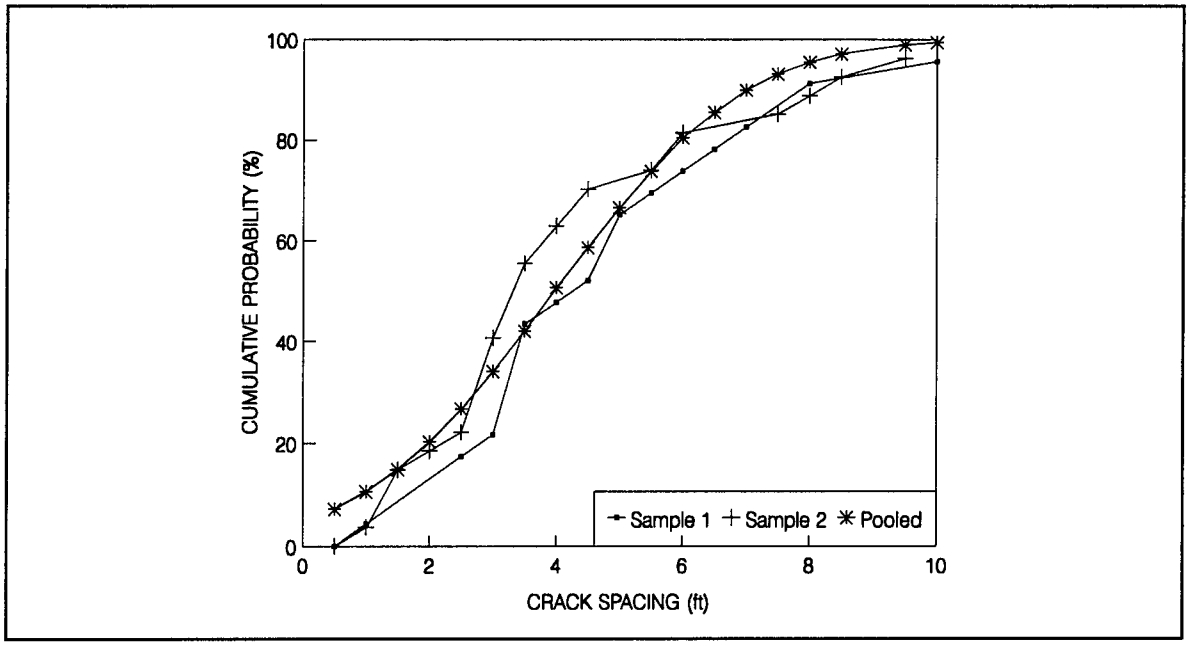

(0.305 m = 1 ft)

Figure 49. Field crack spacing distribution: sample section Illinois-2.

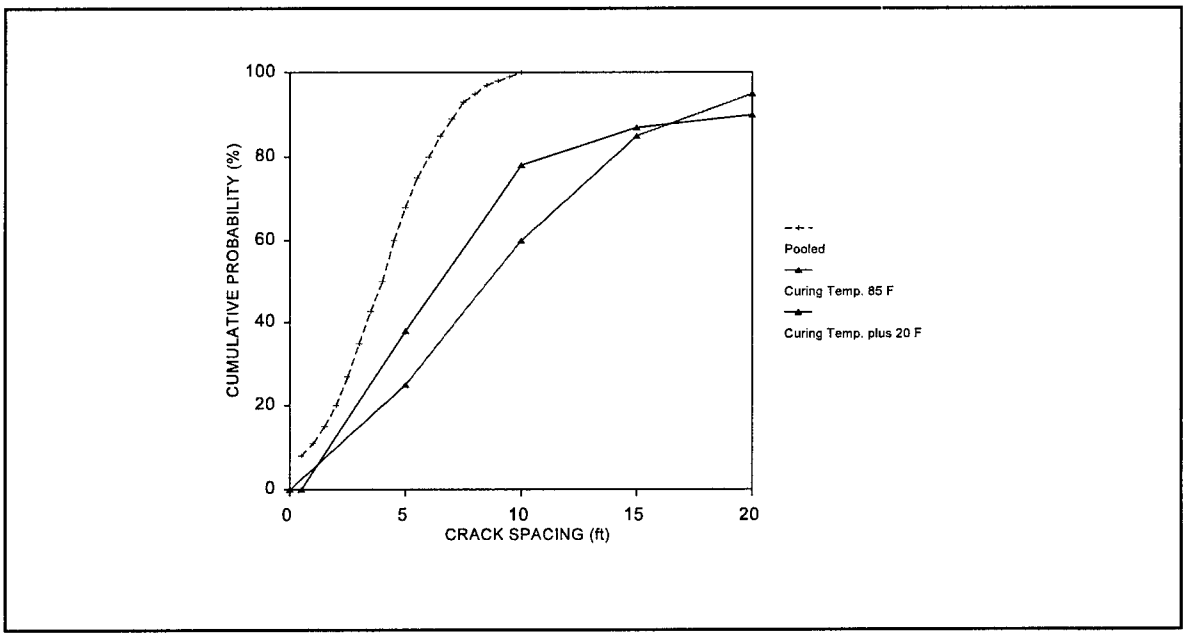

(0.305 m = 1 ft) (28.9 °C = 85 °F) (35 °C = 95 °F)

Figure 50. CRCP-5 crack distribution analysis for two curing temperatures from sample section Illinois-2.

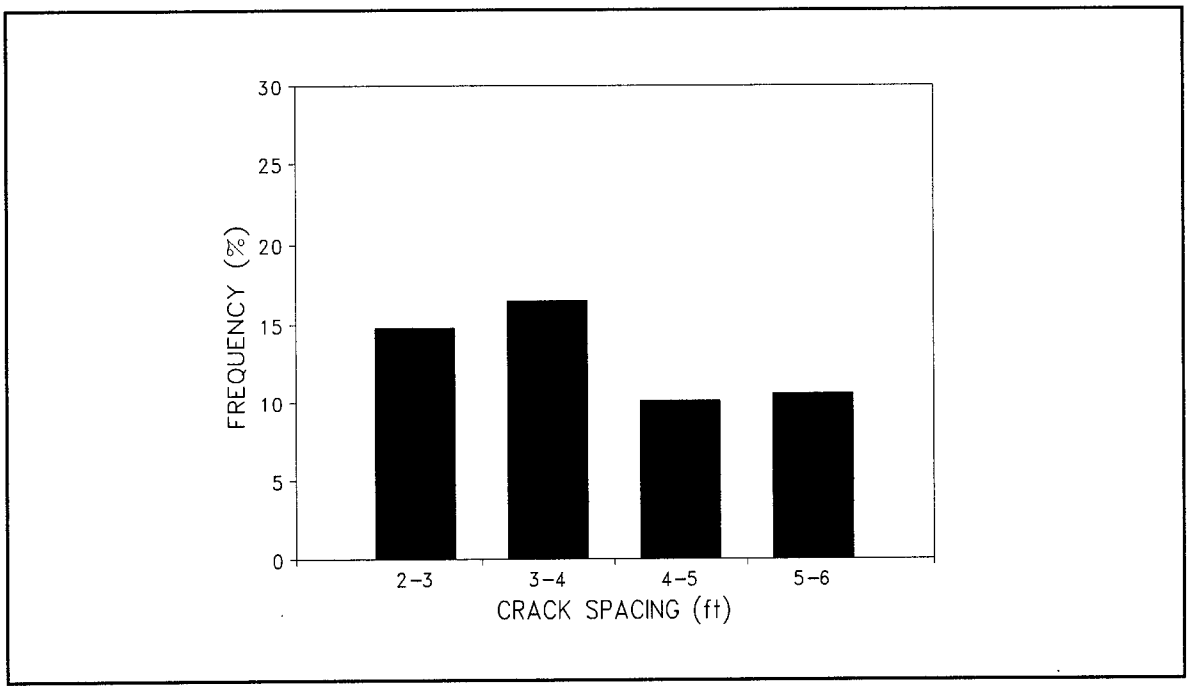

(0.305 m = 1 ft)

Figure 51. Crack spacing frequency: sample section Illinois-2.

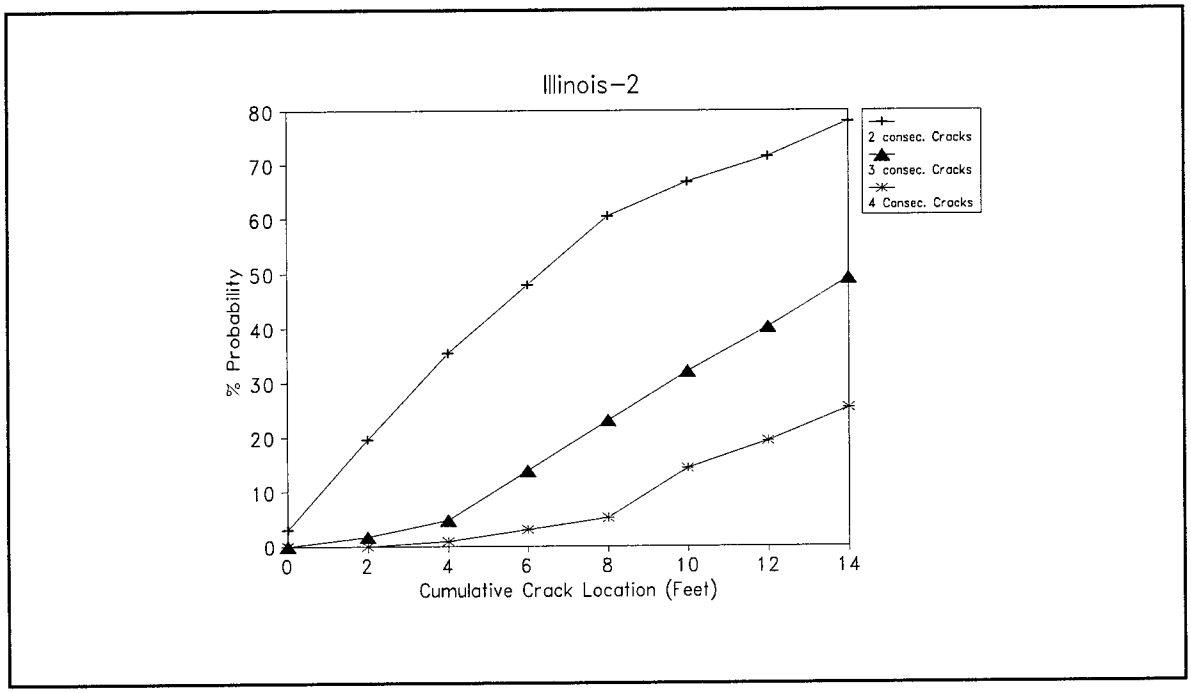

(0.305 m = 1 ft)

Figure 52. Probability of cluster cracking from section Illinois-2.

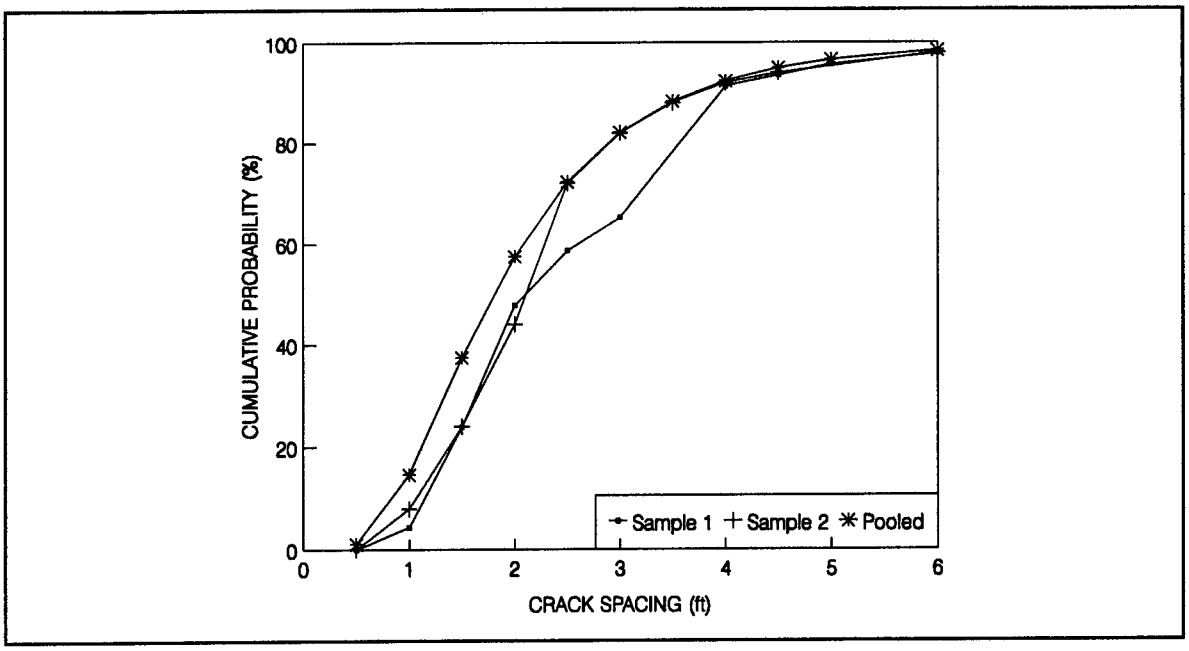

(0.305 m = 1 ft)

Figure 53. Field crack spacing distribution data: sample section Illinois-3.

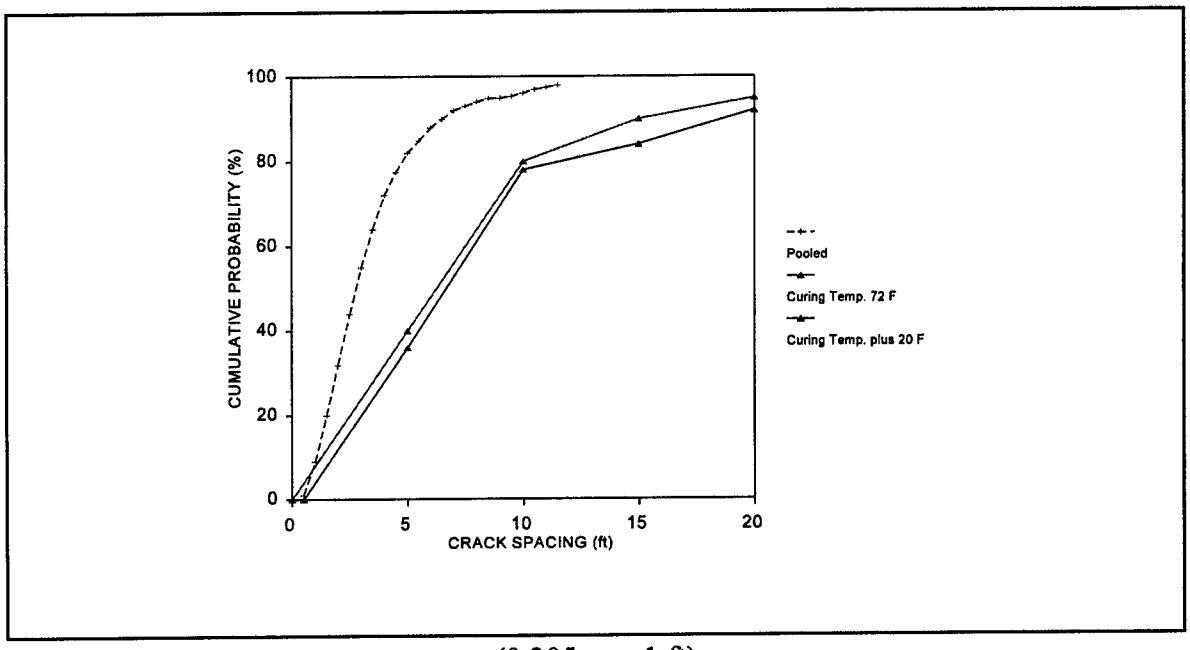

(0.305 m = 1 ft)

Figure 54. CRCP-5 crack distribution analysis for two curing temperatures from sample section Illinois-3.

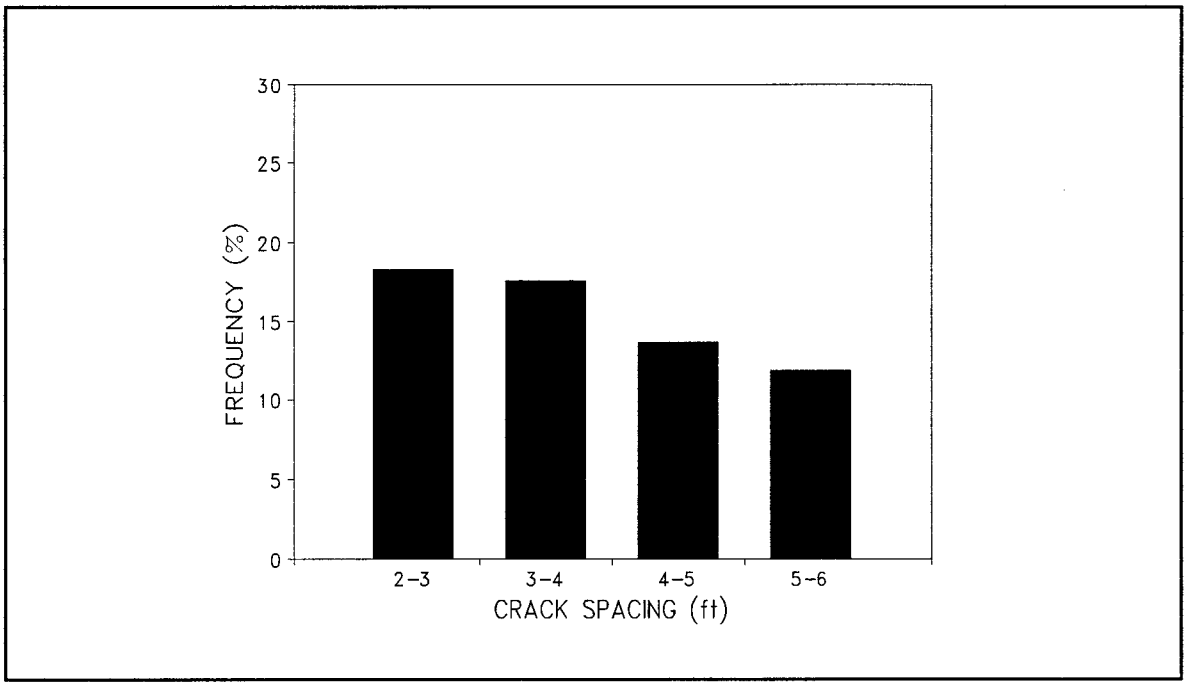

(0.305 m = 1 ft)

Figure 55. Crack spacing frequency: sample section Illinois-3.

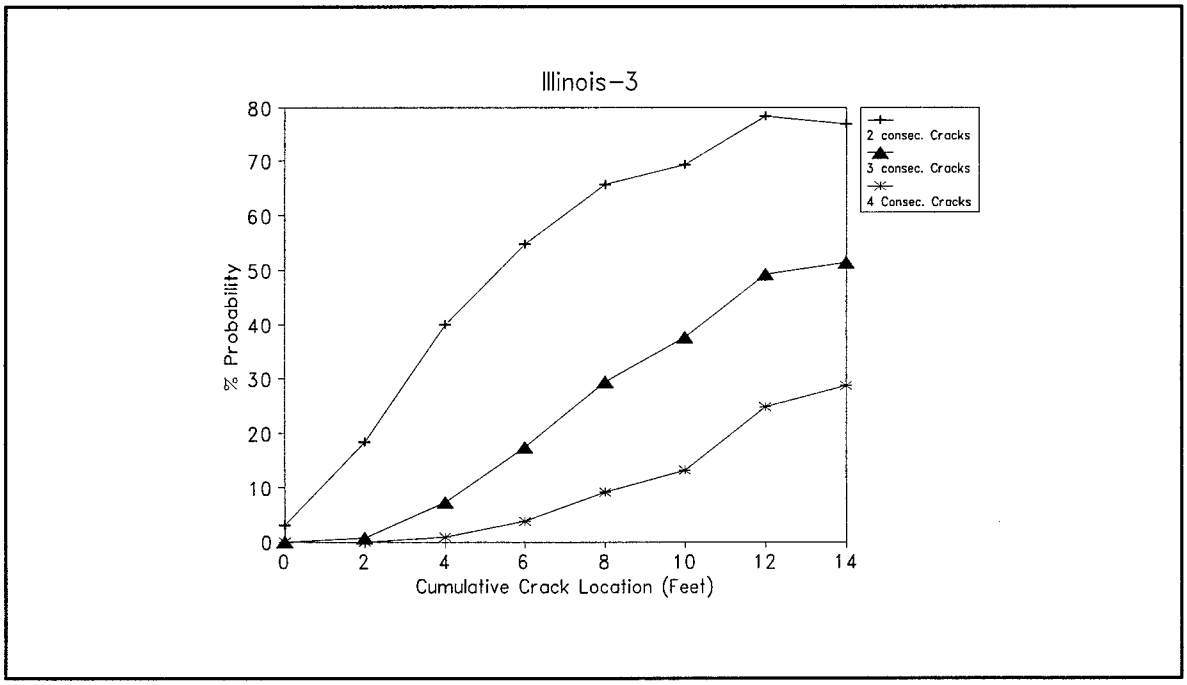

(0.305 m = 1 ft)

Figure 56. Probability of cluster cracking: sample section Illinois-3.

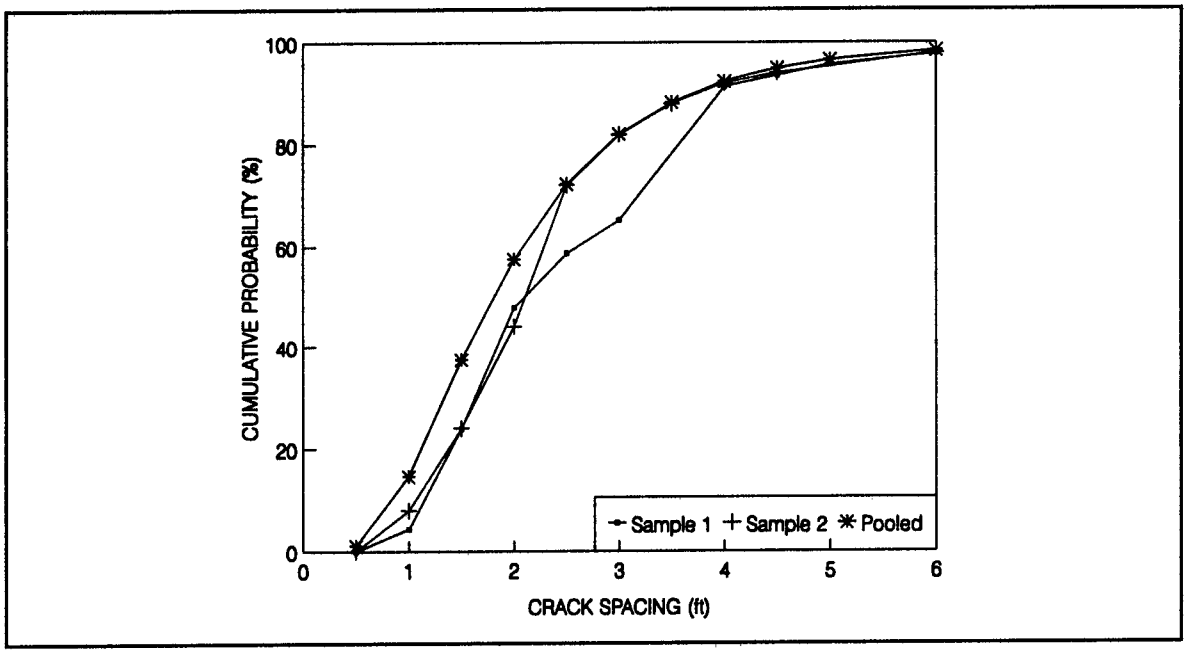

(0.305 m = 1 ft)

Figure 57. Field crack spacing distribution: sample section Illinois-4.

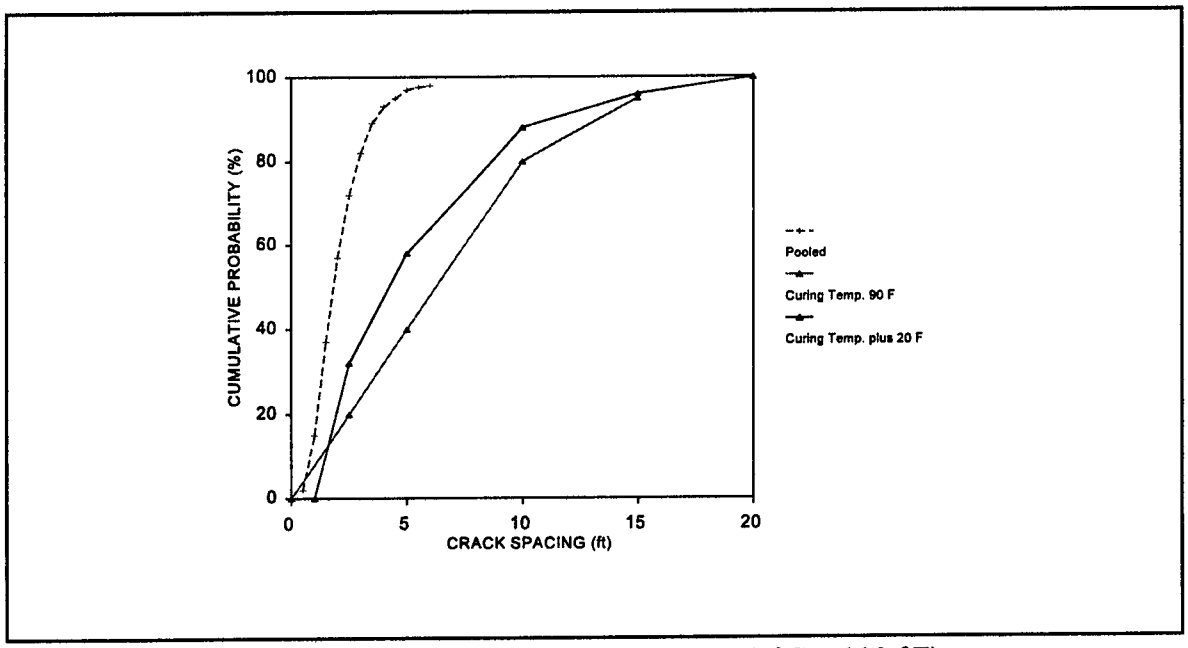

(0.305 m = 1 ft) (32.2 °C = 90 °F) (37.8 °C = 100 °F)

Figure 58. CRCP-5 crack distribution analysis for two curing temperatures from sample section Illinois-4.

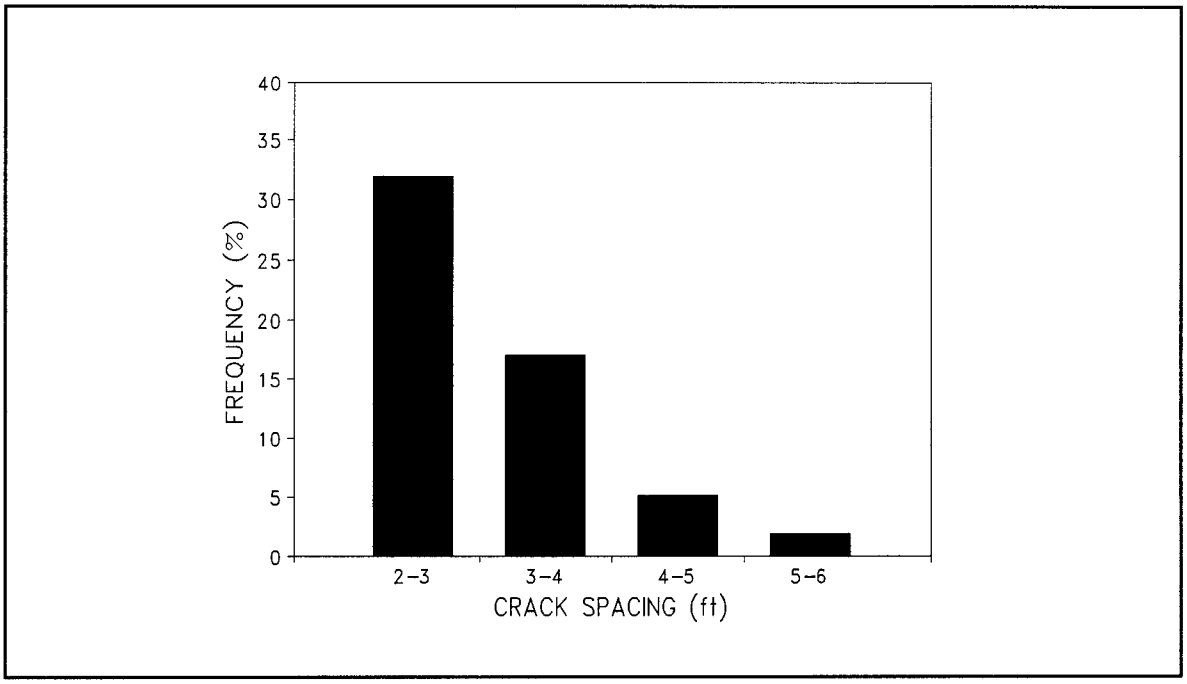

(0.305 m = 1 ft)

Figure 59. Crack spacing frequency: sample section Illinois-4.

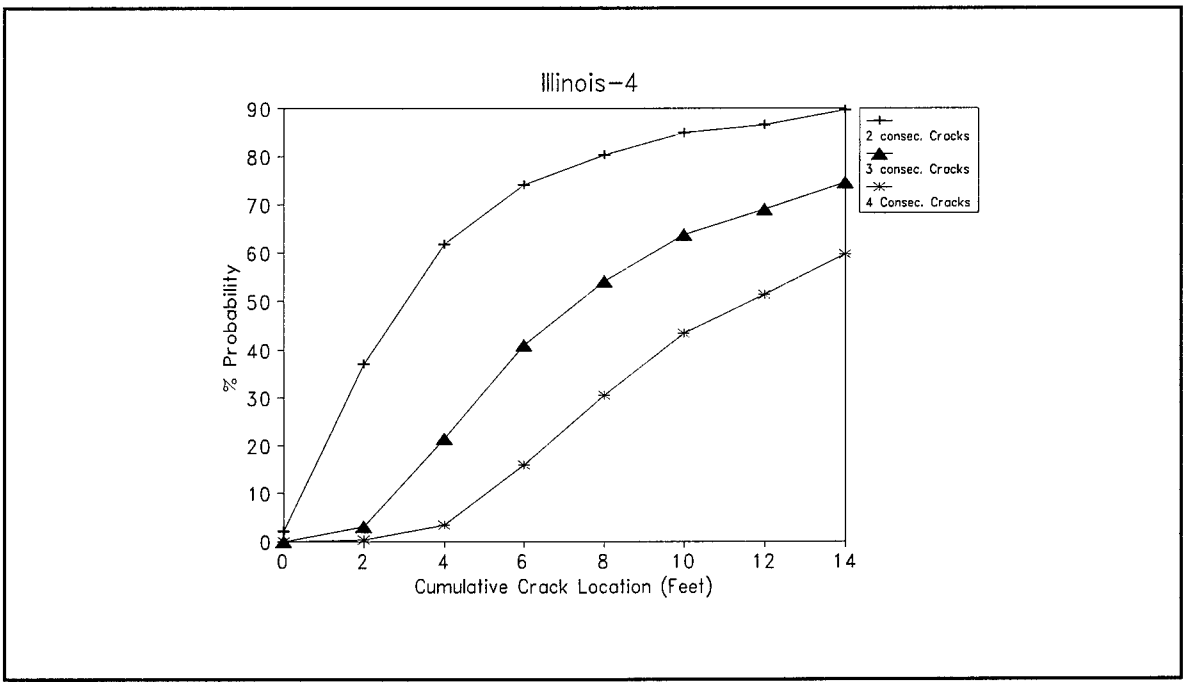

(0.305 m = 1 ft)

Figure 60. Probability of cluster cracking: sample section Illinois-4.

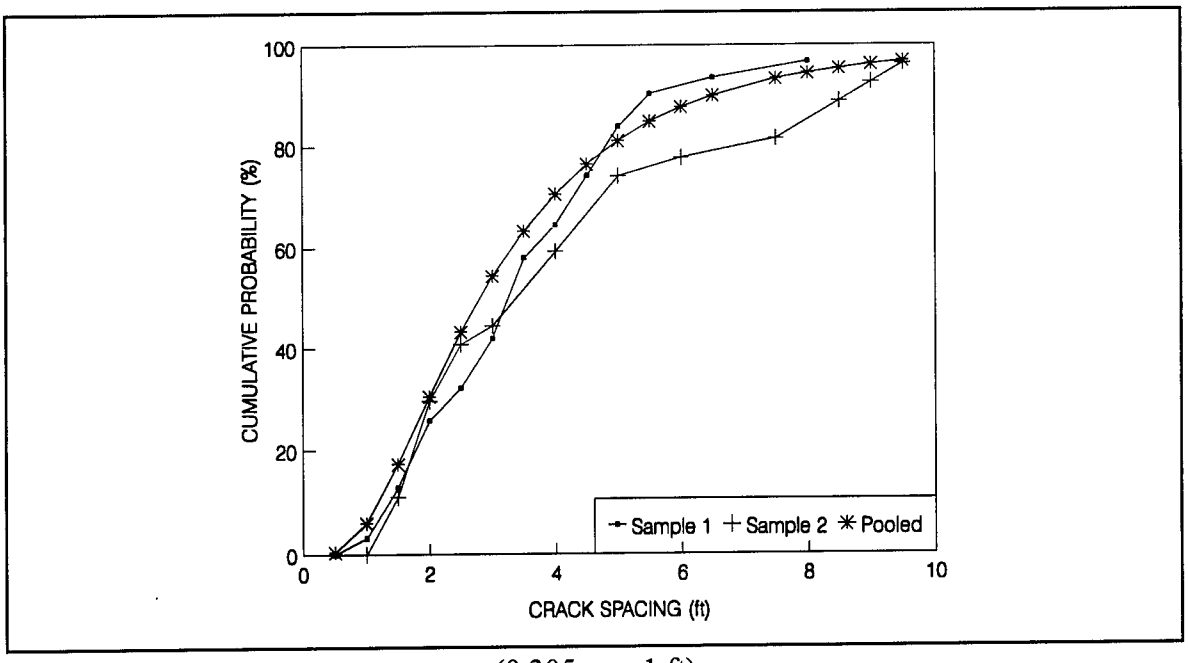

(0.305 m = 1 ft)

Figure 61. Field crack spacing distribution data: sample section Illinois-5.

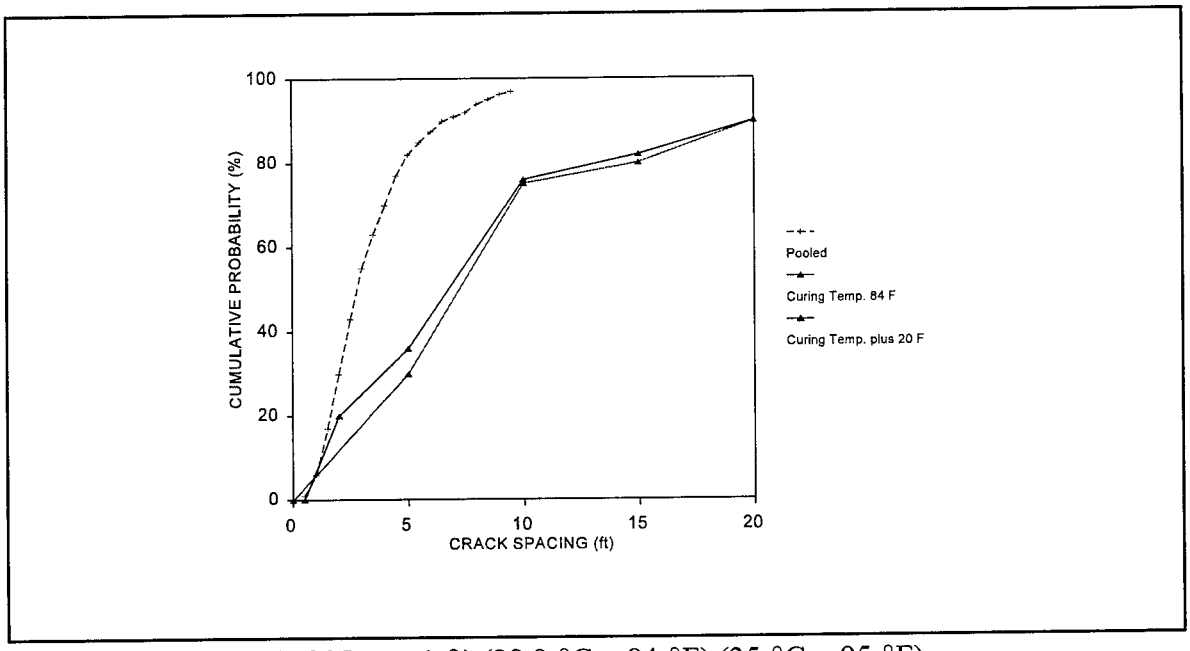

(0.305 m = 1 ft) (28.9 °C = 84 °F) (35 °C = 95 °F)

Figure 62. CRCP-5 crack distribution analysis for two curing temperatures from sample section Illinois-5.

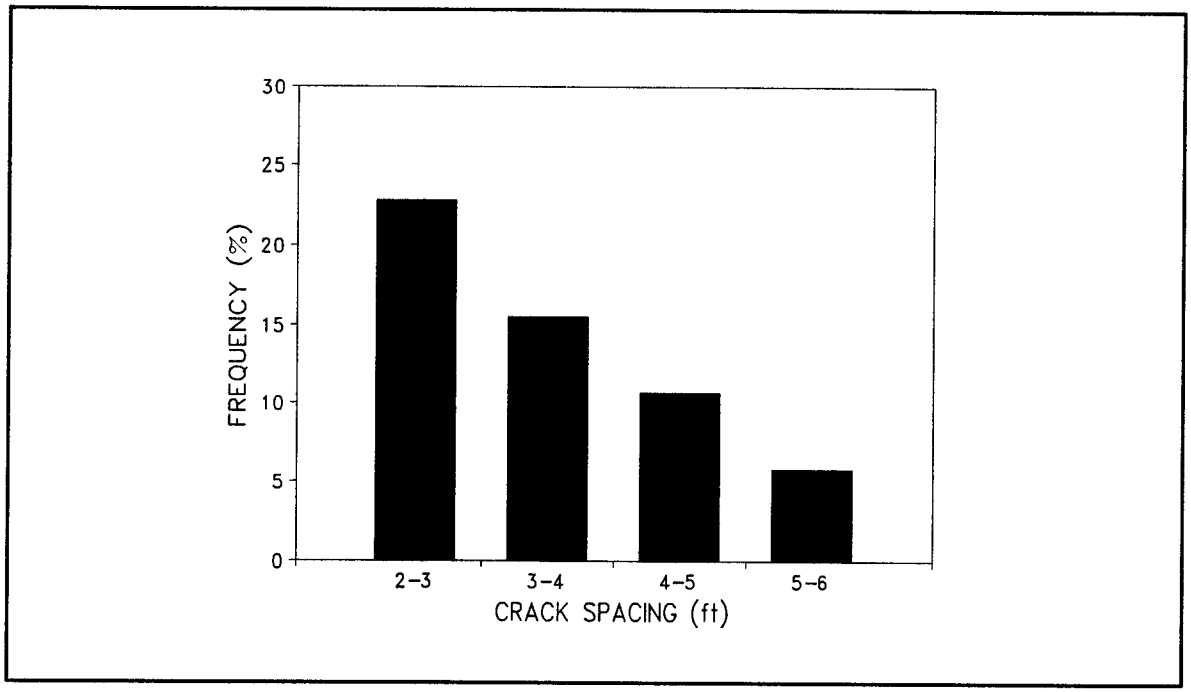

(0.305 m = 1 ft)

Figure 63. Crack spacing frequency: sample section Illinois-5.

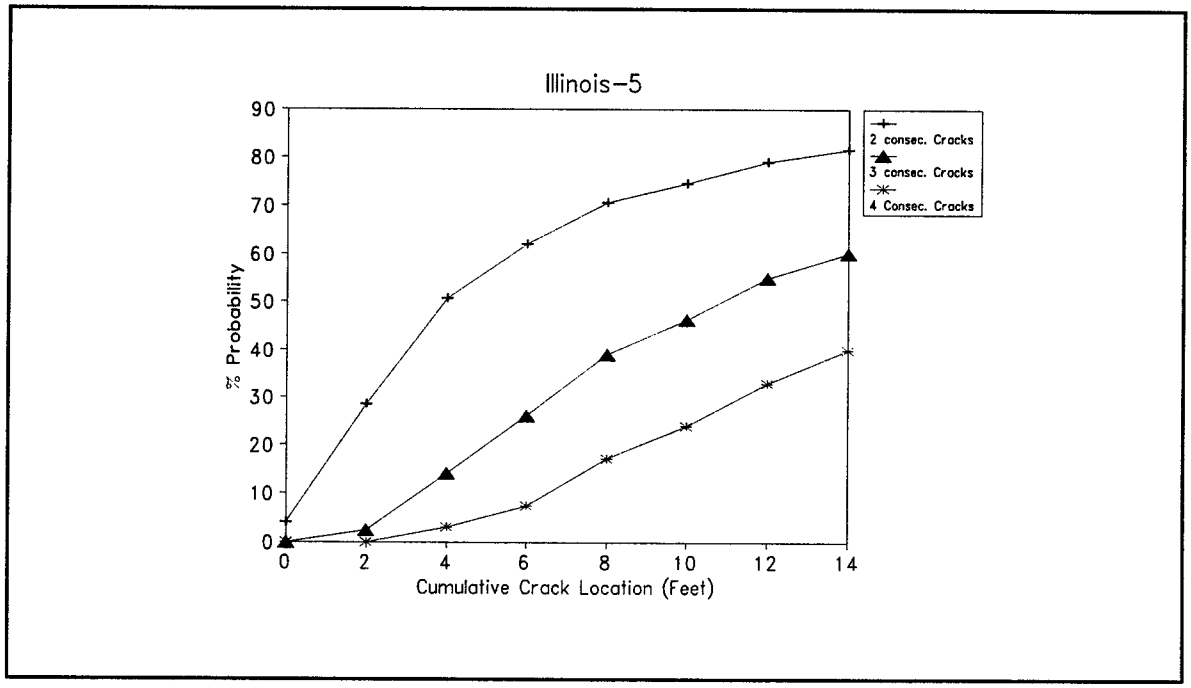

(0.305 m = 1 ft)

Figure 64. Probability of cluster cracking: sample section Illinois-5.

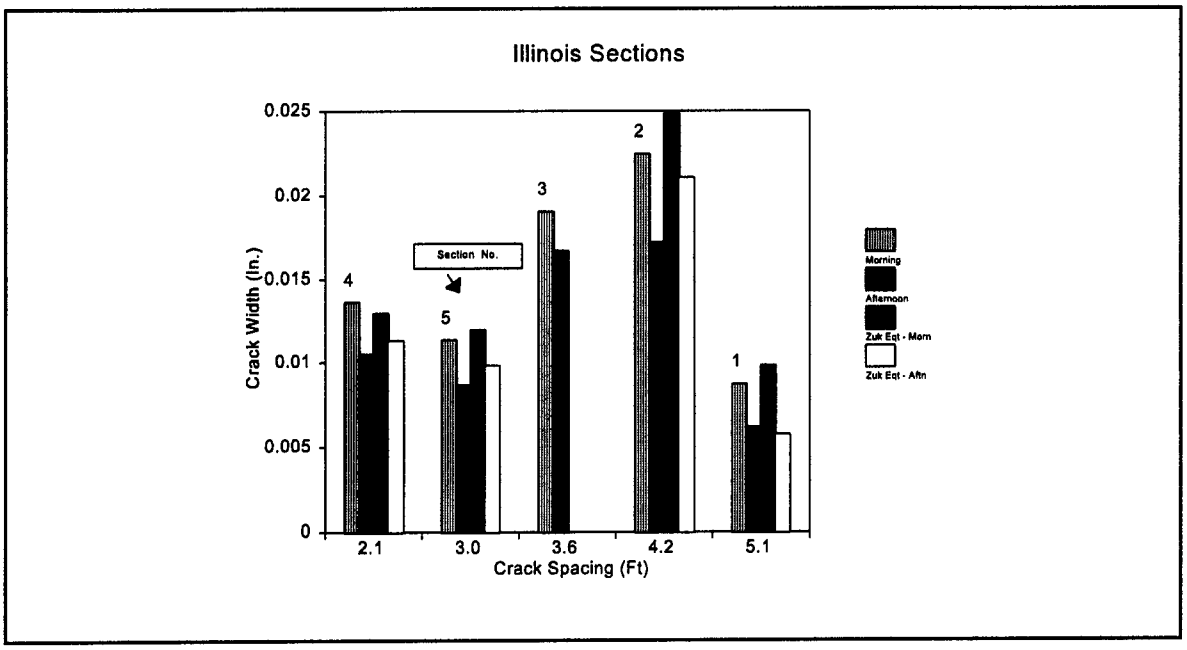

(25.4 mm = 1 in) (0.305 m = 1 ft)

Figure 65. Variation in crack width with crack spacing for Illinois sample sections.

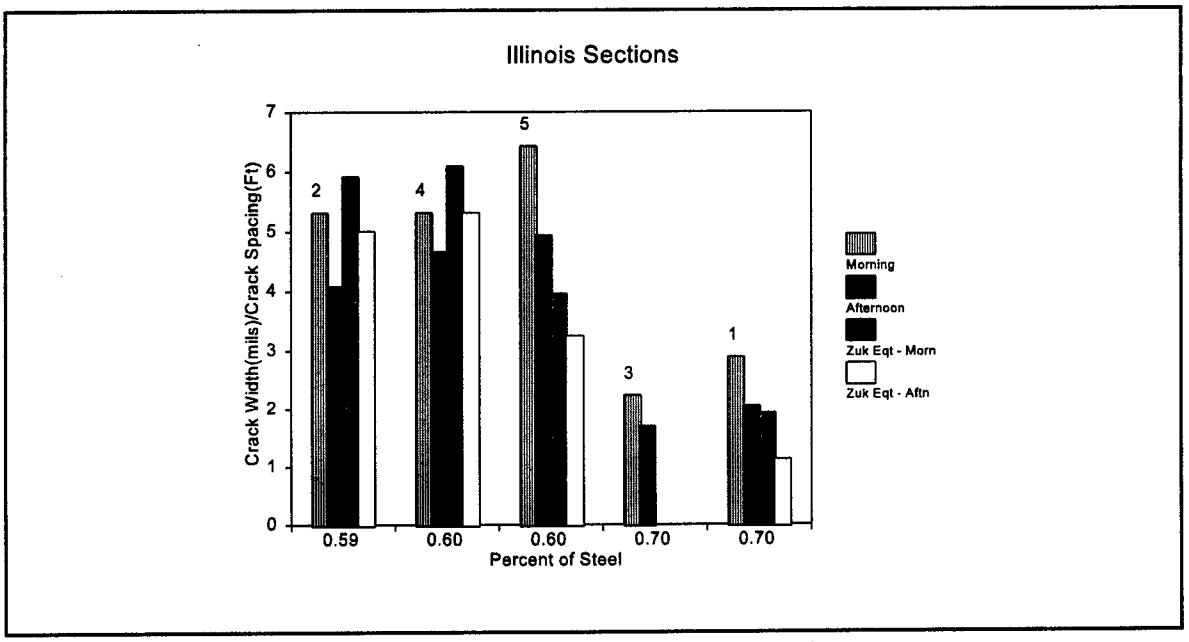

(0.0254 mm = 1 mil) (0.305 m = 1 ft)

Figure 66. Variation in crack width/crack spacing ratio with percent reinforcement for Illinois sample sections.

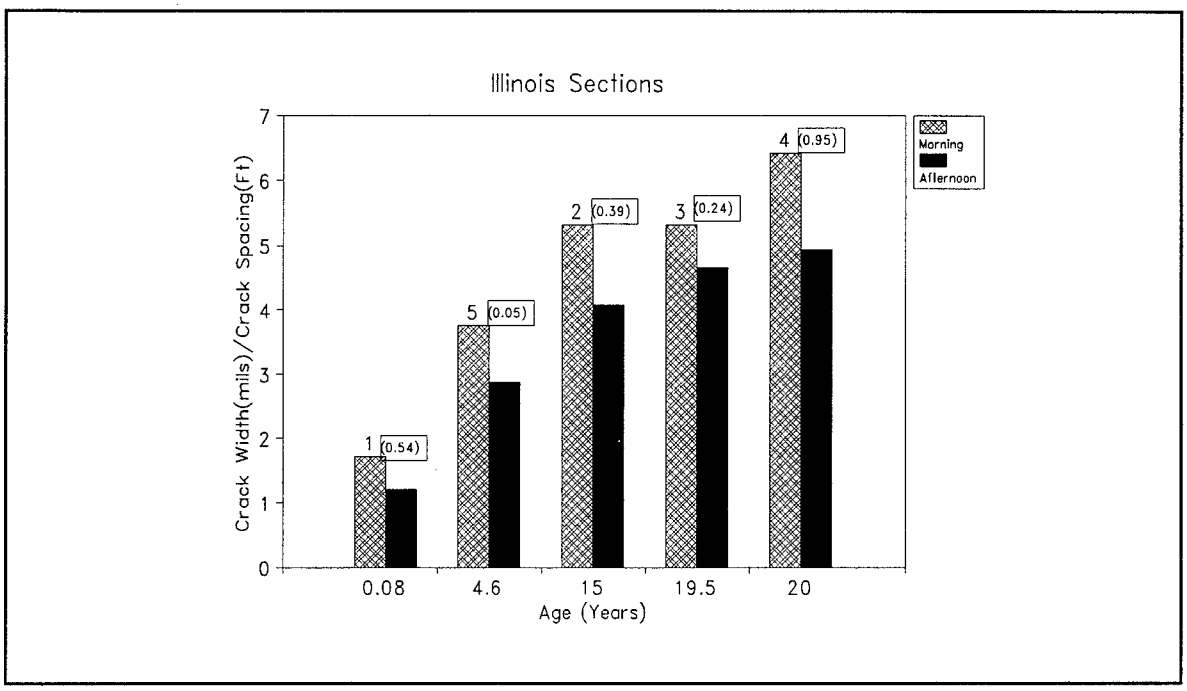

(0.0254 mm = 1 mil) (0.305 m = 1 ft)

Figure 67. Variation in crack width with pavement age for Illinois sample sections.

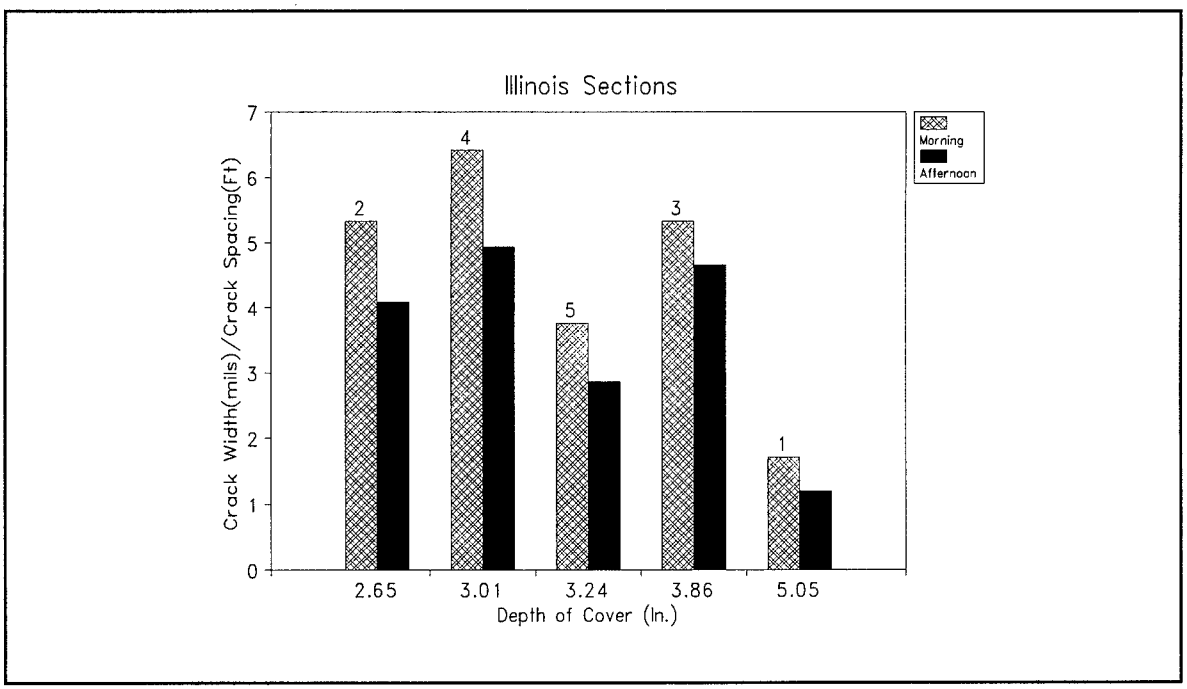

(0.0254 mm = 1 mil) (0.305 m = 1 ft) (25.4 mm = 1 in)

Figure 68. Variation in crack width/crack spacing ratio with depth of cover for Illinois sample sections.

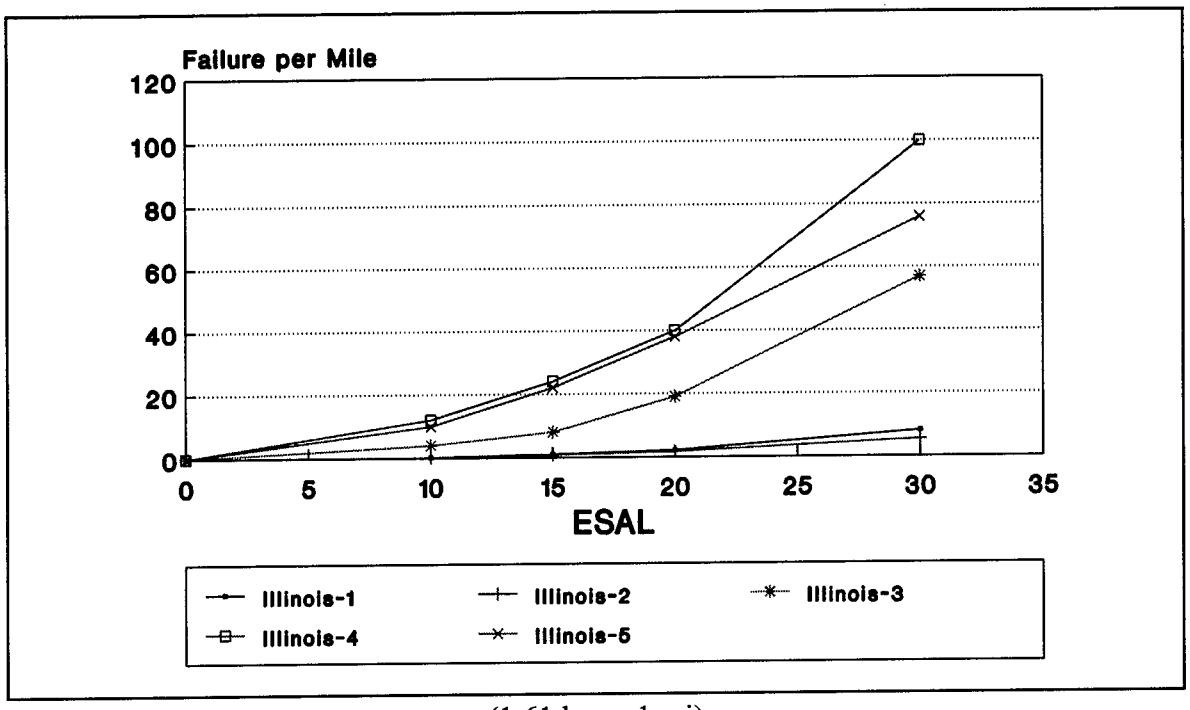

(1.61 km = 1 mi)

Figure 69. Performance prediction for sample sections in Illinois.

APPENDIX B - IOWA TEST SECTIONS DATA ANALYSIS

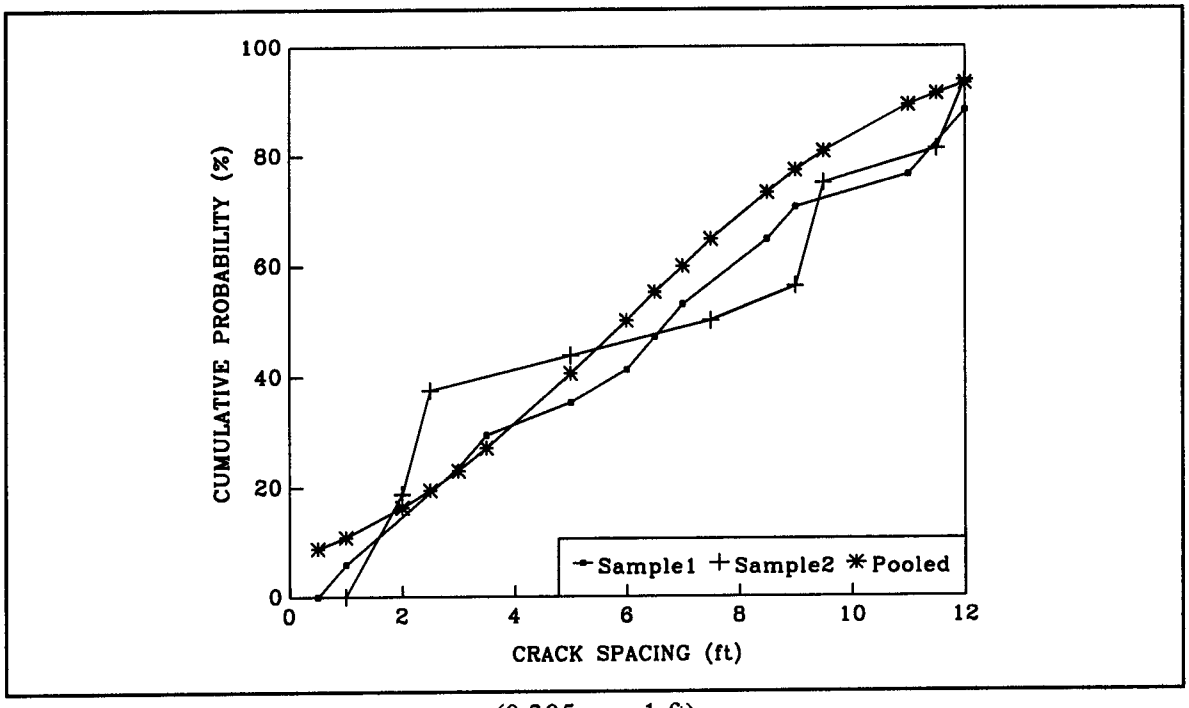

(0.305 m = 1 ft)

Figure 70. Field crack spacing distribution data: sample section Iowa-1.

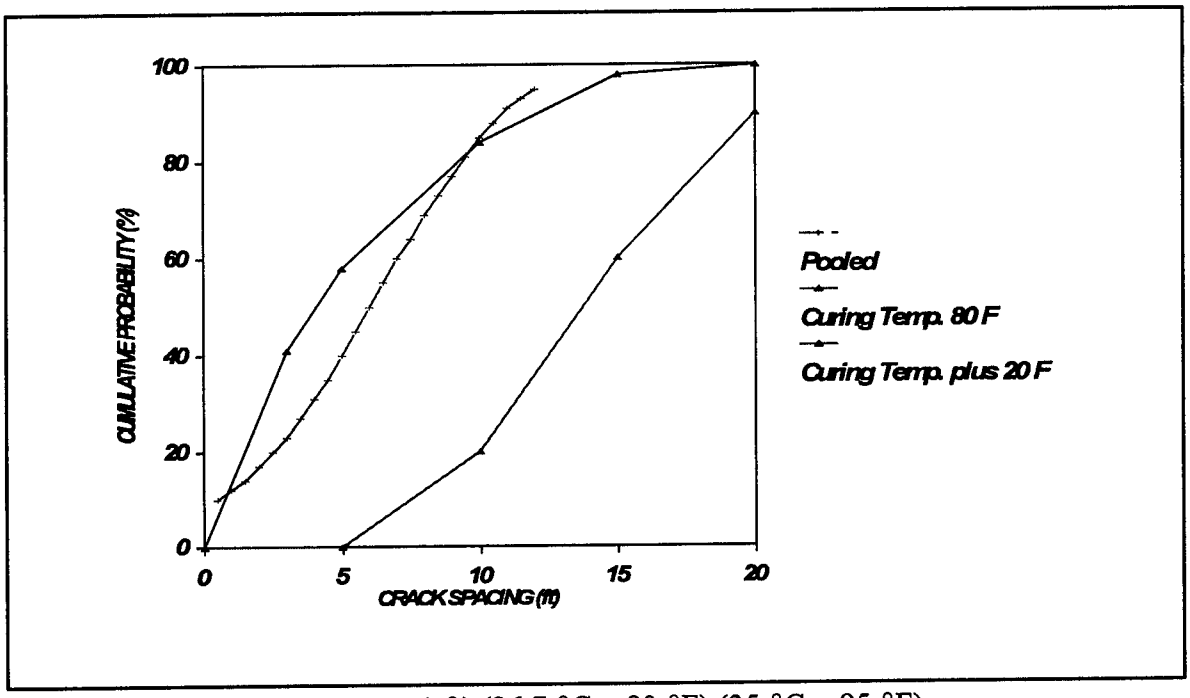

(0.305 m = 1 ft) (26.7 °C = 80 °F) (35 °C = 95 °F)

Figure 71. CRCP-5 crack distribution analysis for two curing temperatures from section Iowa-1.

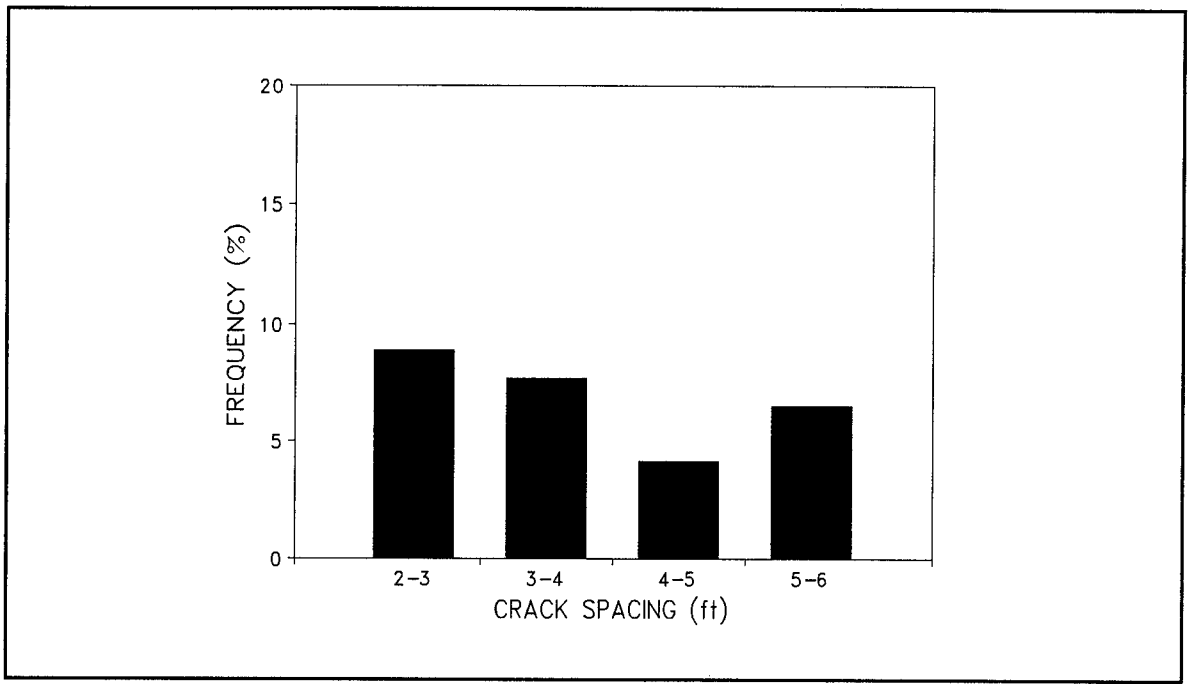

(0.305 m = 1 ft)

Figure 72. Crack spacing frequency: sample section Iowa-1.

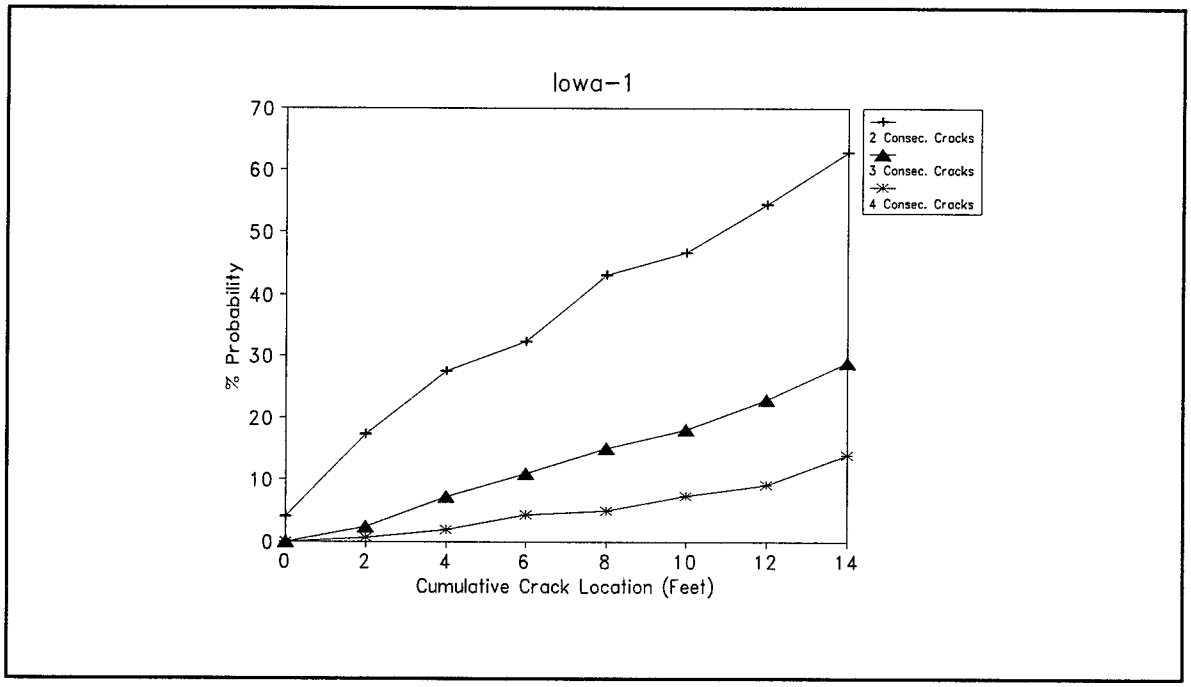

(0.305 m = 1 ft)

Figure 73. Probability of cluster cracking: sample section Iowa-1.

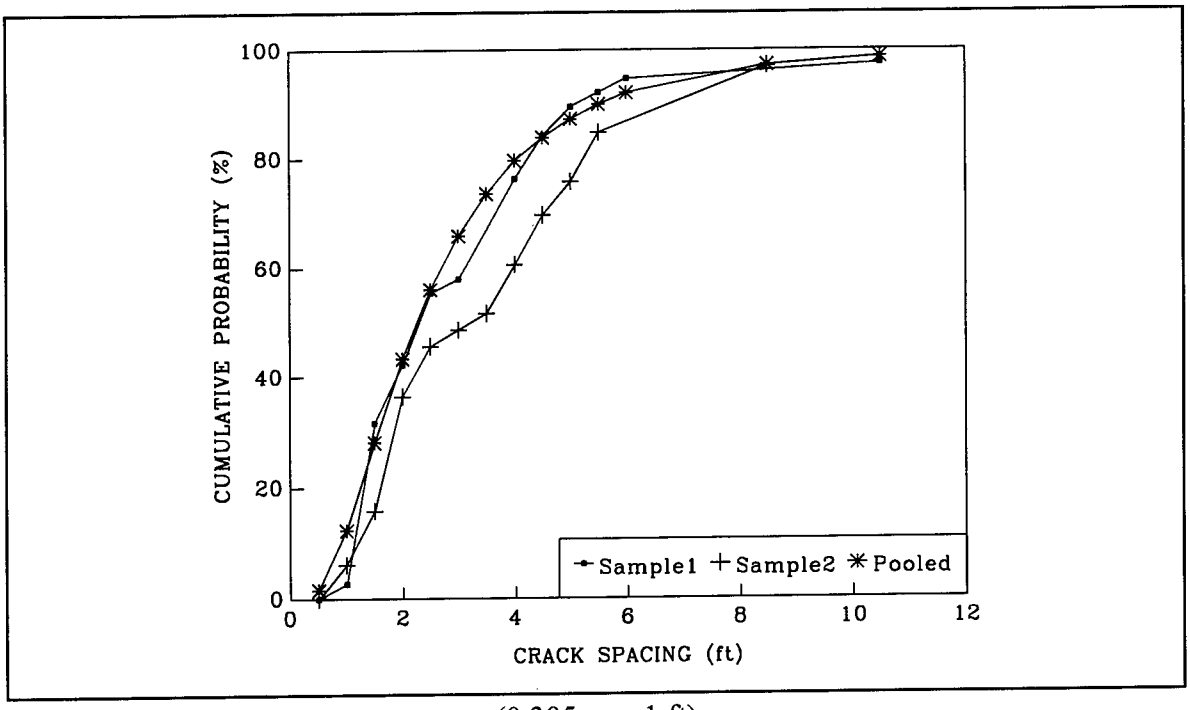

(0.305 m = 1 ft)

Figure 74. Field cracking distribution data: sample section Iowa-2.

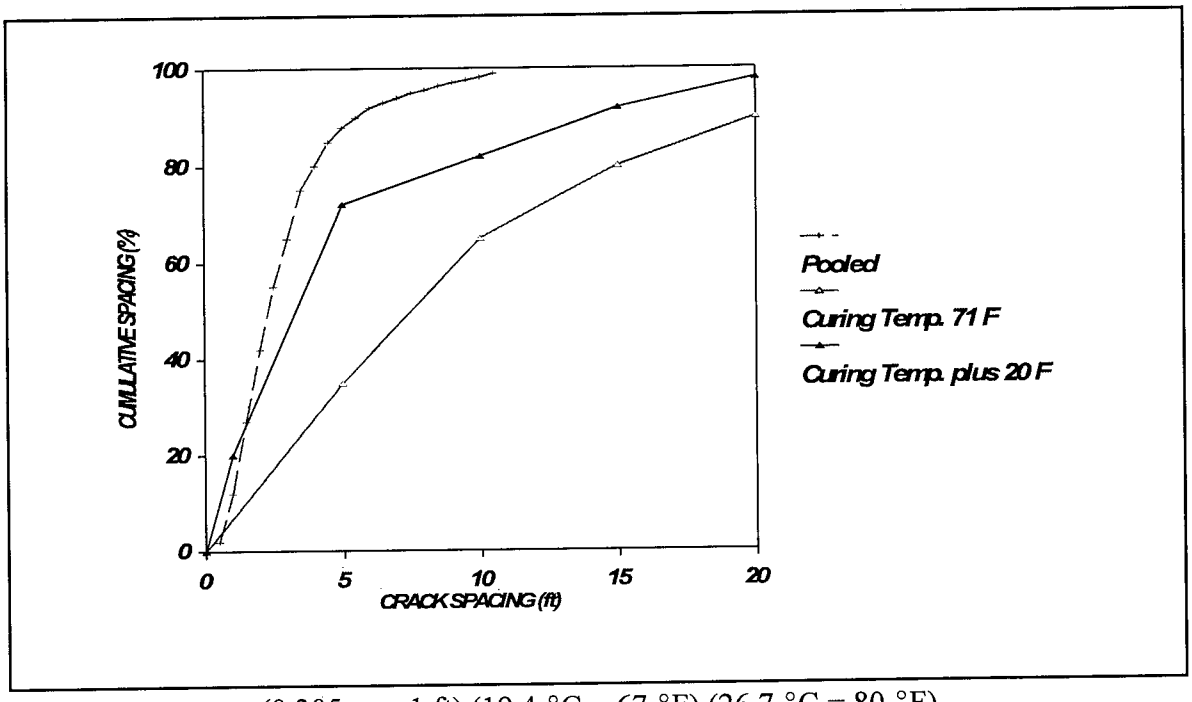

(0.305 m = 1 ft) (19.4 °C = 67 °F) (26.7 °C = 80 °F)

Figure 75. CRCP-5 crack distribution analysis for two curing temperatures from section Iowa-2.

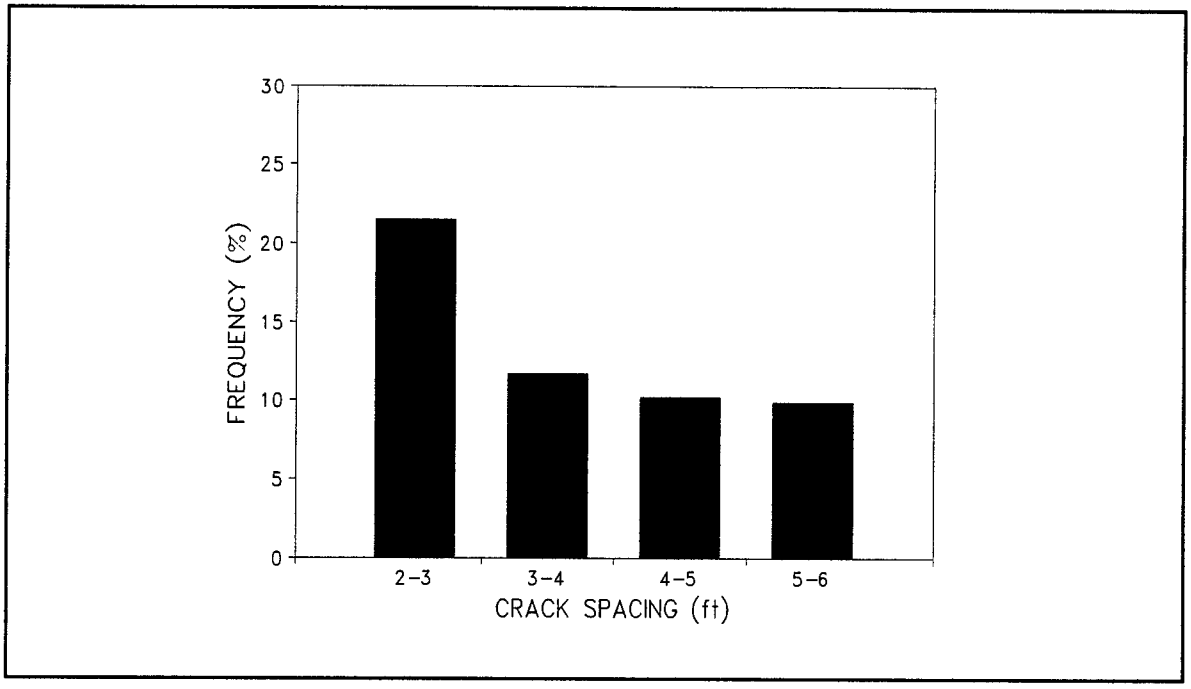

(0.305 m = 1 ft)

Figure 76. Crack spacing frequency: sample section Iowa-2.

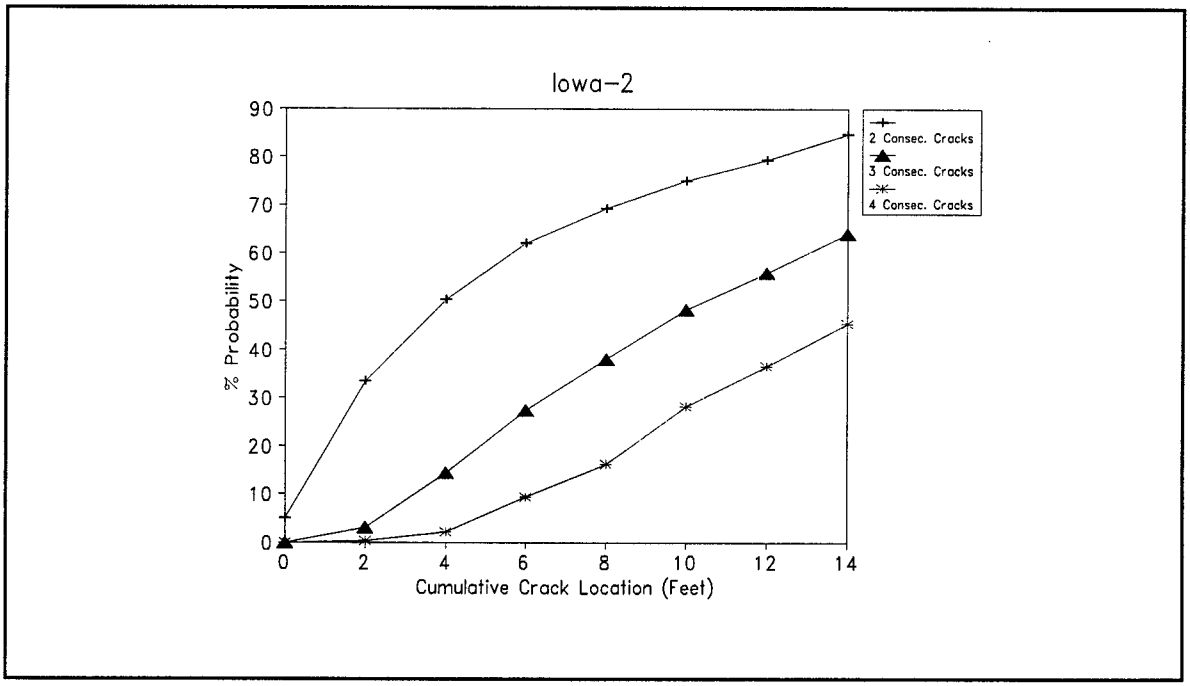

(0.305 m = 1 ft)

Figure 77. Probability of cluster cracking: sample section Iowa-2.

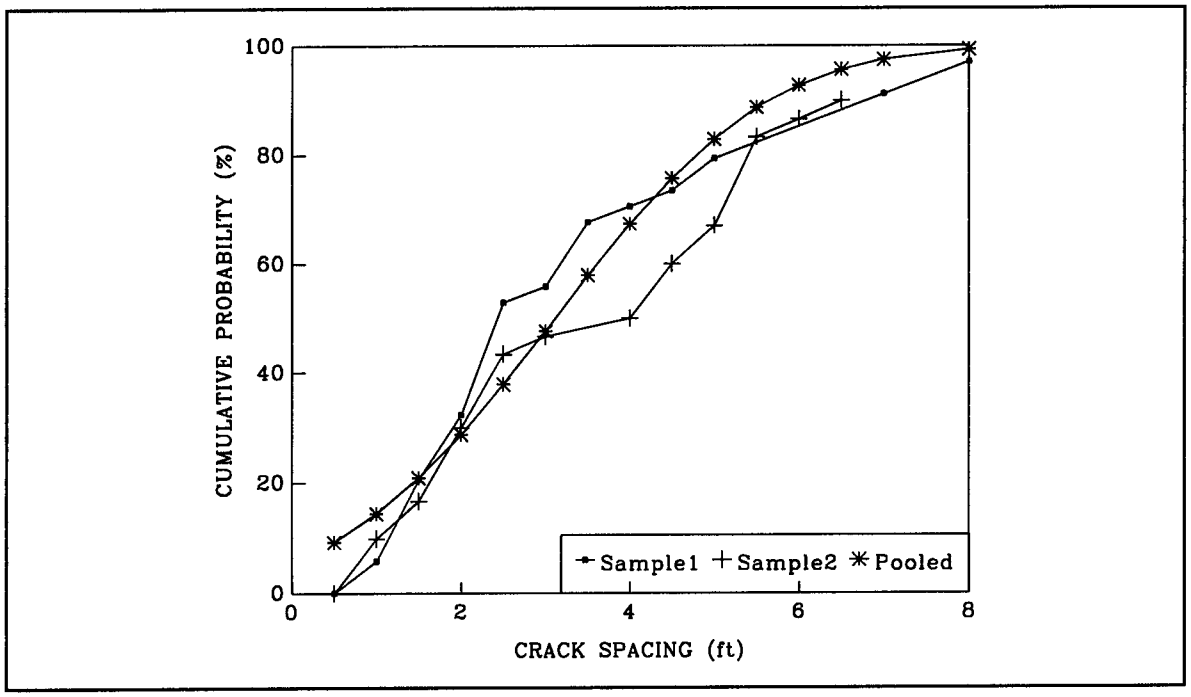

(0.305 m = 1 ft)

Figure 78. Field crack spacing distribution data: sample section Iowa-3.

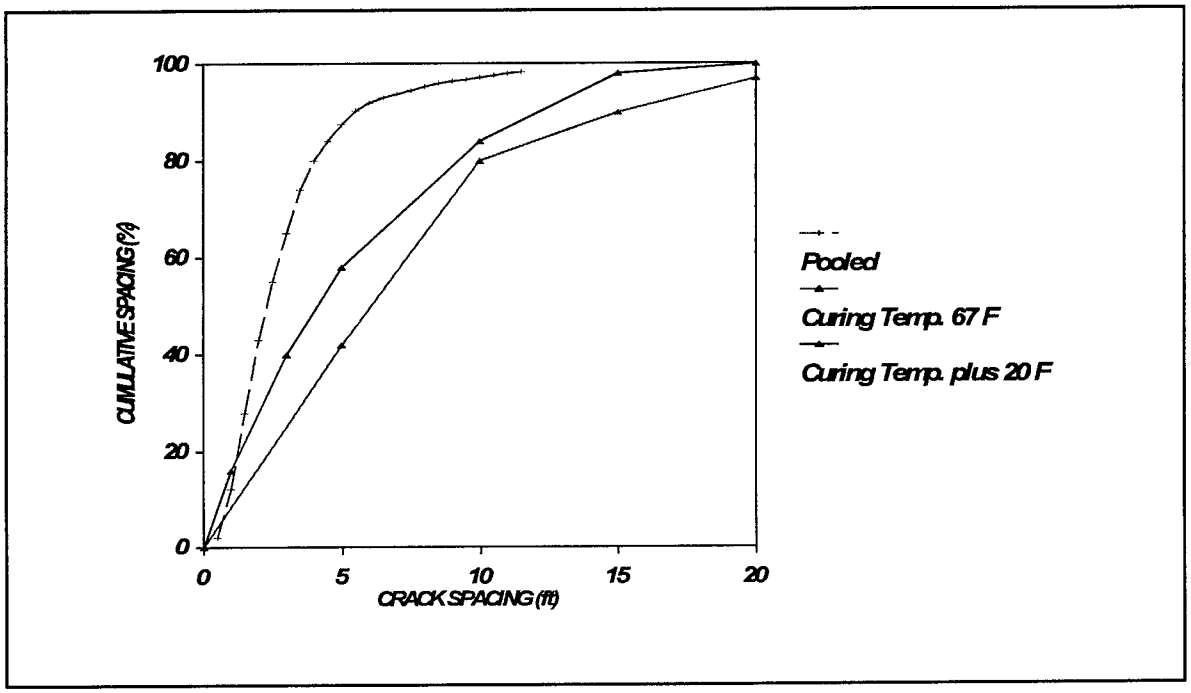

(0.305 m = 1 ft) (19.4 °C = 67 °F) (26.7 °C = 80 °F)

Figure 79. CRCP-5 crack distribution analysis for two curing temperatures from section Iowa-3.

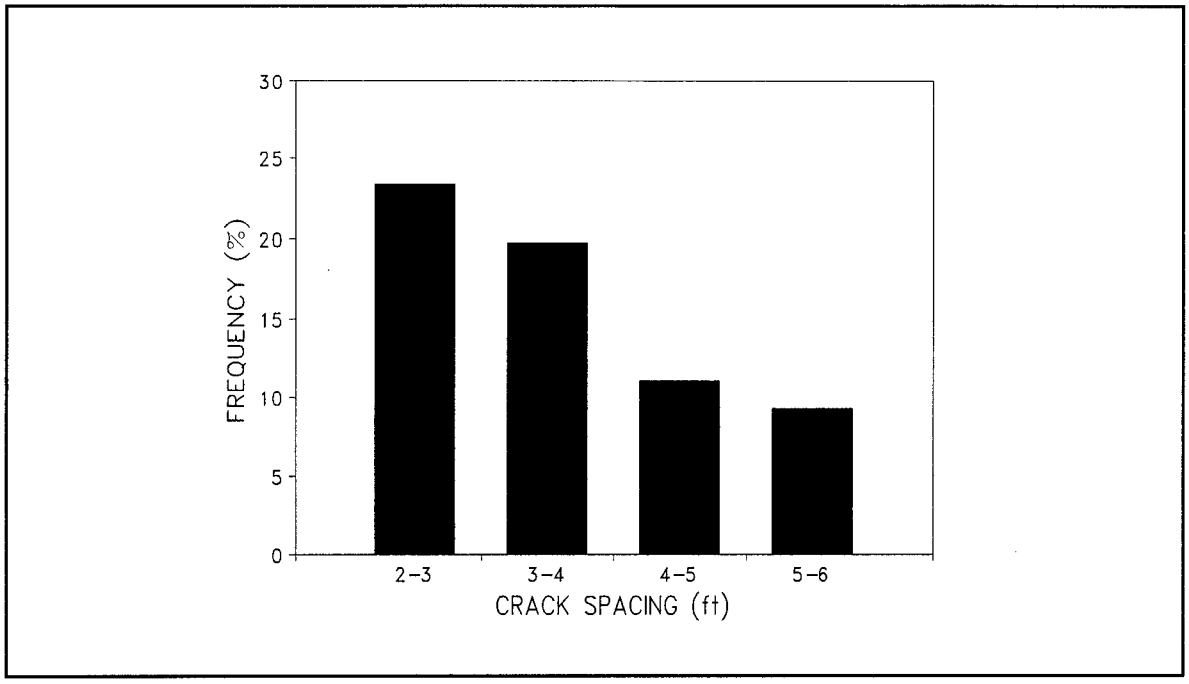

(0.305 m = 1 ft)

Figure 80. Crack spacing frequency: sample section Iowa-3.

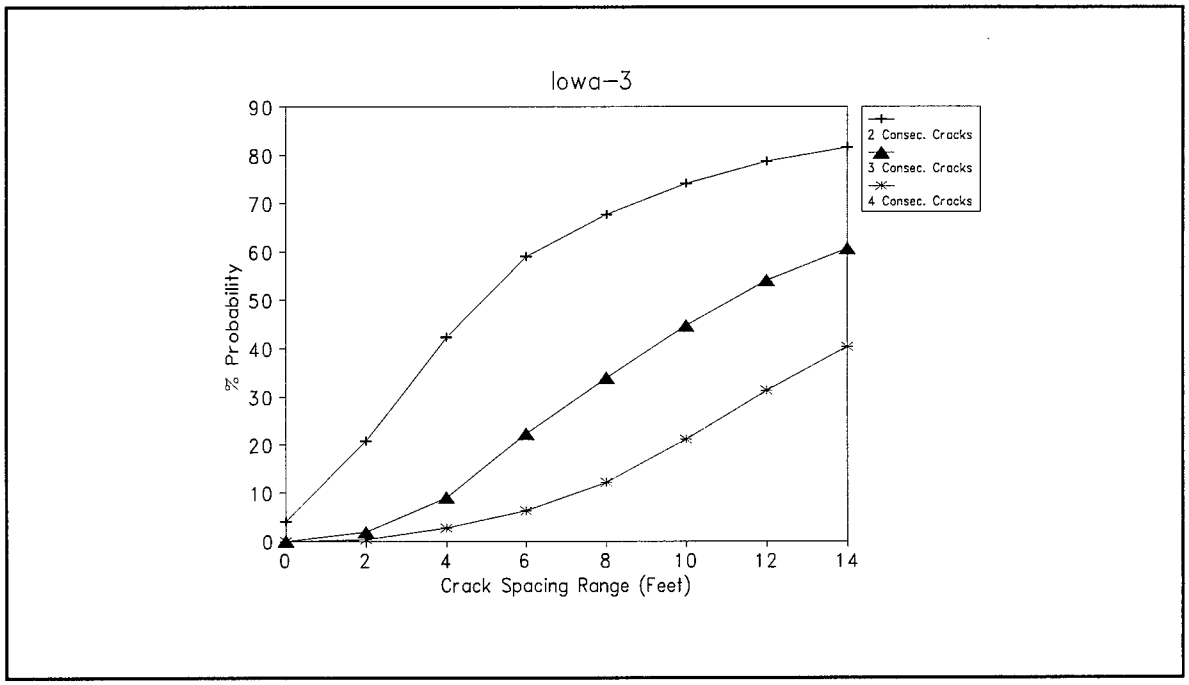

(0.305 m = 1 ft)

Figure 81. Probability of cluster cracking: sample section Iowa-3.

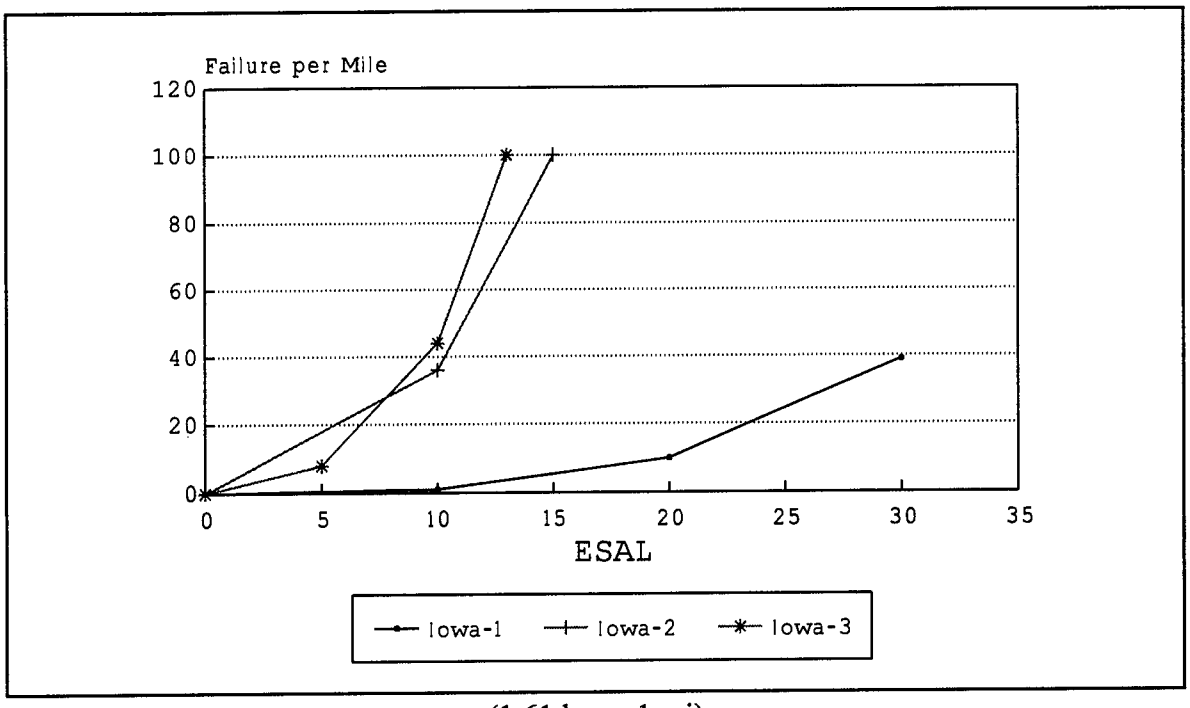

(1.61 km = 1 mi)

Figure 82. Performance prediction for sample sections in Iowa.

APPENDIX C - OKLAHOMA TEST SECTIONS DATA ANALYSIS

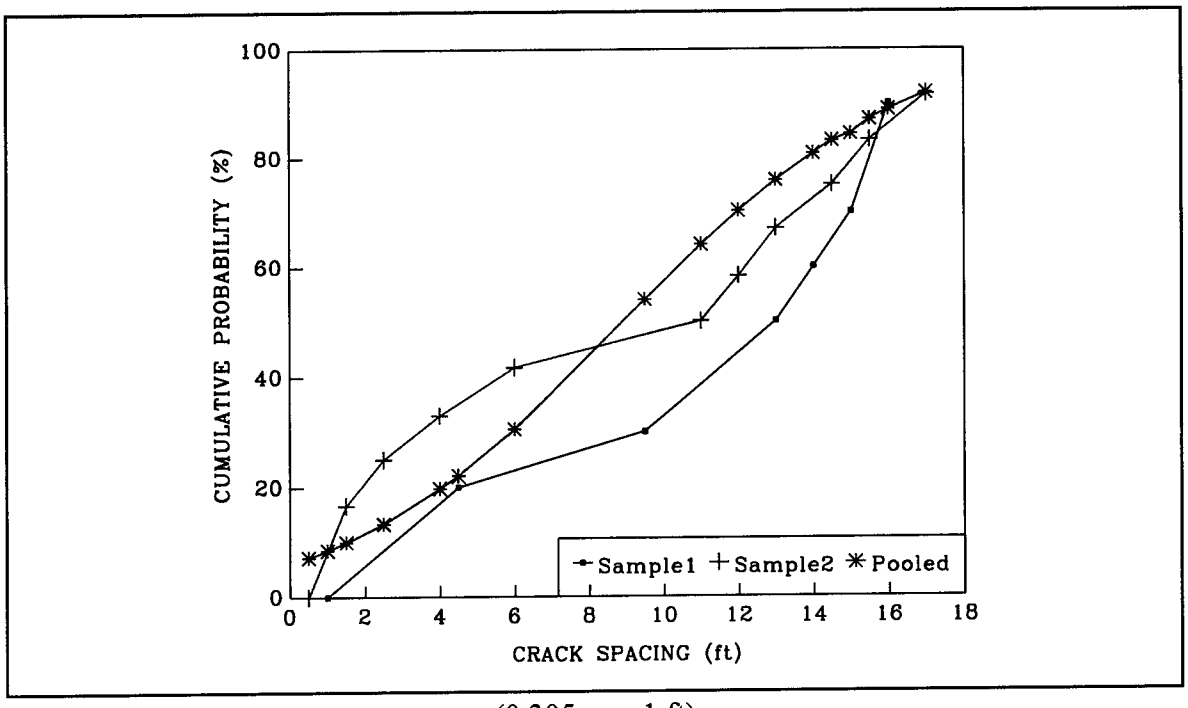

(0.305 m = 1 ft)

Figure 83. Field cracking spacing distribution data: sample section Oklahoma-1.

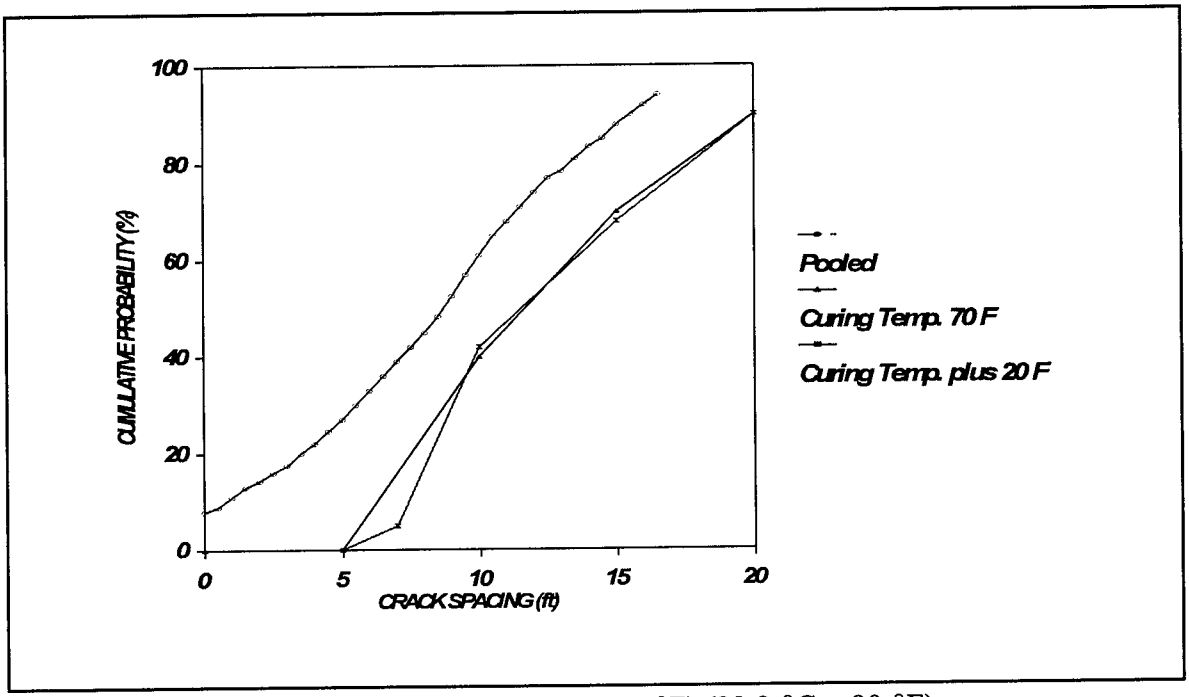

(0.305 m = 1 ft) (23.9 °C = 75 °F) (32.2 °C = 90 °F)

Figure 84. CRCP-5 crack distribution analysis for two curing temperatures from section Oklahoma-1.

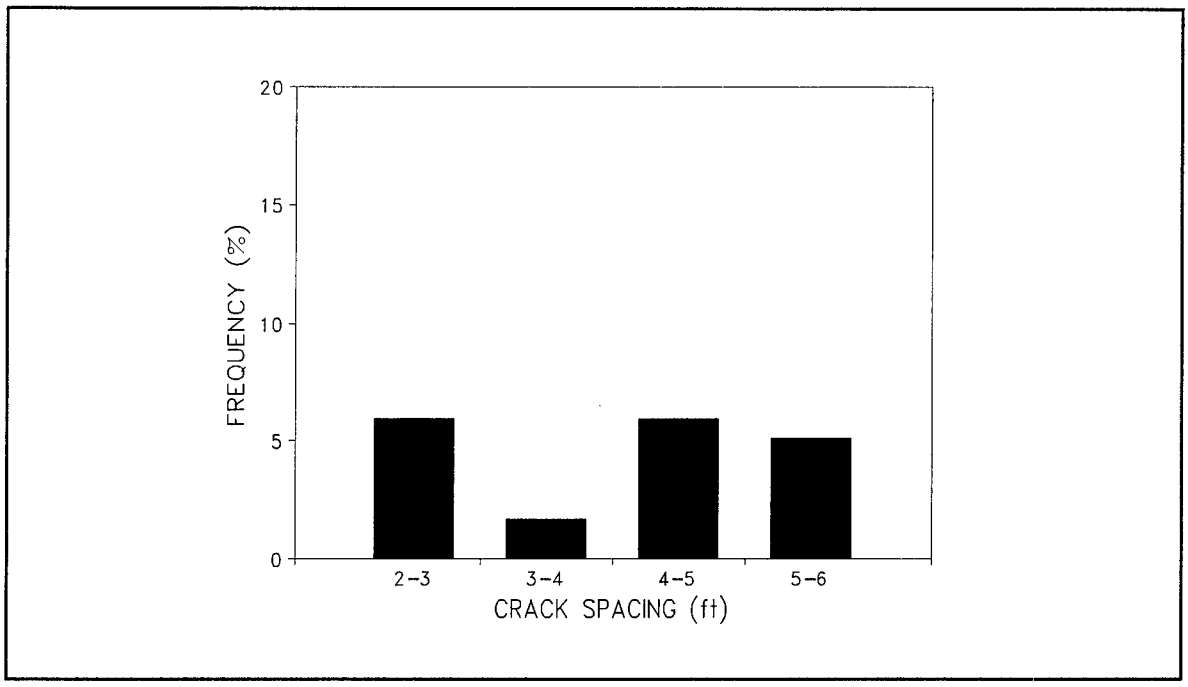

(0.305 m = 1 ft)

Figure 85. Crack spacing frequency: sample section Oklahoma-1.

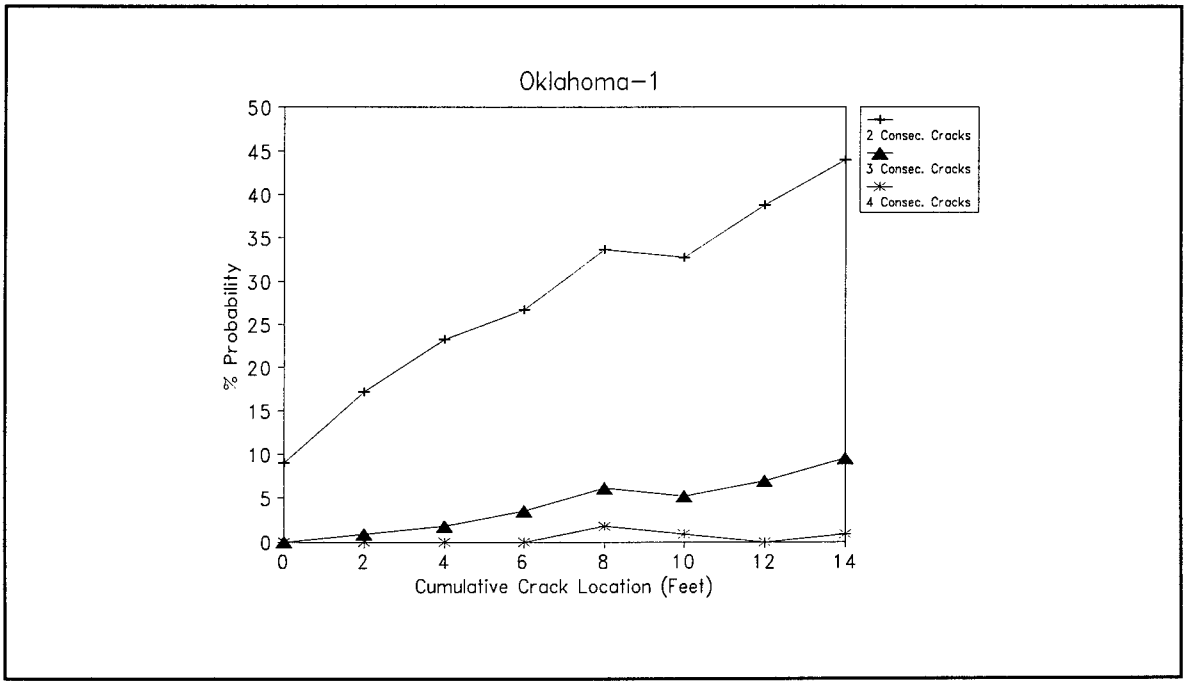

(0.305 m = 1 ft)

Figure 86. Probability of cluster cracking: sample section Oklahoma-1.

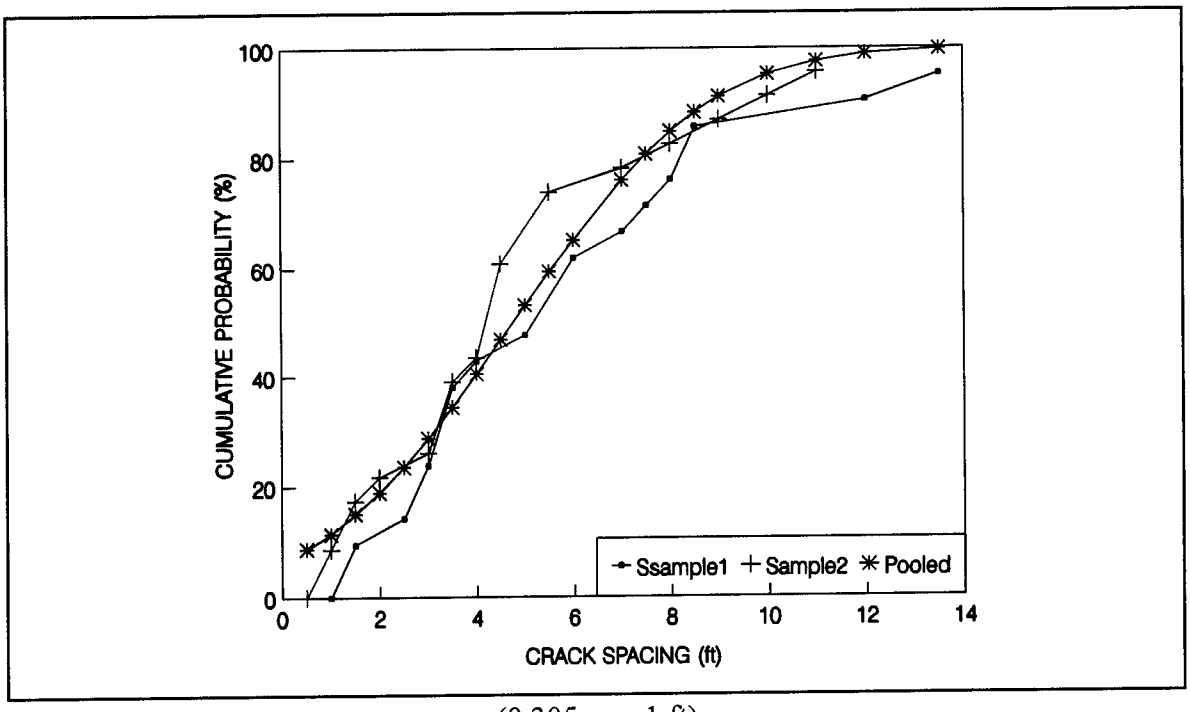

(0.305 m = 1 ft)

Figure 87. Field crack spacing distribution data: sample section Oklahoma-2.

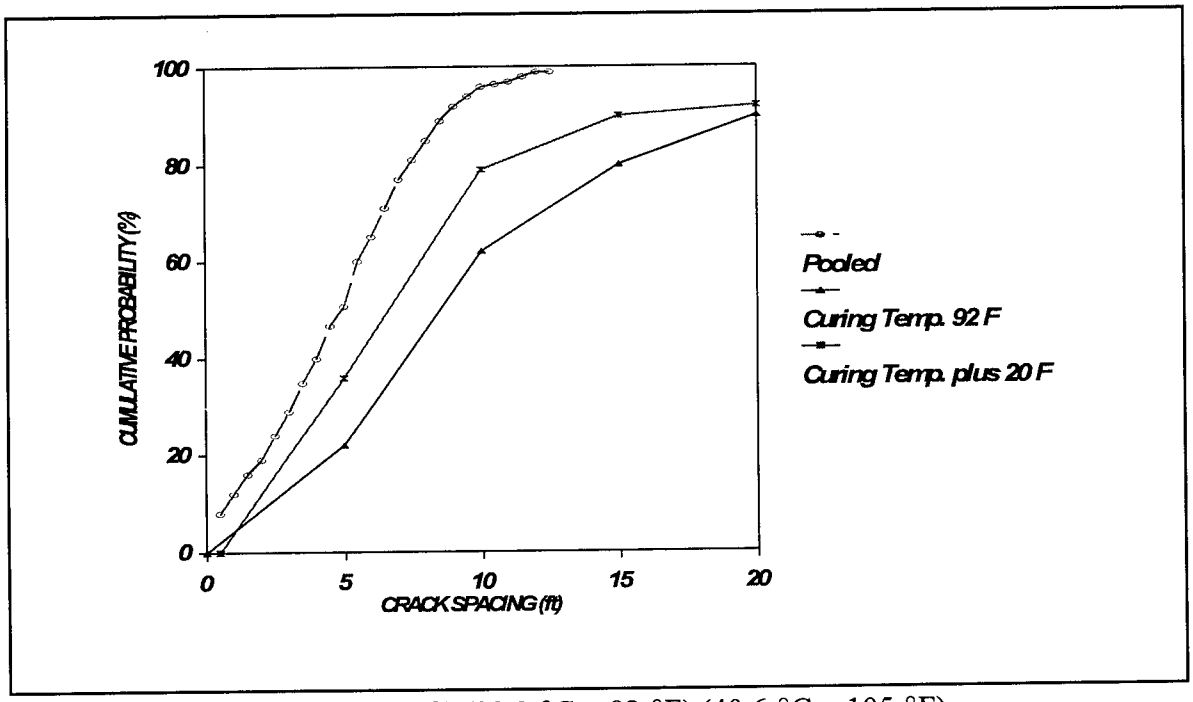

(0.305 m = 1 ft) (33.3 °C = 92 °F) (40.6 °C = 105 °F)

Figure 88. CRCP-5 crack distribution analysis for two curing temperatures from section Oklahoma-2.

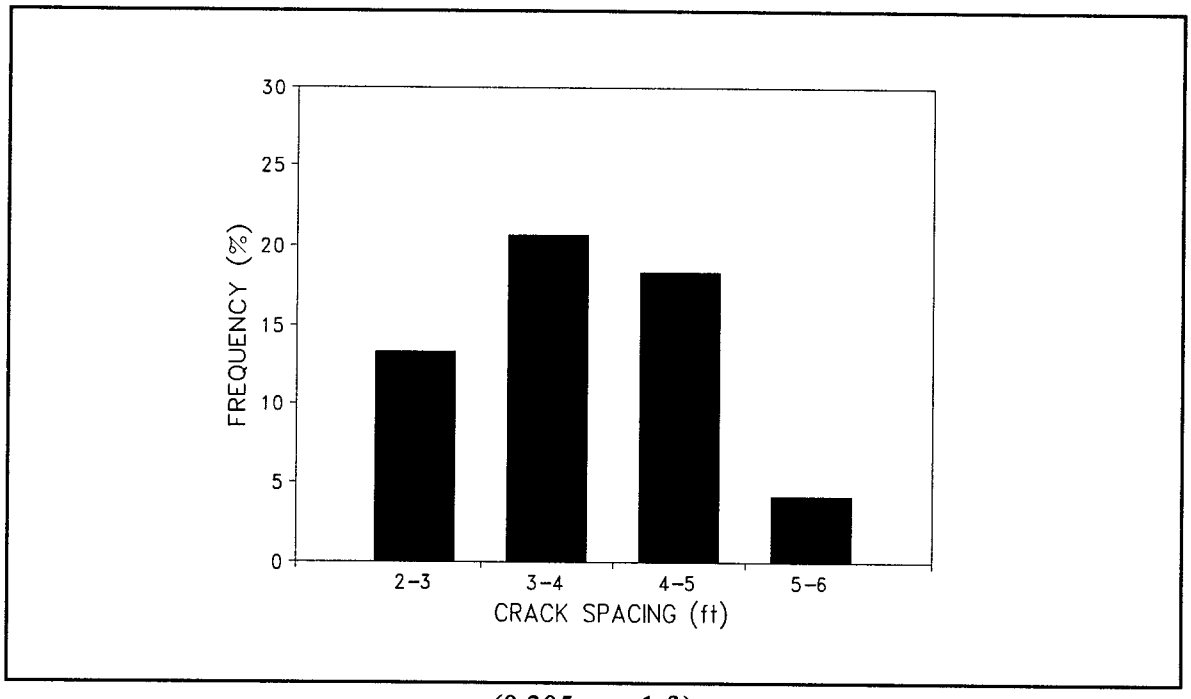

(0.305 m = 1 ft)

Figure 89. Crack spacing frequency: sample section Oklahoma-2.

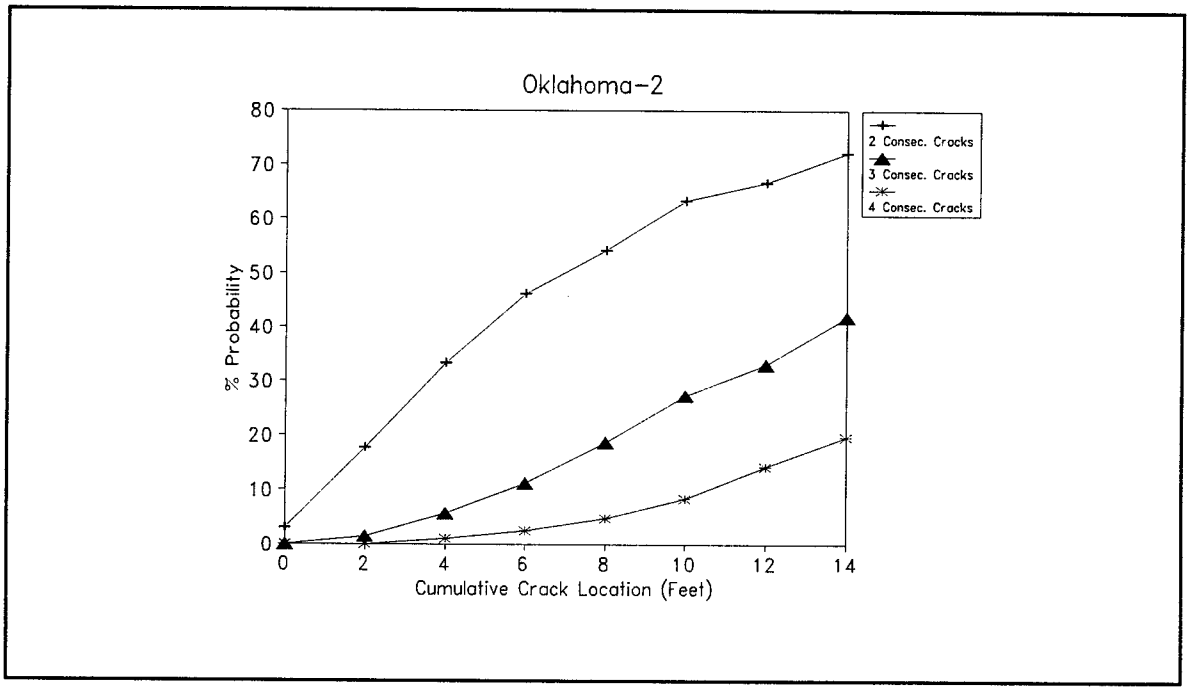

(0.305 m = 1 ft)

Figure 90. Probability of cluster cracking: sample section Oklahoma-2.

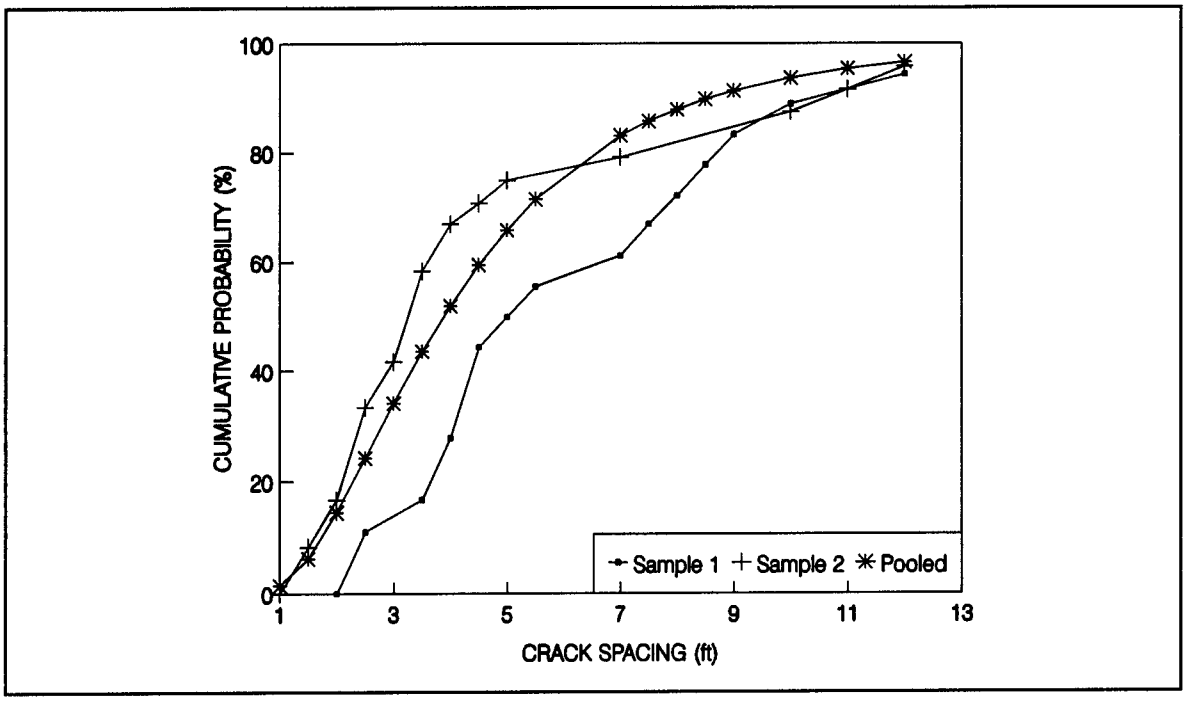

(0.305 m = 1 ft)

Figure 91. Field crack spacing distribution data: sample section Oklahoma-3.

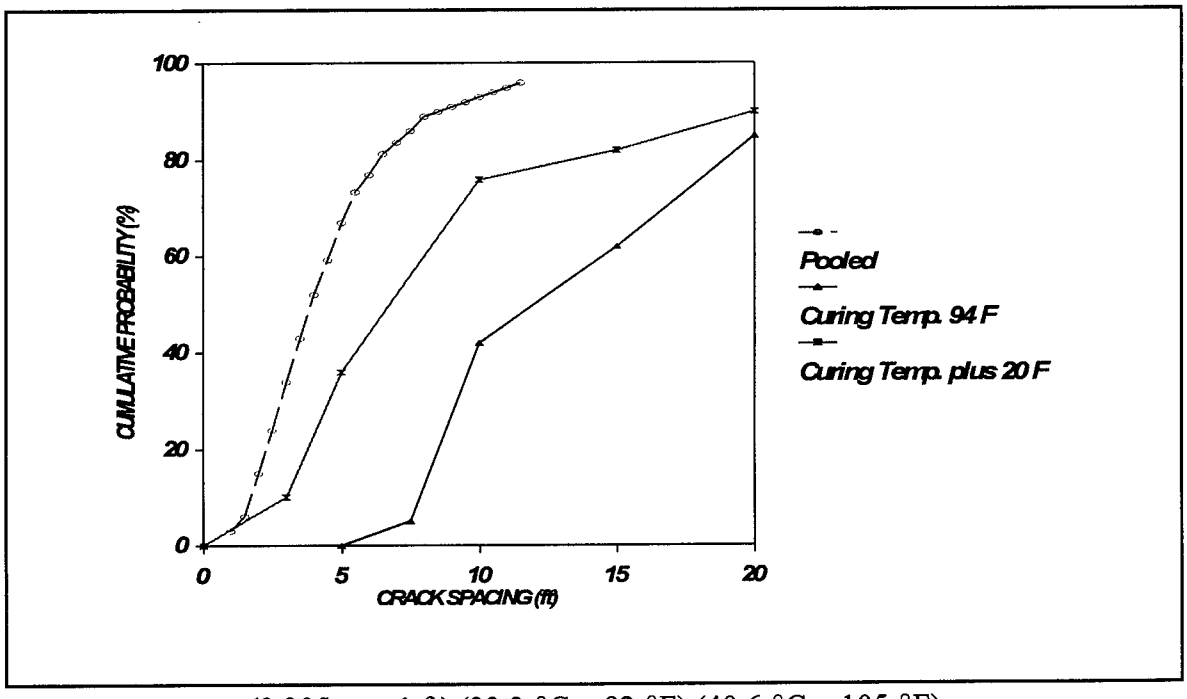

(0.305 m = 1 ft) (33.3 °C = 92 °F) (40.6 °C = 105 °F)

Figure 92. CRCP-5 crack distribution analysis for two curing temperatures from section Oklahoma-3.

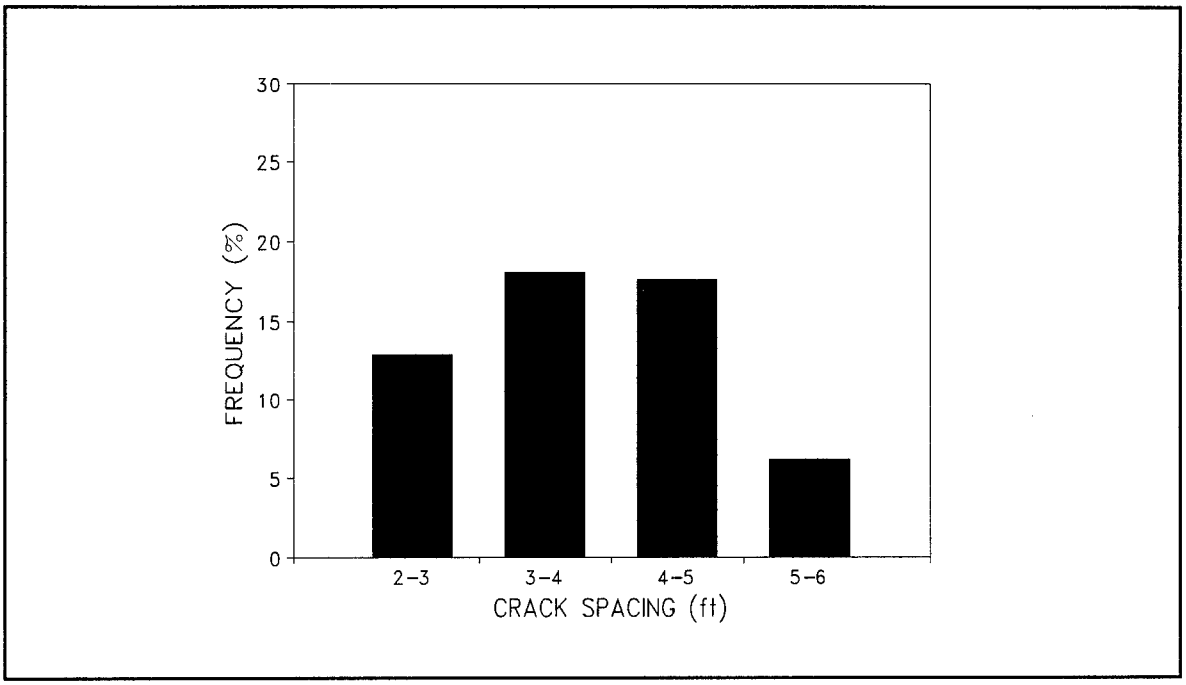

(0.305 m = 1 ft)

Figure 93. Crack spacing frequency: sample section Oklahoma-3.

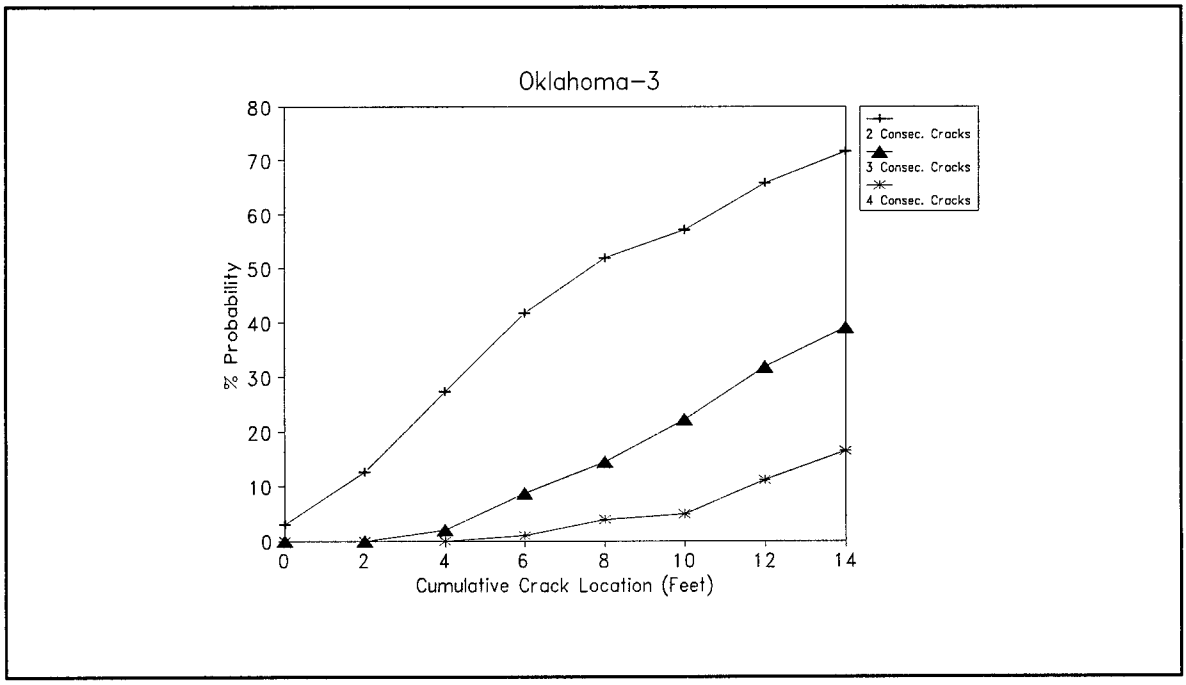

(0.305 m = 1 ft)

Figure 94. Probability of cluster cracking: sample section Oklahoma-3.

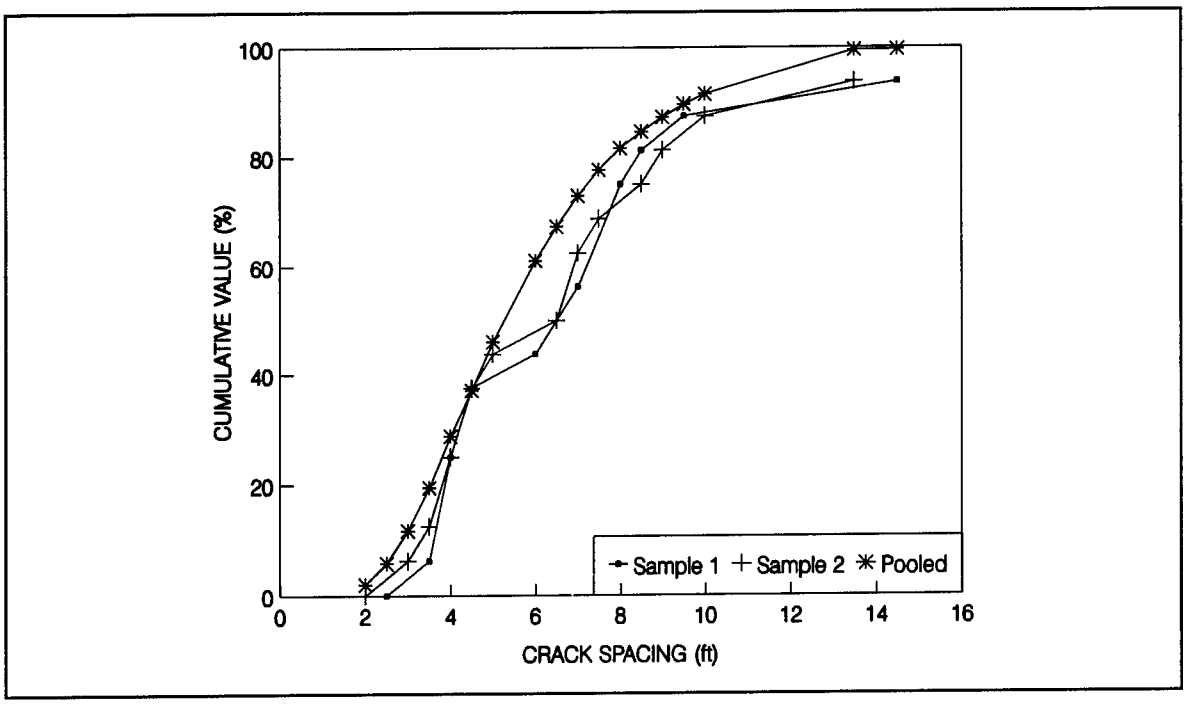

(0.305 m = 1 ft)

Figure 95. Field crack spacing distribution data: sample section Oklahoma-4.

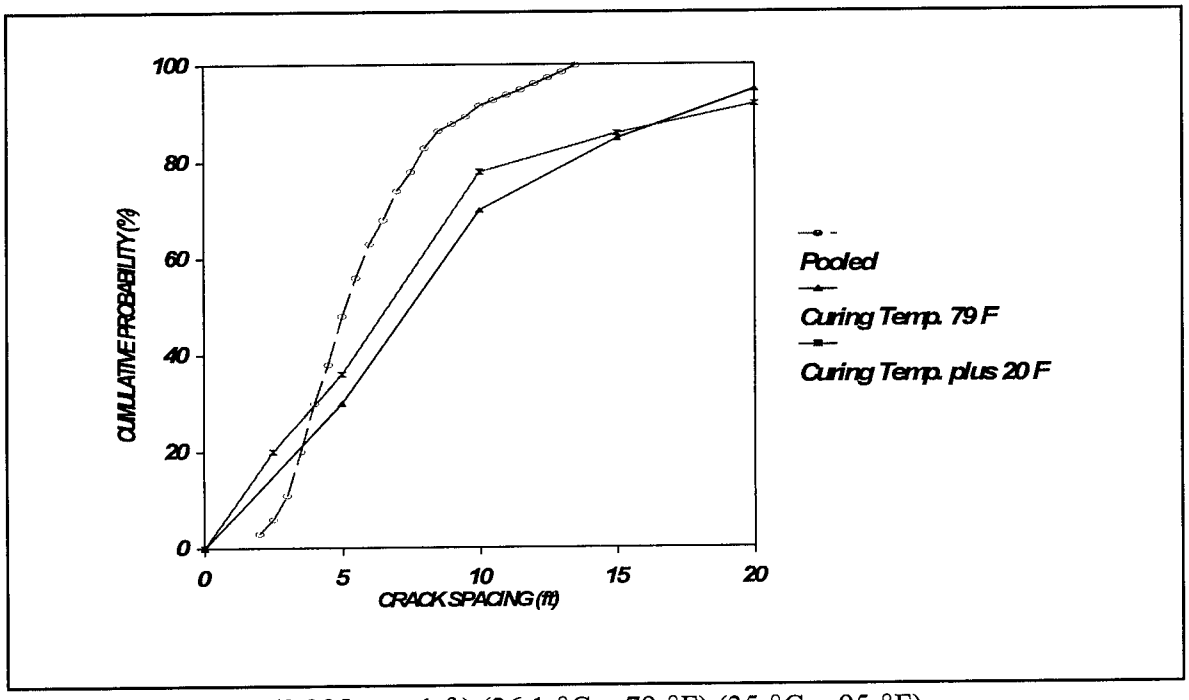

(0.305 m = 1 ft) (26.1 °C = 79 °F) (35 °C = 95 °F)

Figure 96. CRCP-5 crack distribution analysis for two curing temperatures from section Oklahoma-4.

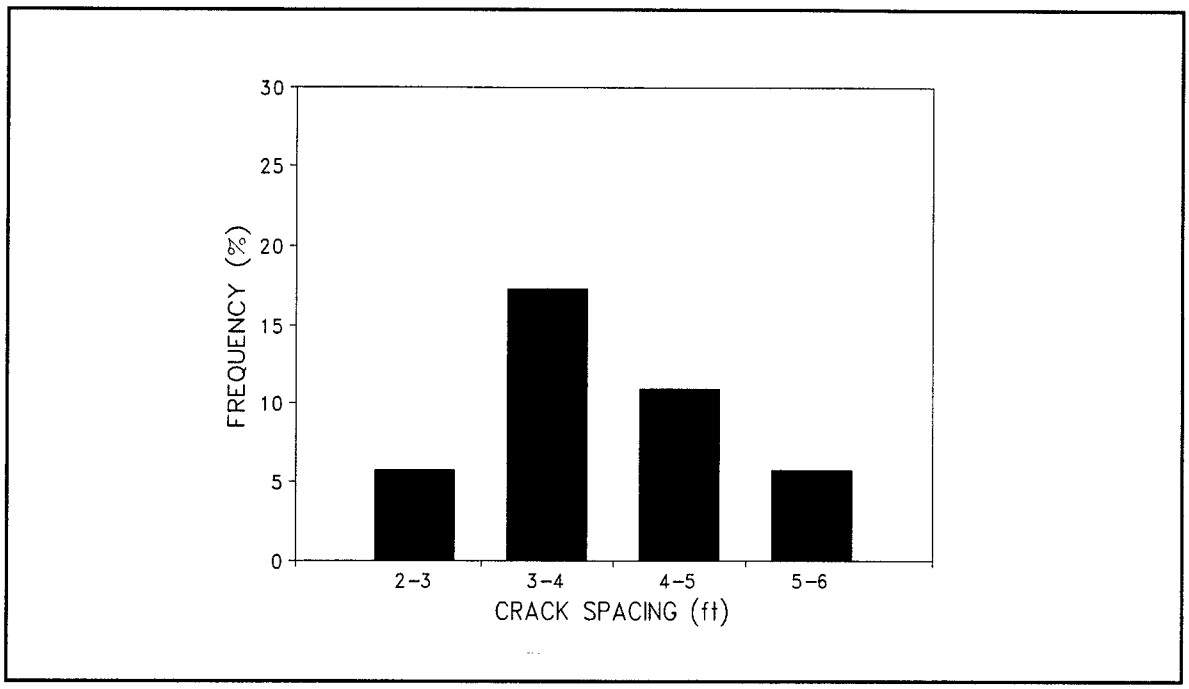

(0.305 m = 1 ft)

Figure 97. Crack spacing frequency: sample section Oklahoma-4.

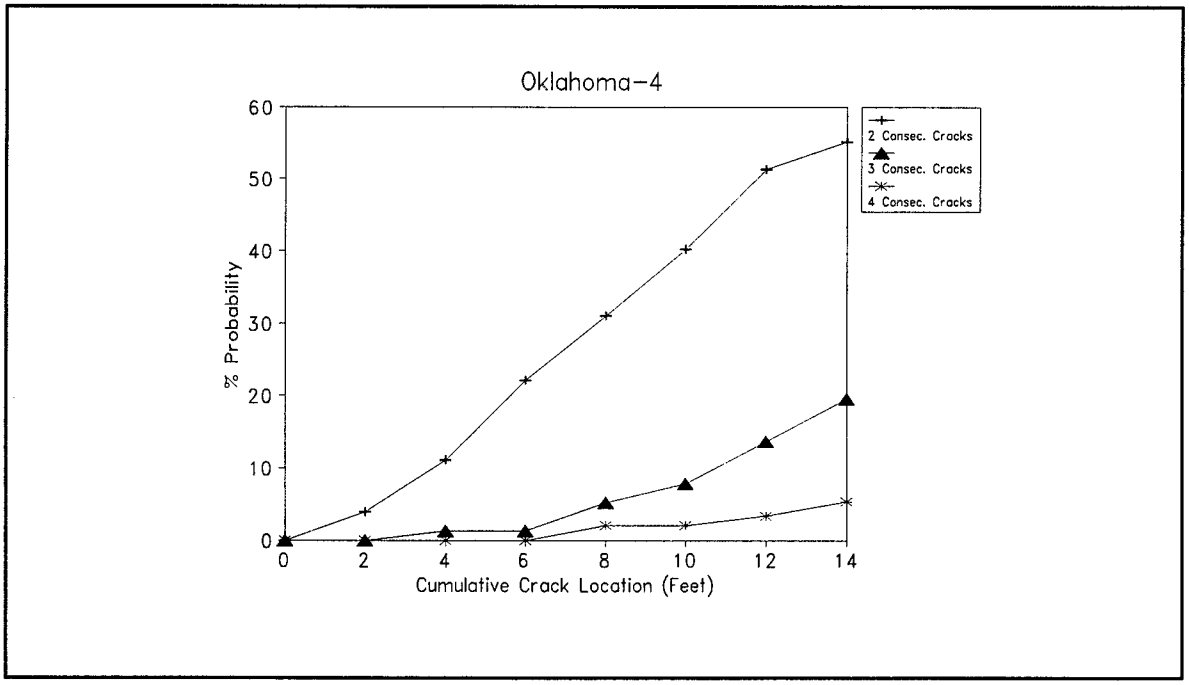

(0.305 m = 1 ft)

Figure 98. Probability of cluster cracking: sample section Oklahoma-4.

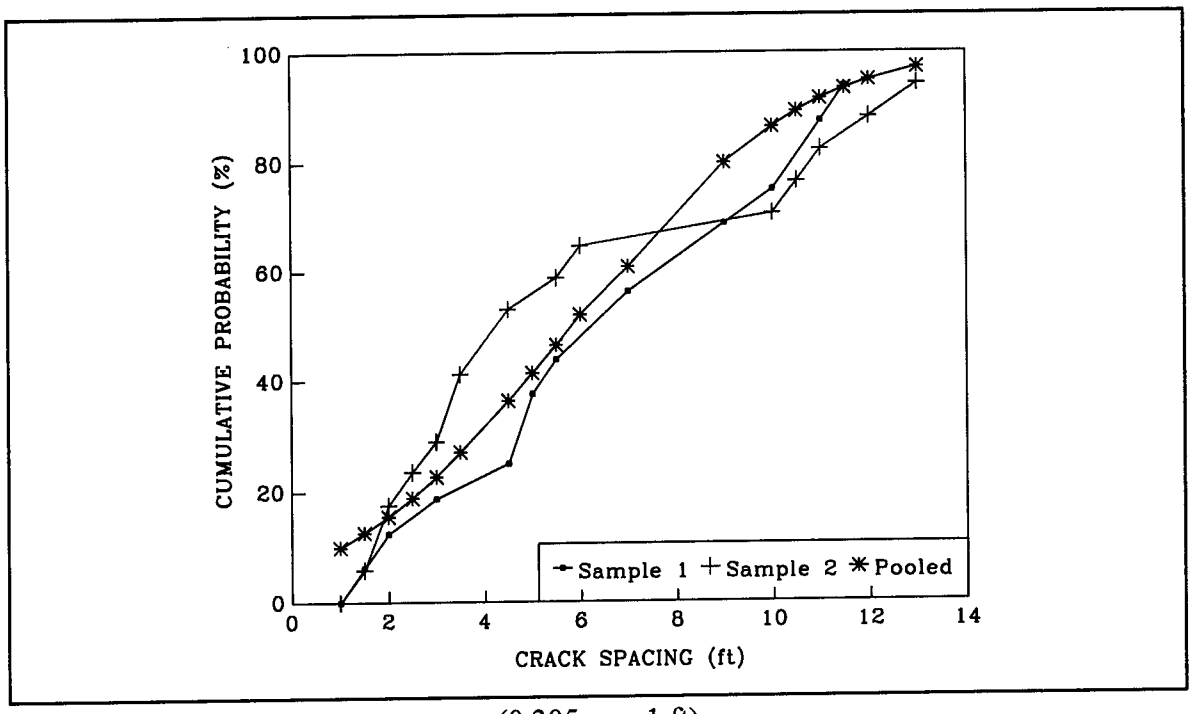

(0.305 m = 1 ft)

Figure 99. Field cracking spacing distribution data: sample section Oklahoma-5.

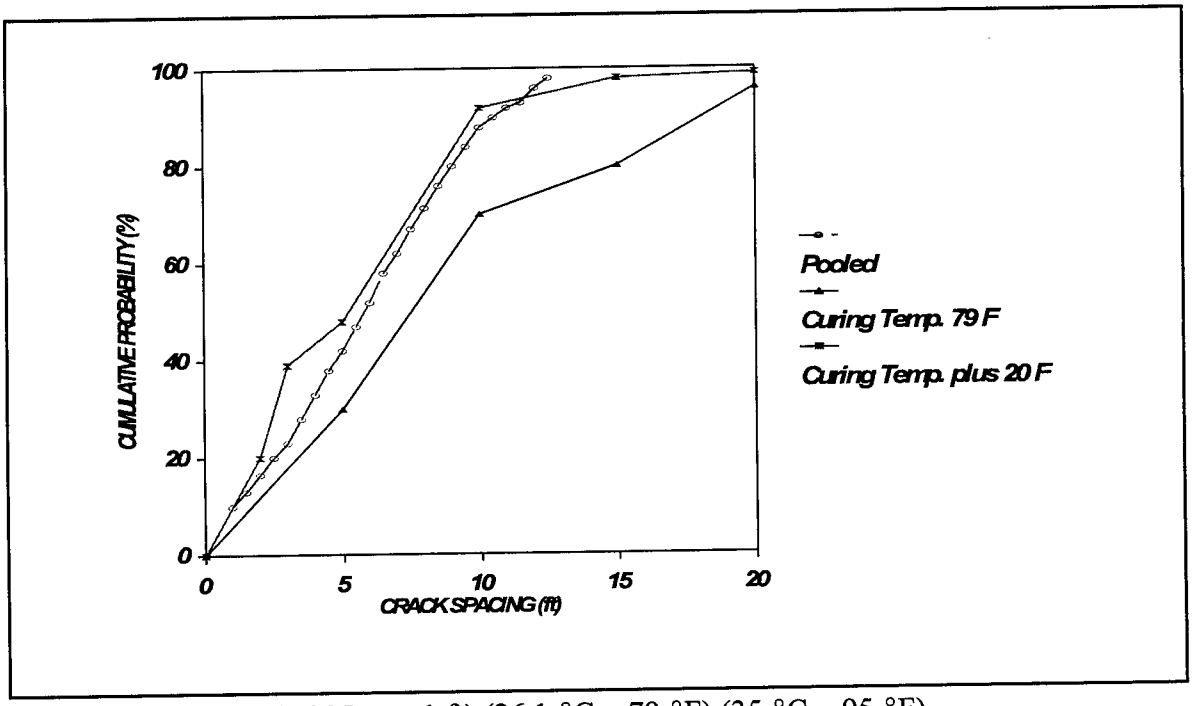

(0.305 m = 1 ft) (26.1 °C = 79 °F) (35 °C = 95 °F)

Figure 100. CRCP-5 crack distribution analysis for two curing temperatures from section Oklahoma-5.

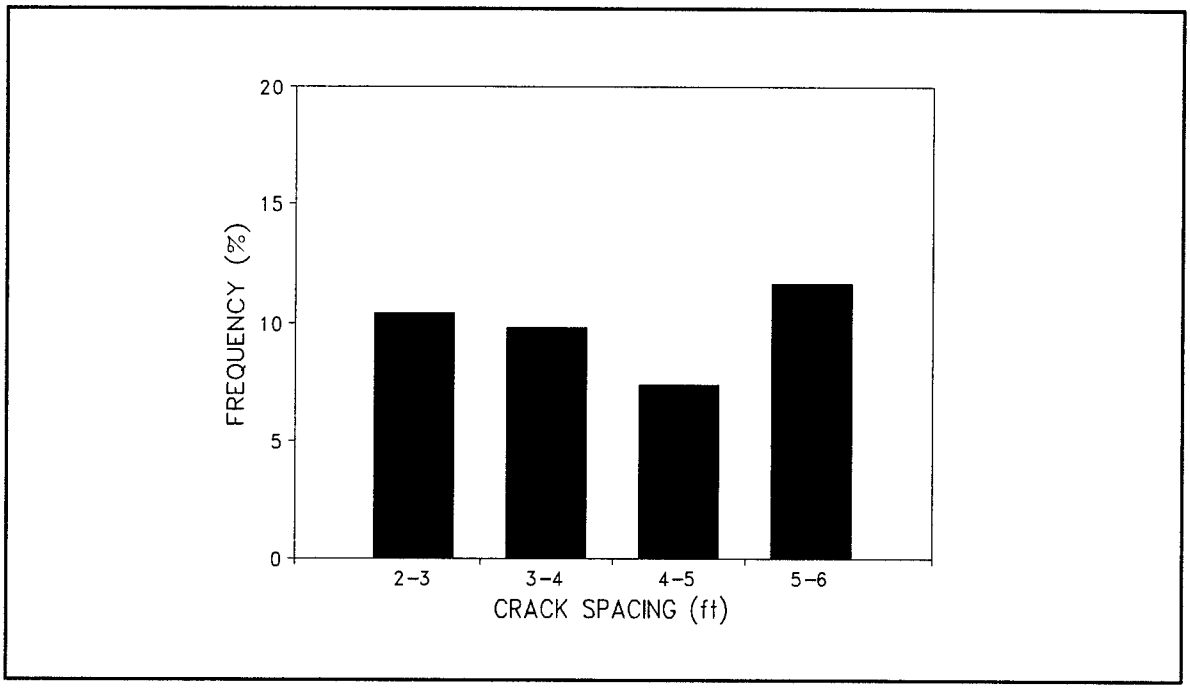

(0.305 m = 1 ft)

Figure 101. Crack spacing frequency: sample section Oklahoma-5.

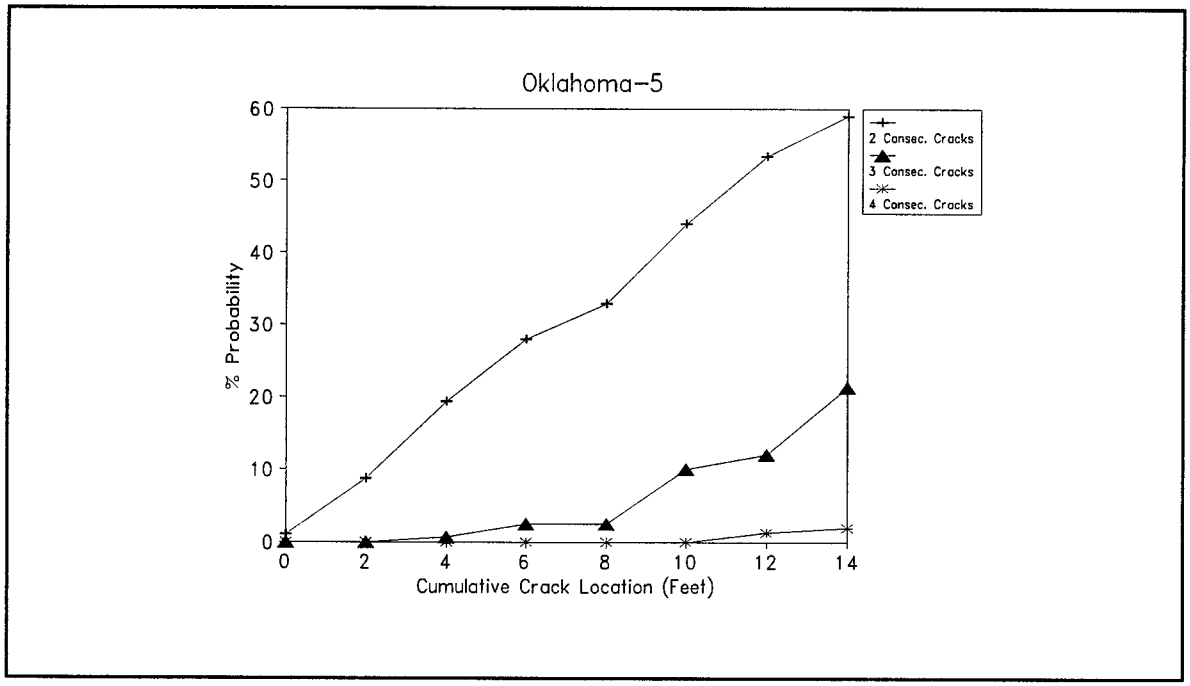

(0.305 m = 1 ft)

Figure 102. Probability of cluster cracking: sample section Oklahoma-5.

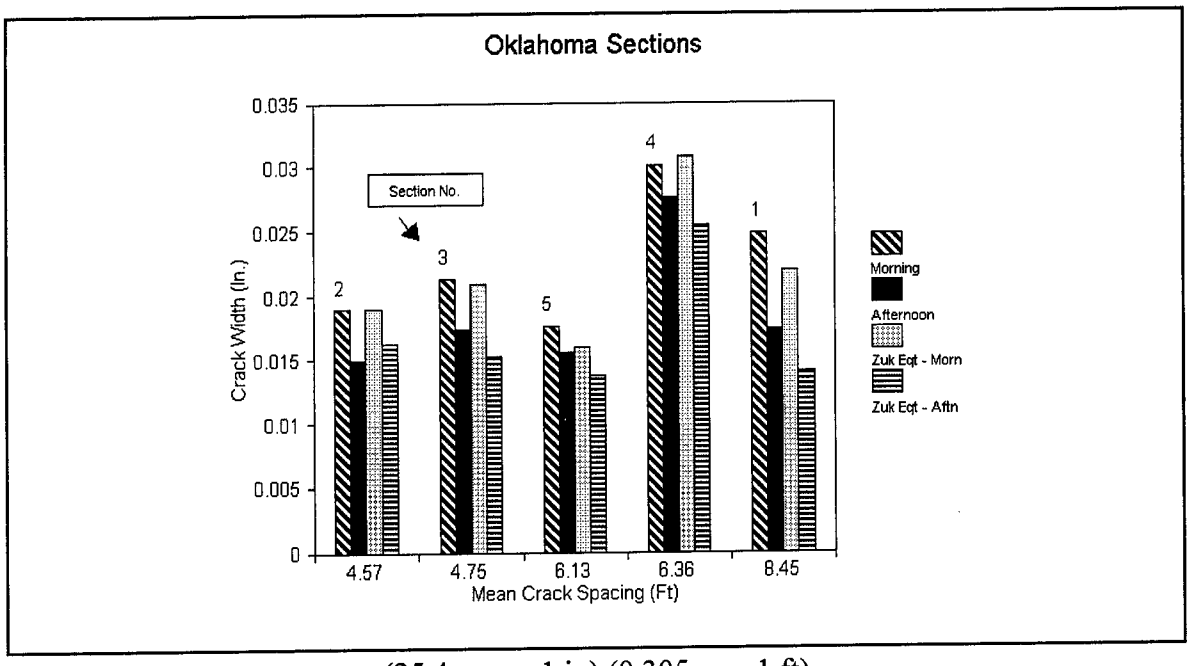

(25.4 mm = 1 in) (0.305 m = 1 ft)

Figure 103. Variation in crack width with crack spacing for Oklahoma sample sections.

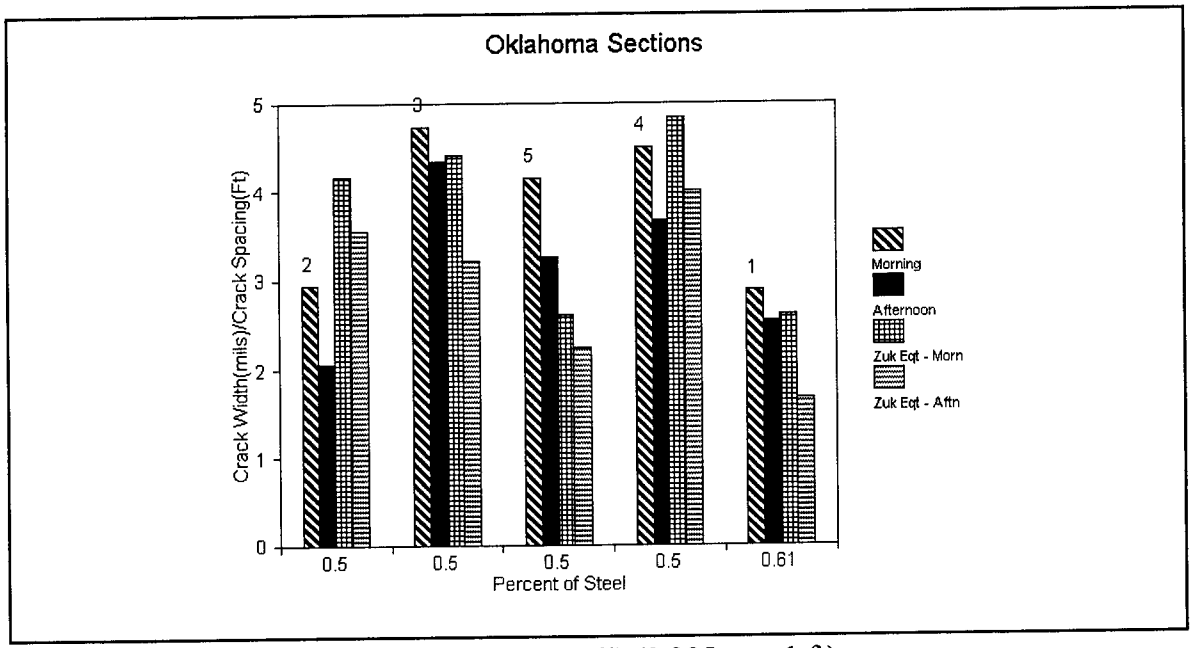

(0.0254 mm = 1 mil) (0.305 m = 1 ft)

Figure 104. Variation in crack width/crack spacing ratio with percent reinforcement for Oklahoma sample sections.

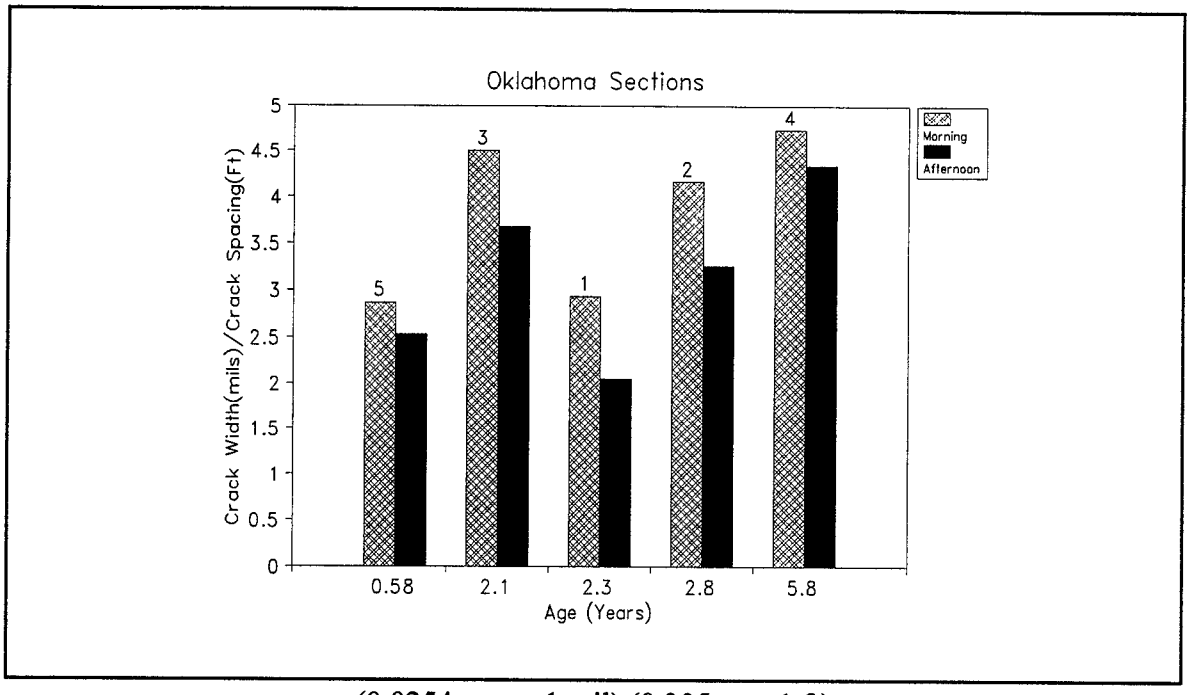

(0.0254 mm = 1 mil) (0.305 m = 1 ft)

Figure 105. Variation in crack width with pavement age for Oklahoma sample sections.

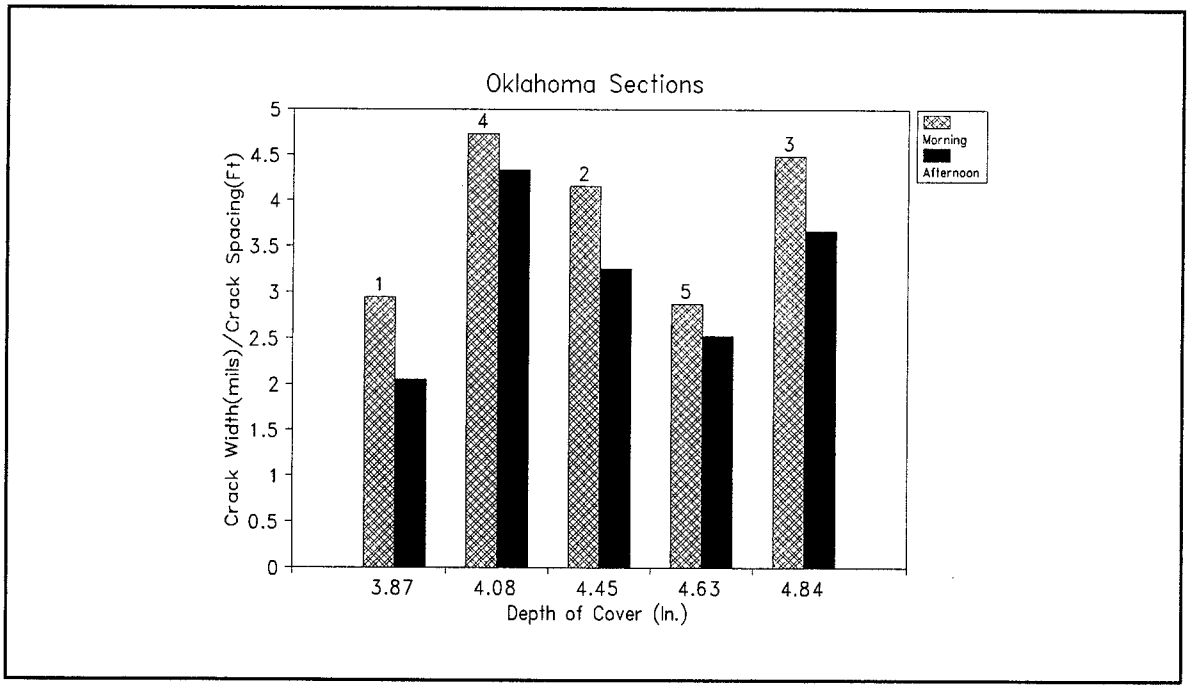

(0.0254 mm = 1 mil) (0.305 m = 1 ft) (25.4 mm = 1 in)

Figure 106. Variation in crack width/crack spacing ratio with depth of cover for Oklahoma sample sections.

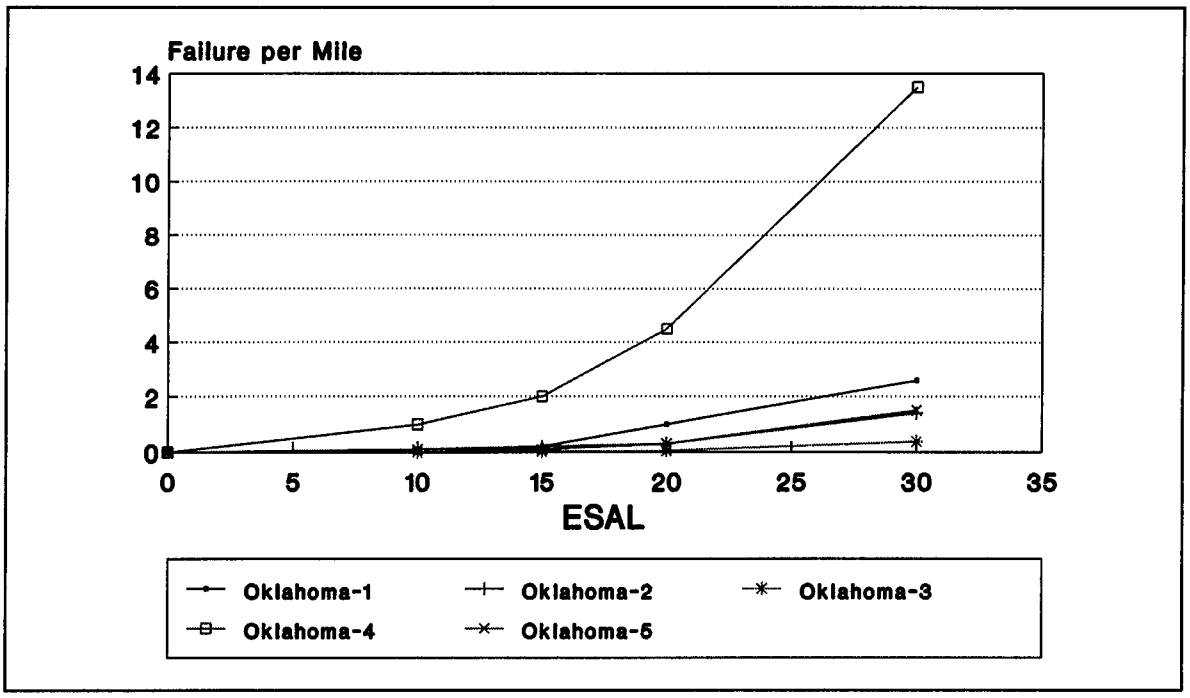

(1.61 km = 1 mi)

Figure 107. Performance prediction for sample sections in Oklahoma.

APPENDIX D - PENNSYLVANIA TEST SECTIONS DATA ANALYSIS

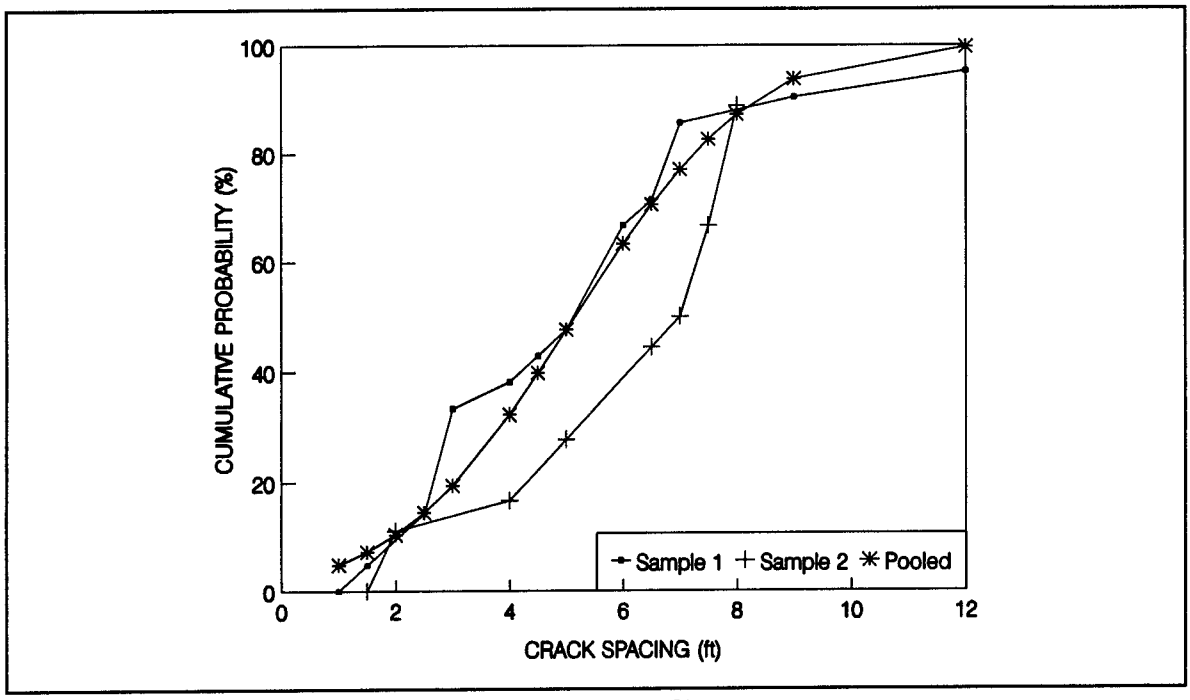

(0.305 m = 1 ft)

Figure 108. Field crack spacing distribution data: sample section Pennsylvania-1.

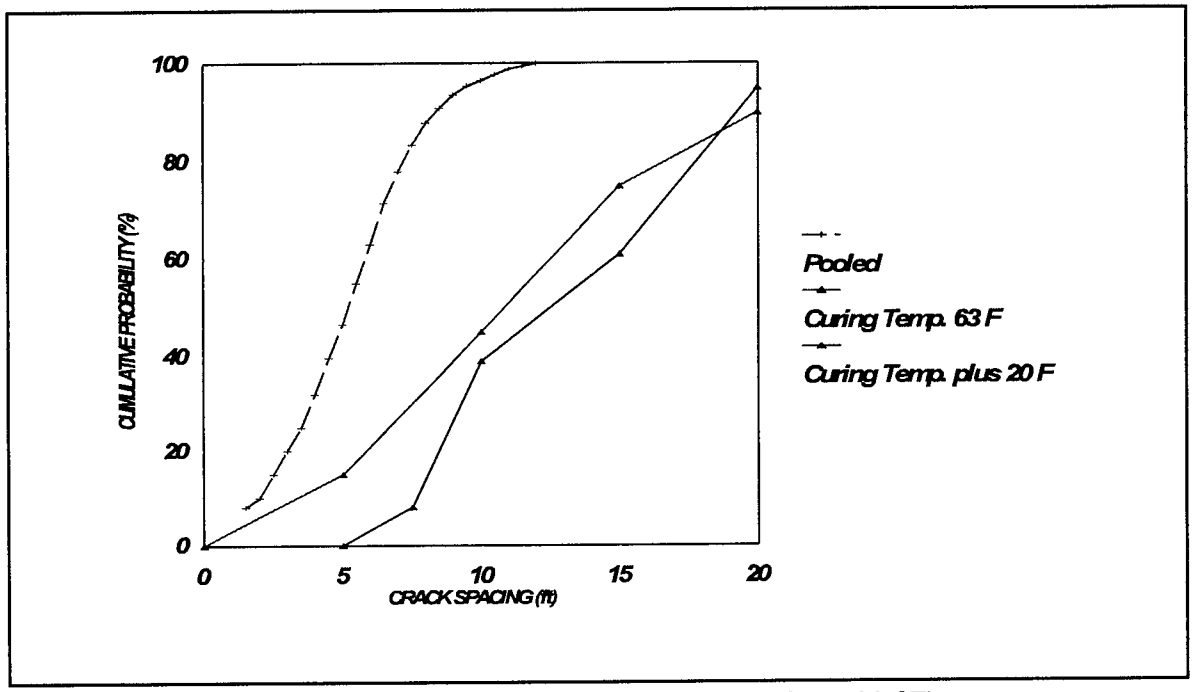

(0.305 m = 1 ft) (17.2 °C = 63 °F) (26.7 °C = 80 °F)

Figure 109. CRCP-5 crack distribution analysis for two curing temperatures from section Pennsylvania-1.

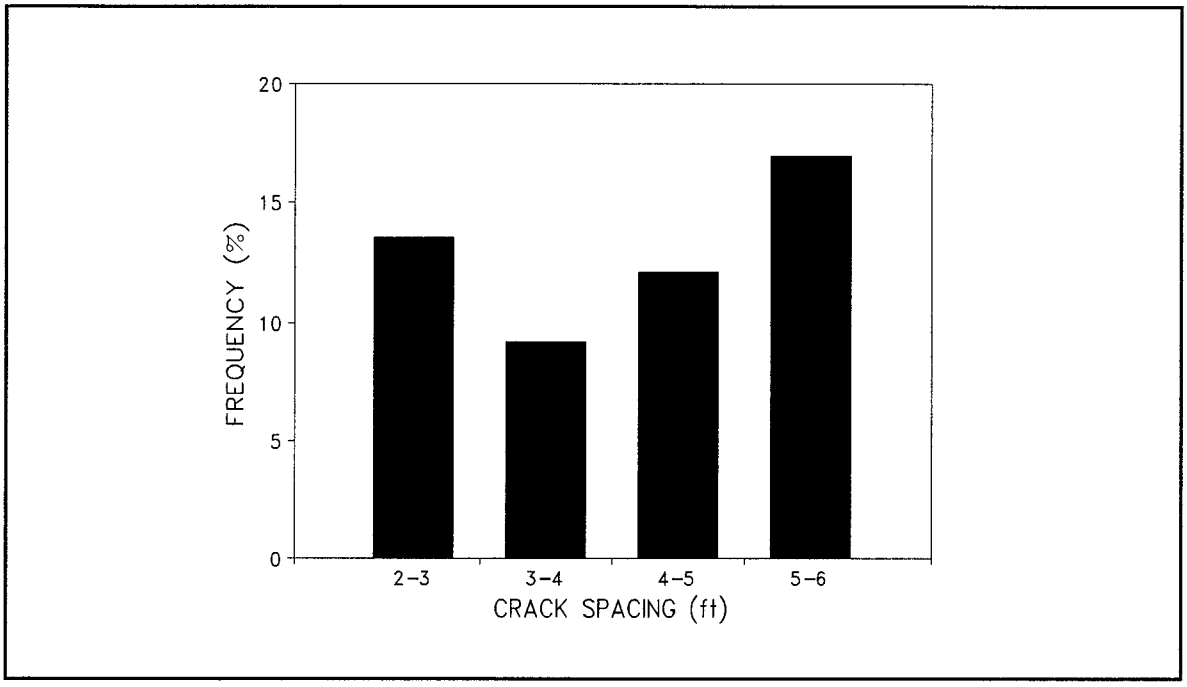

(0.305 m = 1 ft)

Figure 110. Crack spacing frequency: sample section Pennsylvania-1.

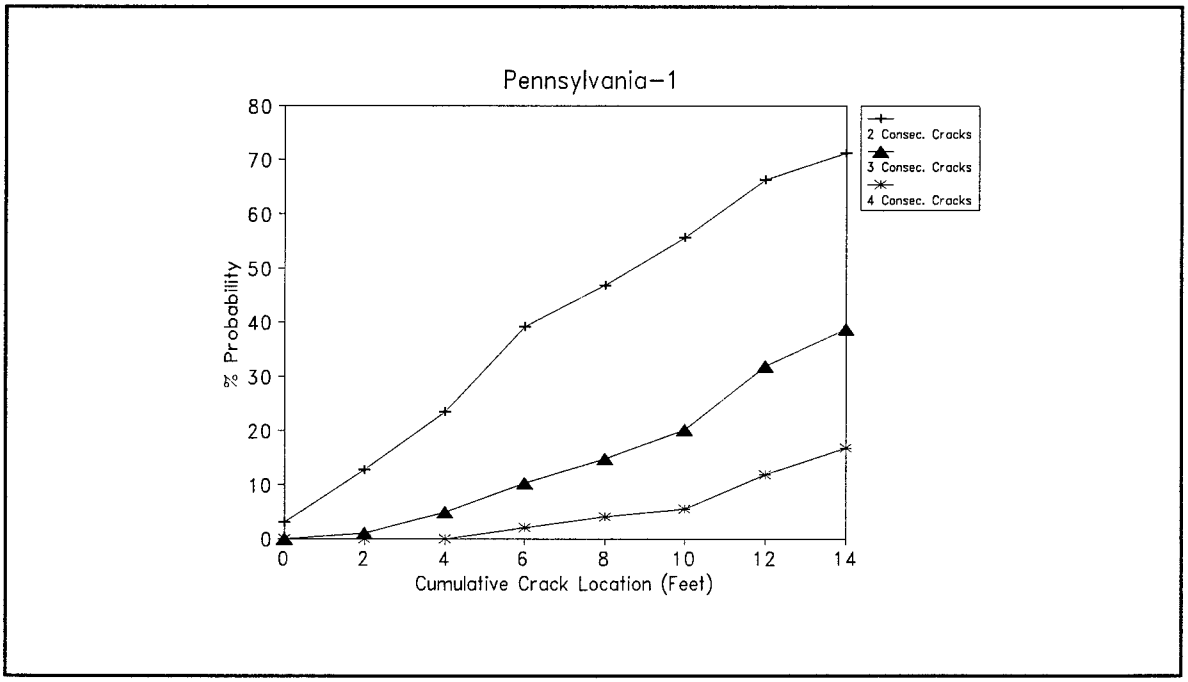

(0.305 m = 1 ft)

Figure 111. Probability of cluster cracking: sample section Pennsylvania-1.

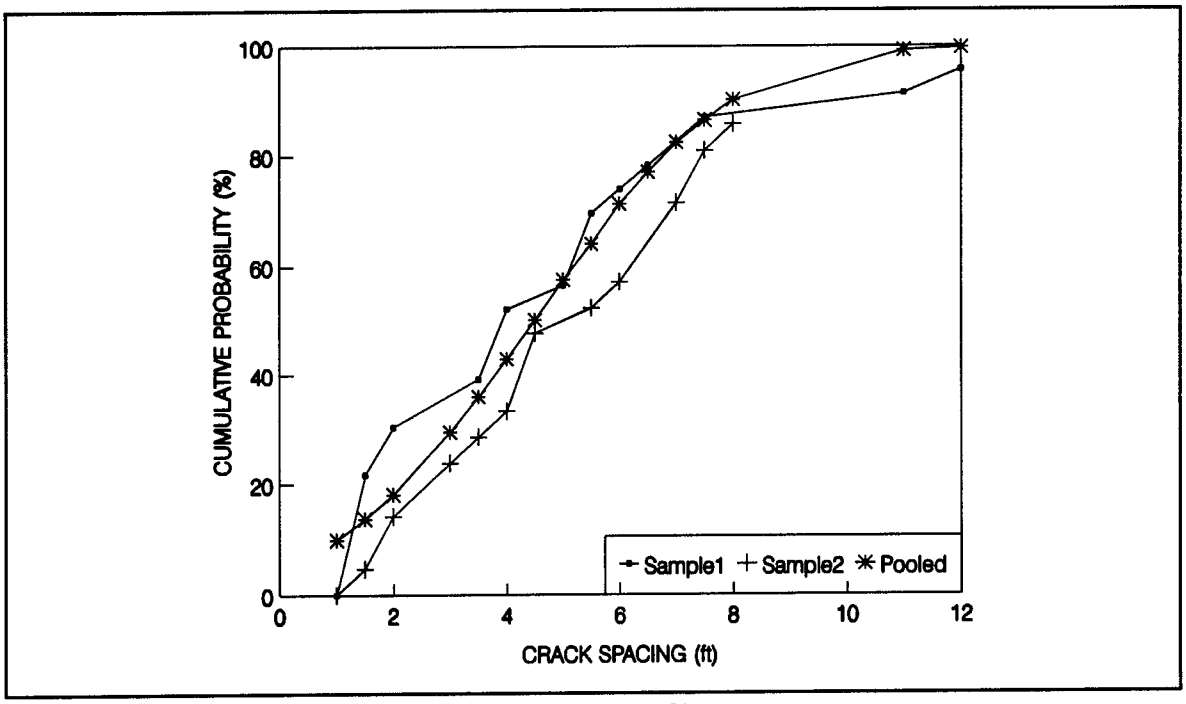

(0.305 m = 1 ft)

Figure 112. Field crack spacing distribution data: sample section Pennsylvania-2.

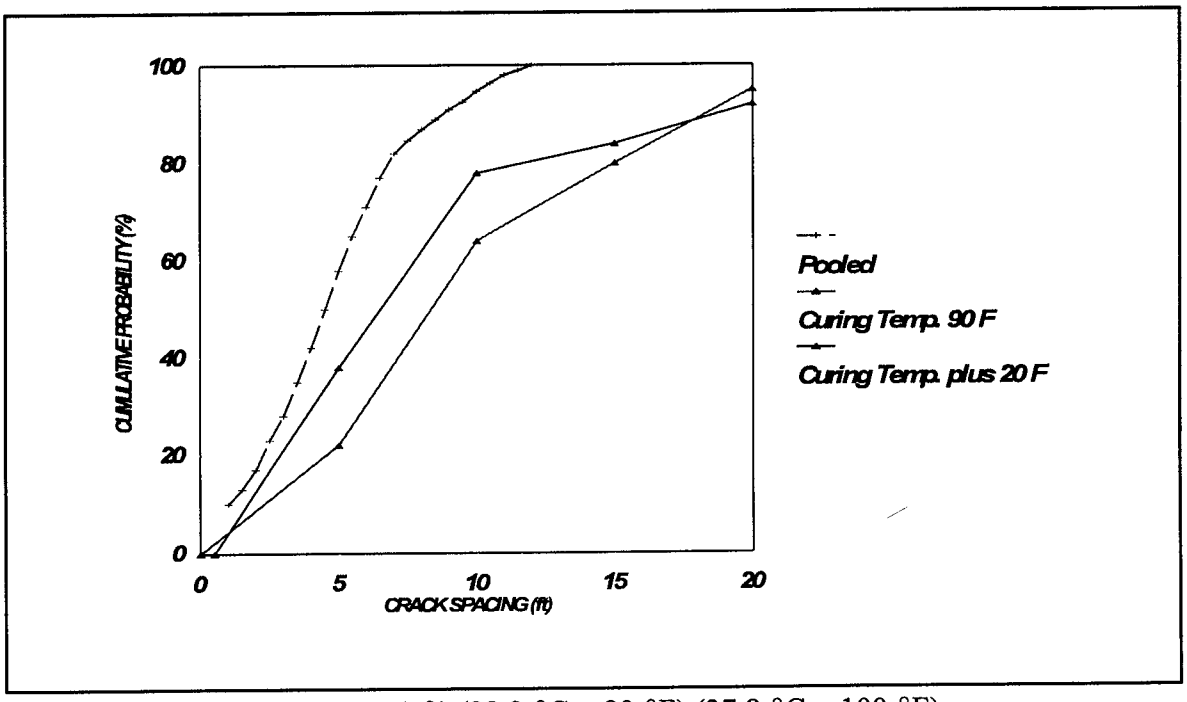

(0.305 m = 1 ft) (32.2 °C = 90 °F) (37.8 °C = 100 °F)

Figure 113. CRCP-5 crack distribution analysis for two curing temperatures from section Pennsylvania-2.

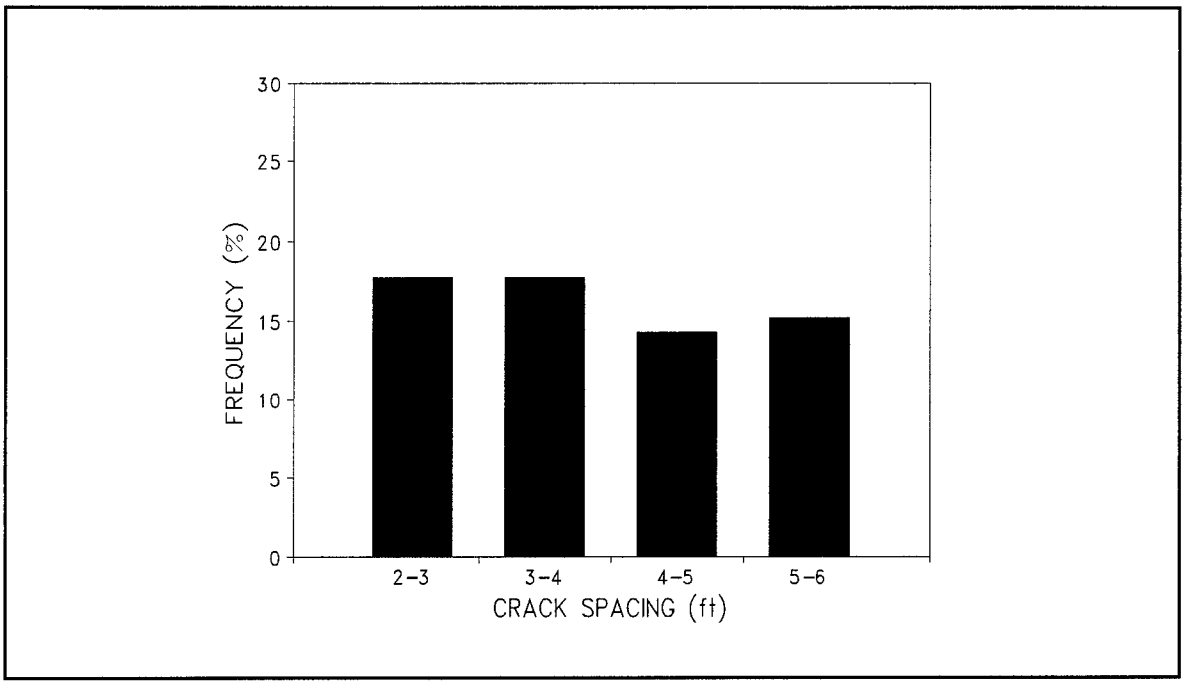

(0.305 m = 1 ft)

Figure 114. Crack spacing frequency: sample section Pennsylvania-2.

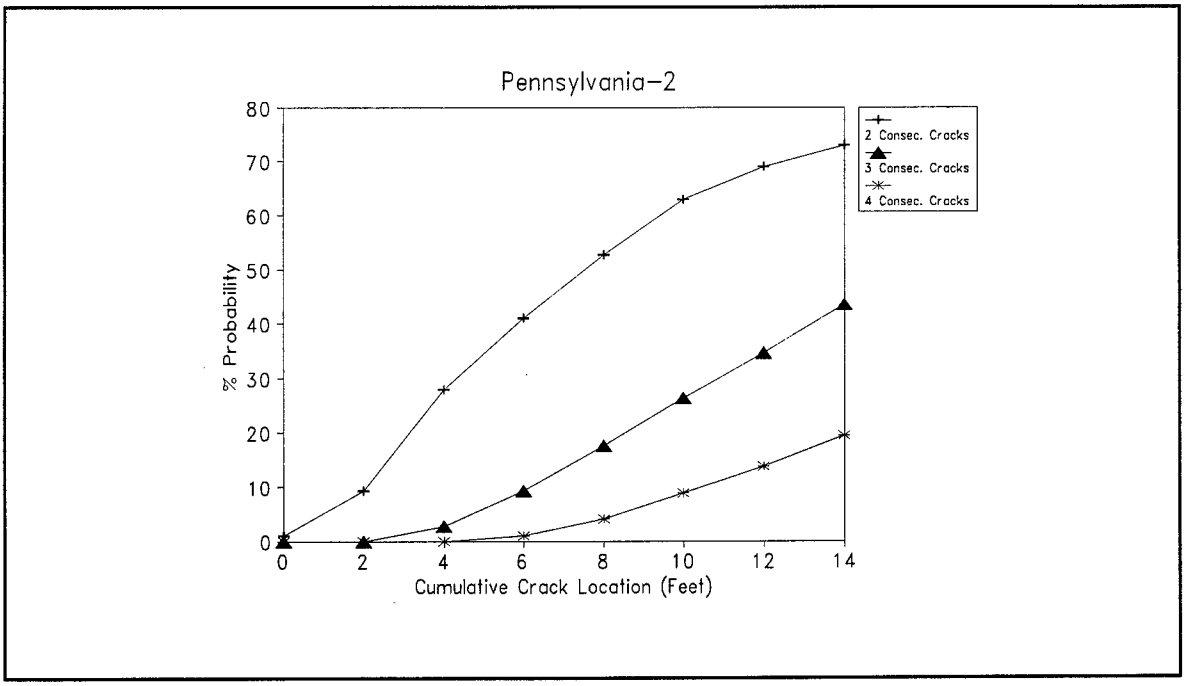

(0.305 m = 1 ft)

Figure 115. Probability of cluster cracking: sample section Pennsylvania-2.

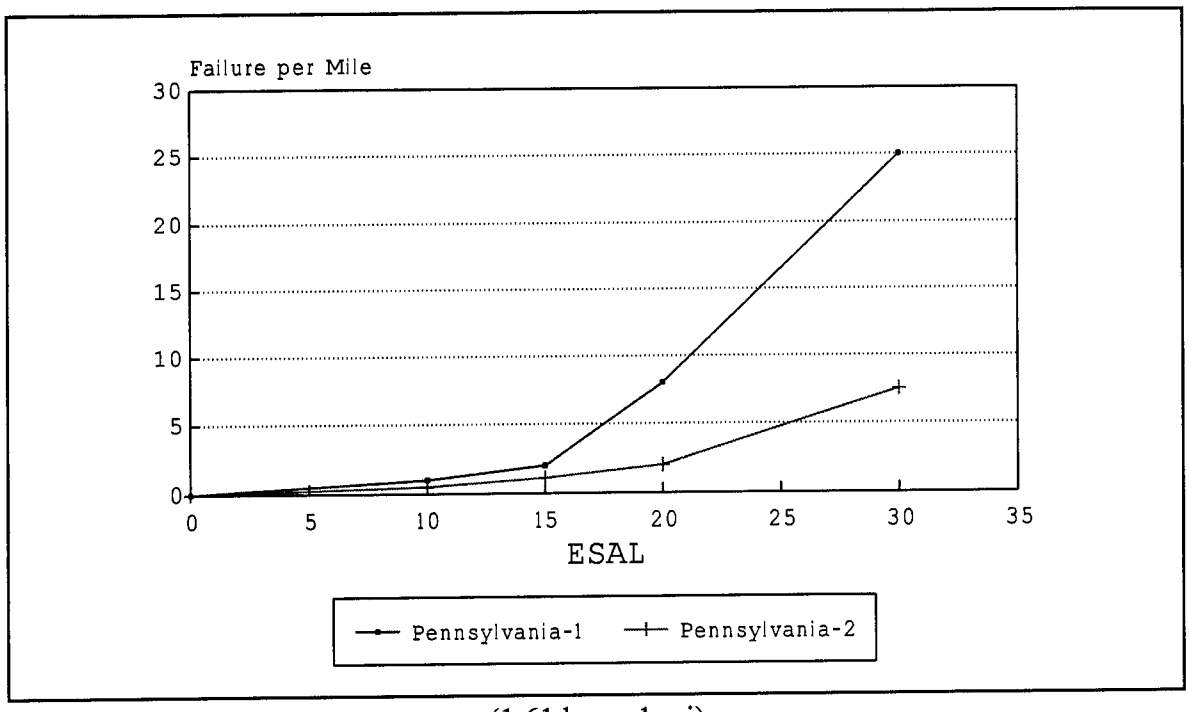

(1.61 km = 1 mi)

Figure 116. Performance prediction for sample sections in Pennsylvania.

APPENDIX E - WISCONSIN TEST SECTIONS DATA ANALYSIS

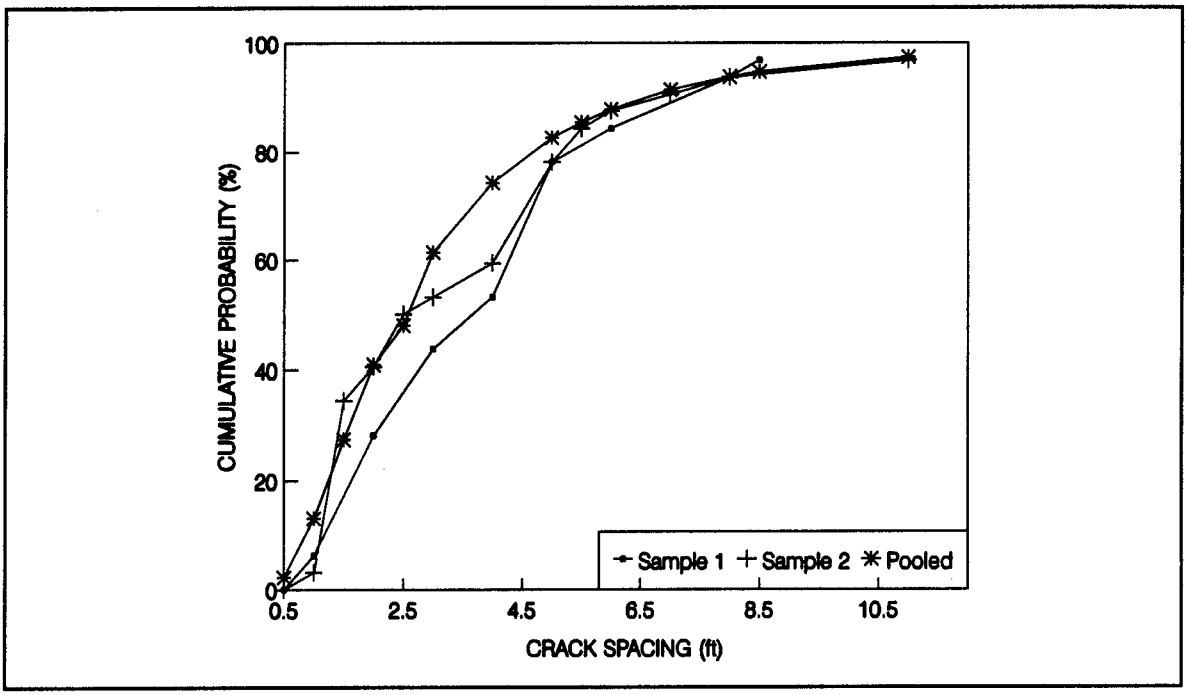

(0.305 m = 1 ft)

Figure 117. Field crack spacing distribution data: sample section Wisconsin-1.

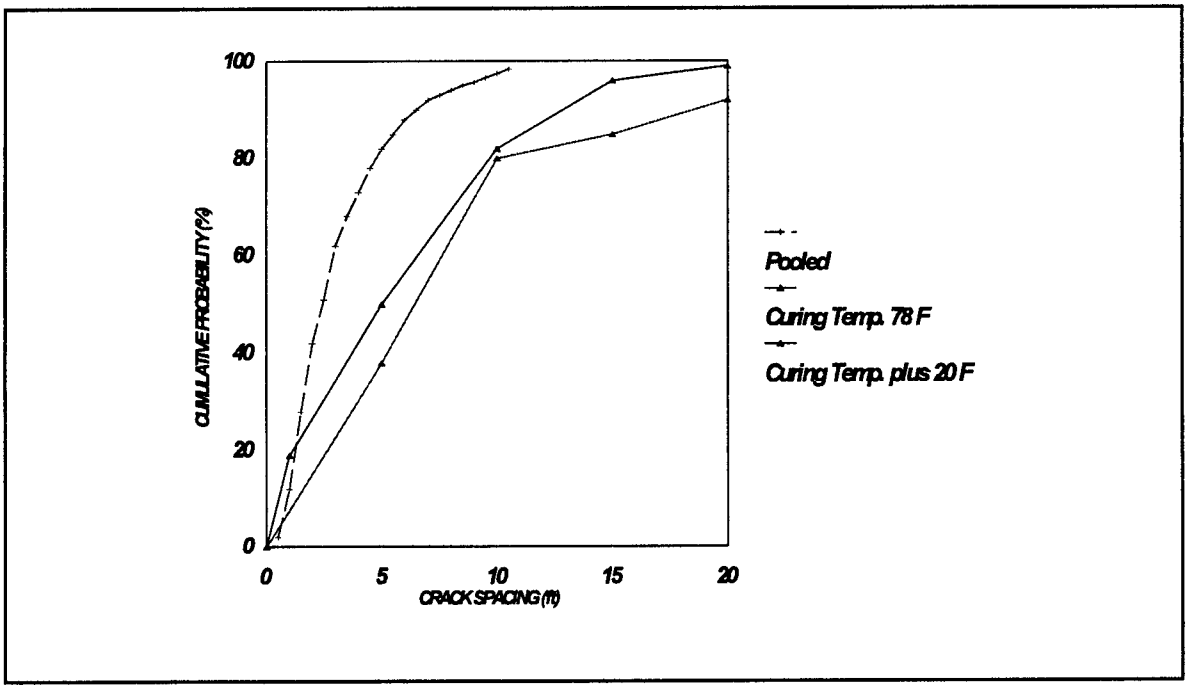

(0.305 m = 1 ft) (25.6 °C = 78 °F) (35 °C = 95 °F)

Figure 118. CRCP-5 crack distribution analysis for two curing temperatures from sample section Wisconsin-1.

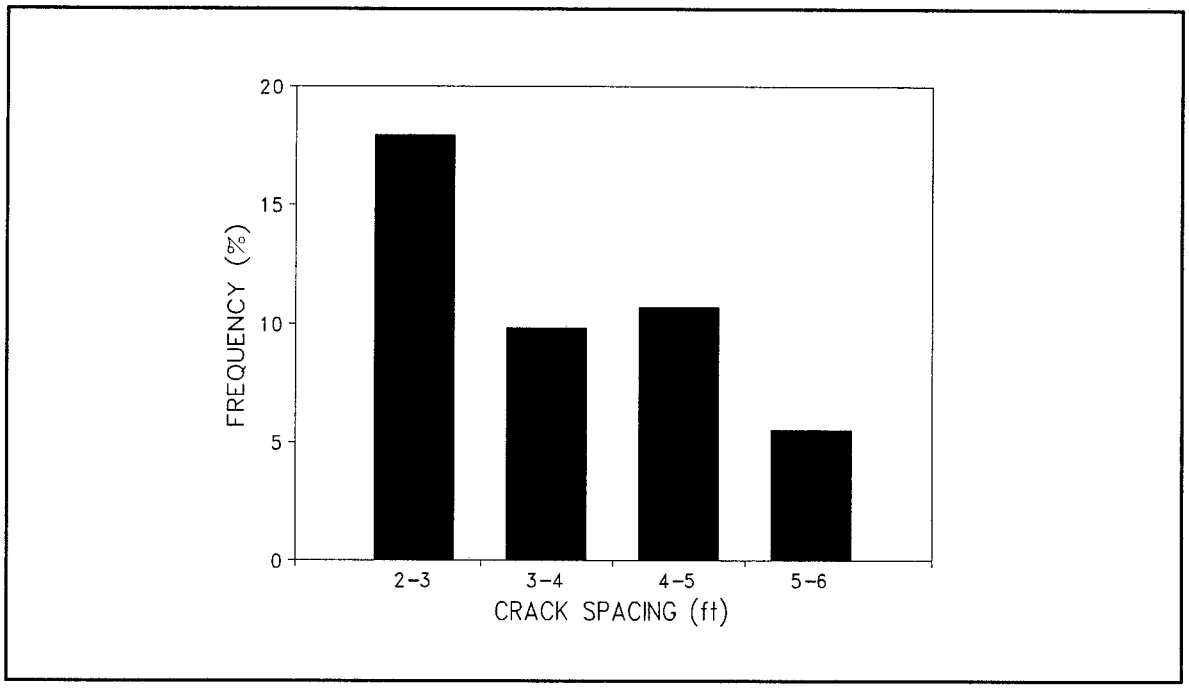

(0.305 m = 1 ft)

Figure 119. Crack spacing frequency: sample section Wisconsin-1.

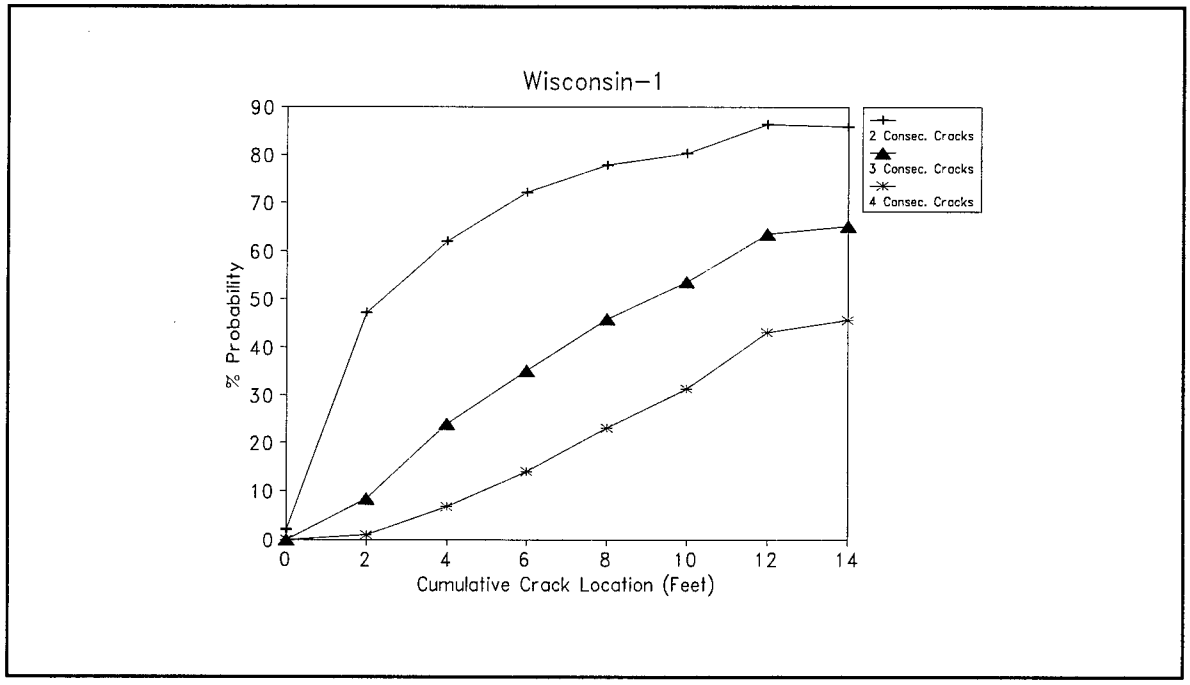

(0.305 m = 1 ft)

Figure 120. Probability of cluster cracking: sample section Wisconsin-1.

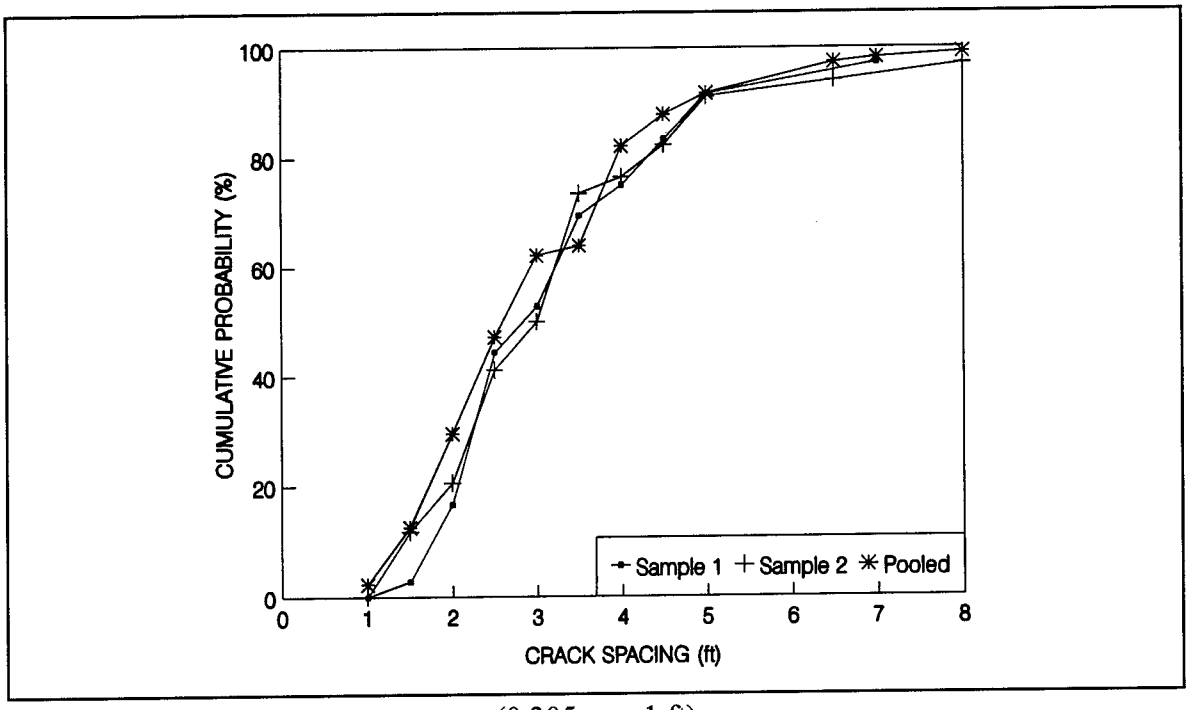

(0.305 m = 1 ft)

Figure 121. Field crack spacing distribution data: sample section Wisconsin-2.

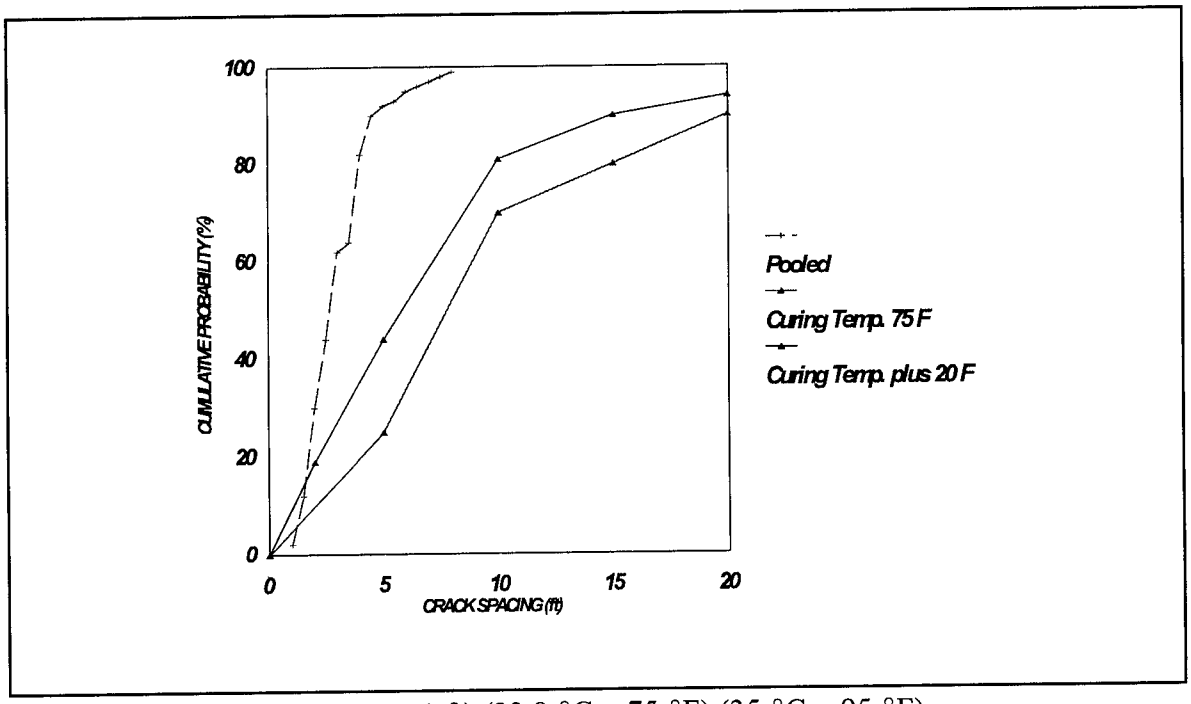

(0.305 m = 1 ft) (23.9 °C = 75 °F) (35 °C = 95 °F)

Figure 122. CRCP-5 crack distribution analysis for two curing temperatures from sample section Wisconsin-2.

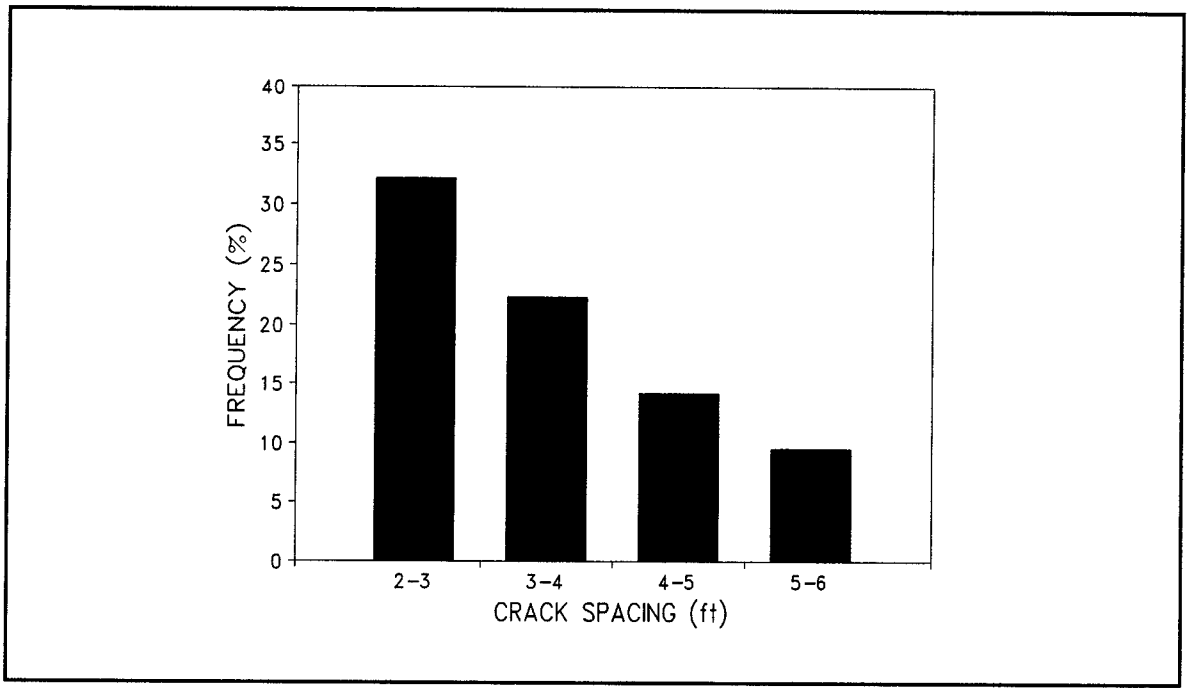

(0.305 m = 1 ft)

Figure 123. Crack spacing frequency: sample section Wisconsin-2.

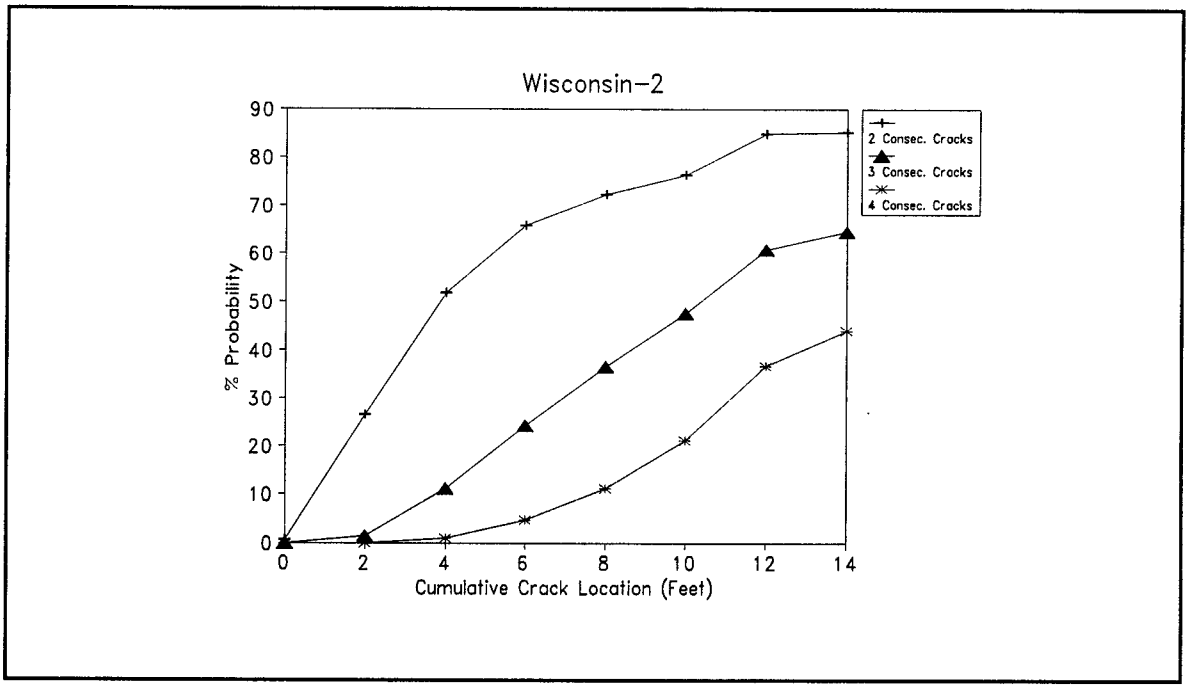

(0.305 m = 1 ft)

Figure 124. Probability of cluster cracking: sample section Wisconsin-2.

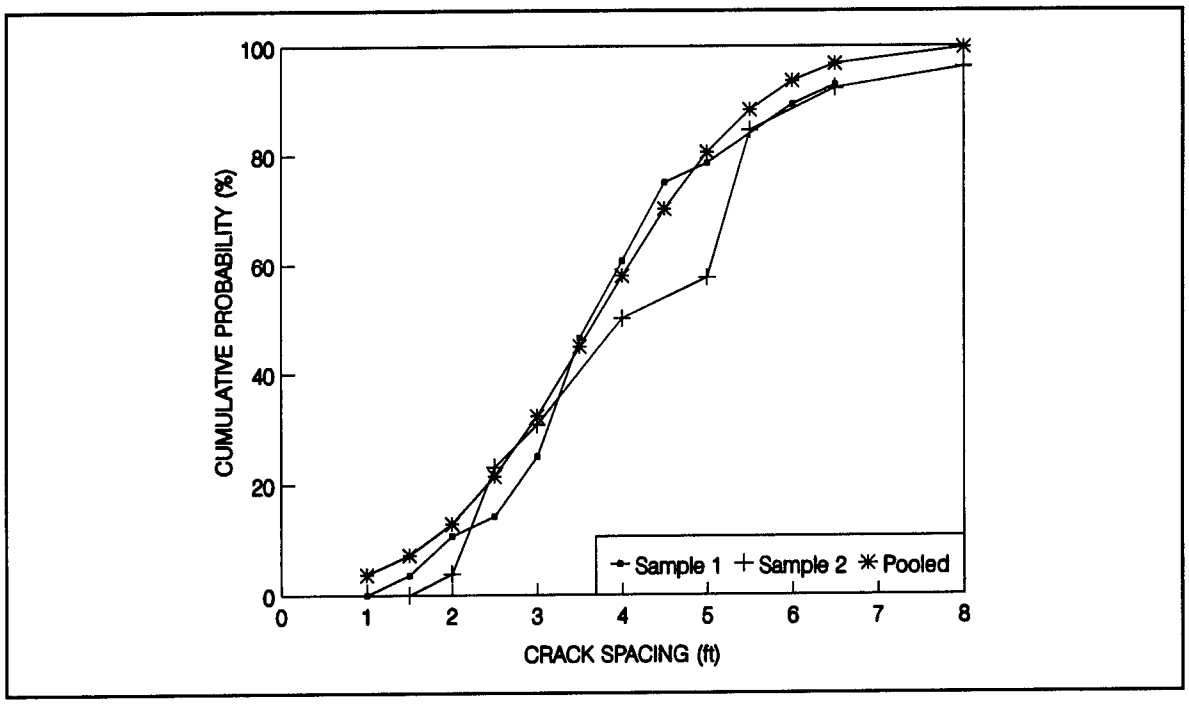

(0.305 m = 1 ft)

Figure 125. Field crack spacing distribution data: sample section Wisconsin-3.

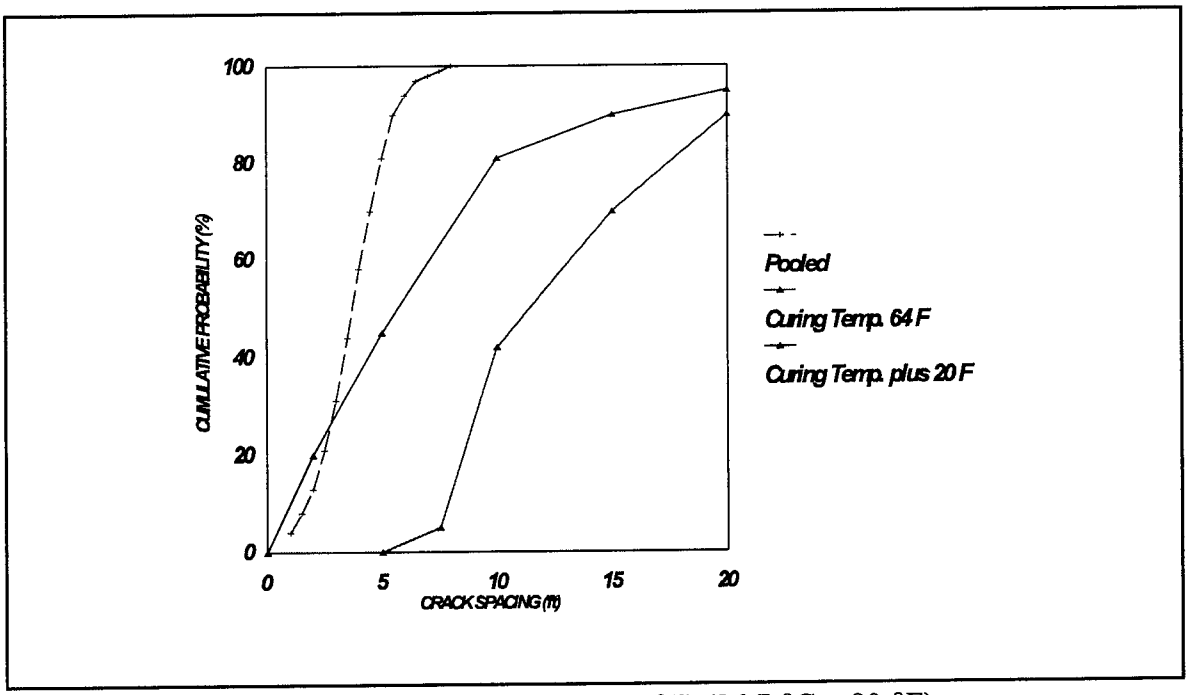

(0.305 m = 1 ft) (17.8 °C = 64 °F) (26.7 °C = 80 °F)

Figure 126. CRCP-5 crack distribution analysis for two curing temperatures from sample section Wisconsin-3.

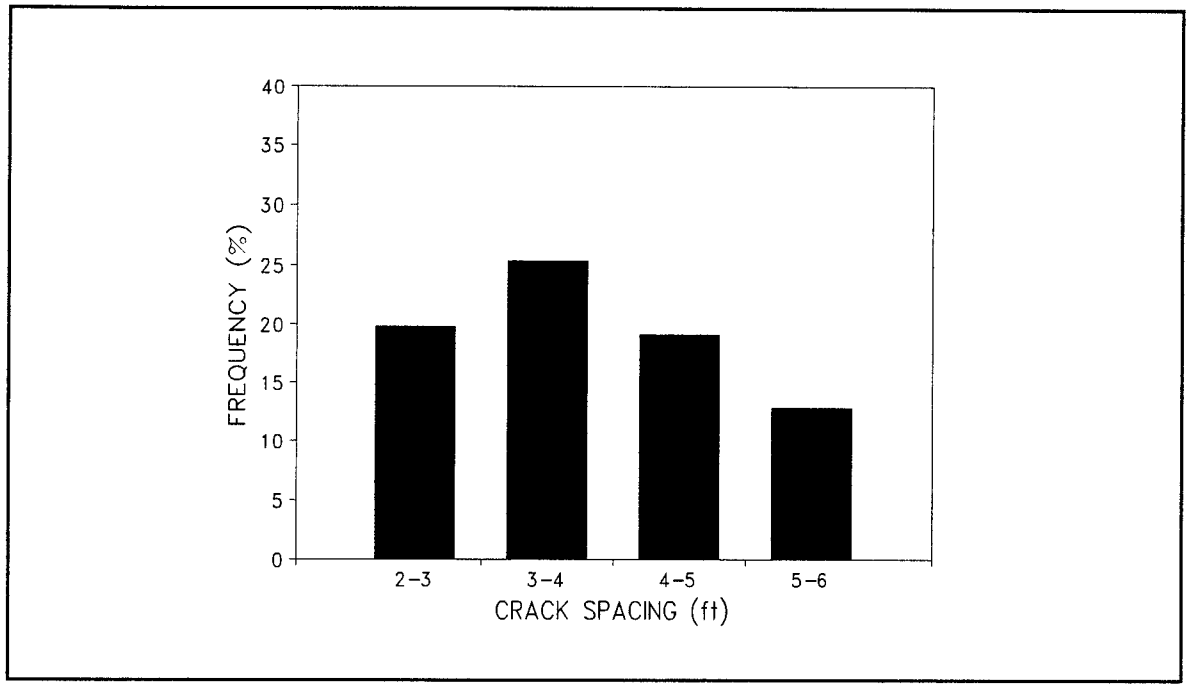

(0.305 m = 1 ft)

Figure 127. Crack spacing frequency: sample section Wisconsin-3.

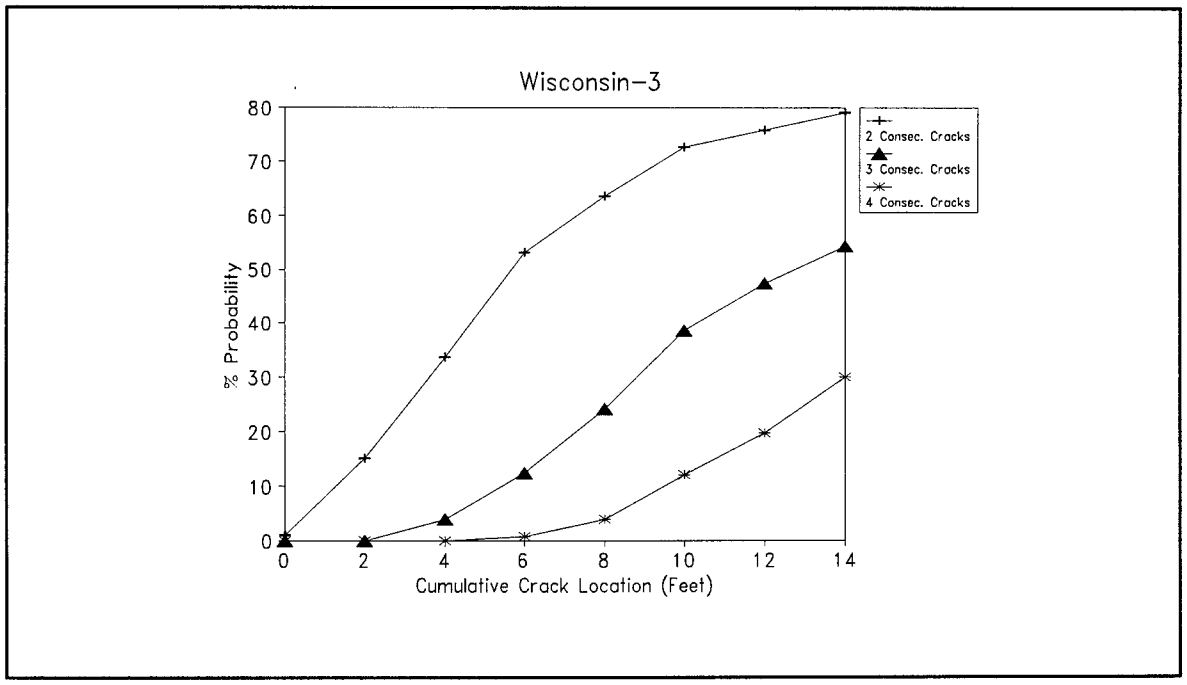

(0.305 m = 1 ft)

Figure 128. Probability of cluster cracking: sample section Wisconsin-3.

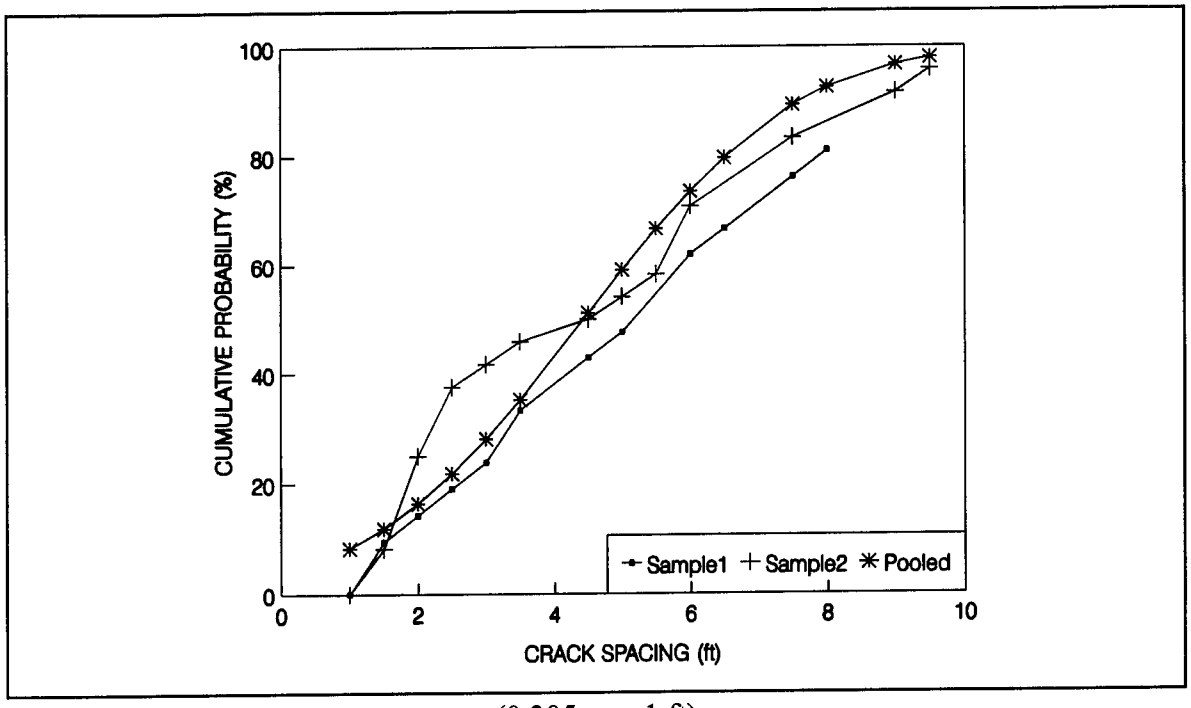

(0.305 m = 1 ft)

Figure 129. Field crack spacing distribution data: sample section Wisconsin-4.

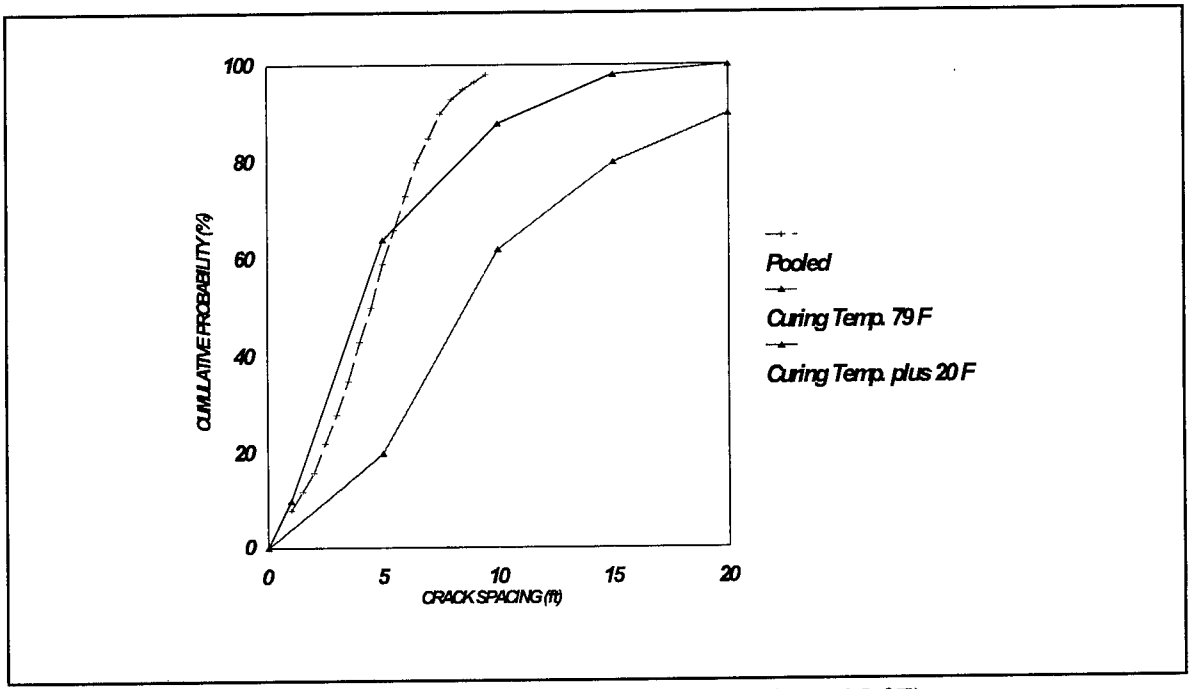

(0.305 m = 1 ft) (25.6 °C = 78 °F) (35 °C = 95 °F)

Figure 130. CRCP-5 crack distribution analysis for two curing temperatures from sample section Wisconsin-4.

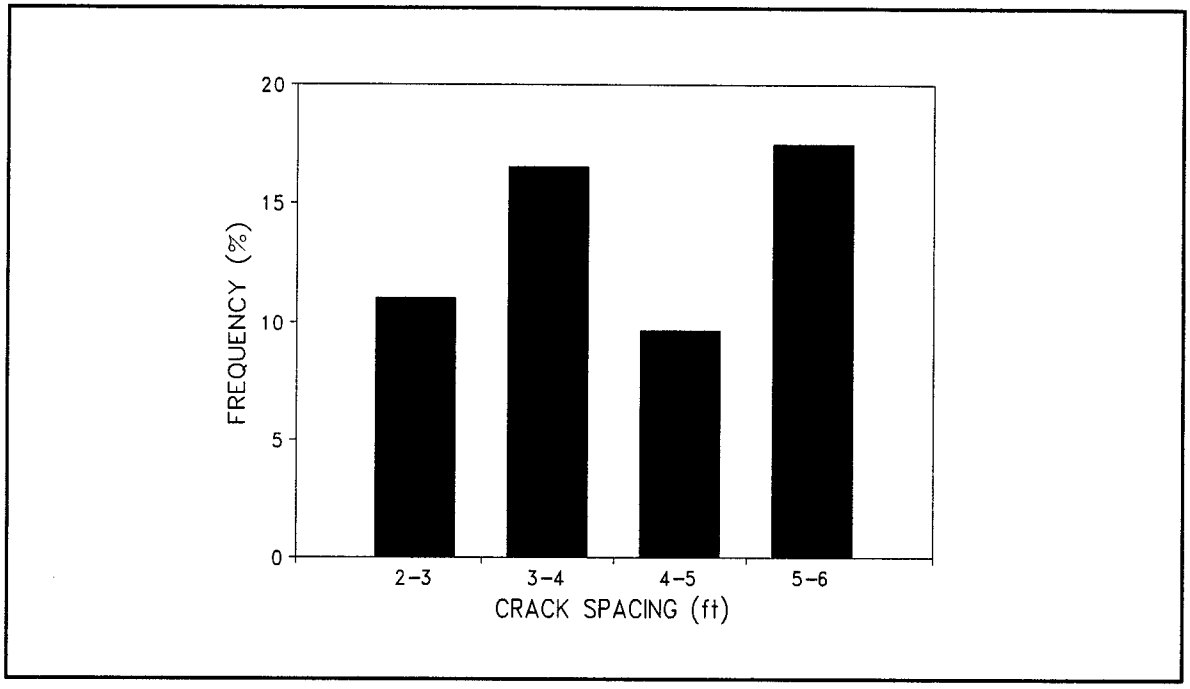

(0.305 m = 1 ft)

Figure 131. Crack spacing frequency: sample section Wisconsin-4.

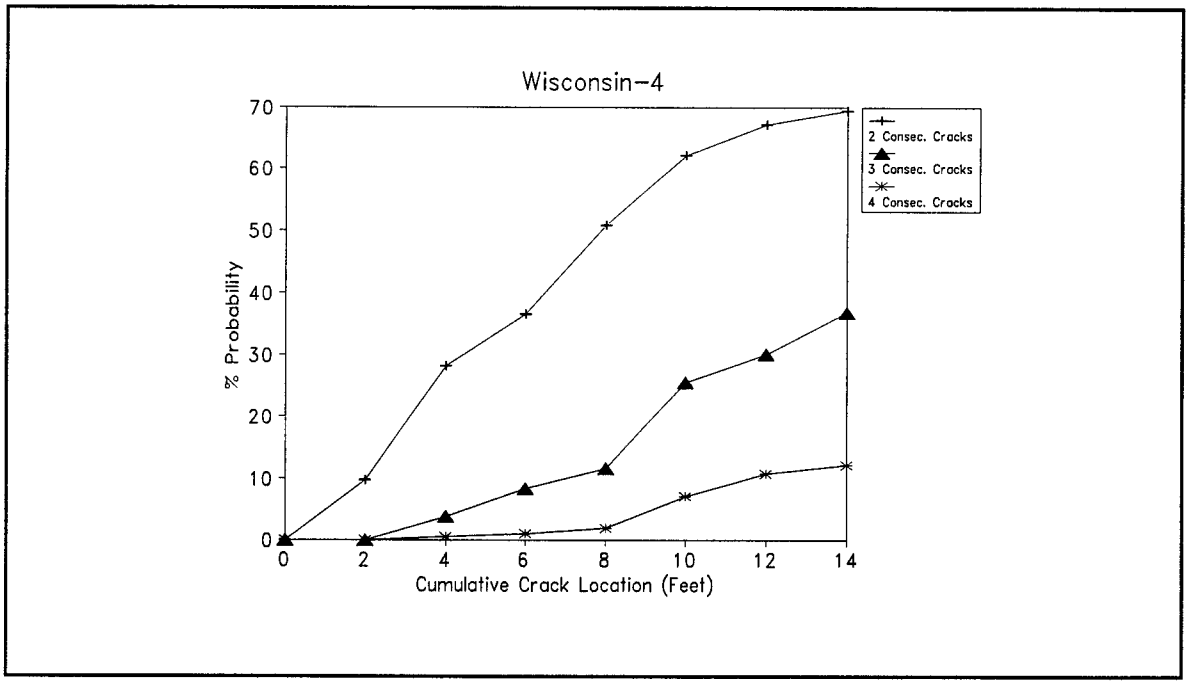

(0.305 m = 1 ft)

Figure 132. Probability of cluster cracking: sample section Wisconsin-4.

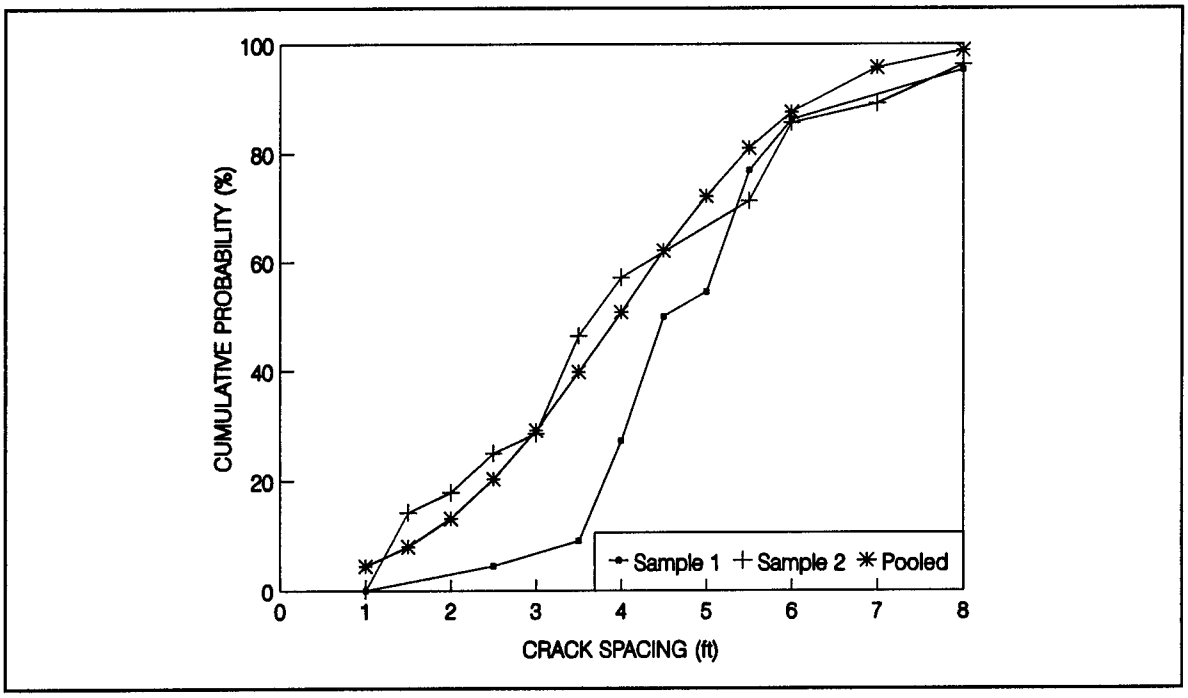

(0.305 m = 1 ft)

Figure 133. Field crack spacing distribution data: sample section Wisconsin-5.

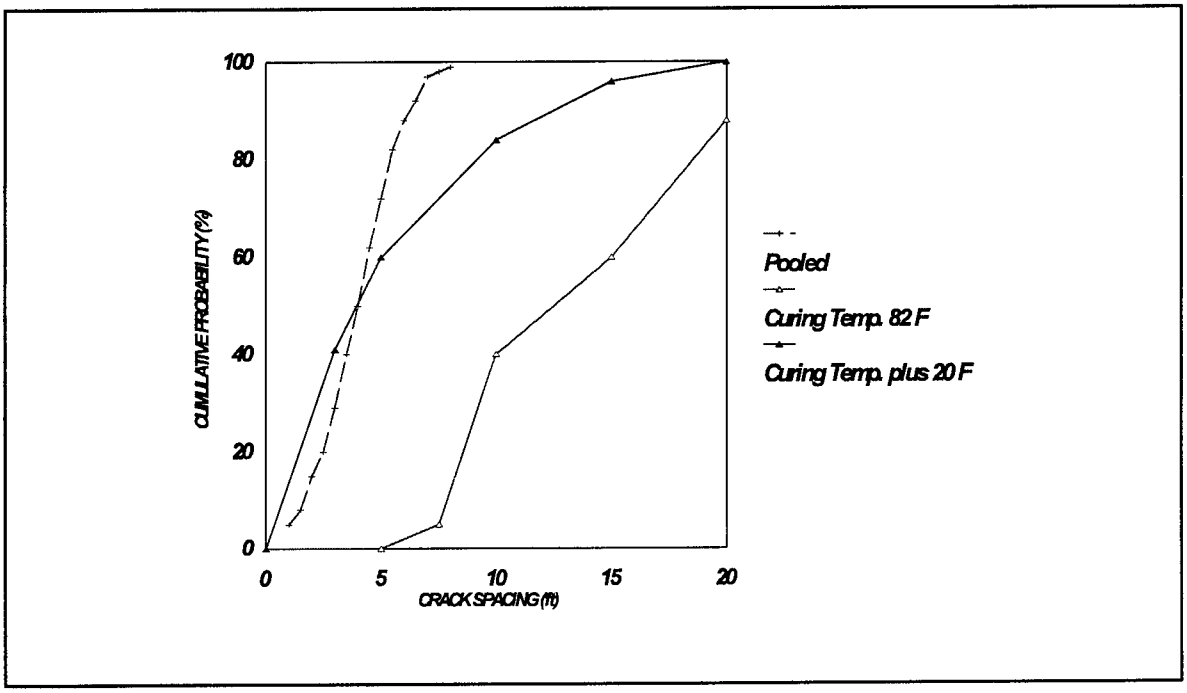

(0.305 m = 1 ft) (27.8 °C = 82 °F) (35 °C = 95 °F)

Figure 134. CRCP-5 crack distribution analysis for two curing temperatures from sample section Wisconsin-5.

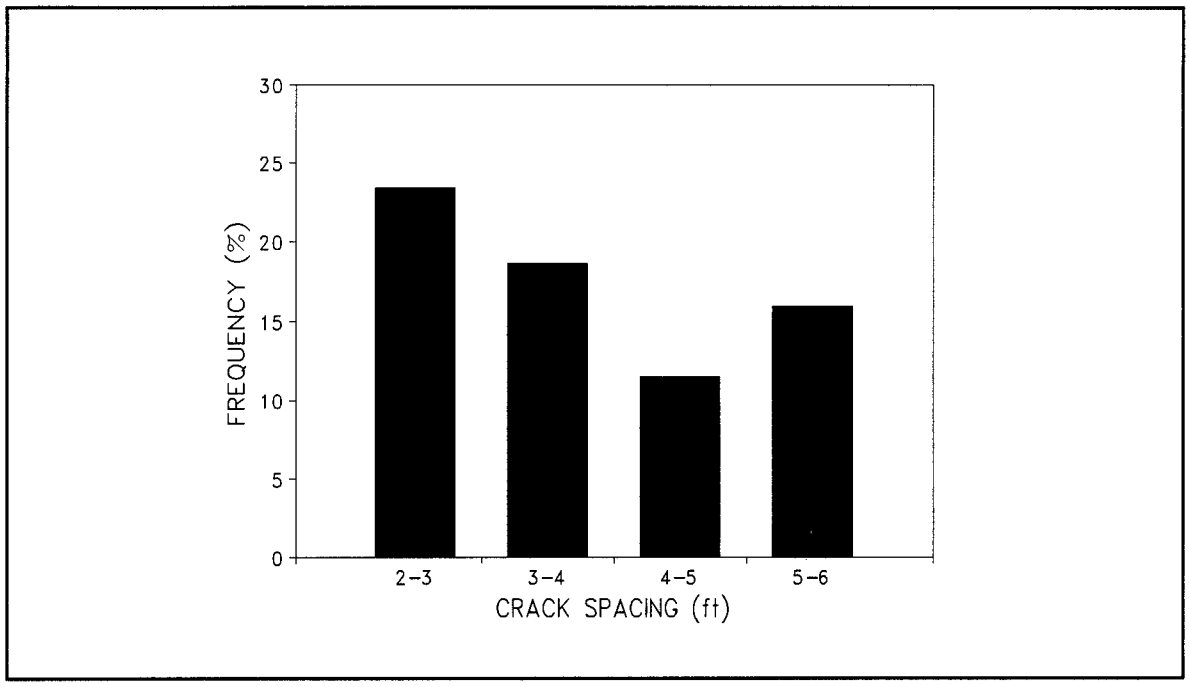

(0.305 m = 1 ft)

Figure 135. Crack spacing frequency: sample section Wisconsin-5.

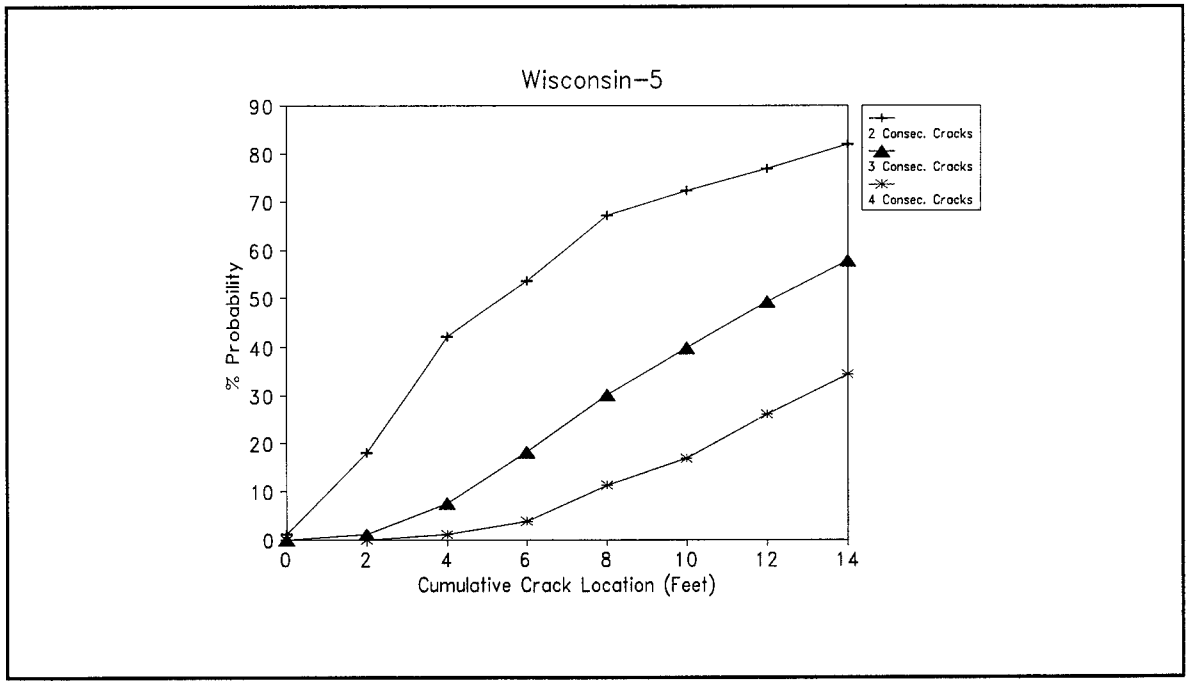

(0.305 m = 1 ft)

Figure 136. Probability of cluster cracking: sample section Wisconsin-5.

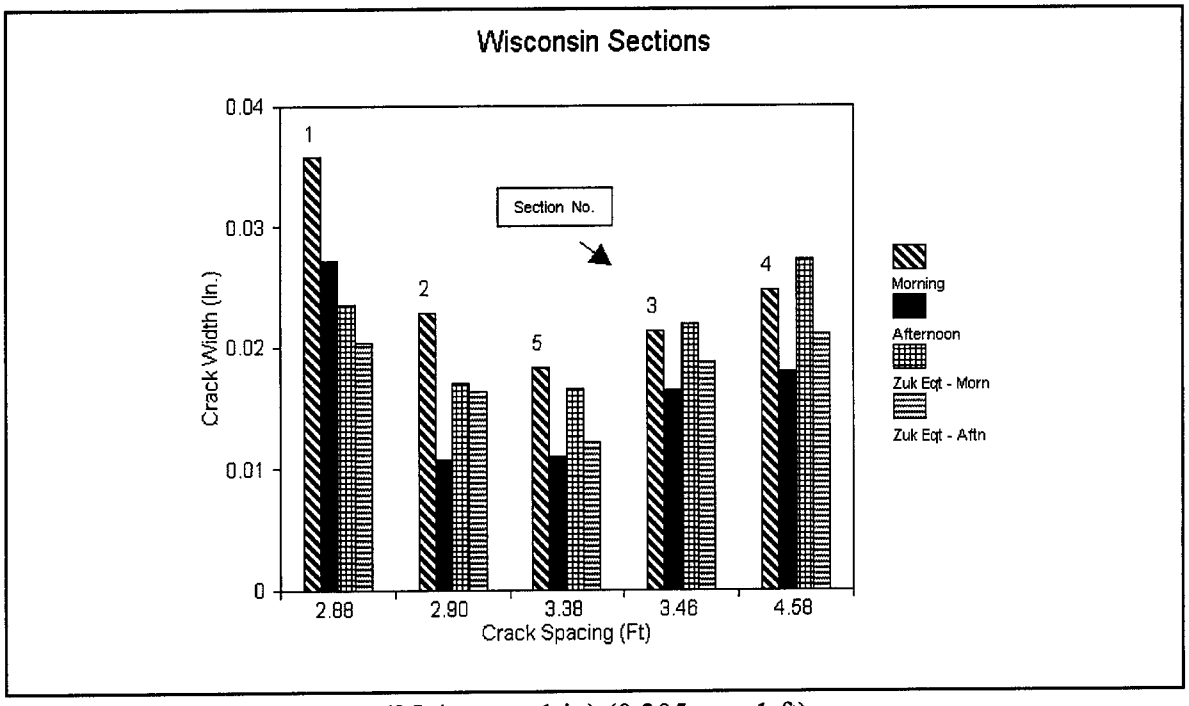

(25.4 mm = 1 in) (0.305 m = 1 ft)

Figure 137. Variation in crack width with crack spacing for Wisconsin sample sections.

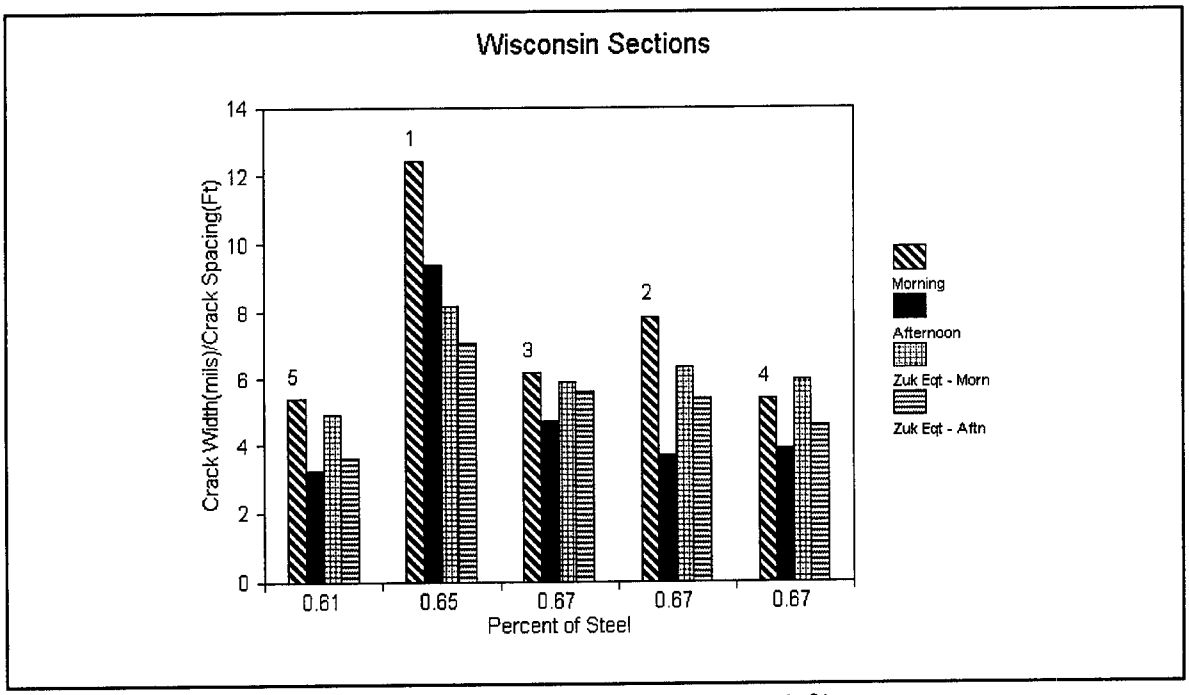

(0.0254 mm = 1 mil) (0.305 m = 1 ft)

Figure 138. Variation in crack width/crack spacing ratio with percent reinforcement for Wisconsin sample sections.

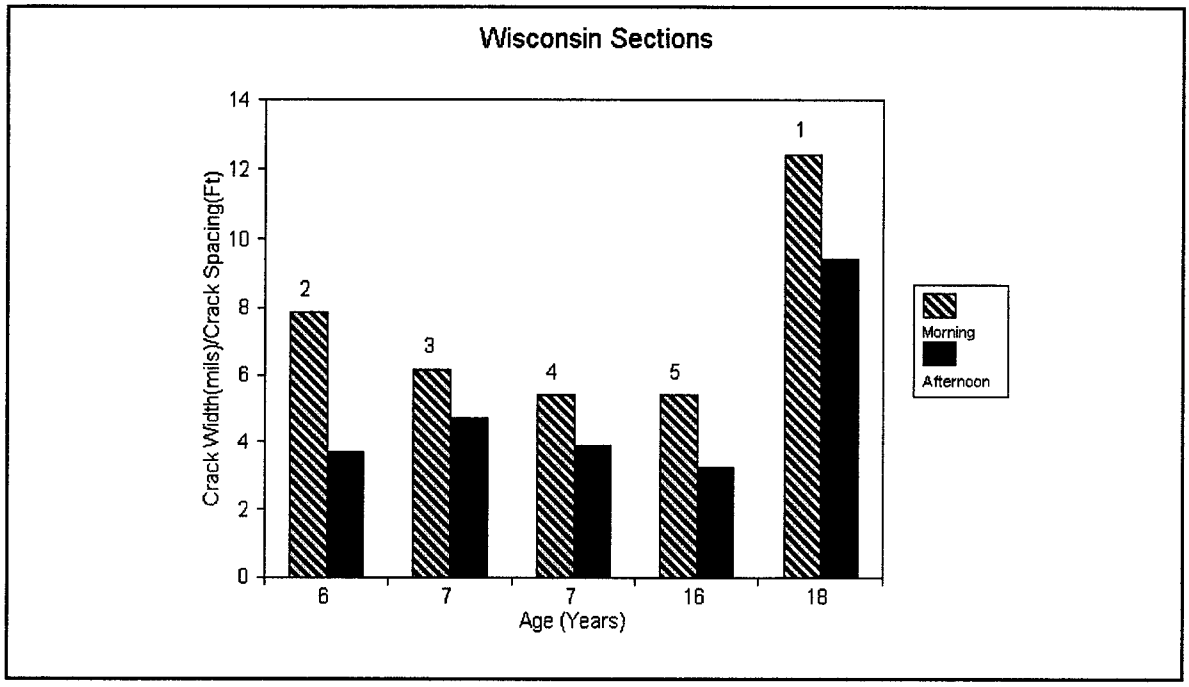

(0.0254 mm = 1 mil) (0.305 m = 1 ft)

Figure 139. Variation in crack width/crack spacing ratio with pavement age for Wisconsin sample sections.

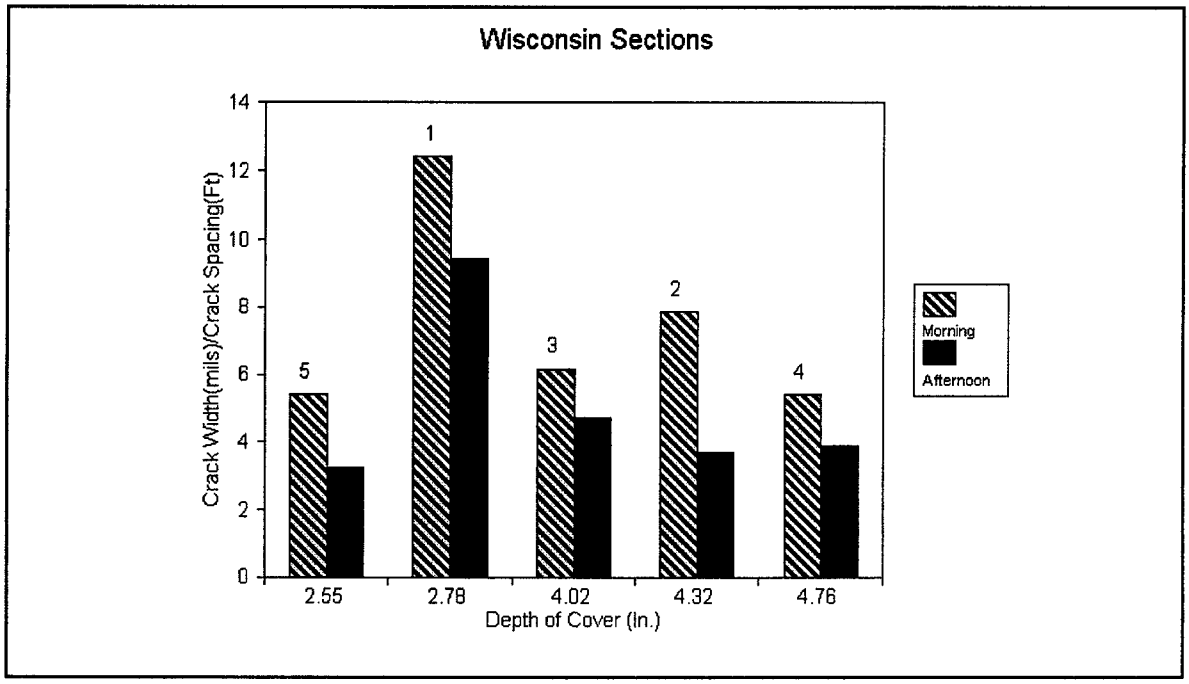

(0.0254 mm = 1 mil) (0.305 m = 1 ft) (25.4 mm = 1 in)

Figure 140. Variation in crack width/crack spacing ratio with depth of cover for Wisconsin sample sections.

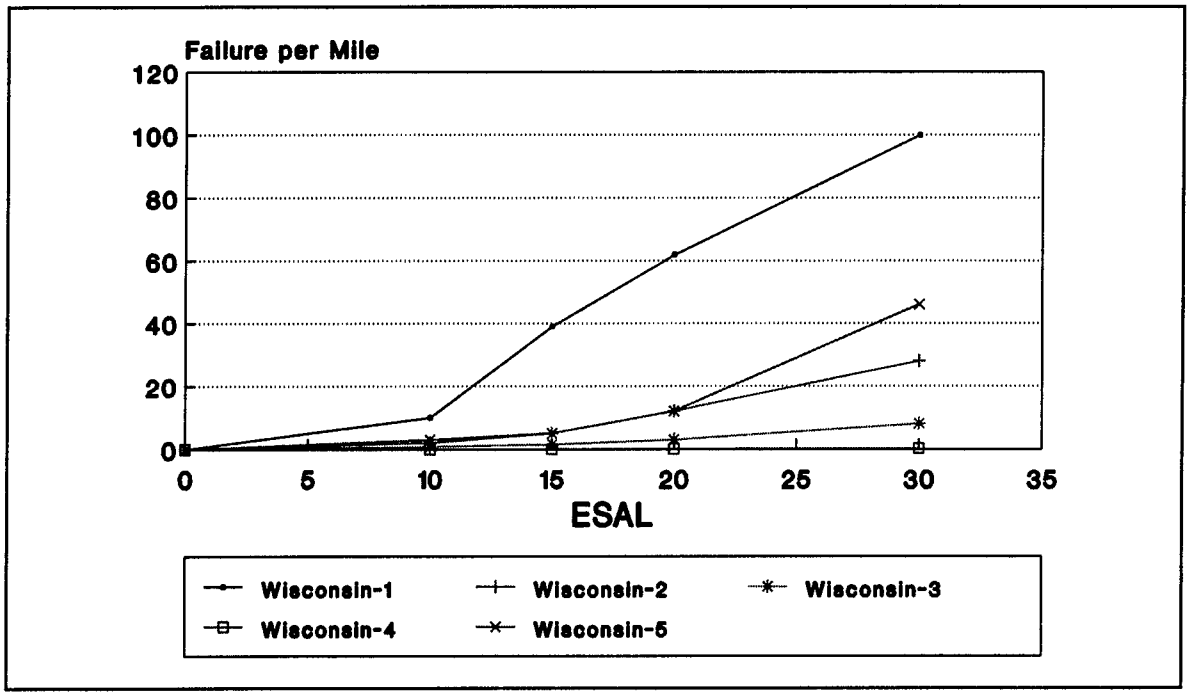

(1.61 km = 1 mi)

Figure 141. Performance prediction for sample sections in Wisconsin.

APPENDIX F - DEVELOPMENT OF CRC PAVEMENT ANALYSIS INPUT

CRCP-5 Program Inputs

The CRCP-5 requires various input parameters in order to function. The parameters that a required by CRCP-5 are listed below:

1. Percent of longitudinal reinforcement.
2. Longitudinal steel bar diameter (in).
3. Yield stress of steel (psi).
4. Elastic modulus of steel (psi).
5. Coefficient of thermal expansion of steel (in/in/°F).
6. Pavement slab thickness (in).
7. Coefficient of thermal expansion of concrete (in/in/°F).
8. Total shrinkage of concrete (in/in).
9. Elastic modulus of concrete (psi).
10. Compressive strength of concrete.
11. The ratio of tensile strength to the modulus of rupture of concrete.
12. Number of pairs of age tensile strength relationships.
13. The coefficient of variation of concrete (COV).
14. Curing temperature of the concrete.
15. Number of days in the analysis period.
16. Minimum temperature that is going to occur immediately after the construction of the pavement.
17. The days before reaching the minimum temperature i.e., the time gap between the construction of the pavement to the occurrence of the minimum temperature.
18. Number of days before the pavement is open to traffic.
19. Wheel load (lb).
20. Wheel load base radius (in).
21. Modulus of subgrade reaction (pci).
22. Frictional characteristics of subbase.

The CRCP-5 requires numerical values for the above parameters. Input data set was created for an individual section. Overall 20 data sets were created. These data sets were used as an input in the CRCP-5 program. The values percent of longitudinal steel, longitudinal steel bar diameters, slab thickness, and date of construction of the pavement were obtained from the construction details of the individual projects from the respective states. The ensuing discussion will give how the values were chose for different parameters.

Steel Properties

The steel yield strength is a transition point in the stress/strain curve between elastic and plastic load response. It is a required steel stress limit in design to limit the permanent yielding of the reinforcing steel required to maintain very tight crack widths. The typical crack widths range from 0.05 cm to 0.06 cm.

Billet steel and axle steel (ASTM A615 and A617) are available in grade 40 and Grade 60, while rail steel is available in grade 50 and Grade 60. The Grade designation indicates the yield strength of the steel, i.e., Grade 50 has a yield strength of 50,000 psi and Grade 60 has a yield strength of 60,0000 psi. Grade 60 is required for longitudinal reinforcement in CRCP, but either Grade 60, Grade 50, or Grade 40 is acceptable for transverse reinforcement.

Table 15. Steel reinforcement properties for sample sections.

Test Section	Long. Percent Steel (%)	Long. Bar Size	Placement of Steel	Epoxy Coated	Depth of Cover	
					Mean	STD
PA-1	0.45	5	Tube Fed	No	3.40	.23
PA-2	0.55	5	Chairs	No	2.73	.13
IL-1	0.70	6	Chairs	No	5.05	.49
IL-2	0.59	5	Tube Fed	No	2.15	.40
IL-3	0.60	5	Chairs	No	3.86	.25
IL-4	0.60	5	Tube Fed	No	3.01	.18
IL-5	0.70	6	Chairs	No	3.24	.17
OK-1	0.50	5	Chairs	No	3.87	.41
OK-2	0.50	5	Chairs	No	4.45	.27
OK-3	0.50	5	Chairs	Yes	4.84	.34
OK-4	0.50	5	Chairs	No	4.08	.31
OK-5	0.61	6	Chairs	No	4.63	.70
WI-1	0.65	4	Chairs	No	2.78	.37
WI-2	0.67	6	Tube Fed	Yes	4.32	.33
WI-3	0.67	6	Tube Fed	Yes	4.02	.36
WI-4	0.67	6	Tube Fed	No	4.76	.37
WI-5	0.61	6	Chairs	No	2.55	.35
IA-1	0.65	6	Tube Fed	No	4.22	.27
IA-2	0.65	6	Tube Fed	No	3.11	.34
IA-3	0.65	6	Tube Fed	No	3.16	.30

The modulus of elasticity of steel is taken as 2.9×10^6 psi for all the sections. The coefficient of thermal expansion of steel is assumed to be 5×10^6 in/in/°F for all the sections. Table 15 gives the percentage of longitudinal steel used in the test sections and also the longitudinal bar diameter used in the sections. It also gives the information regarding the placement of steel and whether the steel is epoxy coated or not.

Concrete Properties

The thermal coefficient of expansion varies with such factors as water-cement ratio, concrete age, richness of the mix, relative humidity, and type of aggregate. The type of coarse aggregate exerts a great influence on the thermal coefficient. Recommended values of thermal coefficients are listed in table 16 as a function of coarse aggregate.

Table 16. Recommended value of the thermal coefficient of concrete for various coarse aggregate types.
(0.6 °C = 1 °F)

Type of Coarse Aggregate in Concrete	Thermal Coefficient of Concrete (10^{-6}/°F)
Quartz	6.6
Sandstone	6.5
Gravel	6.0
Granite	5.3
Basalt	4.8
Limestone	3.8

Elastic modulus of concrete was calculated from tensile strength using the formula:

$$E_c = 4730 * 147.8 \left[\frac{f_t}{0.09 * 147.8}\right]^{\frac{1}{2}} \quad \textbf{(22)}$$

where: E_c = Elastic modulus of concrete (psi).
f_t = Tensile strength of concrete (psi).

The ratio of the direct strength of concrete to the compressive strength of concrete ranges from about 0.07 to 0.11. An average value of 0.09 is taken for all the test sections. The compressive strength of the concrete is calculated from the formula:

$$f_c = \frac{f_t}{0.09} \quad \textbf{(23)}$$

where: f_c = Compressive strength of the concrete (psi).
f_t = Tensile strength of the concrete (psi).

The ratio of modulus of rupture to the tensile strength of the concrete is assumed to be 0.6. The flexural strength of the concrete is assumed to be equal to the tensile strength of the concrete in the analysis.

Total Drying Shrinkage

Loss of water from concrete is known as drying shrinkage of concrete and is a significant factor in the reinforcement design. The rate of shrinkage decreases with age. The value of shrinkage at 28 days is used for the design shrinkage value. Both shrinkage and strength of the concrete are strongly dependent upon the water-cement ratio. As more water is added to the mix, the higher the shrinkage and the lower the strength. Therefore, shrinkage may be proportional to strength. There are many methods to calculate the shrinkage. Some of them are listed below.

Most of the shrinkage formulations suggested are experimentally bases and are empirical in nature. The American Concrete Institute (ACI) expresses shrinkage in concrete in terms of time and ultimate shrinkage. The following general equation is provided by ACI for the prediction of shrinkage in concrete:

$$(\varepsilon_{sh})_t = \frac{t^{\alpha}}{f + t^{\alpha}} \tag{24}$$

where: f = Time in days.
t = Age of concrete.
α = Constant for a given shape and size of structure.
$(\varepsilon_{sh})_t$ = Ultimate shrinkage.

The total shrinkage $\varepsilon_{cs}(t, t_s)$ can be computed by CEB 1990 method from the following equations:

$$\varepsilon_{cs}(t, t_s) = \varepsilon_{cso}\, \beta_s (t - t_s) \tag{25}$$

$$\varepsilon_{cso} = \varepsilon_s (f_{cm})\, \beta_{RH} \tag{26}$$

$$\varepsilon_s (f_{cm}) = \left[160 + 10\beta_{ac} \left(9 - \frac{f_{cm}}{f_{cmo}} \right) \right] * 10^{-6} \tag{27}$$

$$\beta_s (t - t_s) = \left[\frac{(t - t_s)/t_1}{350(h/h_o)^2 + (t - t_s)/t_1} \right]^{0.5} \tag{28}$$

where: t = Age of concrete (days)
t_s = Age of concrete (days) at the beginning of the shrinkage
t_1 = 1 day
ho = 100 mm
f_{cm} = Mean compressive strength of concrete at the age of 28 days (MPA)
f_{cmo} = 10 MPA
β_{sc} = Coefficient (4 for slowly hardening cements, 5 for normal or rapid hardening cements, 6 for rapid hardening high strength cements)
β_{RH} = -1.55 [1 - RH/100)3] for 40 % ≤ RH < 99%
β_{RH} = 0.25 for RH ≥ 99%

Drying shrinkage was also calculated using the temperature and crack width data using the following equations:

$$Drying\ shrinkage = \varepsilon_{cw} - \varepsilon_{tem} \quad (29)$$

ε_{cw} = Shrinkage due to crack widths
ε_{tem} = Shrinkage width of cracks/crack spacing
ε_{cw} = Total width of cracks/crack spacing
ε_{tem} = $(T_{cur} - T_{amb})\alpha$

where: Tcur = Curing temperature
T_{amb} = Temperature at the time of crack width measurements
α = Coefficient of thermal expansion of concrete

Table 17 was also used to determine the shrinkage corresponding to the indirect tensile strength of concrete. For Illinois, Wisconsin, and Oklahoma sections the shrinkage was calculated from temperature and crack width data. Due to the lack of crack width data for Iowa and Pennsylvania the shrinkage was calculated using table 17. Table 18 gives shrinkage values for the sample sections.

Table 17. Approximate relationship between shrinkage and indirect tensile strength of concrete.
(6.89 kPa = 1 psi) (25.4 mm = 1 in)

Indirect Tensile Strength (psi)	Shrinkage, in/in
300 or less	0.0008
400	0.0006
500	0.00045
600	0.0003
700 or more	0.0002

Table 18. Total shrinkage using CRSI table and crack widths.
(25.4 mm = 1 in)

Test Section	Total Shrinkage (in/in)	
	Table 4.3	Using Crack Width Data
IL-1	4.7E-04	4.2E-05
IL-2	3.3E-04	4.1E-04
IL-3	3.0E-04	2.9E-04
IL-4	4.9E-04	3.5E-04
IL-5	4.8E-04	2.3E-04
OK-1	4.8E-04	2.7E-04
OK-2	3.4E-04	1.5E-04
OK-3	4.5E-04	2.5E-04
OK-4	4.9E-04	2.7E-04
OK-5	4.8E-04	7.1E-06
WI-1	4.0E-04	5.8E-04
WI-2	4.7E-04	3.7E-04
WI-3	5.3E-04	4.7E-04
WI-4	3.0E-04	3.5E-04
WI-5	4.2E-04	1.9E-04
IA-1	4.8E-04	---
IA-2	4.4E-04	---
IA-3	3.6E-04	---

Temperature

The curing temperature is based on the date of construction reported for the pavement section. The maximum temperature of the day was taken from the day of the construction to the 30 days after the construction of the pavement and it was averaged to get the curing temperature in °F. This temperature data was obtained from the individual climatological records for the given State. The minimum winter temperature was also taken from the same source of information. The analysis period was assumed to be 28 days. The analysis program requires a daily minimum temperature throughout the analysis period. The analysis period was assumed to be started from the first day of the construction of the pavement which required daily temperatures for the analysis. Table 19 gives the curing temperature and minimum temperature data for each pavement site.

Wheel Load

Eighteen kip wheel load is taken as a standard for all the test sections. The wheel base radius is taken as 150 mm (6 in). In the analysis program the number of days before the pavement is open to traffic is set to a maximum limit of 28 days. If number of days before opening to traffic exceeds 28 days, the program will assume 28 days as the required days. This is a reason why the analysis period in the program was also assumed as 28 days. The analysis program requires tensile strength and temperature data for this analysis period. For the 28 day analysis period the traffic load may not make much difference so, the wheel load stress is assumed as zero in the program for the analysis.

Frictional Characteristics

The tensile strength of concrete is the dominant factor which affects the crack spacing in CRC pavements. Therefore careful consideration was given for tensile strength of concrete in the analysis. The analysis program requires the tensile strength data at 1st, 3rd, 5th, 7th, 14th, 21st, and at the 28th day of the analysis period. The 28th day tensile strength is known for all the test sections and was used to calculate the tensile strength at the other days of the analysis period. The following formulas are used to calculate the tensile strength. The formulas are given in terms of modulus of rupture. It was assumed that the ratio of tensile strength of the concrete to the modulus of rupture is 0.5.

The 28 day tensile strength was converted to modulus of rupture using the above ratio. By doing this we can calculate the 28 day modulus of rupture (F_{28}). The modulus of rupture at any time T(F_A) can be calculated once the F_{28} values are known. Table 20 gives the tensile strength for the sample sections using the following equation:

$$F_A = 1.22 + 0.17 log_{10}T - 0.05 (log_{10}T)^2 \quad \textbf{(30)}$$

where: F_A = Ratio of the modulus of rupture at time T to the modulus of rupture at 28 days.

T = time since slab construction in years.

Table 19. Concrete pavement properties for sample sections.
(25.4 mm = 1 in) (1.8 mm/mm/°C = 1 in/in/°F) (6.89 kPa = 1 psi)

Test Section	Slab Thickness (in)	Thermal Coefficient (in/in/°F)	Compressive Stress (psi)	E_c (psi)	σ_f (psi)
PA-1	9.1	6.0E-06	5367	4.21E+6	483
PA-2	9.5	6.0E-06	6056	4.48E+6	545
IL-1	10.2	3.8E-06	5444	4.24E+6	490
IL-2	8.8	3.8E-06	6422	4.61E+6	578
IL-3	8.2	3.8E-06	6689	4.71E+6	602
IL-4	9.2	3.8E-06	5244	4.17E+6	472
IL-5	8.5	3.8E-06	5367	4.21E+6	483
OK-1	9.3	3.8E-06	5311	4.19E+6	478
OK-2	9.2	3.8E-06	6367	4.59E+6	573
OK-3	10.3	3.8E-06	5522	4.27E+6	497
OK-4	9.4	3.8E-06	5278	4.18E+6	475
OK-5	10.1	3.8E-06	5356	4.21E+6	482
WI-1	8.0	6.5E-06	7367	4.94E+6	663
WI-2	10.0	6.5E-06	5411	4.23E+6	487
WI-3	10.0	6.5E-06	4967	4.05E+6	447
WI-4	10.6	6.5E-06	7367	4.94E+6	633
WI-5	8.0	6.5E-06	5744	4.36E+6	517
IA-1	8.25	3.8E-06	5367	4.21E+6	483
IA-2	7.9	3.8E-06	5656	4.31E+6	509
IA-3	8.1	3.8E-06	6222	4.54E+6	560

Table 20. Curing temperature and minimum temperature after construction of the pavement.
(0.6°C = 1°F)

Test Section	Curing Temperature (°F)	Minimum Temperature After the Construction of Pavement (°F)
PA-1	63	-14
PA-2	90	4
IL-1	84	-4
IL-2	85	-13
IL-3	72	-4
IL-4	90	-7
IL-5	84	-4
OK-1	70	1
OK-2	92	9
OK-3	94	-17
OK-4	79	-11
OK-5	79	-3
WI-1	78	-22
WI-2	75	-22
WI-3	64	-25
WI-4	79	-30
WI-5	82	-15

The modulus of rupture (F) can be estimated at any time T using the following expression:

$$F = F_A\,(F_{28}) \tag{31}$$

where: F = Modulus of rupture at time T.
F_{28} = Modulus of rupture at 28 days.

Table 21. Subgrade characteristics for sample sections.
(0.27 MPa/m = 1 pci) (6.89 kPa = 1 psi) (25.4 mm = 1 in)

Test Section	Subbase Type	AASHTO Class	k (pci)	F (psi)	Y (in)
PA-1	Unbound Granular	A-2-6	225	3.0	-0.02
PA-2	Unbound Granular	A-2-6	225	3.0	-0.02
IL-1	Permeable Concrete	A-7-5	125	1.1	-0.052
IL-2	Cement Treated	A-6	155	15.4	-0.015
IL-3	Asphalt Treated	A-7-5	125	1.6	-0.03
IL-4	Asphalt Treated	A-7-5	125	1.6	-0.03
IL-5	Lean Concrete	A-7-5	125	3.0	-0.024
OK-1	Asphalt Treated	A-6	155	1.6	-0.011
OK-2	Asphalt Treated	A-7-5	125	1.6	-0.011
OK-3	Asphalt Treated	A-4	200	1.6	-0.011
OK-4	Soil Asphalt	A-6	155	0.4	-0.2
OK-5	Permeable Concrete	A-2-6	225	0.6	-0.03
WI-1	Unbound Granular	A-1-a	400	3.0	-0.02
WI-2	Unbound Granular	A-1-a	400	3.0	-0.02
WI-3	Unbound Granular	A-1-a	400	0.6	-0.03
WI-4	Unbound Granular	A-3	250	4.0	-0.03
WI-5	Unbound Granular	A-3	250	3.0	-0.02
IA-1	Cement Treated	A-3	250	15.4	-0.025

Table 22. Tensile strength of the concrete at different days.
(6.89 kPa = 1 psi)

Test Section	Tensile Strength of Concrete (psi)							
	Day 0	Day 1	Day 3	Day 5	Day 7	Day 14	Day 21	Day 28
PA-1	0	331	470	524	566	637	676	725
PA-2	0	342	486	547	586	659	699	750
IL-1	0	353	502	565	605	681	722	775
IL-2	0	387	550	619	664	747	792	850
IL-3	0	365	518	583	625	703	746	800
IL-4	0	319	454	510	547	615	652	700
IL-5	0	376	535	601	644	725	769	825
OK-1	0	376	535	601	644	725	769	825
OK-2	0	362	514	549	619	697	739	793
OK-3	0	342	486	547	586	659	699	750
OK-4	0	331	470	524	566	637	676	725
OK-5	0	324	460	518	554	624	662	710
WI-1	0	383	544	612	656	738	783	840
WI-2	0	319	454	510	547	615	652	700
WI-3	0	319	454	506	547	615	652	700
WI-4	0	334	475	530	572	644	683	733
WI-5	0	410	583	657	703	791	839	900
IA-1	0	399	567	637	683	769	815	875
IA-2	0	328	467	525	562	633	671	720
IA-3	0	296	421	474	508	571	606	650

APPENDIX G - CORRELATIONS OF CLUSTER RATIOS

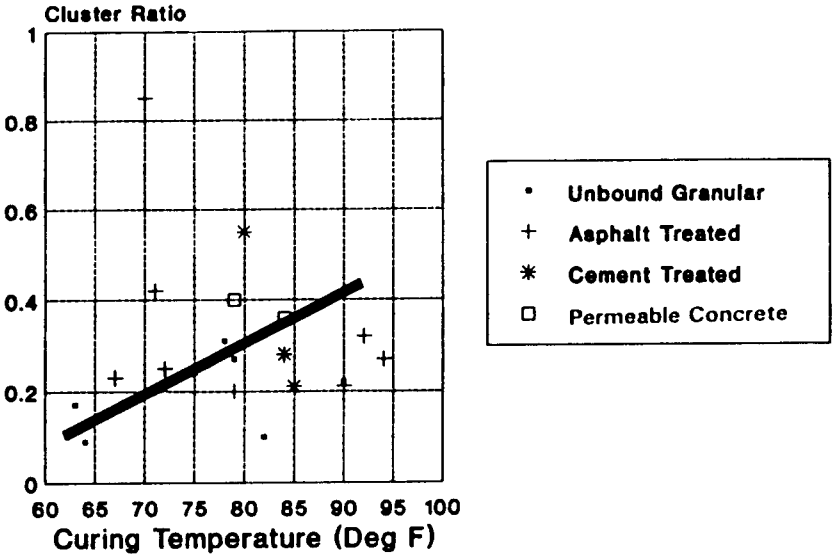

(0.6 °C = 1 °F)

Figure 142. Cluster ratio versus curing temperature for different subbase types.

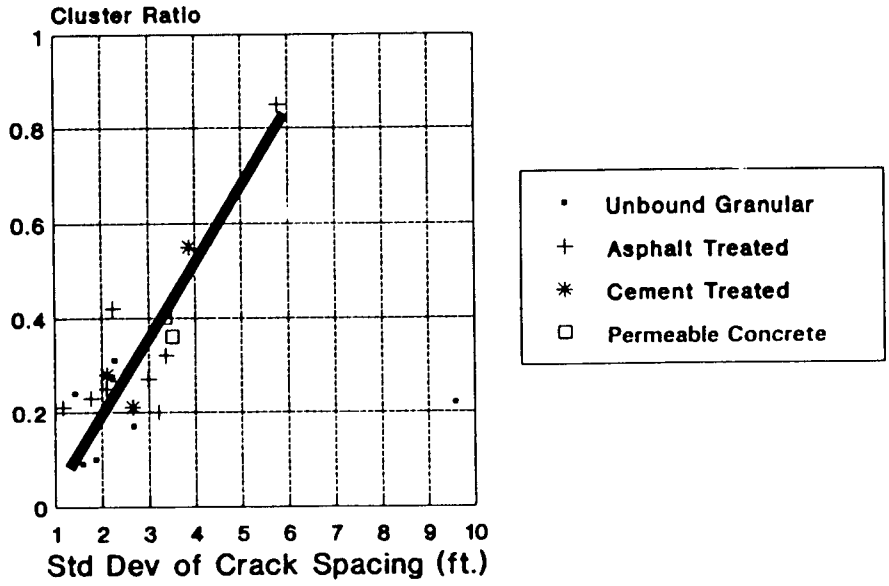

(0.305 m = 1 ft)

Figure 143. Cluster ratio versus standard deviation of crack spacing for different subbase types.

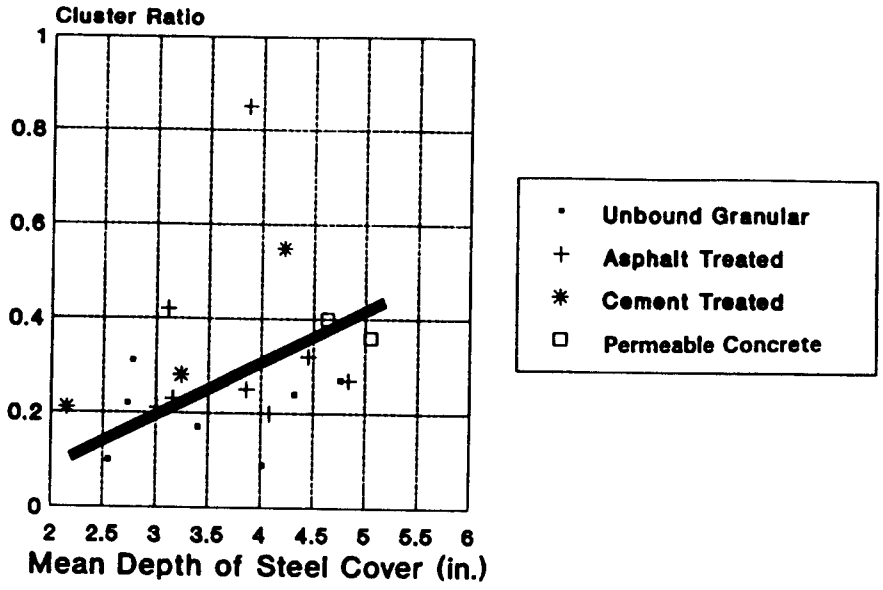

(25.4 mm = 1 in)

Figure 144. Cluster ratio versus mean depth of steel cover for different subbase types.

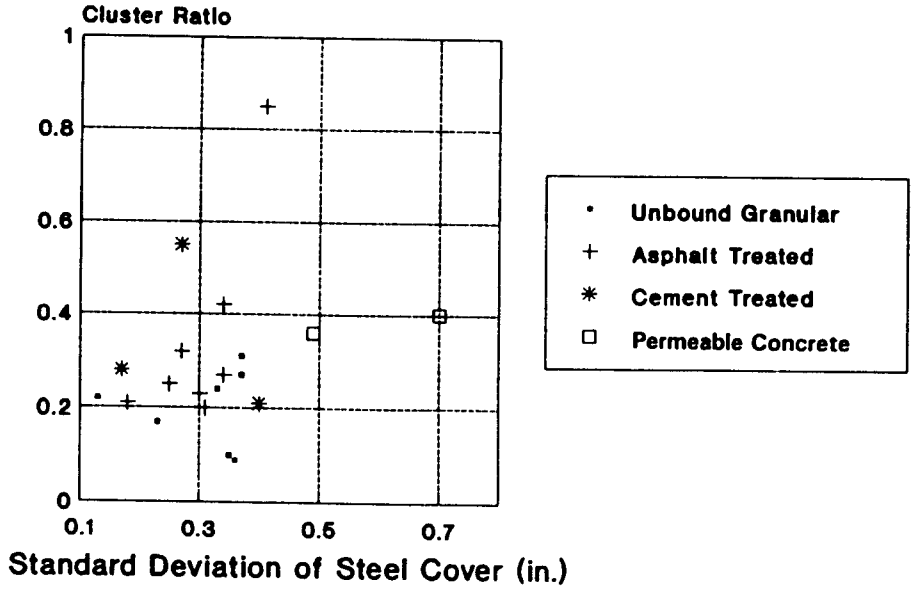

(25.4 mm = 1 in)

Figure 145. Cluster ratio versus the standard deviation of steel cover for different subbase types.

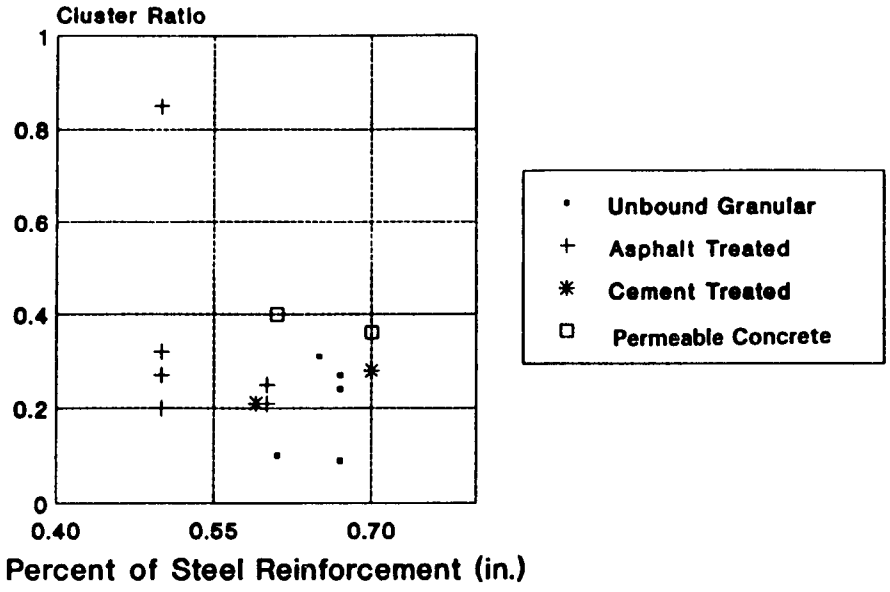

(25.4 mm = 1 in)

Figure 146. Cluster ratio versus percent of steel reinforcement for different subbase types.

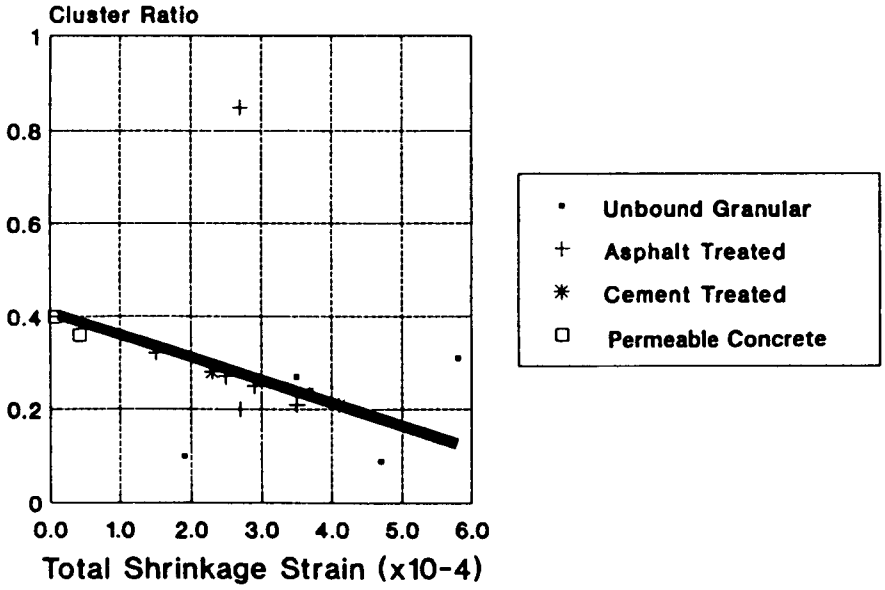

Figure 147. Cluster ratio versus total shrinkage strain for different subbase types.

APPENDIX H - CORRELATIONS OF Y CRACKING

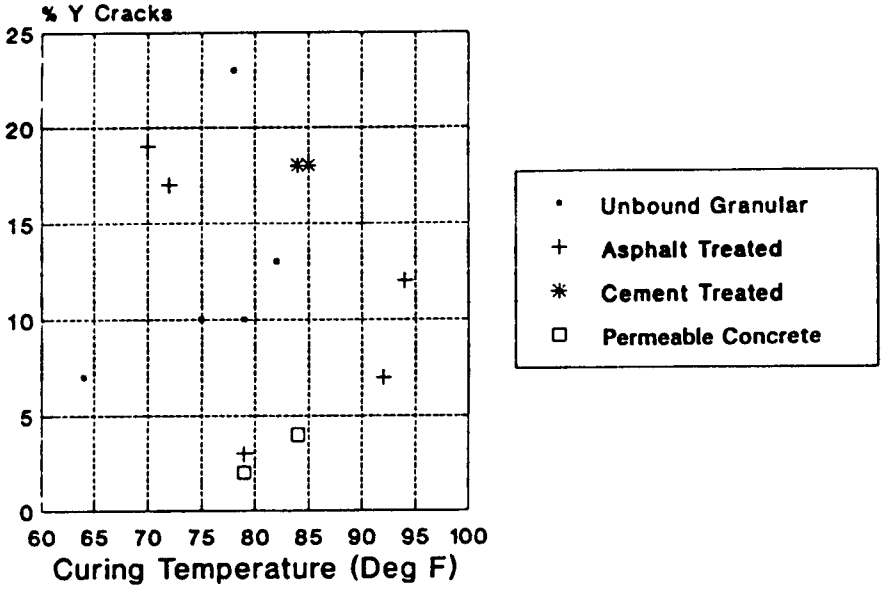

(0.6 °C = 1 °F)

Figure 148. Y cracking versus curing temperature of different subbase types.

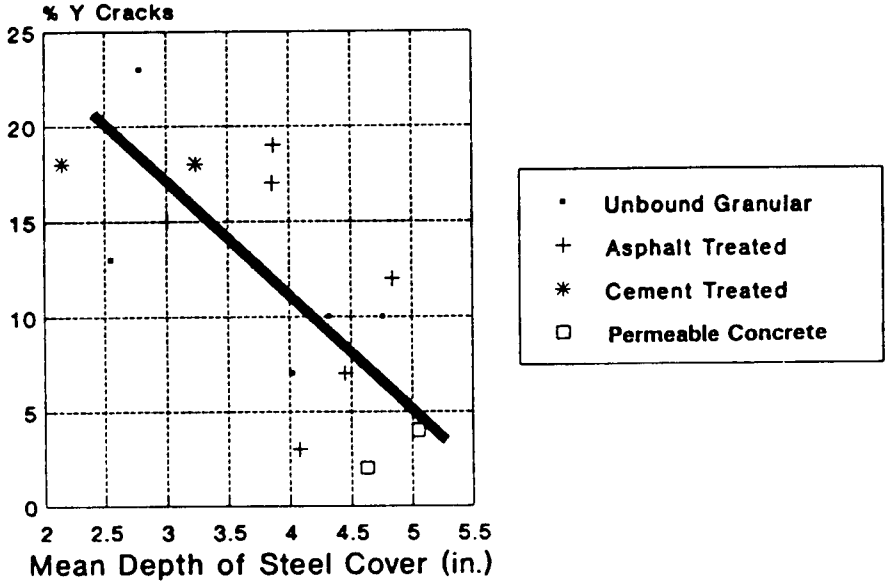

(25.4 mm = 1 in)

Figure 149. Y cracking versus mean depth of steel cover for different subbase types.

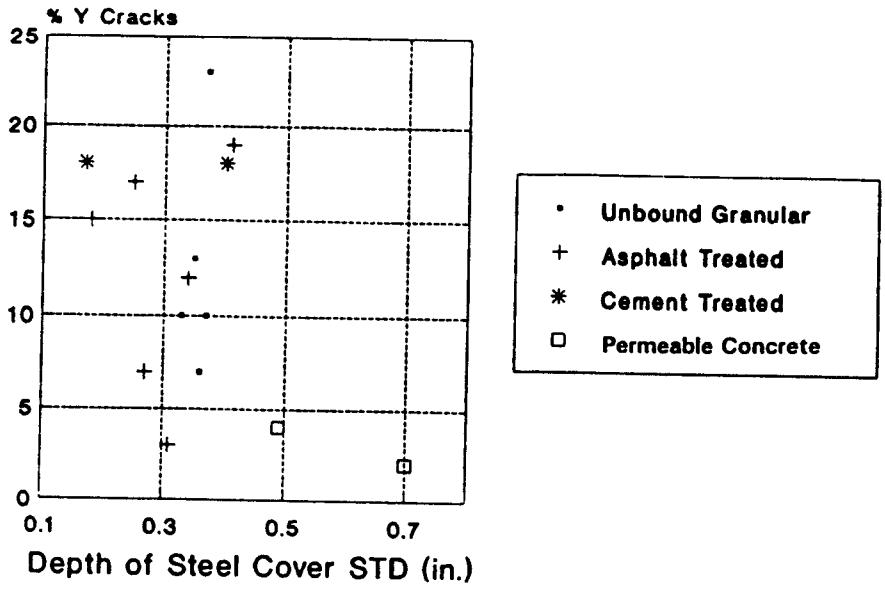

(25.4 mm = 1 in)

Figure 150. Y cracking versus standard deviation of steel cover for different subbase types.

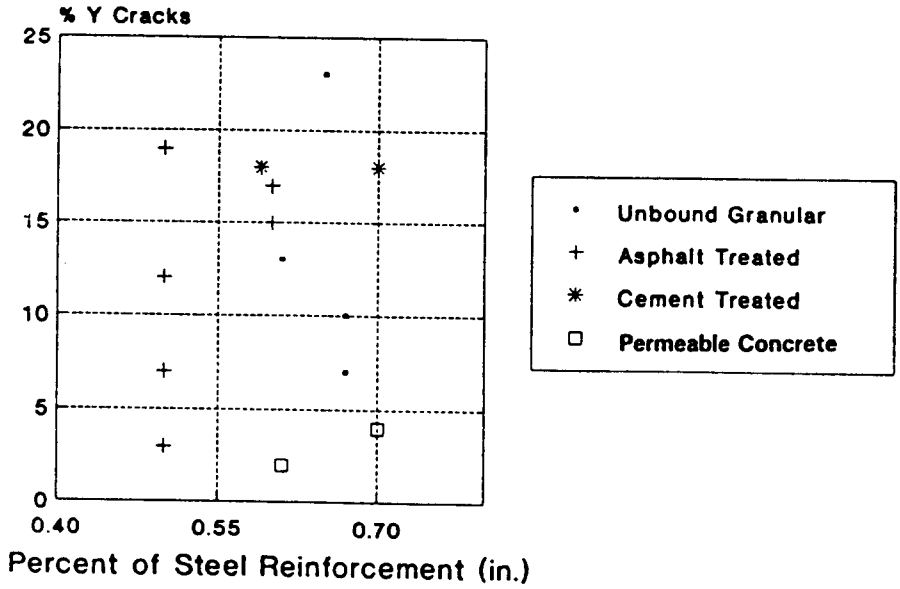

(25.4 mm = 1 in)

Figure 151. Y cracking versus percent of steel for different subbase types.

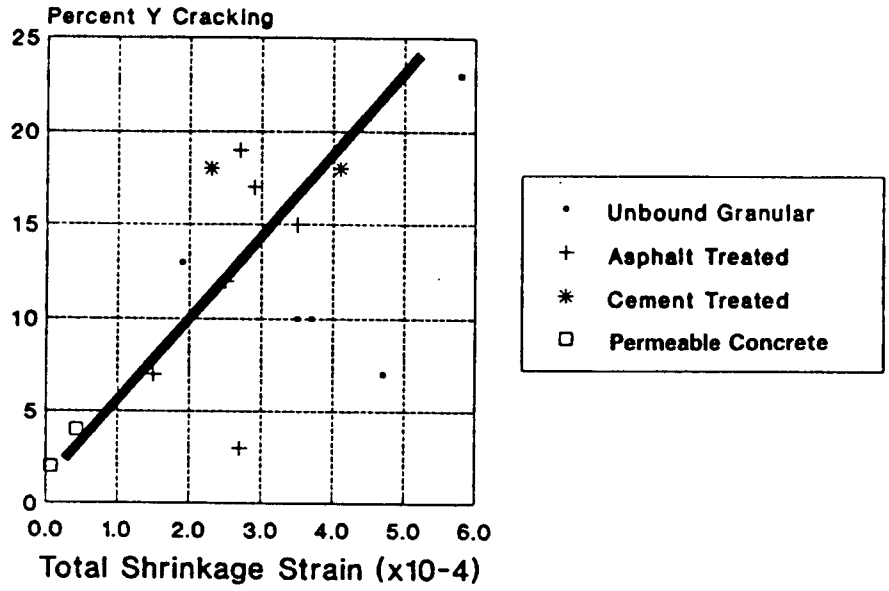

Figure 152. Y cracking versus total shrinkage strain for different subbase types.

REFERENCES

1. Paterson, W.D., "Road Deterioration and Maintenance Effects - Models for Planning and Management," published for the World Bank by the John Hopkins University Press, Baltimore and London, 1987.

2. Hadley, W.O., "PSI Estimates from SHRP Profilometer Roughness," Tech memo No. AU-215 prepared by Texas Research and Development Foundation, Austin, Texas for Strategic Highway Research Program, September 30, 1992.

3. Daleidan, J.F., et al, "Early Analysis of LTPP General Pavement Studies Data: Volume 4 - Evaluation of the AASHTO Design Equations and Recommended Improvements," Report prepared for Strategic Highway Research Program, Washington, DC, August 1993.

4. "AASHTO Guide for Design of Pavement Structures," American Association of State Highway and Transportation Officials, Washington, DC, 1993.

5. Won, M., Hankins, K., and McCullough, B.F., "Mechanistic Analysis of CRC Pavements Considering Material Characteristics, Variability, and Fatigue," Research Report 1169-2, Center for Transportation Research, The University of Texas at Austin, April 1990.

6. Palmer, R., Olsen, M., and Lytton R., "TTICRCP - A Mechanistic Model for the Prediction of Stresses, Strains, and Displacements in CRC Pavements," Report No. FHWA/TX-88/371-2F, Texas Transportation Institute, College Station, Texas, July 1988.

7. Zuk, W., "Analysis of Special Problems in CRC Pavements," Highway Research Bulletin 214, Transportation Research Board, Washington, D.C., 1959.

8. Ioannides, A.M., "Program ILLI-BACK - A Closed-Form Backcalculation Procedure for Rigid Pavements," Copyright 1988. (Program commercially distributed by A.M. Ioannides, Ph.D., Savoy, Illinois).

9. Zollinger, D.G. and Barenberg, E.J., "Continuously Reinforced Pavements: Punchouts and Other Distresses and Implications for Design," Report FHWA/IL/UI-227, FHWA, U.S. Department of Transportation, March 1990.

10. "Data Collection Guide for Long-Term Pavement Performance Studies," Operational Guide No. SHRP-LTPP-OG-001, Strategic Highway Research Program (SHRP), Washington, DC, January 1990 (Revised October 1993, Federal Highway Administration (LTPP Division), Washington, DC).

11. "Laboratory Material Handling and Testing," Operational Guide No. SHRP-LTPP-OG-004, Strategic Highway Research Program, Washington, DC, February 1991 (Revised - Version 2.0, October 1992).

12. SHRP-LTPP Guide for Laboratory Materials Handling and Testing, Operational Guide No. SHRP-LTPP-OG-004, SHRP, Washington, DC, November 1989 (Revised July 1993, Federal Highway Administration (LTPP Division), Washington, DC).

13. Distress Identification Manual for the Long-Term Pavement Performance Project, Report No. SHRP-P-338, Strategic Highway Research Program, Washington, DC, 1993.

14. Verhoeven, K., "Cracking and Corrosion in Continuously Reinforced Concrete Pavements," Proceedings of the 5th International Conference on Concrete Pavement Design and Rehabilitation, held April 20-22, 1993 at Purdue University, West Lafayette, Indiana.